5-2012

Rationalizing Structure, Stability, and Chemical Bonding of Pure and Doped Clusters, Isolatied and Sovanted Multiply Charged Anions, and Solid State Materials

Alina P. Sergeeva
Utah State University

RATIONALIZING STRUCTURE, STABILITY, AND CHEMICAL BONDING OF PURE AND DOPED CLUSTERS, ISOLATED AND SOLVATED MULTIPLY CHARGED ANIONS, AND SOLID STATE MATERIALS

by

Alina P. Sergeeva

A dissertation submitted in partial fulfillment
of the requirements for the degree

of

DOCTOR OF PHILOSOPHY

in

Chemistry

Approved:

Alexander I. Boldyrev Major Professor	Steve Scheiner Committee Member
Alvan Hengge Committee Member	Charles G. Torre Committee Member
David Farrelly Committee Member	Mark R. McLellan Vice President for Research and Dean of the School of Graduate Studies

UTAH STATE UNIVERSITY
Logan, Utah

2012

ABSTRACT

Rationalizing Structure, Stability, and Chemical Bonding of Pure and Doped Clusters, Isolated and Solvated Multiply Charged Anions, and Solid-State Materials

by

Alina P. Sergeeva, Doctor of Philosophy

Utah State University, 2012

Major Professor: Dr. Alexander I. Boldyrev
Department: Chemistry and Biochemistry

Chemistry is the study of materials and the changes that materials undergo. One can tune the properties of the known materials and design the novel materials with desired properties knowing what is responsible for the chemical reactivity, structure, and stability of those materials. The unified chemical bonding theory could address all these questions, but we do not have one available yet. The most accepted general theory of chemical bonding was proposed by Lewis in 1916, though Lewis's theory fails to explain the bonding in materials with delocalized electron density such as sub-nano and nanoclusters, as well as aromatic organic and organometallic molecules. The dissertation presents a set of projects that can be considered the steps towards the development of the unified chemical bonding theory by extending the ideas of Lewis. The dissertation also presents the studies of the properties of multiply charged anions, which tend to undergo Coulomb explosion in the isolated state and release the excess energy stored in them. It is shown how the properties of multiply charged anions can be tuned upon changing the

chemical identity of the species or interaction with solvent molecules. Our findings led to the discovery of a new long-lived triply charged anionic species, whose metastability was explained by the existence of a repulsive Coulomb barrier. We also proposed two ways to restore high symmetry of compounds by suppression of the pseudo Jahn-Teller effect, which could lead to the design of new materials with the restored symmetry and therefore the novel properties.

(343 pages)

CONTENTS

Page

LIST OF TABLES

LIST OF FIGURES

LIST OF SCHEMES

CHAPTER 1

INTRODUCTION AND LITERATURE REVIEW

1-1. Personal Statement

I find theoretical chemistry the most amazing of all the molecular sciences because it has potential to understand our nature's behavior. It is not limited to a particular class of molecules, but rather has immense breadth of application: from clusters to solids, from inorganic to organic and biomolecules. There are two approaches on how to do theoretical chemistry. Some theoreticians embark on a search for novel chemical species or develop models, which can be used for rational design of materials and molecules with tailored properties that can guide future experimental synthesis and characterization of these species. Other theoreticians work in close collaboration with experimentalists by providing the theoretical interpretations of the experimental data.

I joined the theoretical chemistry lab of Professor Boldyrev at USU in 2007 where I was lucky to get exposed to both the purely theoretical inventive research and the collaborative initiative with one of the best experimentalists in the world. Most of my research projects were devoted to the development of the unified chemical bonding theory, which could explain structure, stability and reactivity of every single chemical species and allow design of materials and molecules with desired properties. The most generally accepted theory of chemical bonding now-a-days, which is taught in every general chemistry course, is the one proposed by Lewis in 1916.[1] Almost a century later the development of the general theory of chemical bonding is still far from completion. Extending the ideas of Lewis we were able to rationalize structure, stability and reactivity

of various pure and doped clusters,[2-10] two-dimensional materials,[11] building blocks of crystalline phases,[12] and organometallic compounds.[13]

Almost half of my projects were done in collaboration with experimentalists specializing in photoelectron electron spectroscopy (Professor Bowen, Johns Hopkins University; Professor Wang, Brown University). Our main goal was to determine the most stable structures of novel clusters. Though isolated clusters themselves are certainly exotic species, their chemical bonding, structure, stability and reactivity could help one rationalize the corresponding properties of novel materials, catalysts and nanoparticles. Experiment alone cannot provide structural characterization of the clusters obtained in an electron beam. Theory alone can simulate the experiment and predict the most stable structures of the clusters, but these predictions are never sufficient to make a solid assignment of the most viable chemical species for a given stoichiometry. Only synergetic efforts of experimentalists and theoreticians allow accurate structural characterization of the global minima of clusters. All these endeavors led to a number of exciting discoveries. We showed that one can find analogues of organic aromatic molecules among the realm of inorganic clusters[2-4] and that we can use the concepts of aromaticity beyond organic chemistry to explain structure, stability and reactivity of clusters.[2-4,7,8,10,11-15] For instance, we found boron analogues of prototypical aromatic molecules such as coronene[3] and naphthalene.[2,4] We showed that one of the most stable diatomic molecules (N_2) could be broken upon interaction with gallium clusters.[6]

We demonstrated that the method of presenting a chemical bonding pattern as composed of *n*-center two-electron bonds works in a wide range of chemical species.[2-15] Our chemical bonding models explained possibility of fluxional behavior of molecular

Wankel motors.[10] We proposed the way to design three-dimensional gold clusters.[9] We rationalized the perfectly symmetric structure of a recently synthesized organometallic sandwich complex.[13] We explained the intricate structure of a two-dimensional boron material analogous to graphene.[11]

In addition we investigated properties of various multiply charged anions in the gas phase and when solvated by water molecules.[16-18] Sulfate interactions with water are essential for understanding its chemistry in aqueous solution. Our findings provided molecular-level information about the solute−solvent interactions and critical data to test theoretical methods for weakly bounded species.[18] We were the first to discover the triply charged pyrene-based sulfonate anion, which has negative electron binding energy.[16] Negative electron binding energy is a unique feature of multiply charged anions.[16-17] Such metastable species provide a fertile background to study electron-electron and vibronic interactions in complex molecules.

Another very interesting part of my research was devoted to Jahn-Teller vibronic effects, which are the only source of instability of high-symmetry configurations of polyatomic systems.[19-21] We reported two ways of how one could restore high symmetry in otherwise distorted molecules.[22,23] The first way led to the prediction that if the $Mg(Si_5H_5)_2$ solid compound were synthesized, it could have planar building blocks, similar to ferrocene.[22] The second way explained why the reaction of the puckered silicon Si_6Cl_{12} molecule with a Lewis base (e.g., Cl^-) gave highly symmetric planar $[Si_6Cl_{14}]^{2-}$ dianionic complex.[23] Additionally, the second pathway for the suppression of pseudo-Jahn–Teller effect has been proved by the synthesis and characterization of novel compounds containing planar Si_6 ring.[23] This work demonstrated for the first time that

suppression of the pseudo Jahn–Teller effect could be useful in the rational design of materials with novel properties.

1-2. Overview of the Research Projects Presented in the Dissertation

Chemistry is the study of materials and the changes that materials undergo. One can tune the properties of the known materials and design the novel materials of desired properties knowing what is responsible for the chemical reactivity, structure, and stability of those materials. The unified chemical bonding theory could address all these questions, but we do not have one available yet. Most of the projects I was involved in throughout my Ph. D. degree were the steps towards the development of the unified chemical bonding theory (projects 1 and 2). We have also investigated the properties of multiply charged anions, which tend to undergo the Coulomb explosion in the isolated state and release the excess energy stored in them, and how these properties can be tuned upon changing the chemical identity of the species or interaction with solvent molecules. Our findings led to the discovery of a new long-lived species and showed which factors affect stability of multiply charged anions (project 3). We proposed two ways to restore high symmetry of compounds by suppression of the pseudo Jahn-Teller effect, which could lead to the design of new materials with the restored symmetry and therefore the novel properties (project 4).

All the projects pursued throughout my Ph. D. studies led to 16 peer reviewed journal papers and 3 chapters in the books.[2-18,22,23] I've decided to include only 11 papers to my dissertation. You can find the outline of the projects, the cross-references to the

chapters presented in the dissertation, and the corresponding literature review in the following sections.

1-2.1. Project 1: Structure and chemical bonding of pure and doped clusters

Nanotechnology has become a very popular direction of contemporary science. It may lead to creation of a variety of new materials and devices with a vast range of applications, such as in medicine, electronics, biomaterials and energy production. It is not possible to advance nanotechnology without fully understanding the nano-objects that include atomic clusters among others. Clusters are hard to synthesize and therefore characterize. Clusters show very unique, size-dependent properties, and they are very distinct from both molecules and solid state materials;[24-29] therefore, atomic clusters represent a big challenge both to theoretical chemists and experimentalists. Only synergetic efforts of both experimentalists and theoreticians can allow accurate structural characterization of clusters.[30,31]

The projects on elucidating structure, stability and chemical bonding in novel clusters were done in collaboration with experimental groups of Professor Wang (Brown University) and Professor Bowen (John Hopkins University).[2-6] The experimentalists obtained the clusters in an electron beam and recorded their photoelectron spectra, while we theoretically: (a) determined the most viable chemical structures of the clusters; (b) simulated the photoelectron spectra of the clusters to match the experimental ones in order to confirm the assignment of the global minimum structure; (c) performed chemical bonding analysis to explain what governs stability of the most stable structures of the clusters.

Having one valence electron less than carbon, boron is known to build mainly cage-like structures,[32,33] such as those found in elemental solid state boron,[34] boranes,[35] or boron-rich compounds.[36] Though, if one considers sub-nanoscale, boron atoms tend to form planar and quasi-planar structures of boron clusters.[37] Pure boron clusters are promising molecules for coordination chemistry as potential new ligands and for materials science as new building blocks.[37] Chapter 2 of the dissertation represents a continuation of joint theoretical and experimental studies of pure boron clusters. We show that neutral and anionic boron clusters composed of 16 atoms continue to be planar, and the planarity is governed by π-aromaticity. The structure and stability of B_{16}^{2-} is explained in the view of its similarity to a prototypical aromatic molecule known as naphthalene.[2] Chapter 3 reveales that the B_{19}^{-} cluster attains a beautiful concentric planar structure due to concentric double π-aromaticity reminiscent of that of coronene and [10]annulene.[3] Our studies on chemical bonding of B_{19}^{-} led to the discovery of the first molecular Wankel motor by the groups of Professor Merino and Professor Heine.[38] Both of the papers were highlighted in News of the Week of C&EN.[39] We later combined our studies in the search of other members of molecular Wankel motor family: our collaborators performed the Born-Oppenherimer molecular dynamics studies, which demonstrated that B_{13}^{+} is a fluxional molecule, while we explained the reason for internal rotation in B_{13}^{+}.[10] Chapter 4 summarizes the discovery of the second example of Wankel motors and explains its fluxionality by means of chemical bonding analysis. It was concluded that other boron clusters may possess rotating inner moieties since they exhibit localized bonding on the periphery while the bonding inside of the clusters is delocalized.[10] The planarity of the clusters presented in Chapters 2-4 of the dissertation is

electronic in origin. Chapter 5 rationalizes non-planarity of the B_7^- and B_{12}^- clusters and shows that it is mechanical in origin, according to the careful investigation of properties and structures of AlB_6^- and AlB_{11}^-, which are valence isoelectronic to B_7^- and B_{12}^-.

We have also published purely theoretical articles on structure and chemical bonding of clusters where we finally resolved the controversial issue on chemical bonding in trinuclear rhenium chloride,[7] then confirmed that the proposed model works for the isoelectronic transition-metal halide clusters,[8] as well as proposed the way to design small 3D gold clusters.[9] The chemical bonding picture of rhenium trichloride is shown to change dramatically upon addition of two excess electrons in Chapter 8. The definition of aromaticity in cyclic systems is also revisited. Chapter 9 demonstrates the importance of not restricting oneself to Lewis bonding theory. Small gold clusters may have three-dimensional structures only if they contain tetrahedral four-atomic units each encompassing a four-center two-electron bond. It is important that gold tetrahedra are arranged in such a way that they get to share vertices to account for the least repulsion of electron pairs.

We published three invited chapters in the books where we set the ground rules of chemical bonding that govern chemical structure, stability, and reactivity of clusters.[12,14,15] Clusters exhibit very unique properties, mostly different from those of solid state materials, but we were able to pick the model clusters capable of explaining the bonding in crystalline phases of a set of materials and draw the line connecting clusters and solids.[12] We made a careful analysis of chemical bonding in pure boron clusters, which explained the experimental studies on the reactivity performed by Anderson and co-workers.[40-46]

1-2.2. Project 2: Structure and chemical bonding of solid-state materials and other complexes

Our chemical bonding approach in determining factors that rule structure, stability, and reactivity of clusters is not limited to exotic clusters only. Chapter 6 explains the intricate structure and chemical bonding of an all-boron α-sheet[11] (a 2D-material analogous to graphene). It is shown that all-boron α-sheet has no localized bonds in contrast to carbon-based graphene, and that local π-aromaticity determines holed structure of this material. Chapter 7 rationalizes structure and stability of a recently synthesized remarkable triple-decker sandwich complex $[Pd_4(\mu_4\text{-}C_9H_9)(\mu_4\text{-}C_8H_8)][BAr^f{}_4]$ ($BAr^f{}_4$ = $B\{3,5\text{-}(CF_3)_2(C_6H_3)\}_4$) composed of cyclononatetraenyl anion and cyclooctatetraene as "bread pieces" and square tetrapalladium dication as "meat." We show that according to our chemical bonding analysis the bonding in the Pd_4^{2+} unit of this complex is of δ-character, making the triple-decker sandwich complex the first synthesized compound identified as having delocalized δ-bonding in its cyclic building block when it is in solution or in a crystalline state.[12]

1-2.3. Project 3: Structure and stability of gas phase and solvated multiply charged anions (MCAs)

Multiply charged anions (MCAs) are common in nature,[2] ranging from simple inorganic anions and coordination complexes to organic anions and complex biological molecules. Multiply charged anions contain significant intramolecular Coulomb repulsions and are stabilized in the condensed phase by solvent in solution or counterions in crystals. As isolated species, MCAs are usually unstable against either electron

[2] The next two paragraphs are coauthored by Jie Yang, Xiao-Peng, Xue-Bin, Lai-Sheng Wang, Alina P. Sergeeva and Alexander I. Boldyrev. Reproduced with permission from *J. Chem. Phys.* **2008**, 128, 091102. Copyright 2008, American Institute of Physics.

autodetachment or charge-separation fragmentation and therefore are difficult to study experimentally.[47-53] The electrospray ionization technique[54] made it possible to produce intense beams of MCAs and allowed their first spectroscopic characterization by photoelectron spectroscopy (PES).[55-57] One of the most interesting and unusual features of PES of multiply-charged anions is the detection of the repulsive Coulomb barrier (RCB), which prevents slow electrons from being emitted. The RCB provides dynamic stability for MCAs, allowing metastable species to be observed experimentally.[58-64] Metastable MCAs result in photoelectrons with kinetic energies (KE) higher than the photodetachment photon energy ($h\nu$), leading to negative electron binding energies (BE) on the basis of Einstein's photoelectric equation, BE = $h\nu$ – KE.

Metastable MCAs are interesting molecular species because they store excess electrostatic energies, which are released upon photodetachment. Most small MCAs with negative electron binding energies are too shorted-lived to allow experimental observation, which typically requires 10's of microseconds. An interesting question concerned how much excess energy can be stored in an MCA that would still render it sufficient lifetime to allow experimental observation and interrogation. The first MCA observed with a negative electron binding energy was a fairly large quadruply charged anion,[58,60] copper phthalocyanine tetrasulfonate [$CuPc(SO_3)_4^{4-}$], which was measured to possess 0.9 eV excess energy. Negative electron binding energies have also been measured in a relatively small doubly-charged anion, $PtCl_4^{2-}$, as -0.25 eV.[59,61] The metastabilities of these MCAs have been confirmed by direct observation of autodetachment via tunneling through the RCB in a Fourier transform ion cyclotron resonance mass spectrometer.[62-64] Their half-lives have been measured at room

temperature as 2.5 s for $PtCl_4^{2-}$ and ~275 s for $CuPc(SO_3)_4^{4-}$. We reported the observation of negative electron binding energies in a triply-charged anion, 1-hydroxy-3,6,8-pyrene-trisulfonate ($HPTS^{3-}$).[16] Stable gaseous trianions have been observed and discussed previously,[58,60,65] but negative electron binding energies have not been measured for any trianions. We have determined that $HPTS^{3-}$ possesses a RCB of ~3.3 eV with a relatively high negative electron binding energy of -0.66 eV.[16] This work was followed by exploration of the limits of electronic metastability presented in Chapter 10 of the dissertation.[17] We also studied interactions of a very important inorganic chemistry MCA (SO_4^{2-}) with water, which elucidated the complexity of the water-sulfate potential energy landscape and the importance of the temperature control in studying the solvent-solute systems.[18]

1-2.4. Project 4: Restoration of high symmetry of otherwise distorted molecules

Jahn-Teller effects is the only source of instability of high-symmetry configurations of polyatomic systems.[19-21] We theoretically proposed two pathways to suppress the pseudo Jahn-Teller (PJT) effect and predicted potential high-symmetry molecules that could be synthesized.[22,23] One of the pathways was confirmed by synthesis and experimental characterization of novel compounds.[23]

Chapter 11 reports the theoretical prediction of flattening of the puckered Si_5 ring by suppression of the pseudo Jahn−Teller effect through coordination of two Mg^{2+} cations to the $Si_5H_5^-$ anion to make an inverse $[Mg^{2+}Si_5H_5^-Mg^{2+}]$ sandwich complex. The pseudo Jahn-Teller effect was suppressed through the gaps increase between occupied and unoccupied interacting states. We believe that if the $Mg(Si_5H_5)_2$ solid compound were synthesized, it could have planar $Si_5H_5^-$ building blocks, similar to

ferrocene ($Fe(C_5H_5)_2$). Chapter 12 reports the experimental and theoretical characterization of the neutral Si_6X_{12} (X = Cl, Br) molecules that contain D_{3d} distorted six-member silicon rings due to a pseudo Jahn–Teller effect. The reaction of Si_6Cl_{12} with a Lewis base (e.g., Cl-) to give planar $[Si_6Cl_{14}]^{2-}$ dianionic complexes presents an experimental proof that suppression of the PJT effect is an effective strategy in restoring high Si_6 ring symmetry. Additionally, the proposed pathway for the suppression of pseudo Jahn–Teller effect has been proved by the synthesis and characterization of novel compounds containing planar Si_6 ring, namely, $[^nBu_4N]_2[Si_6Cl_{12}I_2]$, $[^nBu_4N]_2[Si_6Br_{14}]$, and $[^nBu_4N]_2[Si_6Br_{12}I_2]$. This work represented the first demonstration that PJT effect suppression is useful in the rational design of materials with novel properties.

References

1 G. N. Lewis, *J. Am. Chem. Soc*., 1931, **53**, 1367.

2 A. P. Sergeeva, D. Y. Zubarev, H. J. Zhai, A. I. Boldyrev and L. S. Wang, *J. Am. Chem. Soc.,* 2008, **130**, 7244.

3 W. Huang, A. P. Sergeeva, H. J. Zhai, B. B. Averkiev L. S. Wang and A. I. Boldyrev, *Nature Chem.,* 2010, **2**, 202.

4 A. P. Sergeeva, B. B. Averkiev, H. J. Zhai, A. I. Boldyrev and L. S. Wang, *J. Chem. Phys.,* 2011, **134**, 224304.

5 C. Romanescu, A. P. Sergeeva, W. L. Li, A. I. Boldyrev and L. S. Wang, *J. Am. Chem. Soc.,* 2011, **133**, 8646.

6 H. Wang, Y. J. Ko, K. H. Bowen, A. P. Sergeeva, B. B. Averkiev and A. I. Boldyrev, *J. Phys. Chem. A,* 2010, **114**, 11070.

7 A. P. Sergeeva and A. I. Boldyrev, *Comments Inorg. Chem*., 2010, **31**, 2.

8 P. F. Weck, A. P. Sergeeva, E. Kim, A. I. Boldyrev and K. R. Czerwinski, *Inorg. Chem*., 2011, **50**, 1039.

9 A. P. Sergeeva and A. I. Boldyrev, *J. Clust. Sci.*, 2011, **22**, 321.

10 G. Martínez-Guajardo, A. P. Sergeeva, A. I. Boldyrev, T. Heine, J. M. Ugalde and G. Merino, *Chem. Commun*., 2011, **47**, 6242.

11 T. R. Galeev, Q. Chen, J. Guo, H. Bai, C. Q. Miao, H. G. Lu, A. P. Sergeeva, S. D. Li and A. I. Boldyrev, *Phys. Chem. Chem. Phys*., 2011, **13**, 11575.

12 A. P. Sergeeva and A. I. Boldyrev, in *Aromaticity and Metal clusters. Atoms, Molecules, and Clusters. Structure, Reactivity, and Dynamics book series*, ed. P. K. Chattaraj, CRC Press, Taylor & Francis Group, Boca Raton, 2010, pp. 55-68.

13 A. P. Sergeeva and A. I. Boldyrev, *Phys. Chem. Chem. Phys*., 2010, **12**, 12050.

14 A. P. Sergeeva, B. B. Averkiev and A. I. Boldyrev, in *Metal-Metal Bonding. Structure and Bonding book series,* ed. G. Parkin, Volume 136, Springer, Berlin/Heidelberg, 2010, pp. 275-306.

15 D. Y. Zubarev, A. P. Sergeeva and A. I. Boldyrev, in *Chemical Reactivity Theory. A Density Functional View,* ed. P. K. Chattaraj, CRC Press. Taylor & Francis Group, New York, 2009, pp. 439-452.

16 J. Yang, X. P. Xing, X. B. Wang, L. S. Wang, A. P. Sergeeva and A. I. Boldyrev, *J. Chem. Phys*., 2008, **128**, 091102-1-4.

17 X. B. Wang, A. P. Sergeeva, X. P. Xing, M. Massaouti, T. Karpuschkin, O. Hampe, A. I. Boldyrev, M. M. Kappes and L. S. Wang, *J. Am. Chem. Soc.,* 2009, **131**, 9836.

18 X. B. Wang, A. P. Sergeeva, J. Yang, X. P. Xing, A. I. Boldyrev and L. S. Wang, *J. Phys. Chem. A,* 2009, **113**, 5567.

19 I. B. Bersuker, *Chem. Rev.*, 2001, **101**, 1067.

20 I. B. Bersuker, *The Jahn-Teller Effect*, Cambridge University Press, New York, 2006.

21 I. B. Bersuker, *The Jahn-Teller Effect and Beyond: Selected Works of Issac Bersuker with Commentaries*, eds. J. E. Boggs and V. Z. Polinger, The Academy of Sciencies of Moldova: Chisinau, Moldova, 2008.

22 A. P. Sergeeva and A. I. Boldyrev, *Organometallics*, 2010, **29**, 3951.

23 K. Pokhodnya, C. Olson, X. Dai, D. L. Schulz, P. Boudjouk, A. P. Sergeeva and A. I. Boldyrev, *J. Chem. Phys*., 2011, **134**, 014105.

24 *Physics and Chemistry of Small Metal Clusters*, eds. P. Jena, S. N. Khanna and B. K. Rao, Plenum, New York, 1987.

25 S. Sugano, *Microcluster Physics,* Springer, Berlin, 1991.

26 *Clusters of Atoms and Molecules*, ed. H. Haberland, Springer, Berlin, 1994.

27 *Quantum Phenomena in Clusters and Nanostructures*, eds. S. N. Khanna and A. W. Castleman Jr., Springer, Berlin, 2003.

28 T. D. Mark and A. W. Castleman Jr., *Adv. Atomic Mol. Phys.,* 1985, **20**, 65.

29 A. W. Castleman Jr. and R. G. Keesee*, Chem. Rev.* 1986, **86**, 589.

30 X. B. Wang, C. F. Ding, L. S. Wang, A. I. Boldyrev and J. Simons, *J. Chem. Phys.*, 1999, **110**, 4763.

31 A. I. Boldyrev and L. S. Wang, *Chem. Rev.*, 2005, **105**, 3716.

32 N. Vast, S. Baroni, G. Zerah, J. M. Besson, A. Polian, M. Grimsditch and J. C. Chervin, *Phys. Rev. Lett*., 1997, **78**, 693.

33 M. Fujimori, T. Nakata, T. Nakayama, E. Nishibori, K. Kumura, M. Takata and M. Sakata, *Phys. Rev. Lett*., 1999, **82**, 4452.

34 N. N. Greenwood and A. Earnshaw, *Chemistry of the Elements*, 2nd ed., Butterworth-Heinemann, Oxford, 1997.

35 E. D. Jemmis, M. N. Balakrishnarajan and P. D. Pancharatna, *Chem. Rev*. 2002, **102**, 93.

36 *Handbook on the Physics and Chemistry of Rare Earths*, Vol. 38, eds. K. A. Gschneidner Jr., J. C. Bunzli and V. Pecharsky, Elsevier, Amsterdam, 2008.

37 A. N. Alexandrova, A. I. Boldyrev, H.-J. Zhai and L. S. Wang, *Coord. Chem. Rev*., 2006, **250**, 2811.

38 J. O. C. Jimenez-Halla, R. Islas, T. Heine and G. Merino, *Angew. Chem. Int. Ed*. 2010, **49**, 5668.

39 S. Ritter, *Chem. Eng. News*, 2010, **88** , Issue 28, p. 9.

40 L. Hanley and S. L. Anderson, *J. Phys. Chem.,* 1987, **91**, 5161.

41 L. Hanley and S. L. Anderson, *J. Chem. Phys.,* 1988, **89**, 2848.

42 L. Hanley, J. L. Whitten and S. L. Anderson*, J. Phys. Chem*., 1988, **92**, 5803.

43 P. A. Hintz, S. A. Ruatta and S. L. Anderson, *J. Chem. Phys*., 1990, **92**, 292.

44 S. A. Ruatta, P. A. Hintz and S. L. Anderson, *J. Chem. Phys*., 1991, **94**, 2833.

45 P. A. Hintz, M. B. Sowa, S. A. Ruatta and S. L. Anderson, *J. Chem. Phys*., 1991, **94**, 6446.

46 M. B. Sowa-Resat, J. Smolanoff, A. Lapiki and S. L. Anderson, *J. Chem. Phys*., 1997, **106**, 9511.

47 S. N. Schauer, P. Williams and R. N. Compton, *Phys. Rev. Lett*., 1990, **65**, 625.

48 A. I. Boldyrev and J. Simons, *J. Phys. Chem*., 1994, **98**, 2298.

49 J. Kalcher and A. F. Sax, *Chem. Rev.*, 1994, **94**, 2291.

50 M. K. Scheller, R. N. Compton and L. S. Cederbaum, *Science*, 1995, **270**, 1160.

51 A. I. Boldyrev, M. Gutowski and J. Simons, *Acc. Chem. Res*., 1996, **29**, 497.

52 G. R. Freeman and N. H. March, *J. Phys. Chem.*, 1996, **100**, 4331.

53 A. Dreuw and L. S. Cederbaum, *Chem. Rev.,* 2002*,* **102**, 181.

54 J. B. Fenn, *Angew. Chem. Int. Ed.,* 2003, **42**, 3871.

55 X. B. Wang, C. F. Ding and L. S. Wang, *Phys. Rev. Lett*., 1998, **81**, 3351.

56 L. S. Wang, C. F. Ding, X. B. Wang and J. B. Nicholas, *Phys. Rev. Lett*., 1998, **81**, 2667.

57 L. S. Wang and X. B. Wang, *J. Phys. Chem. A*, 2000, **104**, 1978.

58 X. B. Wang and L. S. Wang, *Nature*, 1999, **400**, 245.

59 X. B. Wang and L. S. Wang, *Phys. Rev. Lett*., 1999, **83**. 3402.

60 X. B. Wang, K. Ferris and L. S. Wang, *J. Phys. Chem. A*, 2000, **104**, 25.

61 X. B. Wang and L. S. Wang, *J. Am. Chem. Soc.*, 2000, **122**, 2339.

62 P. Weis, O. Hampe, S. Gilb, and M. M. Kappes, *Chem. Phys. Lett*., 2000, **321**, 426.

63 M. N. Blom, O. Hampe, S. Gilb, P. Weis and M. M. Kappes, *J. Chem. Phys*., 2001, **115**, 3690.

64 K. Arnold, T. S. Balaban, M. N. Blom, O. T. Ehrler, S. Gilb, O. Hampe, J. E. v. Lier, J. M. Weber and M. M. Kappes, *J. Phys. Chem. A,* 2003, **107**, 794.

65 S. Feuerbacher and L. S. Cederbaum, *J. Phys. Chem. A*, 2005, **109**, 11401.

CHAPTER 2

A PHOTOELECTRON SPECTROSCOPIC AND THEORETICAL STUDY OF B_{16}^- AND B_{16}^{2-}: AN ALL-BORON NAPHTHALENE[1]

Although boron clusters were experimentally studied shortly after the discovery of the fullerenes,[1] their structural characterization was only possible fairly recently when we combined photoelectron spectroscopy (PES) and theoretical calculations to investigate the structures and bonding of boron clusters.[2-5] Early theoretical studies[6] indicated that small boron clusters do not assume cage-like structures, which are common in bulk boron and compounds; instead, planar or quasi-planar structures were suggested. The combined PES and theoretical studies show indeed boron clusters with up to 15 atom are planar[2,3,5] and only at B_{20} does a three-dimensional (3D) structure (double ring) become energetically competitive,[4] whereas B_{20}^- still remains planar. A recent ion mobility and theoretical study showed that for B_n^+ the double-ring 3D structure becomes competitive at B_{16}^+.[7]

More interestingly, chemical bonding analyses reveal that π bonding plays an important role in the planar boron clusters.[2,3,5,8] In particular, we have found both aromatic and antiaromatic clusters according to the Hückel rules,[2e,3] analogous to hydrocarbon molecules. In the current work, we focus on B_{16}^- and B_{16}, whose structures and bonding have not been characterized. We show that both B_{16}^- and B_{16} possess quasi-planar structures (C_{2h}). More importantly, we find that addition of an electron to B_{16}^- results in a perfectly planar (D_{2h}) B_{16}^{2-}, which possesses 10 π electrons with a π bonding

[1] Coauthored by Alina P. Sergeeva, Dmitry Yu. Zubarev, Hua-Jin Zhai, Alexander I. Boldyrev, and Lai-Sheng Wang. Reproduced with permission from *J. Am. Chem. Soc.* **2008**, 130, 7244-7246. Copyright 2008, American Chemical Society

pattern similar to that in naphthalene. Thus, B_{16}^{2-} can be considered as an "all-boron naphthalene."

Details of the magnetic-bottle PES apparatus used for this study have been described before.[9] Briefly, the B_{16}^- cluster was produced by laser vaporization of a ^{10}B-enriched target and was mass-selected using time-of-flight mass spectrometry. PES spectra were obtained at two photon energies, as shown in Figure 2-1. The resolution of our PES apparatus was $\Delta E/E \sim 2.5\%$, i.e., ~25 meV for 1 eV electrons.

The 266 nm spectrum reveals three broad and well resolved bands (X, A, B). The broad band widths suggest that there must be significant structural changes between the anion and the neutral final states. The X band defines the ground state vertical detachment energy (VDE) at 3.39 ± 0.04 eV and an adiabatic detachment energy (ADE) of 3.25 ± 0.05 eV, which also represents the electron affinity of B_{16}. At 193 nm, the relative intensity of the B band is increased and another broad band C, which overlaps with band B, also becomes prominent. The 193 nm spectrum is less well resolved and beyond 4.8 eV there is a series of overlapping spectral transitions, which are labeled for the sake of discussion. The VDEs of all the spectral features are given in Table 2-1, compared with theoretical calculations, as discussed in the next section.

Theoretically we first searched for the global minimum of B_{16} using the Gradient Embedded Genetic Algorithm (GEGA) program[10] at the B3LYP/3-21G level of theory and then recalculated geometries of the low-lying isomers at the B3LYP/6-311+G* level. The lowest energy structures identified for B_{16} were used as initial structures for B_{16}^- and B_{16}^{2-}. The VDEs of B_{16}^- were calculated using the R(U)CCSD(T)/6-311+G*, the Outer Valence Green Function method [UOVGF/6-311+G(2df)] and the time-dependent DFT

method [TD-B3LYP/6-311+G(2df)] at the B3LYP/6-311+G* geometries. All calculations were performed using the Gaussian 03 program.[11a] MO visualization was done using the MOLDEN3.4[11b] and MOLEKEL4.3[11c] programs.

The global minimum of B_{16}^- is shown in Figure 2-2, **I.1** (C_{2h}, ^2A_u), which is similar to a low-lying isomer found for B_{16}^+.[7] Alternative structures can be found in Figure 2-3. The second lowest isomer **I.2** (C_s, $^2A''$) is 0.7 kcal/mol (B3LYP/6-311+G*) and 3.7 kcal/mol (CCSD(T)/6-311+G(2df)//B3LYP/6-311+G*) higher in energy. The double-ring structure **I.4** of B_{16}^- (C_s, $^2A'$), analogous to the predicted global minimum structure of B_{20},[4] was found to be 36 kcal/mol higher, very different from B_{16}^+, for which the double-ring structure is a low-lying isomer.[7]

The VDEs for the global minimum structure **I.1** of B_{16}^- have been computed using three methods and are compared to the PES data in Table 2-1. The first two detachment channels are calculated using the ΔCCSD(T) method, which yields VDEs in close agreement with the TD-B3LYP method. The OVGF VDEs appear to be off by as much as 0.3 eV compared to the TD-B3LYP values. We have shown previously for smaller B_n^- (n = 10–15) clusters that the TD-B3LYP method gives VDEs in very good agreement with PES data with errors in the range of 0.1-0.2 eV.[3] Indeed, as can be seen from Table 2-1 and Figure 2-1b, the VDEs from the first four detachment channels, which are well resolved in the PES spectra, are in excellent agreement with the experiment. The first VDE (X) corresponds to detachment from the singly-occupied $6a_u$-HOMO with the singlet final state ^1A_g. The second (A) and third (B) VDEs correspond to detachment from the $5a_u$-HOMO-1, leading to the triplet (^3A_g) and singlet (^1A_g) final states, respectively. The forth VDE (C) derives from detachment from the $5b_g$-HOMO-2

leading to the triplet final state (^3B_u). The VDE (5.12 eV) for the corresponding singlet state (^1B_u) is similar to the next detachment channel from the $7b_u$-HOMO-2 with a calculated VDE of 5.11 eV. Higher detachment channels give a series of closely-spaced VDEs, consistent with the highly congested PES spectrum in the high binding energy side (Figure 2-1b). On the other hand, the calculated first VDE (3.69 eV at TD-B3LYP) for the second lowest isomer (**I.2** in Figure 2-3) is significantly higher than the experimental value of 3.39 eV and this isomer can be ruled out as a contributor to the experiment. The good agreement between the calculated and experimental VDEs for structure **I.1** provides considerable credence for its being the global minimum for B_{16}^-.

Structure **I.1** is quasi-planar because two of the four inner B atoms are slightly out of plane by 0.08 Å. We note that the global minimum of B_{16} is similar to that of B_{16}^- but with more severe out-of-plane distortions by 0.24 Å (**II.1** in Figure 2-2), consistent with the broad ground state transition in the PES spectrum (Figure 2-1). However, upon addition of an electron to the $6a_u$-HOMO of B_{16}^- (C_{2h}, ^2A_u), we find that the resulting B_{16}^{2-} dianion becomes a perfect planar (D_{2h}) and closed-shell (^1A_g) species (**III.1**, Figure 2-2). More interestingly, further analyses of the canonical MOs of B_{16}^{2-} show that it possesses 10 π electrons and its π-system is analogous to that of the well-known aromatic naphthalene (Figure 2-4). Thus, B_{16}^{2-} can be considered as an "all-boron naphthalene", adding a new member to the hydrocarbon analogues of boron clusters.

It is interesting to note that upon removal of two π electrons from the HOMO of B_{16}^{2-} the neutral B_{16} becomes π-anti-aromatic and undergoes out-of-plane deformations, analogous to the out-of-plane distortion in the classical antiaromatic cyclooctatetraene (C_8H_8). In B_{16}, two of the four inner boron atoms (at the terminal positions) distort above

and below the molecular plane by 0.24 Å (Figure 2-2), respectively. The open shell B_{16}^- is in between the π-antiaromatic B_{16} and the π-aromatic B_{16}^{2-} and thus suffers much smaller out-of-plane distortions by only 0.08 Å.

The σ bonding patterns in B_{16}^{2-} are also very interesting and should play important roles in shaping its overall planar structure. It is elucidated using the recently developed adaptive natural density partitioning (AdNDP) method, which is an extension of the popular natural bond orbital (NBO) analysis. This approach leads to partitioning of the charge density into elements with the highest possible degree of localization of electron pairs. If some part of the density cannot be localized in this manner, it is left "delocalized" (*i.e.*, localized on several atoms in the system), giving rise to *n*-center two electron (nc-2e) bonds. Thus, AdNDP incorporates naturally the idea of delocalized (globally aromatic) bonds and achieves seamless description of chemical bonding in the most general sense.

According to our AdNDP analysis shown in Figure 2-5, the σ-bonding framework of B_{16}^{2-} consists of 12 peripheral 2c-2e B-B bonds with occupation numbers above 1.89 |e|, six 3c-2e bonds with occupation number above 1.86 |e|, and two 4c-2e bonds with the occupation number 1.97 |e|. The four inner boron atoms are bonded to the peripheral boron ring via the 3c-2e and 4c-2e bonds. Out of the twenty canonical valence σ-MOs (Figure 2-6), twelve ($3b_{3g}$, $4b_{1u}$, $3b_{1u}$, $2b_{3g}$, $3a_g$, $2b_{2u}$, $2b_{1u}$, $1b_{3g}$, $1b_{2u}$, $2a_g$, $1b_{1u}$, $1a_g$) are responsible for the formation of the above-mentioned 2c-2e peripheral B-B bonds formed from the sp-hybridized AOs of boron atoms. The other eight valence canonical σ-MOs ($5b_{2u}$, $4b_{3g}$, $5b_{1u}$, $6a_g$, $4b_{2u}$, $3b_{2u}$, $5a_g$, $4a_g$) form delocalized σ-bonds, formally satisfying the 4*n* rule for σ-antiaromaticity. This may be responsible for the globally elongated

shape of B_{16}^{2-}, in contrast to the perfectly circular shape of B_8^{2-} and B_9^-, which are both π- and σ-aromatic.[2e]

To assess the viability of using B_{16}^{2-} as building blocks for cluster-assembled nanomaterials, we also optimized structures of B_{16}^{2-} stabilized by two Li^+ cations in Li_2B_{16} (Figure 2-7). We found that the planar B_{16}^{2-} unit is quite flexible and can be bent or "rippled" upon coordination by Li^+. This flexibility is probably due to the relatively weak delocalized, in-plane B-B σ bonding, in contrast to the strong C-C σ-bond that forms the framework of naphthalene. Other than the bending distortion induced by Li^+, the bonding and structural integrity of B_{16}^{2-} are not altered significantly in Li_2B_{16}, suggesting its stability and viability as a structural and material building blocks.

Boron clusters with 6 π-electrons have been found before, including, B_8^{2-} and B_9^-,[2e] B_{10}, B_{11}^-, and B_{12},[3] as well as B_{13}^+,[8] which can be viewed as all-boron analogs of benzene. Globally π-antiaromatic boron clusters with 8 π-electrons have also been found, including B_{13}^- and B_{14},[3] as well as B_{16}, which can be viewed as analogs of antiaromatic cyclobutadiene or cyclooctatetrene. Here we show that B_{16}^{2-} with 10 π-electrons is an all-boron analog of naphthalene. A natural question is if we can extend this analogy further to larger all-boron π-aromatic systems and find analogs of anthracene or other polycyclic aromatic hydrocarbons, which are being actively pursued in our laboratories.

References

(1) (a) Hanley, L.; Anderson, S. L. *J. Phys. Chem.* **1987**, *91*, 5161. (b) Hanley, L.; Anderson, S. L. *J. Chem. Phys*. **1988**, *89*, 2848. (c) Hanley, L.; Whitten, J. L.; Anderson, S. L. *J. Phys. Chem*. **1988**, *92*, 5803. (d) Hintz, P. A.; Ruatta, S. A.;

Anderson, S. L. *J. Chem. Phys*. **1990**, *92*, 292. (e) Ruatta, S. A.; Hintz, P. A.; Anderson, S. L. *J. Chem. Phys*. **1991**, *94*, 2833. (f) Hintz, P. A.; Sowa, M. B.; Ruatta, S. A.; Anderson, S. L. *J. Chem. Phys*. **1991**, *94*, 6446. (g) Sowa-Resat, M. B.; Smolanoff, J.; Lapiki, A.; Anderson, S. L. *J. Chem. Phys*. **1997**, *106*, 9511. (h) La Placa, S. J.; Roland, P. A.; Wynne, J. J. *Chem. Phys. Lett*. **1992**, *190*, 163.

(2) (a) Zhai, H. J.; Wang, L. S.; Alexandrova, A. N.; Boldyrev, A. I. *J. Chem. Phys.* **2002**, *117*, 7917. (b) Alexandrova, A. N.; Boldyrev. A. I.; Zhai, H. J.; Wang, L. S.; Steiner, E.; Fowler, P. W. *J. Phys. Chem. A* **2003**, *107*, 1359. (c) Zhai, H. J.; Wang, L. S.; Alexandrova, A. N.; Boldyrev, A. I.; Zakrzewski, V. G. *J. Phys. Chem. A* **2003**, *107*, 9319. (d) Kuznetsov, A. E.; Boldyrev, A. I. *Struct. Chem.* **2002**, *13*, 141. (e) Zhai, H. J.; Alexandrova , A. N.; Birch, K. A.; Boldyrev, A. I.; Wang. L. S. *Angew. Chem. Int. Ed.* **2003**, *42*, 6004. (f) Alexandrova, A. N.; Boldyrev, A. I.; Zhai, H. J.; Wang, L. S. *J. Phys. Chem. A* **2004**, *108*, 3509. (g) Alexandrova, A. N.; Zhai, H. J.; Wang, L. S.; Boldyrev, A. I. *Inorg. Chem.* **2004**, *43*, 3552. (h) Alexandrova, A. N.; Boldyrev, A. I.; Zhai, H. J.; Wang, L. S. *J. Chem. Phys.* **2005**, *122*, 054313. (i) Alexandrova, A. N.; Kayle, E.; Boldyrev, A. I. *J. Mol. Mod.* **2006**, *12*, 569. (j) Zhai, H. J.; Wang, L. S.; Zubarev, D. Y.; Boldyrev, A. I. *J. Phys. Chem. A* **2006**, *110*, 1689.

(3) Zhai, H. J.; Kiran, B.; Li, J.; Wang, L. S. *Nat. Mater.* **2003**, *2*, 827.

(4) (a) Kiran, B.; Bulusu, S.; Zhai, H. J.; Yoo, S.; Zeng, X. C.; Wang, L. S. *Proc. Natl. Acad. Sci*. (USA) **2005**, *102*, 961. (b) An, W.; Bulusu, S.; Gao, Y.; Zeng, X. C. *J. Chem. Phys*. **2006**, *124*, 154310.

(5) (a) Alexandrova, A. N.; Boldyrev, A. I.; Zhai, H. J.; Wang, L. S. *Coord. Chem. Rev.* **2006**, *250*, 2811. (b) Zubarev, D. Y.; Boldyrev, A. I. *J. Comput. Chem.* **2007**, *28*, 251.

(6) (a) Bonacic-Koutecky, V.; Fantucci, P.; Koutecky, J. *Chem. Rev*. **1991**, *91*, 1035. (b) Kawai, R.; Weare, J. H. *J. Chem. Phys.* **1991**, *95*, 1151. (c) Kawai, R.; Weare, J. H. *Chem. Phys. Lett.* **1992**, *191*, 311. (d) Martin, J. M. L.; François, J. P.; Gijbels, R. *Chem. Phys. Lett.* **1992**, *189*, 529. (e) Kato, H.; Yamashita, K.; Morokuma, K. *Chem. Phys. Lett.* **1992**, *190*, 361. (f) Boustani, I. *Int. J. Quantum Chem*. **1994**, *52*, 1081. (g) Boustani, I. *Chem. Phys. Lett.* **1995**, *233*, 273. (h) Boustani, I. *Chem. Phys. Lett.* **1995**, *240*, 135. (i) Ricca, A.; Bauschlicher, C. W. Jr. *Chem. Phys.* **1996**, *208*, 233. (j) Boustani, I. *Surf. Sci.* **1997**, *370*, 355. (k) Boustani, I. *Phys. Rev. B,* **1997**, *53*, 16426. (l) Nie, J.; Rao, B. K.; Jena, P. *J. Chem. Phys.* **1997**, *107*, 132. (m) Gu, F. L.; Yang, X.; Tang, A. C.; Jiao, H.; Schleyer, P. v. R. *J. Comput. Chem.* **1998**, *19*, 203. (n) Cao, P. L.; Zhao, W.; Li, B. X.; Song, B.; Zhou, X. Y. *J. Phys.: Condens. Matter* **2001**, *13*, 5065.

(7) Oger, E.; Crawford, R. M.; Kelting, R.; Weis, P.; Kappes, M. M.; Ahlrichs, R. *Angew. Chem. Int. Ed*. **2007**, *46*, 8503.

(8) (a) Fowler, J. E.; Ugalde, J. M. *J. Phys. Chem. A* **2000**, *104*, 397. (b) Aihara, J. *J. Phys. Chem. A* **2001**, *105*, 5486. (c) Aihara, J.; Kanno, H.; Ishida, T. *J. Am. Chem. Soc.* **2005**, *127*, 13324.

(9) Wang, L. S.; Cheng, H. S.; Fan, J. *J. Chem. Phys.* **1995**, *102*, 9480.

(10) (a) Alexandrova, A. N.; Boldyrev, A. I.; Fu, Y. J.; Wang, X. B.; Wang, L. S. *J. Chem. Phys.* **2004**, *121*, 5709. (b) Alexandrova, A. N.; Boldyrev, A. I. *J. Chem. Theory and Comput.* **2005**, *1*, 566.

(11) (a) Frisch, M. J.; et al. *Gaussian 03*, Revision D.01, Gaussian, Inc., Wallingford CT, 2004. (b) MOLDEN 3.4. Schaftenaar, G. MOLDEN3.4, CAOS/CAMM Center: The Netherlands, **1998**. (c) Portmann, S. *MOLEKEL*, Version 4.3; CSCS/ETHZ: Zurich, Switzerland, 2002.

***Table 2-1*:** Comparison of the experimental vertical detachment energies (VDE) with the calculated values of B_{16}^- (structure **I.1**). All energies are in eV.

Feature	VDE (exp.)[a]	Final State and Electronic Configuration	VDE (theo.)		
			TD-B3LYP[b]	OVGF[c]	ΔCCSD(T)[e]
X	3.39 (4)	^1A_g, $7a_g^2 6b_u^2 4b_g^2 7b_u^2 5b_g^2 5a_u^2 6a_u^0$	3.37	3.57 (0.88)	3.27
A	3.78 (4)	^3A_g, $7a_g^2 6b_u^2 4b_g^2 7b_u^2 5b_g^2 5a_u^1 6a_u^1$	3.70	3.53 (0.88)	3.76
B	4.03 (4)	^1A_g, $7a_g^2 6b_u^2 4b_g^2 7b_u^2 5b_g^2 5a_u^1 6a_u^1$	4.03	[d]	
C	4.4 (1)	^3B_u, $7a_g^2 6b_u^2 4b_g^2 7b_u^2 5b_g^1 5a_u^2 6a_u^1$	4.40	4.44 (0.88)	
D	~5.0	^3B_g, $7a_g^2 6b_u^2 4b_g^2 7b_u^1 5b_g^2 5a_u^2 6a_u^1$	5.11	5.36 (0.88)	
		^1B_u, $7a_g^2 6b_u^2 4b_g^2 7b_u^2 5b_g^1 5a_u^2 6a_u^1$	5.12	[d]	
E	~5.2	^3B_u, $7a_g^2 6b_u^2 4b_g^1 7b_u^2 5b_g^2 5a_u^2 6a_u^1$	5.30	5.46 (0.83)	
F	5.40 (10)	^1B_g, $7a_g^2 6b_u^2 4b_g^2 7b_u^1 5b_g^2 5a_u^2 6a_u^1$	5.39	[d]	
G	5.6 ~ 6.2	^3B_g, $7a_g^2 6b_u^1 4b_g^2 7b_u^2 5b_g^2 5a_u^2 6a_u^1$	5.65	5.86 (0.84)	
		^1B_u, $7a_g^2 6b_u^2 4b_g^1 7b_u^2 5b_g^2 5a_u^2 6a_u^1$	5.66	[d]	
		^1B_g, $7a_g^2 6b_u^1 4b_g^2 7b_u^2 5b_g^2 5a_u^2 6a_u^1$	5.77	[d]	
		^3A_u, $7a_g^1 6b_u^2 4b_g^2 7b_u^2 5b_g^2 5a_u^2 6a_u^1$	5.78	6.25 (0.83)	
		^1A_u, $7a_g^1 6b_u^2 4b_g^2 7b_u^2 5b_g^2 5a_u^2 6a_u^1$	5.99	[d]	

[a]Numbers in parentheses represent the uncertainty in the last digit.
[b]VDEs were calculated at TD-B3LYP/6-311+G(2df)//B3LYP/6-311+G* level of theory.
[c]VDEs were calculated at UOVGF/6-311+G(2df)//B3LYP/6-311+G* level of theory. Values in parentheses represent the pole strength of the OVGF calculation.
[d]This transition cannot be calculated at this level of theory.
[e]VDEs were calculated at R(U)CCSD(T)/6-311+G*/B3LYP/6-311+G* level of theory.

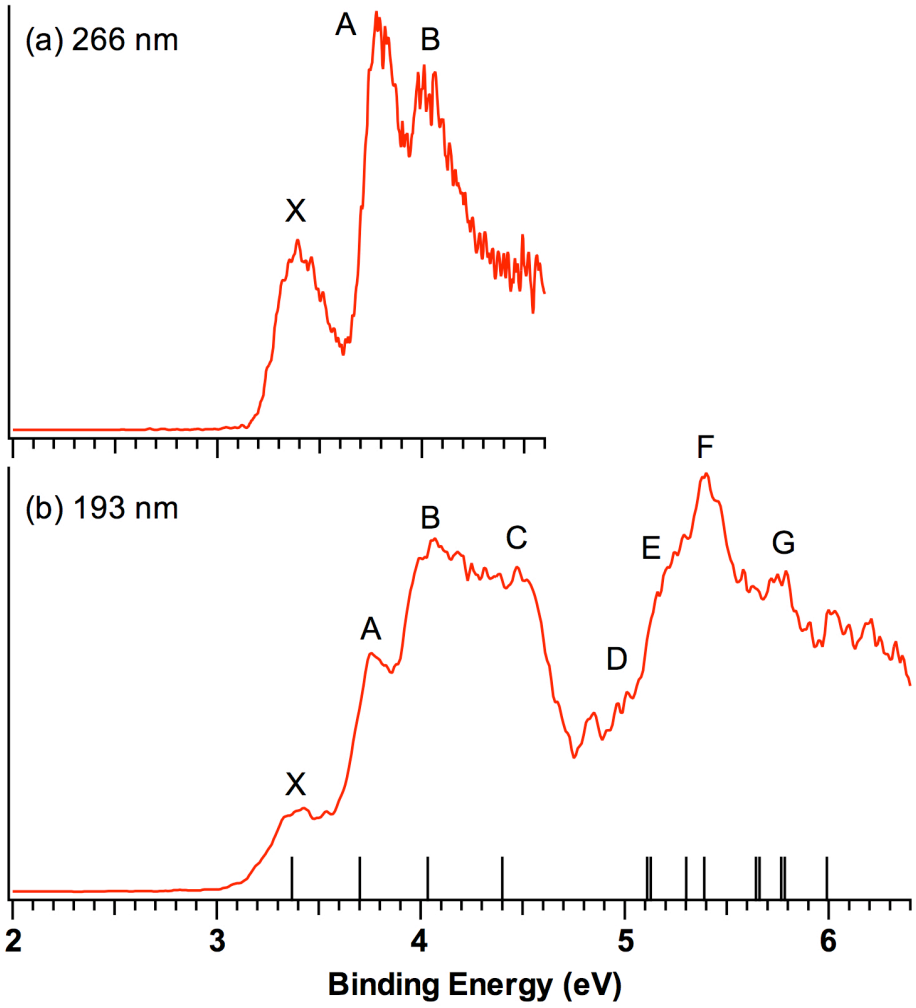

Figure 2-1. Photoelectron spectra of B_{16}^- at (a) 266 nm (4.661 eV) and (b) 193 nm (6.424 eV). The vertical bars represent the calculated VDEs at the TD-B3LYP level (see Table 2-1).

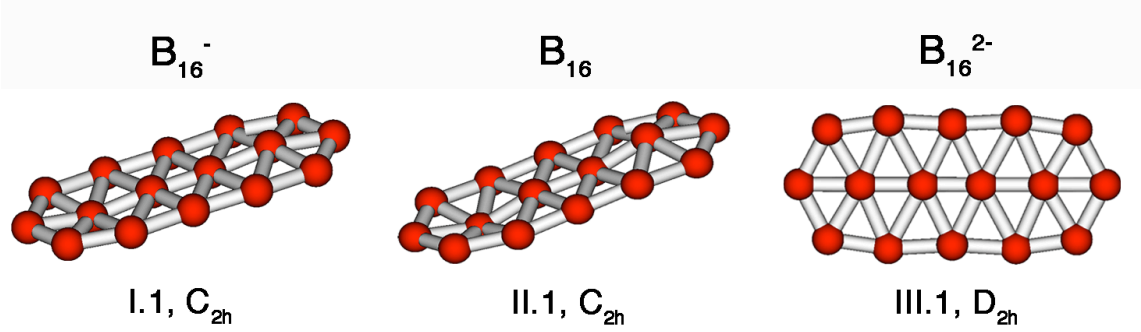

Figure 2-2. The optimized global minimum structures of B_{16}^{-} (^2A_u), B_{16} (^1A_g), and B_{16}^{2-} (^1A_g) at B3LYP/6-311+G*.

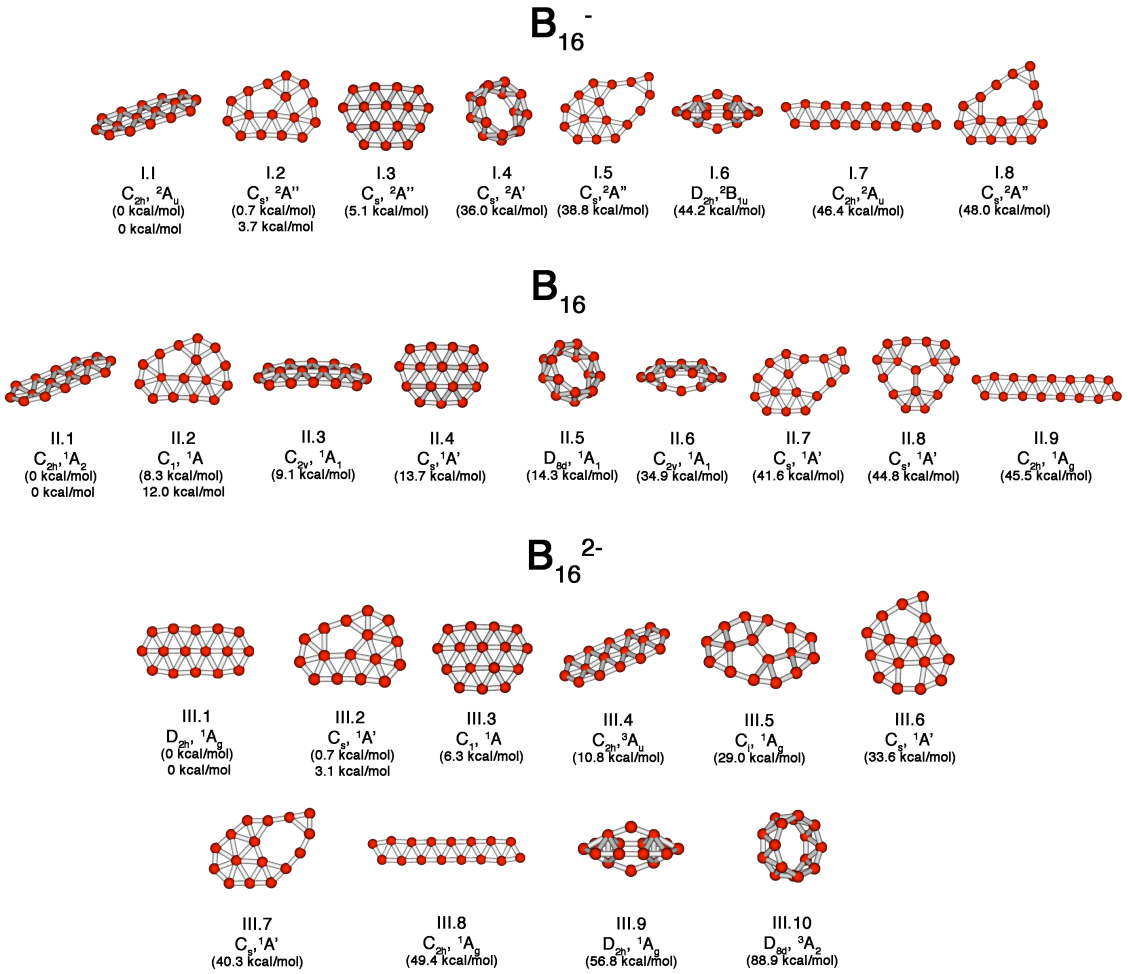

Figure 2-3. Optimized structures for B_{16}^{-}, B_{16}, and B_{16}^{2-}. The number in the parentheses is the relative energy at the B3LYP/6-311+G*//B3LYP/6-311+G* level of theory with ZPE correction. The lower number without parentheses is the relative energy at the R(U)CCSD(T)/6-311G*//B3LYP/6-311+G* level of theory.

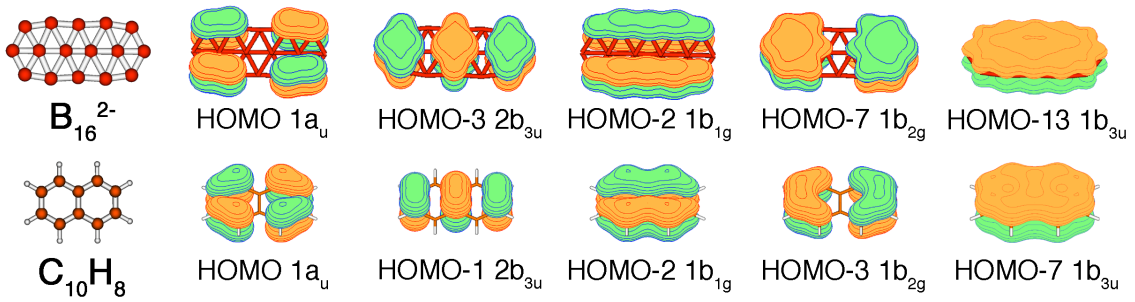

Figure 2-4. Comparison of the structures and π bonding of B_{16}^{2-} (D_{2h}, ^1A_g) and naphthalene.

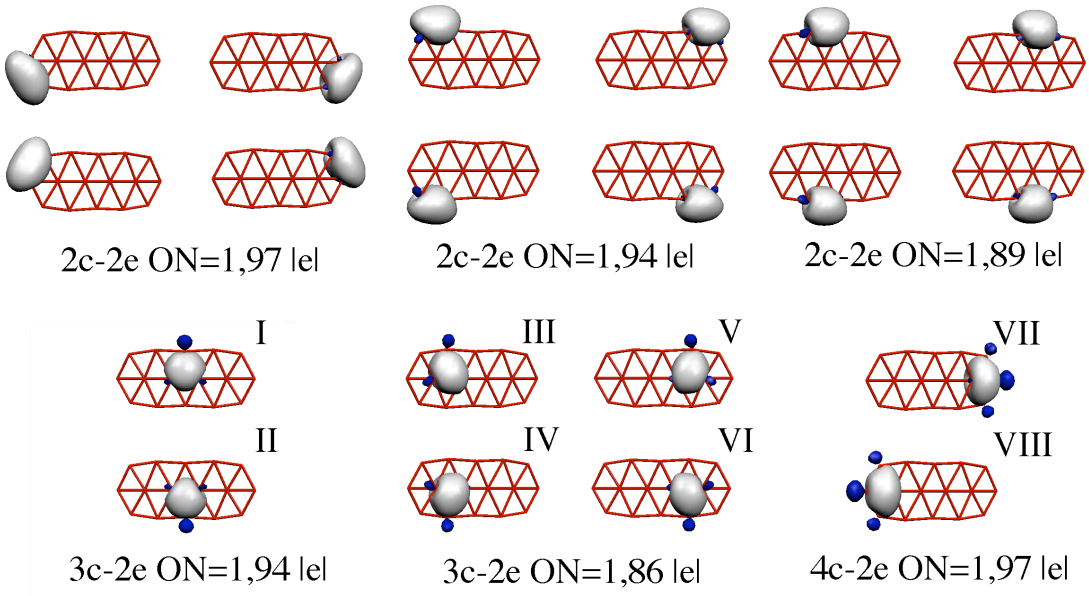

Figure 2-5. Localized nc-2e σ-bonds and occupation numbers in B_{16}^{2-} obtained by AdNDP analyses.

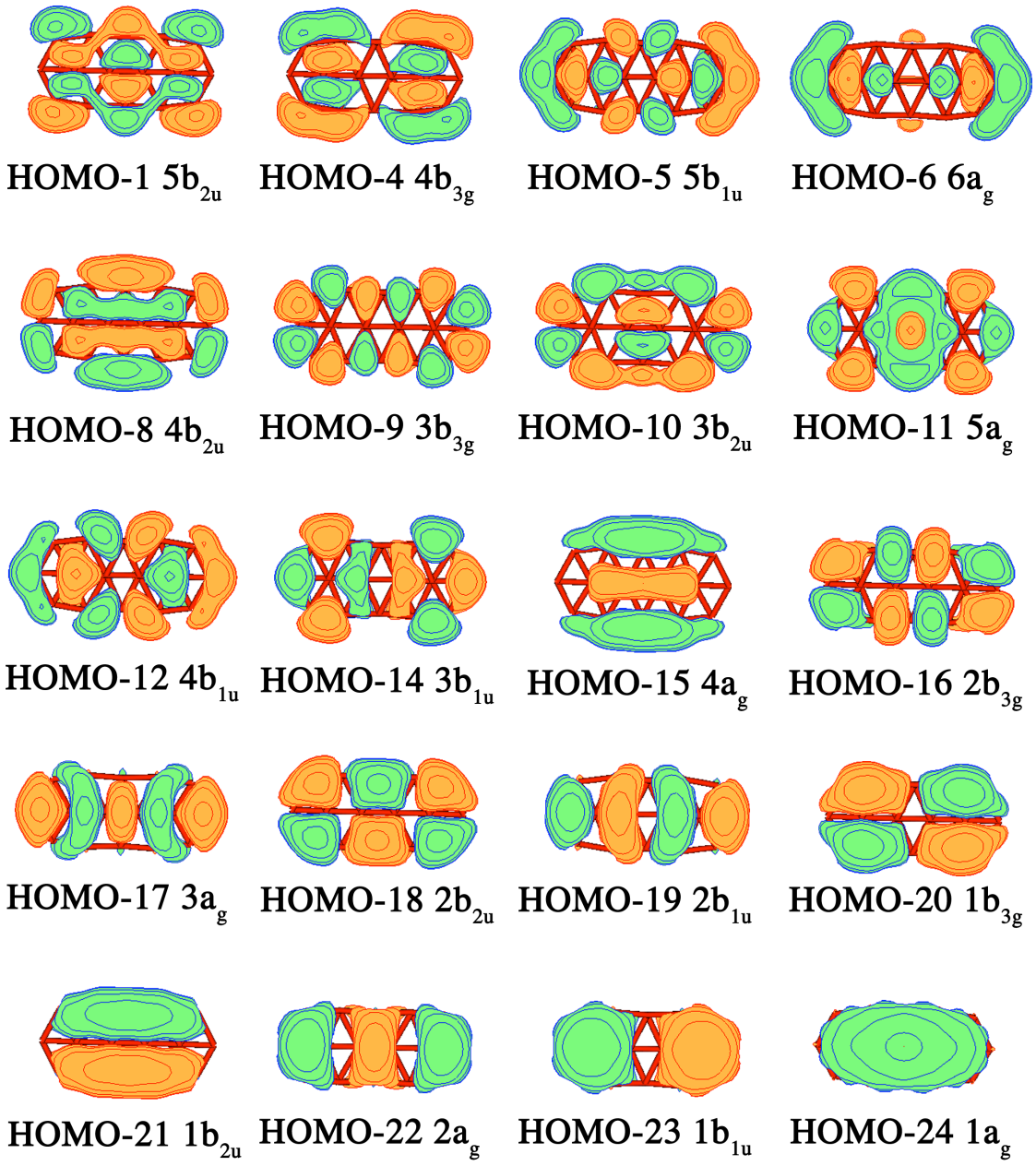

Figure 2-6. Valence canonical σ molecular orbitals for most stable structure of B_{16}^{2-} (D_{2h}, ^1A_g) (structure **III.1**).

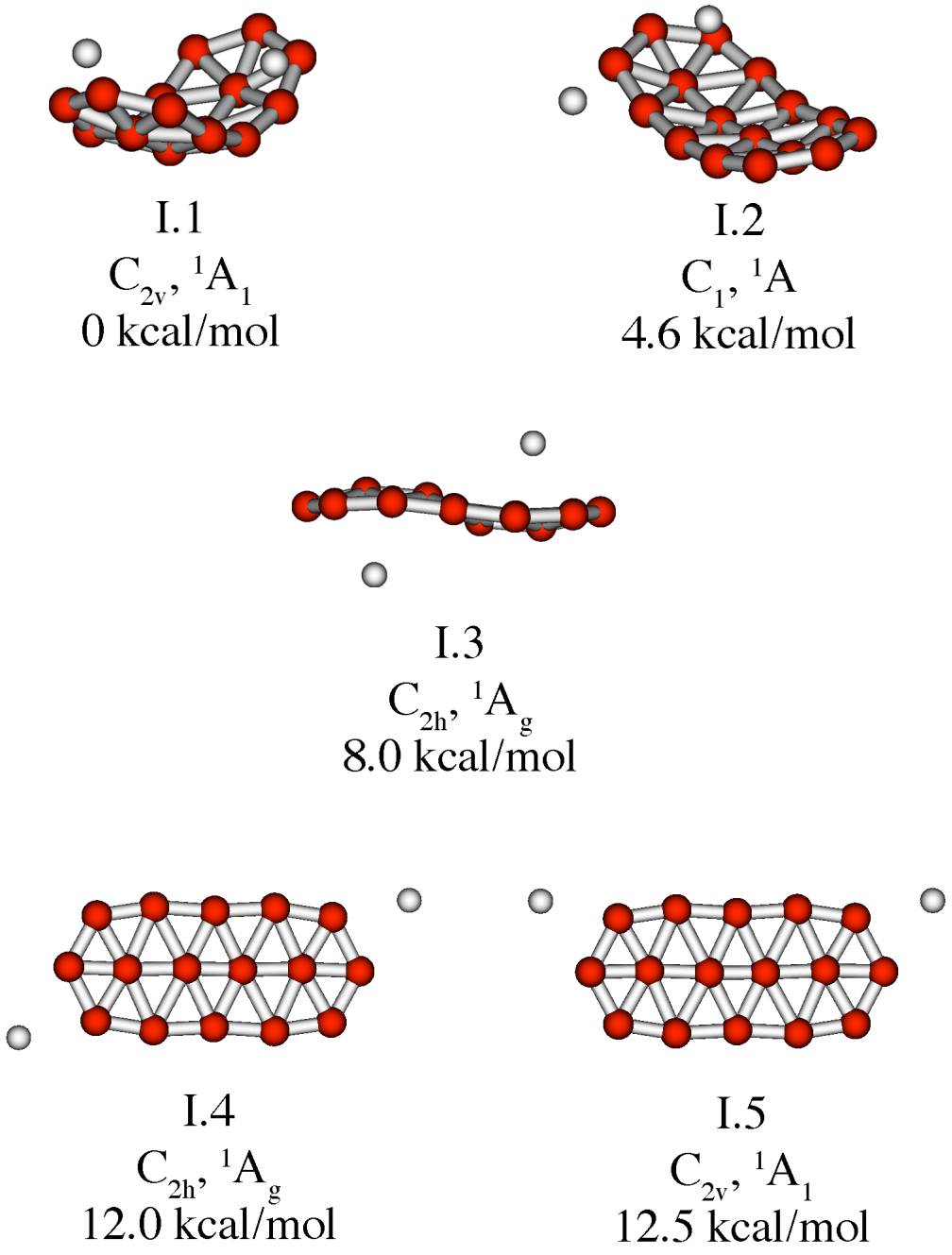

Figure 2-7. Optimized structures of Li_2B_{16}. Relative energies are given at the B3LYP/6-311+G*//B3LYP/6-311+G* level of theory with ZPE correction.

CHAPTER 3

A CONCENTRIC PLANAR DOUBLY π-AROMATIC B_{19}^- CLUSTER[1]

Abstract

Atomic clusters often exhibit unique size-dependent properties and have become a fertile ground for discovering novel molecular structures and chemical bonding. Here we report an investigation of the B_{19}^- cluster, which exhibits chemical bonding reminiscent of those in [10]annulene ($C_{10}H_{10}$) and [6]circulene ($C_{24}H_{12}$). Photoelectron spectroscopy reveals a relatively simple spectrum for B_{19}^- with a high electron binding energy. Theoretical calculations show that the global minimum of B_{19}^- is a nearly circular planar structure with a central B_6 pentagonal unit bonded to an outer B_{13} ring. Chemical bonding analyses reveal that the B_{19}^- cluster possesses unique double π aromaticity in two concentric π systems, with 2 π electrons delocalized over the central pentagonal B_5 unit and another 10 π electrons responsible for the π-bonding between the central pentagonal unit and the outer ring. Such peculiar chemical bonding does not exist in organic compounds; it can only be found in atomic clusters.

Aromaticity in chemistry manifests itself as enhanced stability, high symmetry, low reactivity, bond lengths equalization, enhanced anisotropy of diamagnetic susceptibility, diatropic (low-field) ^{1}H NMR shifts, large negative nucleus independent chemical shift (NICS) values, as well as high electron detachment energies in photoelectron spectra.[1-3] Aromaticity in conjugated hydrocarbons follows Hückel's $4n+2$ π electron rule, which

[1] Coauthored by Wei Huang, Alina P. Sergeeva, Hua-Jin Zhai, Boris B. Averkiev, Lai-Sheng Wang, and Alexander I. Boldyrev. Reproduced with permission from *Nature Chem*. **2010**, 2, 202-206. Copyright 2010, MacMillan Publishers Ltd.

was developed on the basis of symmetry of molecular orbitals of monocyclic C_nH_n (where n is an even number) hydrocarbons known in chemistry as annulenes. The prototypical aromatic molecule with 6 π electrons satisfying the $4n+2$ rule is benzene or [6]annulene (n = 1). The next higher uncharged homologue of benzene with n = 2 is [10]annulene ($C_{10}H_{10}$, planar monocyclic cyclodeca-1,3,5,7,9-pentaene) (Fig. 3-1a, bottom scheme). However, [10]annulene was shown to be neither planar nor aromatic.[4-6] Masamune *et al*. isolated two crystalline forms (A and B) of [10]annulene and came to the conclusion that both possess non-planar geometries. The most recent ab initio calculations[6] showed that there are three lowest isomers for $C_{10}H_{10}$, all being non-planar species: a "twist" structure (the most stable), a "naphthalene-like" structure (1.4 kcal/mol higher in energy), and a "heart-shaped" structure (4.2 kcal/mol higher in energy), all calculated at a high level of theory (Fig. 3-1a, top scheme). Price and Stanton demonstrated that the "twist" isomer corresponds to the crystalline form B of $C_{10}H_{10}$ by comparing experimental NMR shifts with theoretical calculations.[7] The *planar* monocyclic [10]annulene (Fig. 3-1a, bottom scheme) is substantially higher in energy and not even a local minimum on the potential energy surface. The concept of aromaticity has long been extended to the realms outside organic chemistry.[2,3,8] The question is whether one can find analogous 10 π electron systems among other classes of chemical species. Boron clusters could potentially offer such an opportunity since a number of hydrocarbon analogues of boron clusters have been identified recently.[9-12]

Chemical bonding, structure, reactivity, and stability of planar and quasi-planar boron clusters can be rationalized using concepts of aromaticity and antiaromaticity.[9-16] Particularly, B_8^{2-} and B_9^-,[9,16] B_{10}, B_{11}^-, and B_{12},[10] as well as B_{13}^+ boron clusters[13-15] can

be viewed as all-boron analogues of benzene on the basis of their 6 π electrons comprising similar π molecular orbital patterns. Early experimental works on boron clusters involved measurements of appearance potentials and fragmentation patterns using collision-induced dissociations,[17-21] revealing that B_{13}^+ has anomalously high stability and low reactivity in comparison with other cationic boron clusters, consistent with its aromatic nature. Photoelectron spectroscopy in combination with *ab initio* calculations has recently enabled detailed structural characterization of a series of boron clusters,[9-11,22-25] leading to the concept of hydrocarbon analogues of planar boron clusters. The latest example is B_{16}^{2-} with 10 π-electrons, which was shown to be an all-boron analogue of naphthalene.[26] Here we report an experimental and theoretical investigation of the B_{19}^- cluster. We found that B_{19}^- possesses a nearly circular planar structure (Fig. 3-1b) with a pentagonal central B_6 unit inside a B_{13} ring with a π-bonding pattern displaying similarities to those of both the planar aromatic [10]annulene (Fig. 3-1a, bottom scheme) and [6]circulene (Fig. 3-1c). The presented structure/chemical bonding representation of [6]circulene, which avoids resonance description and is consistent with the symmetry of the molecule (Fig. 3-1c) was first proposed by Zubarev and Boldyrev[27] and is not well-known among organic chemists, compared to those of resonance structures widely used in the literature (see Fig. 3-2). According to Zubarev and Boldyrev representation, in [6]circulene 96 valence electrons out of the total of 108 are participating in the localized bonding: 60 comprise thirty 2c-2e C-C σ-bonds, 21 comprise twelve 2c-2e C-H σ-bonds, and 12 comprise six 2c-2e C-C π-bonds. The rest 12 valence electrons participate in delocalized π-bonding. The $4n+2$ rule is applied to the two π-subsystems separately: six π-electrons are responsible for the bonding in the

internal six carbon atoms ($4n + 2 = 6$, $n = 1$), and the other six π-electrons are responsible for the bonding between peripheral C_{18} and the internal C_6 rings ($4n + 2 = 6$, $n = 1$). π bonding in B_{19}^- consists of two concentric π systems, analogous to [6]circulene, with two π-electrons delocalized over the central pentagonal unit and ten additional π electrons delocalized in a circle between the central B_6 unit and the outer B_{13} ring, reminiscent of the ten π electrons in the planar [10]annulene (Fig. 3-1b).

The experiment was performed using a magnetic-bottle photoelectron spectroscopy apparatus equipped with a laser vaporization source (see Methods).[28] Photoelectron spectra of B_{19}^- at two photon energies are shown in Fig. 3-3, compared with the calculated vertical detachment energies (VDEs). The 193 nm spectrum (Fig. 3-3b) shows five resolved bands. At 266 nm (Fig. 3-3a), the band at 4.5 eV was resolved into two sharp peaks (A and B). The ground state band (X) was observed to be fairly broad in the 266 nm spectrum, suggesting a possible geometry change between the anion and neutral ground state. The adiabatic detachment energy of B_{19}^- was estimated to be 4.2 ± 0.1 eV, which is very high. The VDEs of all the spectral features are given in Table 3-1 and compared to the theoretical VDEs (see METHODS) of the two lowest energy isomers of B_{19}^- (I and II).

We searched for the global minimum of B_{19}^- using two programs: a Coalescence Kick[29] program written by Boris Averkiev and a Basin Hopping Search[30] program written by Wei Huang, both at the B3LYP/3-21G level of theory initially. The Coalescence Kick method subjects large populations of randomly generated structures to a coalescence procedure with all atoms gradually pushed to the molecular center of mass to avoid generation of fragmented structures and then optimizes them to the nearest local minima.

Basin Hopping is an unbiased global minimum search method, in which potential energy transformation is combined with Monte Carlo sampling. All low-lying isomers found by both methods were reoptimized at the B3LYP/6-311+G* level of theory with additional further single-point calculations at the CCSD(T)/6-311+G* level of theory using the optimized geometry at the B3LYP/6-311+G* level. The three lowest energy structures together with a tubular one are summarized in Fig. 3-4. A more extensive set of alternative structures is given in Fig. 3-5).

We found that the global minimum of B_{19}^- (I in Fig. 3-4) is a planar spider-web-like structure with one boron atom at the center surrounded by five boron atoms in the first coordination sphere and thirteen boron atoms in the second coordination sphere. The geometric parameters presented in Fig. 3-6 suggest an almost perfect planar and circular structure for the global minimum of B_{19}^-. The distances from the central boron atom to the peripheral atoms vary from 3.01 to 3.28 Å with the maximum deviation from the average distance (3.20 Å) being 0.19 Å or 6%. The appearance of the nearly D_{5h} central B_6 unit (with a maximum of 0.02 Å deviation from the average radius of 1.63 Å) is also quite intriguing, reminiscent of bulk boron, which consists of B_{12} icosahedral cages with local C_{5v} symmetry.[31] This structure is of C_s symmetry ($^1A'$), but after vibrational averaging it is effectively of C_{2v} symmetry ($^1A_1$). The difference in total energies between the C_s and C_{2v} structures is smaller than the difference in zero-point energy corrections for these two structures with the zero-point energy for the C_s structure being slightly larger. Thus, after zero-point energy correction the C_{2v} effective structure is lower in energy.

There is only one low-lying isomer (II in Fig. 3-4), which is 1.75 kcal/mol higher in energy than the global minimum. The second low-lying isomer (III in Fig. 3-4) was found to be 7.23 kcal/mol above the global minimum. The tubular isomer (IV in Fig. 3-4), which was the global minimum for the B_{19}^+ cation,[32] was found to be a very high energy isomer of B_{19}^-.

The calculated VDEs of the global minimum are in excellent agreement with the experimental data, as can be seen in Fig. 3-1 and Table 3-1. The first VDE was calculated to be 4.37 eV compared to the experimental value of 4.34 eV. The next two detachment channels were calculated to be very close in energy, in an exact agreement with the A and B bands resolved in the 266 nm spectrum (Fig. 3-3a). The fourth and fifth detachment channels were also close in energy, corresponding to the C band, which is fairly broad and should contain two unresolved bands like the A/B bands (Fig. 3-3b). The next detachment channel from the global minimum occurs at 6.34 eV, in a good agreement with the observed band E at 6.37 eV. The global minimum B_{19}^- has no detachment channel between 5 and 6 eV. Thus, the D band at 5.8 eV cannot come from the global minimum isomer. However, the sixth detachment channel of isomer II with a calculated VDE of 5.67 eV is in a good agreement with band D, providing evidence that this isomer was populated in our experiment. The other detachment channels from isomer II can also be discerned from the experimental data, as can be seen in Fig. 3-3, though they were not well resolved. In particular, the first detachment channel of isomer II clearly contributed to the lower energy tail of band X. Overall, the agreement between the theoretical and experimental data is excellent, providing considerable credence for the identified global minimum of B_{19}^- and its low-lying isomer.

Molecular orbital analyses show that there are 12 π-electrons in isomer I of B_{19}^- occupying 6 π canonical molecular orbitals (CMOs) of two types, as illustrated in Fig. 3-7. We found five CMOs contributing to the bonding between the inner pentagonal ring and the outer B_{13} ring, namely, HOMO-1, HOMO-2, HOMO-5, HOMO-7, and the sum of HOMO with HOMO-15 that results in a CMO delocalized over the peripheral atoms with no electron density over the pentagonal B_6 unit. The remaining π bond derived from the difference between HOMO and HOMO-15 that gives rise to a CMO with electron density over the pentagonal boron B_6 unit and only contributes to the bonding in the inner B_6 unit. The two types of π bonds can be better interpreted by applying the recently developed Adaptive Natural Density Partitioning Analysis (AdNDP),[33] as shown in Fig. 3-8. The AdNDP analysis is based on the concept of electron pairs as the main elements of chemical bonding. It represents the electronic structure in terms of *n*-center–two-electron (*n*c-2e) bonds. With *n* ranging from one to the total number of atoms in the whole cluster, AdNDP recovers both Lewis bonding elements (1c-2e or 2c-2e objects, i.e., lone pairs or two-center two-electron bonds) and delocalized bonding elements, which are associated with the concepts of aromaticity. Both CMO and AdNDP analyses reveal that the chemical bonding in the B_{19}^- cluster consist of two concentric π aromatic systems: a 10 π-electron system describing the bonding between the inner and outer rings and a 2 π-electrons system delocalized over the central B_6 unit, each satisfying the $4n$+2 Hückel rule independently. The 10 π-electron sub-system is similar to the π-system in the planar aromatic [10]annulene (Fig. 3-1a). The aromaticity of the circular B_{19}^- is also confirmed by NICS analyses,[34] bond equalization in the outer and inner B_{13} and B_5 rings, as well as its high VDE of 4.34 eV. In Table 3-2, we compared the $NICS_{zz}$ values of the

circular B_{19}^- with those of benzene and the planar aromatic [10]annulene. The magnitudes of the negative $NICS_{zz}$ values of B_{19}^- (Table 3-2) clearly show that the circular B_{19}^- cluster is a π-aromatic system.

The concentric aromatic π systems of the circular B_{19}^- are reminiscent of the π bonding in circulenes.[35] Circulenes are cyclic aromatic hydrocarbon compounds and they can be viewed as fused benzene rings, among which [6]circulene or coronene (Fig. 3-1c), consisting of six benzene rings, is a perfect planar D_{6h} molecule. The chemical bonding of coronene was recently analyzed,[36] showing that its π-bonding consists of three parts: 1) six C-C peripheral π-bonds, 2) three π-bonds delocalized over the central C_6 ring, and 3) three delocalized π-bonds responsible for the bonding between the inner C_6 ring and the outer C_{18} ring. The difference between coronene and B_{19}^- is that the former has six π-electrons delocalized over the central part of the molecule and six π-electrons responsible for the bonding between the inner and outer rings, while B_{19}^- has only two electrons delocalized over its inner six boron atoms and ten π-electrons responsible for the bonding between the inner and outer rings. Thus, although there is similarity between the π bonding of the B_{19}^- cluster and coronene, the π-bonding pattern in the boron cluster is unique and does not have an exact counterpart in hydrocarbons.

Interestingly, our structure and bonding analyses showed that the low-lying isomer II of B_{19}^- (Fig. 3-9) is also doubly π aromatic with two similar concentric π systems (Fig. 3-10 and Fig. 3-11) as isomer I, even though isomer II is much less circular. The key structural difference between the two isomers is the arrangement of the central B_6 unit. In isomer I, the B_6 unit is pentagonal with near D_{5h} symmetry resulting in its near circular structure, whereas in isomer II the B_6 unit forms a triangle giving rise to the overall

triangular shape of this isomer. It is conceivable that the less delocalized π bonding in isomer II makes it slightly less stable.

In reality, [10]annulene is not a planar species. Our AdNDP analysis for a *planar* [10]annulene (Fig. 3-12) revealed ten 2c-2e C-C σ-bonds, ten 2c-2e C-H σ-bonds and five 10c-2e delocalized π-bonds that look exactly the same as the canonical π molecular orbitals in B_{19}^-, if the π-orbital on the inner B_6 unit is ignored (Fig. 3-7). However, the unfavourable C-C-C bond angles (144 degrees instead of the ideal 120 degrees for sp^2 hybridization) cause substantial strain energies in [10]annulene (Fig. 3-1a). Apparently, these strain energies outweigh the stabilizing resonance energy derived from π-aromaticity, leading to the out-of-plane distortions in the cyclic $C_{10}H_{10}$ molecule. Thus, boron clusters may provide even more opportunities or flexibilities than the hydrocarbons to design planar aromatic species.

The concentric π aromatic systems in the global minimum of B_{19}^- can give rise to ring currents either in the same direction or opposite to each other, which would be interesting to investigate. The current finding suggests even more interesting structures and chemical bonding may be discovered in more complex cluster systems that will expand established chemical concepts and may find applications in nanotechnology. In particular, there exists the possibility of designing doubly aromatic hetero-clusters by replacing the central B_6 unit in the global minimum of B_{19}^-, for example, by transition metals, which may give rise to concentric δ-aromatic and π-aromatic systems. Such modifications may lead to novel boron-based nano-systems with tunable electronic, optical, and magnetic properties.

3-1. Methods

3-1.1. Experiment

The B_{19}^- cluster was produced by laser vaporization of a ^{10}B-enriched disk target with a helium carrier and was mass-selected using time-of-flight mass spectrometry. Photoelectron spectra were obtained using a magnetic-bottle electron analyzer at two photon energies and calibrated by the known spectra of Au^-. The resolution of our photoelectron apparatus was $\Delta E/E \sim 2.5\%$, i.e., ~25 meV for 1 eV electrons.[28]

3-1.2. Theory

The VDEs of B_{19}^- were calculated using the time-dependent hybrid density functional method (TD-B3LYP) utilizing 6-311+G(2df) basis set at the optimized B3LYP/6-311+G* geometry. In this approach, the first VDE was calculated at the B3LYP level as the lowest transition from the singlet state of the singly charged anion (B_{19}^-) into the final lowest doublet state of the neutral species (B_{19}) at the optimized geometry of the singly charged anion (B_{19}^-). Then the vertical excitation energies in the corresponding neutral species (at the TD-B3LYP level) were added to the lowest VDE in order to get the second and higher VDEs. All calculations were performed using the Gaussian 03 software package.[36] Molecular orbital visualization is done utilizing Molekel 4.3 program.[37]

References

1. Minkin, V.I., Glukhovtsev, M.N. & Simkin, B.Y. *Aromaticity and Antiaromaticity* (Wiley, 1994).

2. Schleyer, P.v.R. (ed.) Special edition on delocalization pi and sigma. *Chem. Rev.* **105**, No. 10 (2005).

3. Schleyer, P.v.R. (ed.) Special edition on aromaticity. *Chem. Rev.* **101**, No. 5 (2001).

4. Masamune, S., Hojo, K., Hojo Kiyomi, Bigam, G. & Rabenstein, D.L. Geometry of [10]annulenes. *J. Am. Chem. Soc.* **93**, 4966-4968 (1971).

5. Masamune, S. & Darby, N. [10]Annulenes and other $(CH)_{10}$ hydrocarbons. *Acc. Chem. Res.* **5**, 272-281 (1972).

6. King, R.A., Crawford, T.D., Stanton, J.F. & Schaefer, H.F. III. Conformations of [10]Annulene: more bad news for density functional theory and second-order perturbation theory. *J. Am. Chem. Soc.* **121**, 10788-10793 (1999).

7. Price, D.R. & Stanton, J.F. Computational study of [10]Annulene NMR spectra. *Org. Lett.* **4**, 2809-2811 (2002).

8. Li, X., Kuznetsov, A.E., Zhang, H.F., Boldyrev, A.I. & Wang, L.S. Observation of all-metal aromatic molecules. *Science* **291**, 859-861 (2001).

9. Zhai, H.J., Alexandrova, A.N., Birch, K.A., Boldyrev, A.I. & Wang, L.S. Hepta- and octacoordinate boron in molecular wheels of eight- and nine-atom boron clusters: observation and confirmation. *Angew. Chem. Int. Ed.* **42**, 6004-6008 (2003).

10. Zhai, H.J., Kiran, B., Li, J. & Wang, L.S. Hydrocarbon analogues of boron clusters — planarity, aromaticity and antiaromaticity. *Nature Materials* **2**, 827-833 (2003).

11. Alexandrova, A.N., Boldyrev, A.I., Zhai, H.J. & Wang, L.S. All-boron aromatic clusters as potential new inorganic ligands and building blocks in chemistry. *Coord. Chem. Rev.* **250**, 2811-2866 (2006).

12. Zubarev, D.Y. & Boldyrev, A.I. Comprehensive analysis of chemical bonding in boron clusters. *J. Comput. Chem.* **28**, 251-268 (2007).

13. Fowler, J.E. & Ugalde, J.M. The curiously stable B_{13}^{+} cluster and its neutral and anionic counterparts: the advantages of planarity. *J. Phys. Chem. A* **104**, 397-403 (2000).

14. Mercero, J.M. & Ugalde, J.M. Sandwich-like complexes based on "all-metal" (Al_4^{2-}) aromatic compounds. *J. Am. Chem. Soc*. **126**, 3380-3381 (2004).

15. Aihara, J. B_{13}^{+} is highly aromatic. *J. Phys. Chem. A* **105**, 5486-5489 (2001).

16. Fowler, P.W. & Gray, B.R. Induced currents and electron counting in aromatic boron wheels: B_8^{2-} and B_9^{-}. *Inorg. Chem.* **46**, 2892-2897 (2007).

17. Hanley, L. & Anderson, S.L. Production and collision-induced dissociation of small boron cluster ions. *J. Phys. Chem*. **91**, 5161-5163 (1987).

18. Hanley, L., Whitten, J.L. & Anderson, S.L. Collision-induced dissociation and ab initio studies of boron cluster ions: determination of structures and stabilities. *J. Phys. Chem*. **92**, 5803-5812 (1988).

19. Hintz, P.A., Ruatta, S.A. & Anderson, S.L. Interaction of boron cluster ions with water: single collision dynamics and sequential etching. *J. Chem. Phys*. **92**, 292-303 (1990).

20. Hintz, P.A., Sowa, M.B., Ruatta, S.A. & Anderson, S.L. Reactions of boron cluster ions (B_n^{+} n=2–24) with N_2O: NO versus NN bond activation as a function of size *J. Chem. Phys*. **94**, 6446-6458 (1991).

21. Sowa-Resat, M.B., Smolanoff, J., Lapiki, A. & Anderson, S.L. Interaction of small boron cluster ions with HF. *J. Chem. Phys*. **106**, 9511-9522 (1997).

22. Zhai, H.J., Wang, L.S., Alexandrova, A.N. & Boldyrev, A.I. Electronic structure and chemical bonding of B_5^- and B_5 by photoelectron spectroscopy and ab initio calculations. *J. Chem. Phys*. **117**, 7917-7924 (2002).

23. Alexandrova, A.N. *et al*. Structure and bonding in B_6^- and B_6: planarity and antiaromaticity. *J. Phys. Chem*. A **107**, 1359-1369 (2003).

24. Zhai, H.J., Wang, L.S., Alexandrova, A.N., Boldyrev, A.I. & Zakrzewski, V.G. Photoelectron spectroscopy and ab initio study of B_3^- and B_4^- anions and their neutrals. *J. Phys. Chem. A* **107**, 9319-9328 (2003).

25. Kiran, B. *et al*. Planar-to-tubular structural transition in boron clusters: B_{20} as the embryo of single-walled boron nanotubes. *Proc. Natl. Acad. Sci. USA* **102**, 961-964 (2005).

26. Sergeeva, A.P., Zubarev, D.Y., Zhai, H.J., Boldyrev, A.I. & Wang, L.S. A photoelectron spectroscopic and theoretical study of B_{16}^- and B_{16}^{2-}: an all-boron naphthalene. *J. Am. Chem. Soc.* **130**, 7244-7246 (2008).

27. Zubarev, D.Y. & Boldyrev, A.I. Revealing intuitively assessable chemical bonding patterns in organic aromatic molecules via Adaptive Natural Density Partitioning. *J. Org. Chem.* **73**, 9251-9258 (2008).

28. Wang, L.S., Cheng, H.S. & Fan, J. Photoelectron spectroscopy of size-selected transition metal clusters: Fe_n^-, n=3–24. *J. Chem. Phys*. **102**, 9480-9493 (1995).

29. Saunders, M. Stochastic search for isomers on a quantum mechanical surface. *J. Comput. Chem*. **25**, 621-626 (2004).

30. Wales, D.J. & Doye, J.P.K. Global optimization by basin-hopping and the lowest energy structures of Lennard-Jones clusters containing up to 110 atoms. *J. Phys. Chem. A* **101**, 5111-5116 (1997).

31. Fujimori, M. *et al*. Peculiar covalent bonds in α-rhombohedral boron. *Phys. Rev. Lett.* **82**, 4452-4455 (1999).

32. Oger, E. *et al*. Boron cluster cations: transition from planar to cylindrical structures. *Angew. Chem. Int. Ed*. **46**, 8503-8506 (2007).

33. Zubarev, D.Y. & Boldyrev, A.I. Developing paradigms of chemical bonding: adaptive natural density partitioning. *Phys. Chem. Chem. Phys*. **10**, 5207-5217 (2008).

34. Schleyer, P.v.R., Maerker, C., Dransfeld, A., Jiao, H.J. & Hommes, N.J.R.V. Nucleus-independent chemical shifts: a simple and efficient aromaticity probe. *J. Am. Chem. Soc*. **118**, 6317-6318 (1996).

35. Clar, E. *The Aromatic Sextet*. J. Wiley & Sons, London (1972).

36. Frisch, M. J. *et al.* The Gaussian 03 program (revision D.01) (Gaussian, 2003).

37. Portmann, S. Molekel, Version 4.3., (Swiss National Supercomputing Centre/Swiss Fedral Institute of Technology Zurich, 2002).

Table 3-1 | Comparison of the Experimental VDEs (VDE^{exp}) with the Calculated Values (VDE^{theo}) for Isomers I and II of B_{19}^- (eV).

Feature	VDE^{exp}	Final state and electronic configuration	VDE^{theo} TD-B3LYP
Isomer I			
X	4.34 ± 0.05	$^2B_1$, $\{...1a_2^{(2)}13a_1^{(2)}10b_2^{(2)}3b_1^{(2)}2a_2^{(2)}4b_1^{(1)}\}$	4.37
A	4.48 ± 0.02	$^2A_2$, $\{...1a_2^{(2)}13a_1^{(2)}10b_2^{(2)}3b_1^{(2)}2a_2^{(1)}4b_1^{(2)}\}$	4.48
B	4.52 ± 0.02	$^2B_1$, $\{...1a_2^{(2)}13a_1^{(2)}10b_2^{(2)}3b_1^{(1)}2a_2^{(2)}4b_1^{(2)}\}$	4.51
C	~5.0	$^2B_2$, $\{...1a_2^{(2)}13a_1^{(2)}10b_2^{(1)}3b_1^{(2)}2a_2^{(2)}4b_1^{(2)}\}$	4.88
		$^2A_1$, $\{...1a_2^{(2)}13a_1^{(1)}10b_2^{(2)}3b_1^{(2)}2a_2^{(2)}4b_1^{(2)}\}$	4.97
E	6.37 ± 0.04	$^2A_2$, $\{...1a_2^{(1)}13a_1^{(2)}10b_2^{(2)}3b_1^{(2)}2a_2^{(2)}4b_1^{(2)}\}$	6.34
Isomer II			
Tail	~4.1	$^2B_1$, $\{...12a_1^{(2)}9b_2^{(2)}10b_2^{(2)}3b_1^{(2)}\ 2a_2^{(2)}13a_1^{(2)}4b_1^{(1)}\}$	4.19
		$^2A_1$, $\{...12a_1^{(2)}9b_2^{(2)}10b_2^{(2)}3b_1^{(2)}\ 2a_2^{(2)}13a_1^{(1)}4b_1^{(2)}\}$	4.40
		$^2A_2$, $\{...12a_1^{(2)}9b_2^{(2)}10b_2^{(2)}3b_1^{(2)}\ 2a_2^{(1)}13a_1^{(2)}4b_1^{(2)}\}$	4.41
		$^2B_1$, $\{...12a_1^{(2)}9b_2^{(2)}10b_2^{(2)}3b_1^{(1)}\ 2a_2^{(2)}13a_1^{(2)}4b_1^{(2)}\}$	4.64
		$^2B_2$, $\{...12a_1^{(2)}9b_2^{(2)}10b_2^{(1)}3b_1^{(2)}\ 2a_2^{(2)}13a_1^{(2)}4b_1^{(2)}\}$	5.42
D	5.8 ± 0.1	$^2B_2$, $\{...12a_1^{(2)}9b_2^{(1)}10b_2^{(2)}3b_1^{(2)}\ 2a_2^{(2)}13a_1^{(2)}4b_1^{(2)}\}$	5.67
		$^2A_1$, $\{...12a_1^{(1)}9b_2^{(2)}10b_2^{(2)}3b_1^{(2)}\ 2a_2^{(2)}13a_1^{(2)}4b_1^{(2)}\}$	6.36

Table 3-2 | $NICS_{zz}$ values of B_{19}^- cluster at the B3LYP/6-311+G* level of theory compared to that of benzene (C_6H_6) and [10]annulene ($C_{10}H_{10}$), both at the B3LYP/6-311++G level of theory.**

Distance above the centre of the molecule, Å	Benzene C_6H_6	[10]annulene $C_{10}H_{10}$	Isomer I of B_{19}^-
	$NICS_{zz}$, ppm	$NICS_{zz}$, ppm	$NICS_{zz}$, ppm
0.0	-14.49	-38.80	-
0.2	-16.26	-38.82	-101.30
0.4	-20.57	-38.80	-83.95
0.6	-25.21	-38.61	-85.28
0.8	-28.33	-38.06	-84.17
1.0	-29.25	-37.04	-79.98

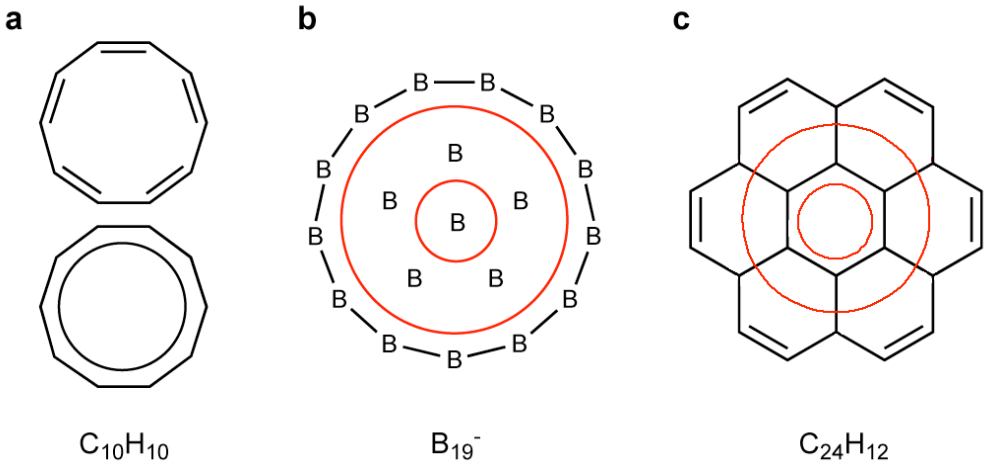

Figure 3-1 | Comparison of structure and chemical bonding of B_{19}^- with two hydrocarbon molecules. a-c, All the schemes show localized 2c-2e σ- and π-bonds (C-C s-bonds, B-B s-bonds, C-C p-bonds being represented as single lines with C-H s-bonds omitted) and delocalized π-bonds (represented as circles). (a) top scheme: the non-planar [10]annulene ($C_{10}H_{10}$), as it exits, features localized bonding only (classic molecule, non-aromatic); bottom scheme: the model planar [10]annulene ($C_{10}H_{10}$) has a circular structure with 10 π-electrons delocalized over the peripheral ring of carbon atoms ($4n$+2=10, n=2, π-aromatic). (b) B_{19}^- consists of two concentric π-systems with 2 π-electrons delocalized over the central pentagonal B_6 unit (4n+2=2, n=0, π-aromatic) and 10 additional π electrons delocalized in a circle between the central B_6 unit and the outer B_{13} ring (4n+2=10, n=2, π-aromatic), as well as 13 peripheral B-B σ-bonds. Six central boron atoms do not participate in the localized σ-bonding, but rather in delocalized σ-bonding. (c) [6]circulene, or coronene ($C_{24}H_{12}$), is composed of six benzene rings with π-bonding consisting of three parts: 1) six localized 2c-2e C-C peripheral π-bonds, 2) six π-electrons delocalized over the central C_6 ring (4n+2=6, n=1, π-aromatic), and 3) six delocalized π-electrons responsible for the bonding between the inner C_6 ring and the outer C_{18} ring (4n+2=6, n=1, π-aromatic).

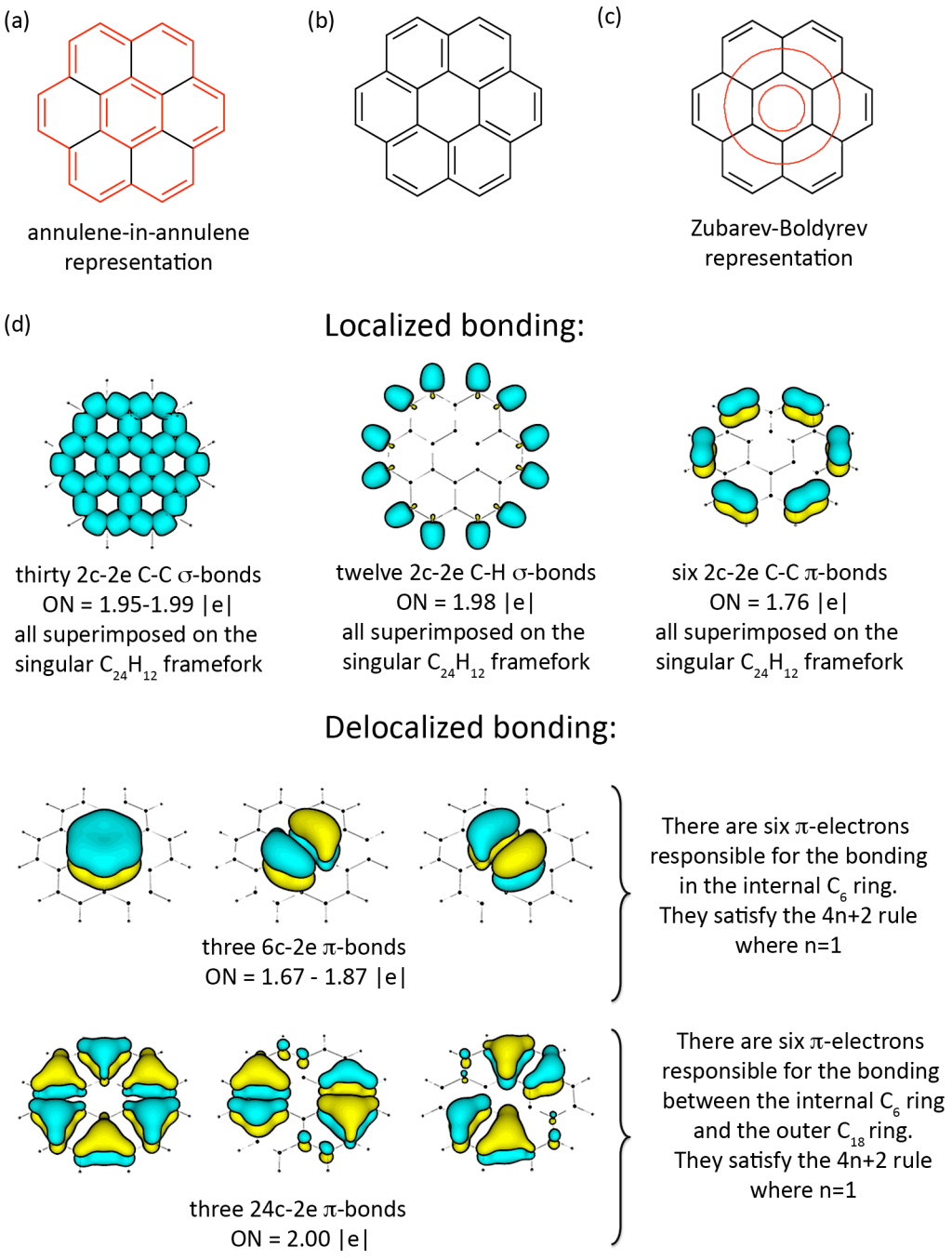

Figure 3-2 | Chemical bonding of $C_{24}H_{12}$ (coronene, [6]circulene). a, b, are the two most accepted Kekule representations of coronene among organic chemists with both representations being resonance structures; **c,** Zubarev-Boldyrev representation according to the results obtained by the AdNDP, which avoids resonance description and is consistent with the point group symmetry of the molecule (D_{6h}); **d,** Adaptive Natural Density Partitioning (AdNDP) Analysis of $C_{24}H_{12}$ (coronene or [6]circulene) at B3LYP/3-21G.

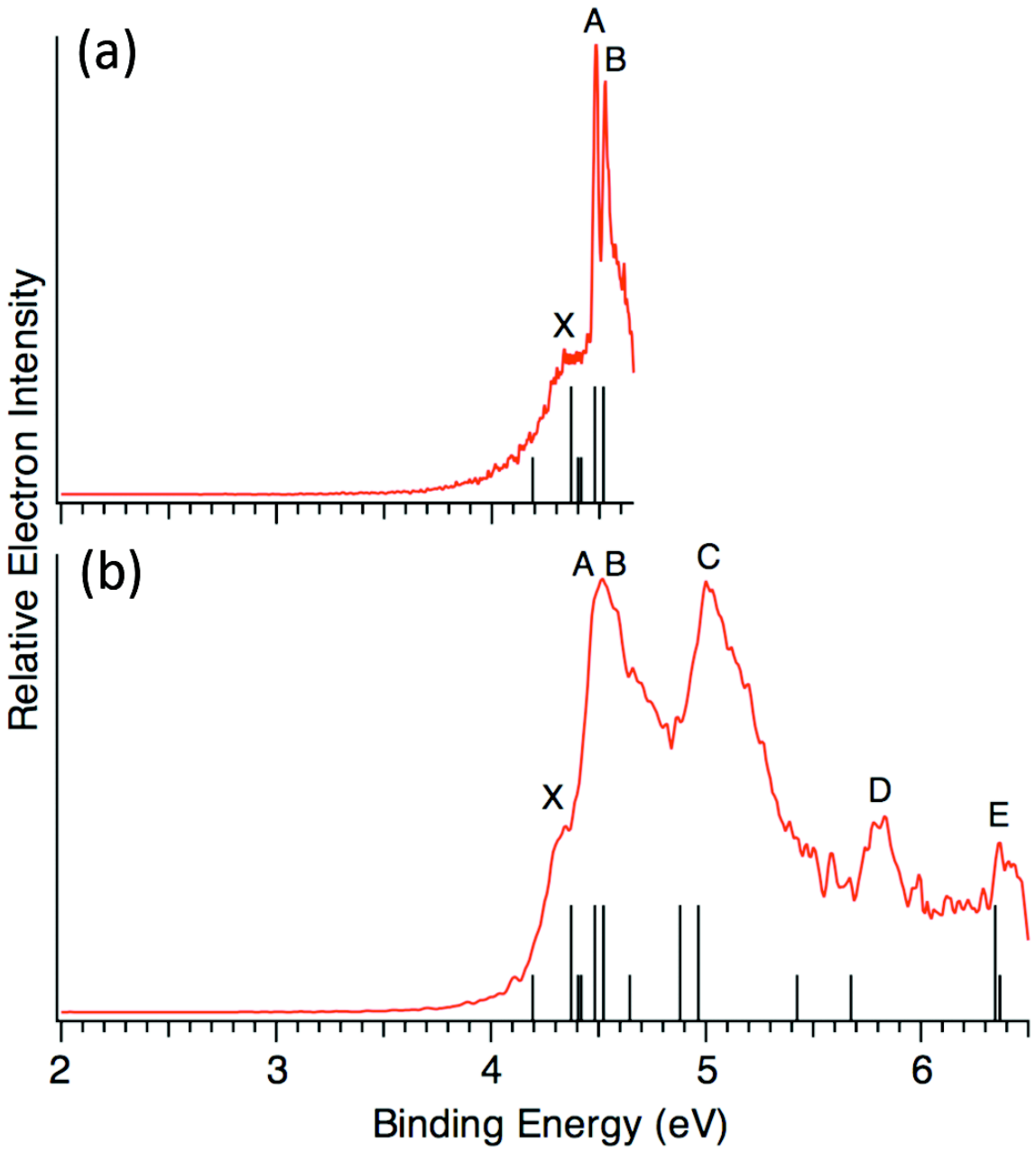

Figure 3-3 | Photoelectron spectra of B_{19}^-. a,b, (a) At 266 nm (4.661 eV). (b) At 193 nm (6.424 eV). The calculated vertical electron detachment energies for two isomers of B_{19}^- are represented as the vertical bars. The long bars correspond to the vertical detachment energies calculated for the global minimum isomer I and the short bars - for the low-lying isomer II.

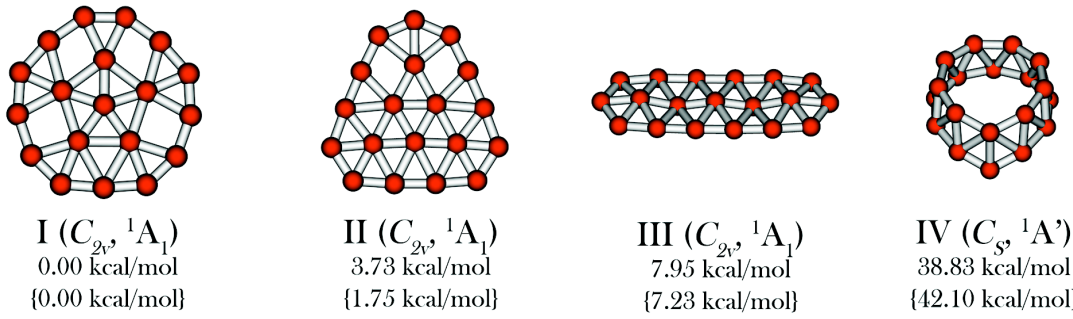

Figure 3-4 | Four representative optimized isomers of B_{19}^-. The relative energies are given at B3LYP/6-311+G* and at CCSD(T)/6-311+G* at the optimized B3LYP/6-311+G* geometry in squiggle brackets, both corrected for zero-point energies at B3LYP/6-311+G*.

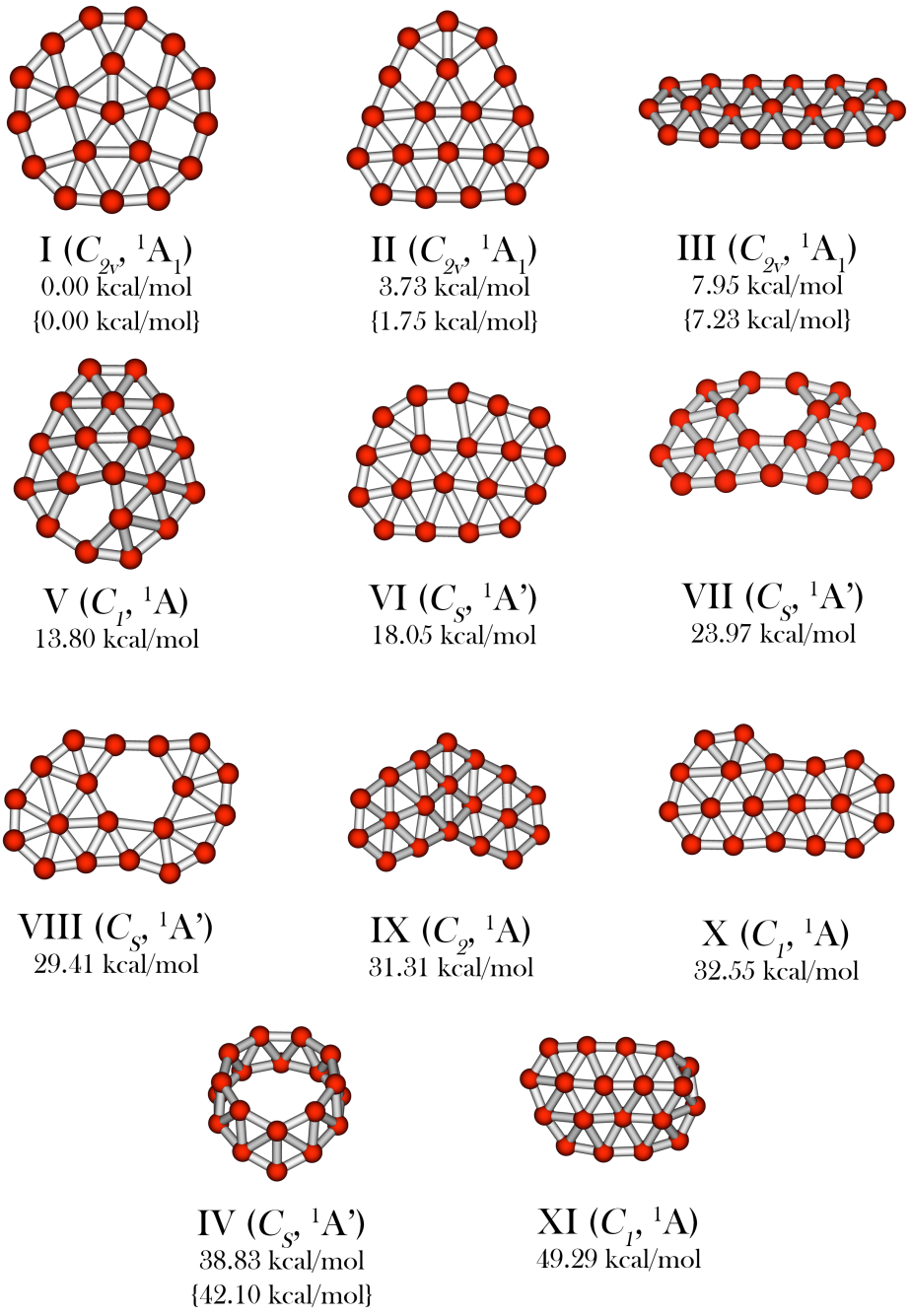

Figure 3-5 | Optimized isomers of B_{19}^- cluster and their relative energies: at B3LYP/6-311+G* and at CCSD(T)/6-311+G* at the optimized B3LYP/6-311+G* geometry {squiggle brackets} both corrected for zero-point energy at B3LYP/6-311+G*.

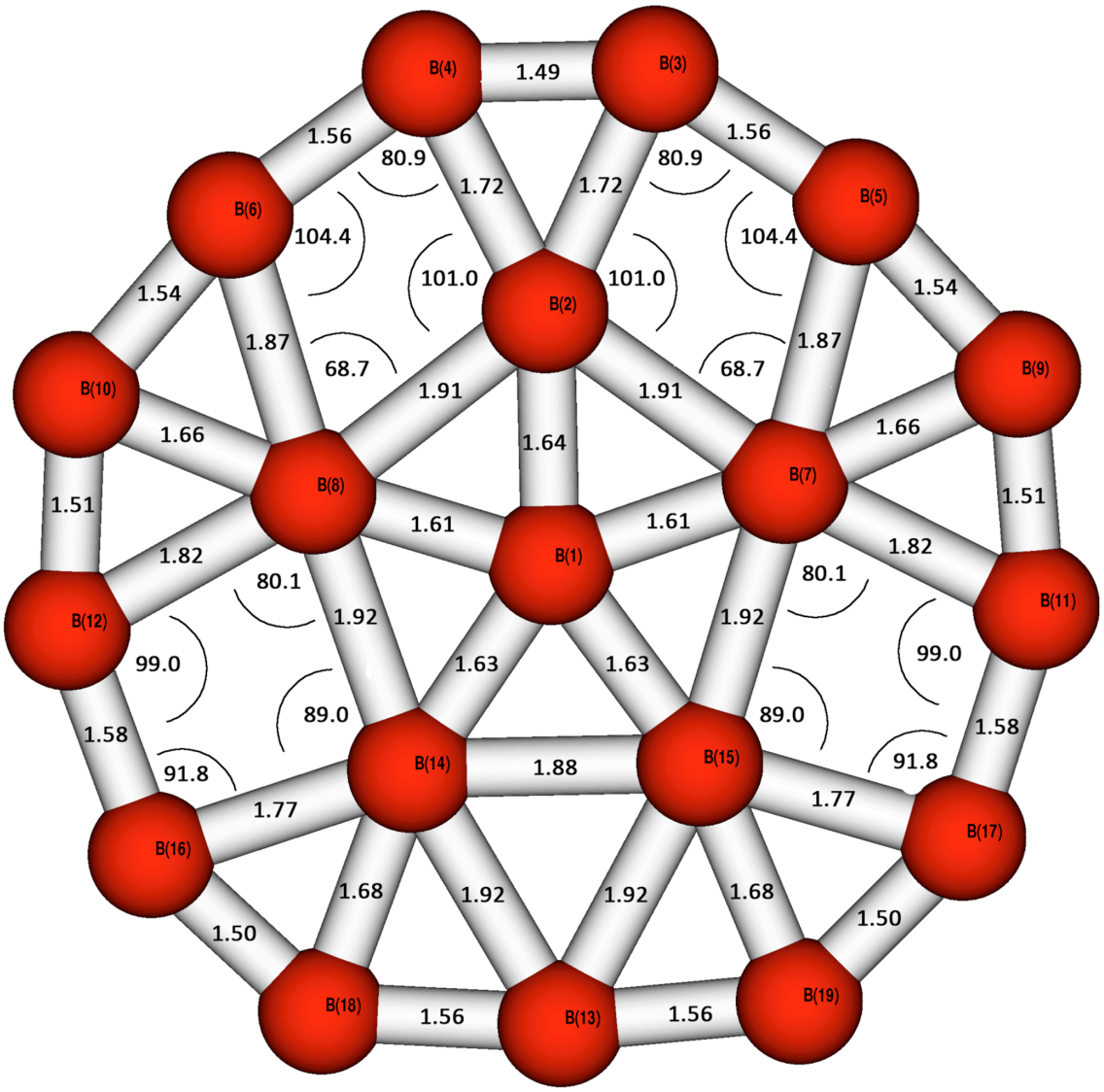

Distances		Angles	
(center – inner B_5 ring)	*(center – outer B_{13} ring)*	*(center – inner B_5 ring)*	*(center – outer B_{13} ring)*
B1-B2 = 1.64 Å B1-B7 = B1-B8 = 1.61 Å B1-B14 = B1-B15 = 1.63 Å	B1-B3 = B1-B4 = 3.28 Å B1-B5 = B1-B6 = 3.07 Å B1-B9 = B1-B10 = 3.27 Å B1-B11 = B1-B12 = 3.17 Å B1-B17 = B1-B16 = 3.22 Å B1-B18 = B1-B19 = 3.28 Å B1-B13 = 3.01 Å	∠B2B1B7 = ∠B2B1B8 = 72.2° ∠B7B1B15 = ∠B8B1B14 = 72.6° ∠B15B1B14 = 70.5°	∠B4B1B3 = 26.4° ∠B3B1B5 = ∠B6B1B4 = 28.3° ∠B5B1B9 = ∠B6B1B10 = 27.9° ∠B9B1B11 = ∠B10B1B12 = 27.2° ∠B11B1B17 = ∠B12B1B16 = 28.6° ∠B17B1B19 = ∠B16B1B18 = 26.7° ∠B19B1B13 = ∠B18B1B13 = 28.2°
B-B(aver)=1.63 Å r_{inner} = 1.61 – 1.64 Å	B-B(aver)= 3.20 Å r_{outer} = 3.01 – 3.28 Å	α_{inner}= 70.5° - 72.6° α_{ideal}= 360°/5= 72.0°	α_{outer}= 26.4° – 28.6° α_{ideal}= 360°/13 ≅ 27.7°

Figure 3-6 | Optimized geometry of isomer I of B_{19}^- (C_{2v}, $^1A_1$) cluster at the B3LYP/6-311+G* level of theory.

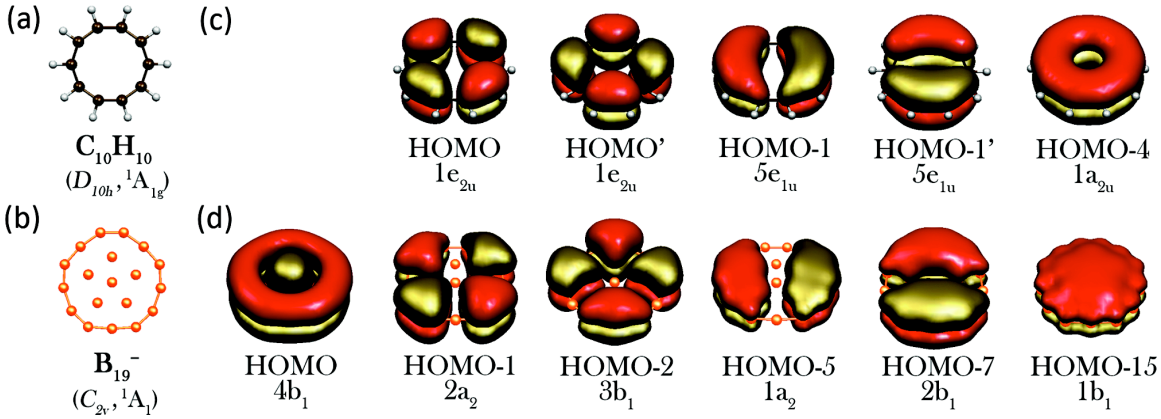

Figure 3-7 | Comparison of the structures and canonical molecular orbitals between [10]annulene ($C_{10}H_{10}$) and the global minimum of B_{19}^-. a-d, The similarity of the π-system of the planar aromatic [10]annulene (a) to the ten π-electron sub-system of B_{19}^- (b) is illustrated. **c,** The canonical molecular orbitals, HOMO-1, HOMO-2, HOMO-5, HOMO-7, and the sum of HOMO with HOMO-15, of the global minimum of B_{19}^- contribute to the bonding between the inner pentagonal B_6 ring and the outer B_{13} ring, which results in an orbital delocalized over the peripheral atoms with no electron density over the pentagonal B_6 unit, reminiscent of those of [10]annulene (HOMO, HOMO', HOMO-1, HOMO-1', and HOMO-4, respectively) shown in (c).

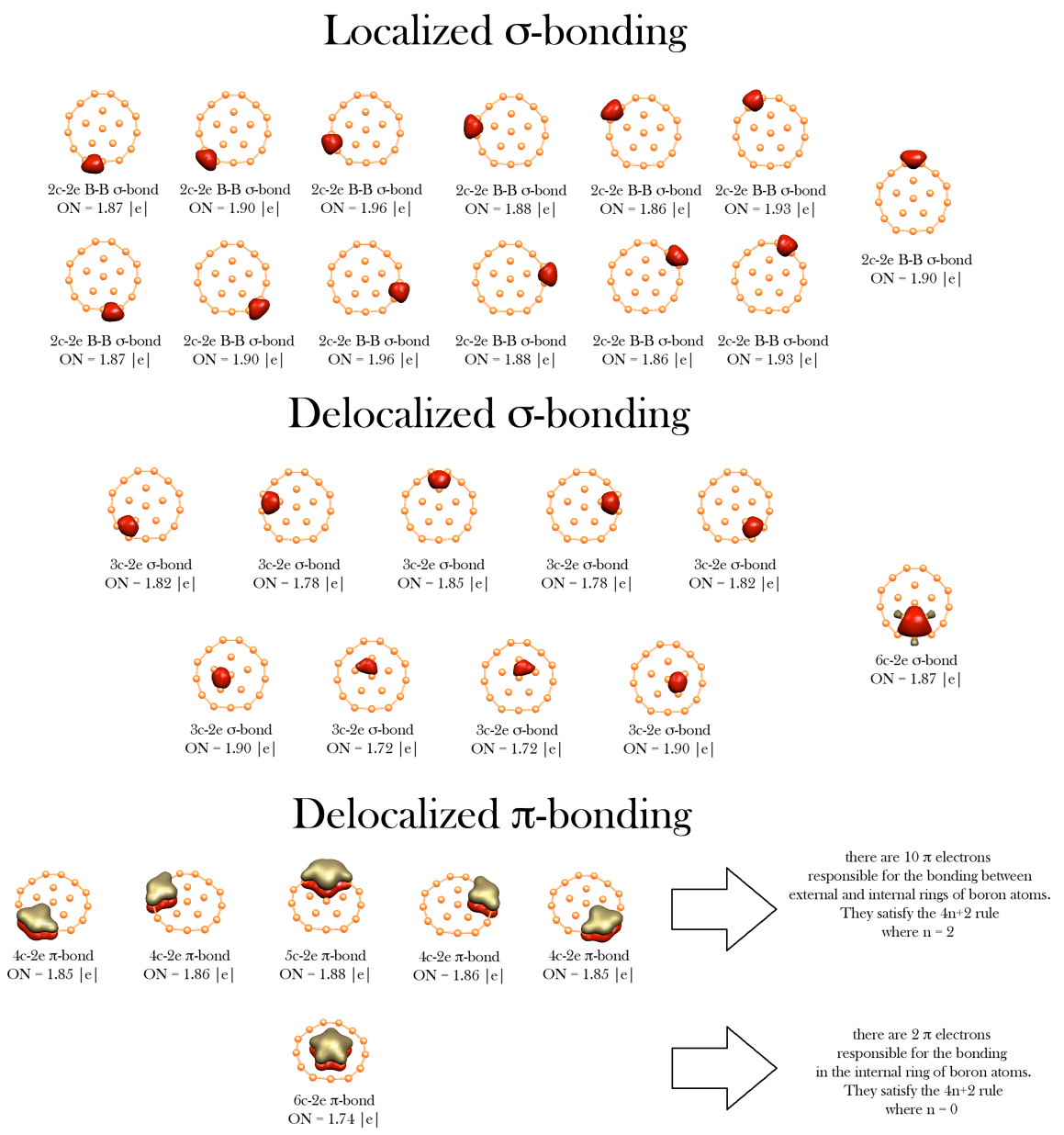

Figure 3-8 | Adaptive Natural Density Partitioning (AdNDP) Analysis of the isomer I of B_{19}^- (C_{2v}, $^1A_1$) cluster at B3LYP/3-21G.

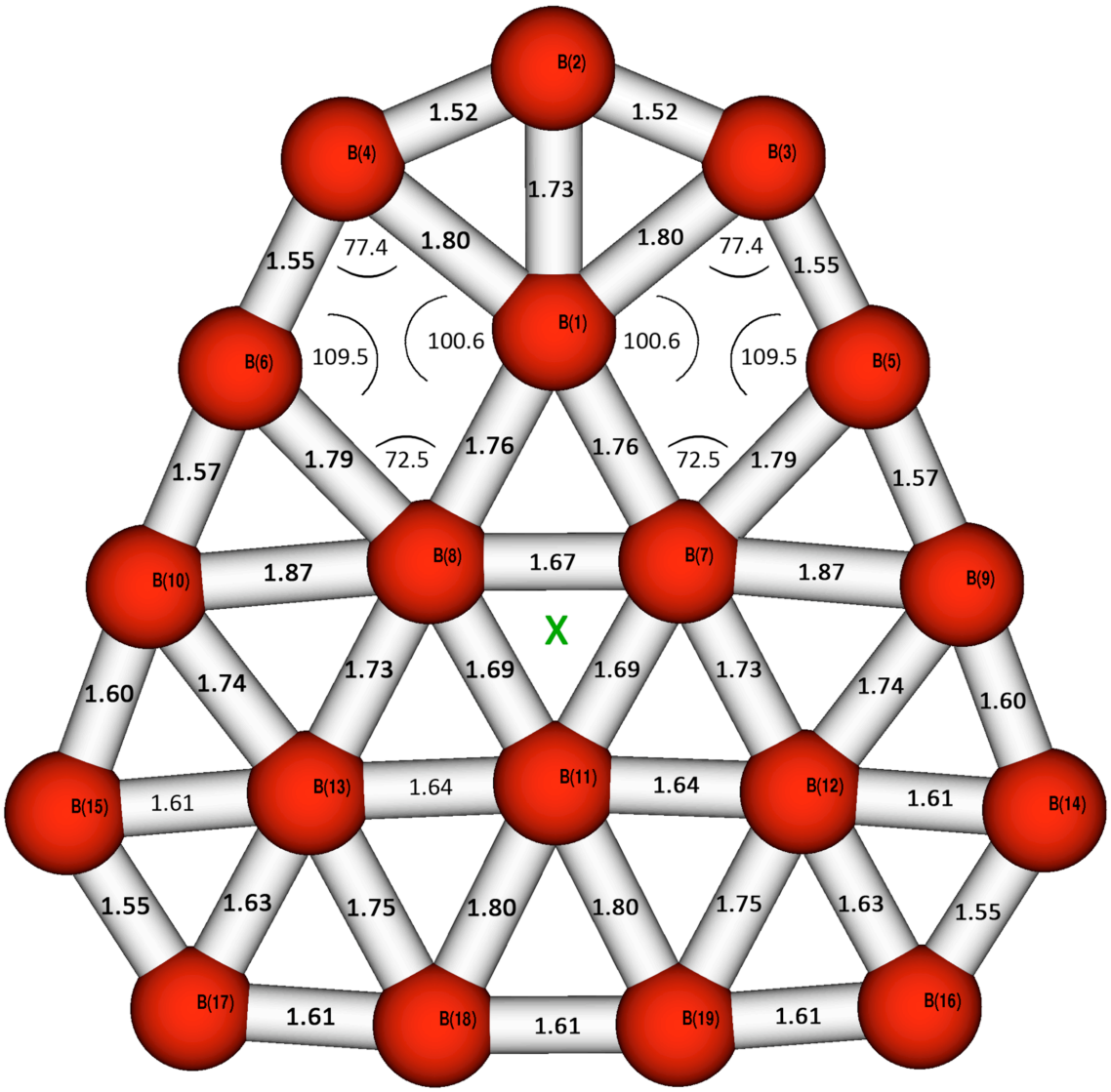

Distances		Angles	
(center – inner B_6 fragment)	*(center – outer B_{13} fragment)*	*(center – inner B_6 fragment)*	*(center – outer B_{13} fragment)*
X-B1 = 2.04 Å X-B7 = X-B8 = 0.97 Å X-B11 = 0.98 Å X-B12 = X-B13 = 1.94 Å	X-B2 = 3.76 Å X-B3 = X-B4 = 3.46 Å X-B5 = X-B6 = 2.74 Å X-B9 = X-B10 = 2.73 Å X-B14 = X-B15 = 3.45 Å	∠B1XB7 = ∠B1XB8 = 59.5° ∠B7XB12 = ∠B8XB13 = 62.8° ∠B12XB11 = ∠B13XB11 = 57.4°	∠B2XB3 = ∠B2XB4 = 23.8° ∠B3XB5 = ∠B4XB6 = 25.7° ∠B5XB9 = ∠B6XB10 = 33.4° ∠B9XB14 = ∠B10XB15 = 26.8° ∠B14XB16 = ∠B15XB17 = 25.9° ∠B16XB19 = ∠B17XB19 = 26.9° ∠B19XB18 = 34.7°
X-B(aver) = 1.47 Å r_{inner} = 0.97 – 2.04 Å	X-B(aver) = 3.17 Å r_{outer} = 2.73 – 3.76 Å	α_{inner}= 70.5° - 72.6° α_{ideal}= 360°/5= 72.0°	α_{outer}= 23.8° – 33.4° α_{ideal}= 360°/13 ≅ 27.7°

Figure 3-9 | Optimized geometry of isomer II of B_{19}^- (C_{2v}, $^1A_1$) cluster at the B3LYP/6-311+G* level of theory.

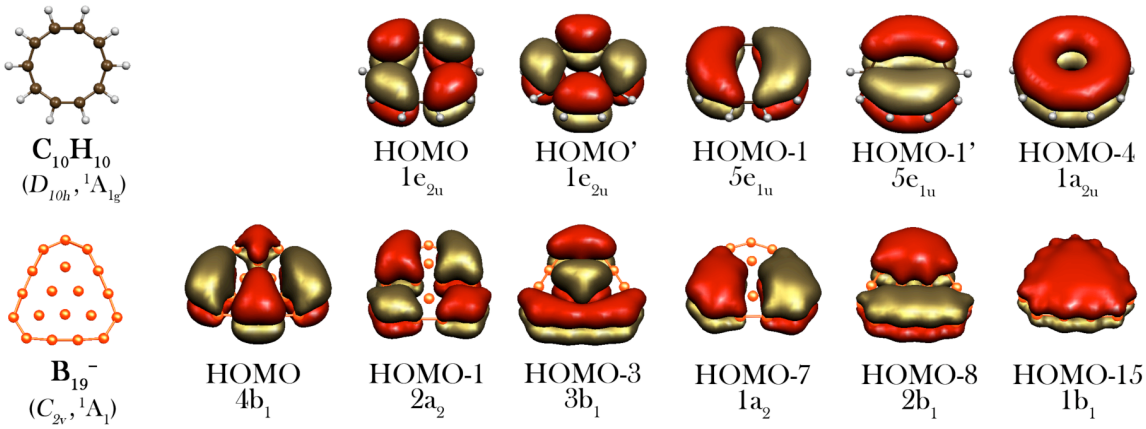

Similarity of CMOs

B_{19}^- (Isomer II)	$C_{10}H_{10}$
HOMO	HOMO'
HOMO-1	HOMO
sum of HOMO-3 and HOMO-15	HOMO-4
HOMO-7	HOMO-1
HOMO-8	HOMO-1'
difference of HOMO-3 and HOMO-15 (responsible for the bonding in the central triangle of boron atoms)	-

Figure 3-10 | Comparison between CMOs of [10]annulene and those of isomer II of B_{19}^-.

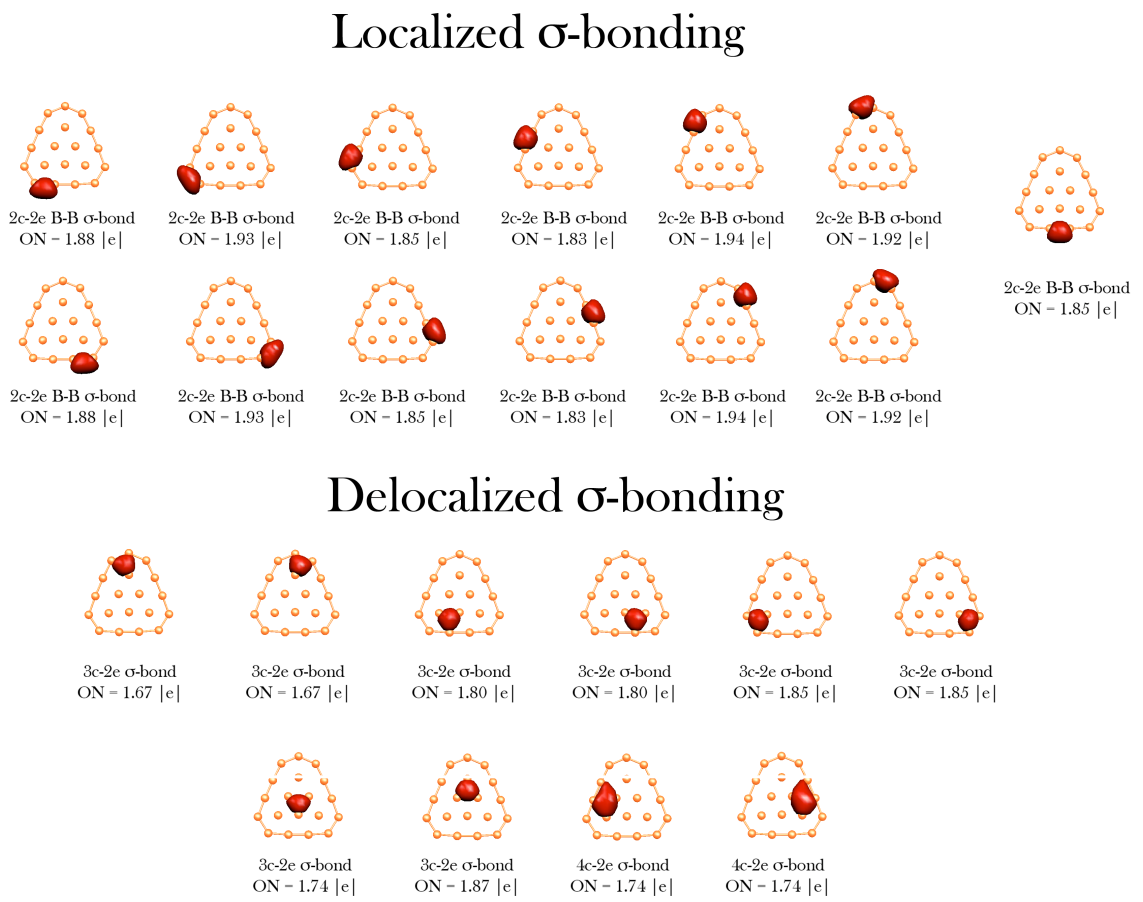

Figure 3-11 | Adaptive Natural Density Partitioning (AdNDP) Analysis of the isomer II of B_{19}^- (C_{2v}, $^1A_1$) cluster at B3LYP/3-21G.

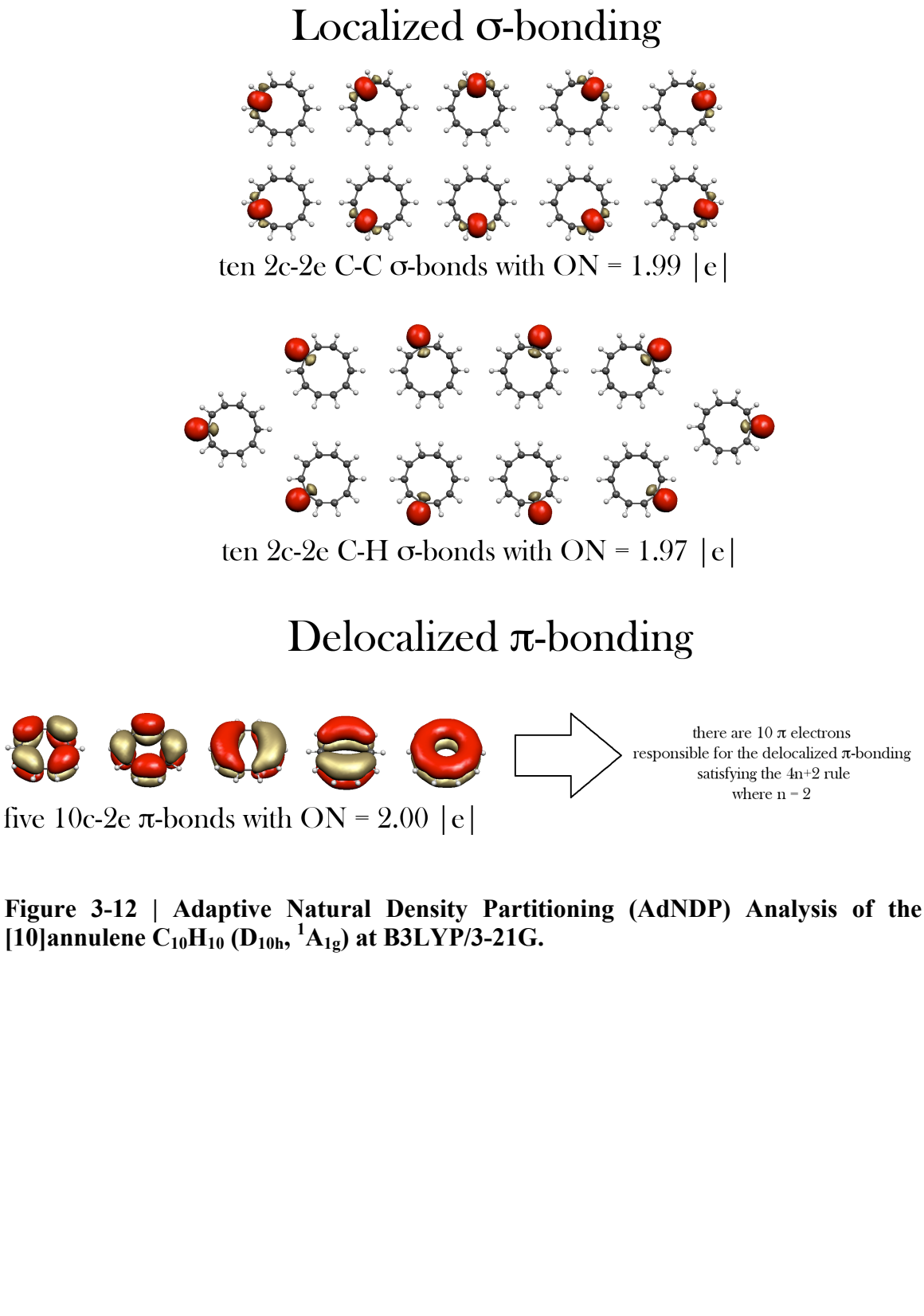

Figure 3-12 | Adaptive Natural Density Partitioning (AdNDP) Analysis of the [10]annulene $C_{10}H_{10}$ (D_{10h}, $^1A_{1g}$) at B3LYP/3-21G.

CHAPTER 4

UNRAVELLING PHENOMENON OF INTERNAL ROTATION IN B_{13}^+ THROUGH CHEMICAL BONDING ANALYSIS[1]

B_{13}^+ had a very peculiar history full of adventure. In 1988, Hanley et al. found that the mass distribution of B_n^+ from laser ablation showed numerous "magic numbers" in the range n=1−20.[1] Particularly, collision-induced dissociation (CID) experiments indicated the presence of two "magic" clusters: B_5^+ and B_{13}^+. In the following years, Anderson's group performed a series of reactivity studies[2] and found that B_{13}^+ had an anomalously low reactivity with O_2, D_2O, CO_2, and N_2O in a molecular beam. These unusual properties of B_{13}^+ inspired several theoretical studies to determine structure and bonding of this cluster. Anderson and co-workers originally postulated that B_{13}^+ had a filled icosahedral structure. However, in 1992 Kawai and Weare made Car-Parrinello MD simulations, which proved that the icosahedral structure was not a minimum.[3] They suggested that the most stable form of B_{13}^+ was a three-dimensional C_{3v} structure.[3] In 1994, Boustani predicted a quasi-planar structure composed of three hexagonal pyramids adjacent to one another in a longitudinal arrangement.[4] Two years later, Ricca and Bauschlicher reported a planar C_{2v} form as the ground state of B_{13}^+ with an inner triangle enclosed into a ten-atomic ring at the B3LYP/6-31G* level.[5] In 1998 Schleyer and co-workers[6] confirmed the findings of Ricca and Bauschlicher by re-examining various structures of B_{13}^+ at the same level. Schleyer and co-workers[6] were first to predict the fluxional behaviour of the C_{2v} global minimum of B_{13}^+. In 2000 Fowler and Ugalde[7] also

[1] Coauthored by Gerardo Martínez-Guajardo, Alina P. Sergeeva, Alexander I. Boldyrev, Thomas Heine, Jesus M. Ugalde, and Gabriel Merino with permission from *Chem. Commun.* **2011**, 47, 6242-6244.

concluded that the B_{13}^+ global minimum structure had a planar C_{2v} geometry with an inner triangle. Thus, the global minimum structure of B_{13}^+ has been firmly established.

Fowler and Ugalde[7] were the first to propose that exceptional stability and low reactivity of B_{13}^+ was related to its π-aromatic character. They showed that the π-molecular orbitals of B_{13}^+ were similar to those of benzene. Aihara[8] evaluated the topological resonance energy (TRE) for π-electrons using graph theory. He established that the TRE value of B_{13}^+ was very large in magnitude and comparable to other aromatic hydrocarbons such as phenalenium. Alexandrova et al.[9] were the first to recognise that B_{13}^+ was doubly σ- and π-aromatic. Furthermore, Zubarev et al. showed that this cluster is doubly σ-aromatic (two concentric aromatic σ-systems) and π-aromatic using the Adaptive Natural Density Partitioning (AdNDP) method.[10] The phenomenon of double σ- and π-aromaticity was discovered by Schleyer and co-workers[11] in their seminal paper on double aromaticity in the 3,5-dehydrophenyl cation.

The groups of Wang and Boldyrev conducted a series of joint studies, where they showed that boron clusters containing up to twenty atoms tend to adopt planar or quasi-planar geometries rather than three-dimensional (3-D) structures.[12,13]

Recently, the groups of Merino and Heine[14] reported remarkable fluxional behaviour of B_{19}^-, which structure and chemical bonding was previously established by Huang et al.[15] The authors[14] demonstrated almost free internal rotation of the pentagon-shaped hub (the inner B_6 ring unit of B_{19}^-) within the B_{13} outer ring unit of B_{19}^- by means of Born-Oppenheimer Molecular Dynamics (BO-MD) calculations. In-plane internal rotation was initially discovered in borocarbon wheels by Erhardt et al.,[16] though all the reported forms are not the lowest energy structures. In this communication, we analyze

the fluxionality of B_{13}^+ and present an explanation, using the AdNDP method, why such a fluxional behaviour is possible.

We first carried out a detailed theoretical study on B_{13}^+, locating the transition states of the inner fragment rotation, and studying the fluxionality using BO-MD calculations. The C_{2v} structure **1**, previously reported as the global minimum,[5] has been reoptimized at the PBE/6-311+G* level. Like B_{19}^-, there is a small vibrational frequency, which corresponds to a soft mode of 137 cm^{-1} regarding the rotation of the inner triangle. Following the frequency mode related to the ring rotation the transition state **2** is found (Figure 4-1), which also exhibits C_{2v} symmetry (its smallest imaginary frequency mode is 132 cm^{-1}) in agreement with the previous results of Schleyer and co-workers.[6] We have ensured that **2** connects truly to the correct minima **1** by performing an IRC calculation at the PBE/6-311+G* level. The energy difference between **1** and **2** is negligible (0.1 $kcal \cdot mol^{-1}$, including the ZPE correction), indicating a quasi-free rotation of the inner ring. BO-MD simulations at the PBE/DZVP-GGA level confirm the B_{13}^+ fluxional behavior.[17] During the BO-MD simulations, the molecule essentially maintains its planar geometry, and internal and external rings rotate nearly freely with respect to each other via a low-energy transition state. In summary, B_{13}^+ could be considered a molecular "Wankel motor" similar to B_{19}^-.

How such rotation of the inner triangle is possible within the outer 10-atomic ring? This question is answered by means of the chemical bonding analysis performed using the AdNDP method. The detailed description of the AdNDP method can be found elsewhere.[10] The AdNDP results were obtained at the B3LYP/3-21G//B3LYP/6-311+G(d) level.[18] It was shown previously that the AdNDP analysis is not sensitive to the

method or basis set used similar to those of the NBO analysis.[10,19] Therefore, the choice of the level is adequate. This analysis revealed ten 2c-2e B-B σ-bonds on the periphery of **1** (See Figure 4-2). There is also one 3c-2e σ-bond, which is delocalized over the central boron triangle. The AdNDP search also recovered five 3c-2e σ-bonds, which are responsible for the bonding between the central triangular unit and the peripheral B_{10} ring. So, there are two concentric σ-systems, which both satisfy the $4n + 2$ Hückel rule separately. Therefore, the global minimum is doubly concentric σ-aromatic. Concurrently, there are six π-electrons satisfying the Hückel rule, which form three delocalized 5c-2e π-bonds. Thus, B_{13}^+ is also π-aromatic. Similar results are found for the transition state **2**, which are presented side by side with those for **1** in Figure 4-2. So, both the global minimum **1** and the transition state **2** are doubly σ- and π-aromatic.

Let's envision the fluxionality of B_{13}^+ as a clockwise rotation of the outer B_{10} ring with respect to inner B_3 triangle, whose atoms positions are held fixed (Figure 4-3). The internal rotation can be then presented as the following process: $\Leftrightarrow \mathbf{1}_1 \Leftrightarrow \mathbf{2}_{1\text{-}2} \Leftrightarrow \mathbf{1}_2 \Leftrightarrow \mathbf{2}_{2\text{-}3} \Leftrightarrow \mathbf{1}_3 \Leftrightarrow \ldots \Leftrightarrow \mathbf{1}_{29} \Leftrightarrow \mathbf{2}_{29\text{-}30} \Leftrightarrow \mathbf{1}_{30} \Leftrightarrow \mathbf{2}_{30\text{-}1} \Leftrightarrow \mathbf{1}_1 \Leftrightarrow$, where $\mathbf{1}_i$ represent the global minima (i = 1-30), which differ in relative arrangement of the outer ring with respect to the fixed inner ring. Each $\mathbf{2}_{i\text{-}j}$ species stands for the transition state connecting global minima $\mathbf{1}_i$ and $\mathbf{1}_j$ (i, j = 1-30). In global minimum $\mathbf{1}_1$ the B7-B8 edge of the inner B_3 triangle is coordinated to the B12-B13 peripheral bond, whereas the B7-B8 edge of the inner triangle is coordinated to the B13-B11 peripheral bond in $\mathbf{1}_4$. On the way from $\mathbf{1}_1$ to $\mathbf{1}_4$ the outer B_{10} ring is slowly and gradually rotating clockwise by one peripheral bond through the transitional species $\Leftrightarrow \mathbf{2}_{1\text{-}2} \Leftrightarrow \mathbf{1}_2 \Leftrightarrow \mathbf{2}_{2\text{-}3} \Leftrightarrow \mathbf{1}_3 \Leftrightarrow \mathbf{2}_{3\text{-}4} \Leftrightarrow$ with respect to the inner triangle, whose atoms positions are held fixed. If we consider the outer ten-atomic ring as

a concentric circle, then the rotation by one peripheral bond of the ten-atomic ring is the same as rotation by 360°/10 = 36 degrees. In other words, the outer B_{10} ring makes a 36°-turn going from $\mathbf{1}_1$ to $\mathbf{1}_4$. To make a full 360°-turn of the outer B_{10} ring with respect to the fixed B_3 triangle, one needs 30 different global minima ($\mathbf{1}_i$, i = 1-30) and 30 different transition states ($\mathbf{2}_{i\text{-}j}$, i, j = 1-30). The atoms of the global minima and the transition states throughout the rotation were numerated on the basis of careful exploration of potential energy surface around the transition state.

Now, how the chemical bonding changes during the internal rotation? The peripheral atoms participate in both localized and delocalized bonding, while the inner three atoms comprising the central boron triangle are involved in delocalized bonding only (Figure 4-2). Note that during the internal rotation the localized peripheral B-B σ-bonds are not breaking/forming, but rather "staying in place." The delocalized π-bonding also does not change during the rotation.

The main change in chemical bonding upon rotation occurs in delocalized σ-framework (see Figures 4-3), where the delocalized 3c-2e σ-bonds are symbolically presented as solid triangles. The electron density migrates from one 3c-2e σ-bond to other 3c-2e σ-bond (see the direction of the arrows in Figure 4-3), while the other pairs of delocalized σ-electrons occupying 3c-2e σ-bonds stay in their places. So, the σ-electron density migration does not violate the $4n + 2$ rule for both concentric σ-systems. The σ-electrons number is constant over the inner triangle (two electrons) and in between the triangle and the peripheral ring (ten electrons) upon internal rotation. The geometry of the inner triangle is rather rigid upon internal rotation. This can be explained by σ-aromaticity in this unit.

The absence of localized 2c-2e σ-bonds between the B_3 and B_{10} moieties is the main reason why almost free internal rotation is possible. High energy would have to be supplied for those bonds to be broken and formed during **1** to **2** transition if these localized bonds existed. The chemical bonding in **1** and **2** can be compared to that of prototypic concentric aromatic hydrocarbon such as coronene ($C_{24}H_{12}$).[20] If we consider an internal rotation of the C_6 moiety inside of coronene, such rotation would require breaking/formation of localized 2c-2e C-C σ-bonds, since σ-framework in coronene consists solely of 2c-2e C-C σ-bonds. We failed to find the transition state for internal rotation inside of coronene showing necessity of delocalized bonding between inner and peripheral moieties for possibility of fluxional behaviour.

Finally, Figure 4-4 shows the isolines of the *z*-component of the induced magnetic field, B^{ind}_z, of an external field applied perpendicular to the molecular plane of **1**.[21] A magnetic field in this direction can induce a ring current in and parallel to the molecular plane. The total magnetic response shows a long-range shielding cone perpendicular to the molecular plane. This cone is even more intense to that observed in benzene. Note that inner triangle lies in the strong shielding area (approximately -71 ppm) of the induced field. The B^{ind}_z intensity diminishes gradually from the inner to the outer boron ring, confirming the presence of two concentric aromatic rings.

Interestingly, the local diamagnetic contributions of the σ-electrons generate a long-range response and a diatropic (shielding) region around the triangle ring. Furthermore, the π-orbital contribution shows the typical response of an aromatic system.

No paratropic contributions are found inside the ring. Outside of the molecule, the field lines form long-range cones (shielding cones). The π-contributions are, however, smaller in magnitude than those of the σ–skeleton, which results in a strong total response. In this sense, B_{13}^+ is a double aromatic system, in agreement to our early analyses. The B^{ind}_z isolines of **2** indicate essentially the same magnetic response in shape and intensity than **1**. Thus, during the rotation the changes in σ- and π-aromaticity are negligible.

In conclusion, the fluxional behaviour of B_{13}^+ has been described as almost free rotation of the inner B_3 moiety inside of the peripheral B_{10} ring. Therefore, B_{13}^+ should be considered as a molecular "Wankel" motor. The chemical bonding analysis revealed that the localized bonding in both global minimum and its transition state is presented by peripheral 2c-2e B-B σ-bonds, while the delocalized bonding can be viewed as two concentric σ-systems and one π-system, each satisfying the $4n + 2$ rule for aromaticity. The doubly aromatic nature of B_{13}^+ was confirmed by the induced magnetic field analyses. The chemical bonding analysis helped to decipher the fluxional behaviour of B_{13}^+. Almost free rotation found for this cluster is due to the fact that the inner triangle is bound to the peripheral ring by delocalized bonds only. Therefore, we believe that other planar boron clusters may exhibit fluxional behaviour similar to B_{13}^+ and B_{19}^-. This kind of internal rotation is a new member of the diamond-square-diamond rearrangements introduced by Lipscomb in 1966.[22]

References

1 L. Hanley, J. L. Whitten and S. L. Anderson, *J. Phys. Chem.* 1988, **92**, 5803.

2 S. A. Ruatta, L. Hanley and S. L. Anderson, *J. Chem. Phys.* 1989, **91**, 226.

3 R. Kawai and J. H. Weare, *Chem. Phys. Lett.* 1992, **191**, 311.

4 I. Boustani, *Int. J. Quant. Chem.* 1994, **52**, 1081.

5 A. Ricca and C. W. Bauschlicher, *Chem. Phys.* 1996, **208**, 233.

6 F. L. Gu, X. M. Yang, A. C. Tang, H. J. Jiao and P. v. R. Schleyer, *J. Comput. Chem.* 1998, **19,** 203.

7 J. E. Fowler and J. M. Ugalde, *J. Phys. Chem. A* 2000, **104**, 397.

8 J. Aihara, *J. Phys. Chem. A* 2001, **105**, 5486.

9 A. N. Alexandrova, A. I. Boldyrev, H.-J. Zhai and L. S. Wang, *Coord. Chem. Rev.* 2006, **250**, 2811.

10 (a) D. Y. Zubarev and A. I. Boldyrev, *Phys. Chem. Chem. Phys.* 2008, **10**, 5207. (b) D. Y. Zubarev, A. P. Sergeeva and A. I. Boldyrev, in *Chemical Reactivity Theory: A Density Functional View,* ed. P. K. Chattaraj, CRC Press, Taylor & Francis Group, New York, 2009, pp. 439-452.

11 J. Chandrasekhar, E.D. Jemmis, and P.v.R. Schleyer. Tetrahedron Letters 1979, 3707.

12 (a) H.-J. Zhai, L. S. Wang, A. N. Alexandrova and A. I. Boldyrev, *J. Chem. Phys.* 2002, **117**, 7917. (b) A. N. Alexandrova, A. I. Boldyrev. H.-J. Zhai, L. S. Wang, E. Steiner and P. W. Fowler, *J. Phys. Chem. A* 2003, **107**, 1359. (c) H.-J. Zhai, L. S. Wang, A. N. Alexandrova, A. I. Boldyrev and V. G. Zakrzewski, *J. Phys. Chem. A* 2003, **107**, 9319. (d) H.-J. Zhai, A. N. Alexandrova , K. A. Birch, A. I. Boldyrev and L. S. Wang. *Angew. Chem. Int. Ed.* 2003, **42**, 6004. (e) A. N. Alexandrova, A. I. Boldyrev, H.-J. Zhai and L. S. Wang, *J. Phys. Chem. A* 2004, **108**, 3509. (f) H.-J. Zhai, L. S. Wang, D. Y. Zubarev and A. I. Boldyrev, *J. Phys. Chem. A* 2006, **110**,

1689. (g) H.-J. Zhai, B. Kiran, J. Li and L. S. Wang, *Nature Materials* 2003, **2**, 827. (h) D. Y. Zubarev and A. I. Boldyrev, *J. Comput. Chem.* 2007, **28**, 251.

13 (a) B. Kiran, S. Bulusu, H.-J. Zhai, S. Yoo, X. C. Zeng and L. S. Wang, *Proc. Natl. Acad. Sci*. (USA) 2005, **102**, 961. (b) W. An, S. Bulusu, Y. Gao and X. C. Zeng, *J. Chem. Phys*. 2006, **124**, 154310.

14 J. O. C. Jimenez-Halla, R. Islas, T. Heine and G. Merino, *Angew. Chem. Int. Ed.* 2010, **49**, 5668.

15 W. Huang, A. P. Sergeeva, H.-J. Zhai, B. B. Averkiev, L. S. Wang and A. I. Boldyrev, *Nat. Chem.* 2010, **2**, 202.

16 S. Erhardt, G. Frenking, Z. F. Chen and P. v. R. Schleyer, *Angew. Chem. Int. Ed.* 2005, **44**, 1078.

17 The deMon program package (A. M. Köster, *et. al.* deMon2k, The deMon Developers Community, Mexico, 2008) was used for such calculations; B. Hammer, L. B. Hansen, J. K. Norskov, *Phys. Rev. B.* 1999, **59**, 7413; N. Godbout, D. R. Salahub, J. Andzelm and E. Wimmer, *Can. J. Chem.* 1992, **70**, 560. The simulation was started at the equilibrium geometry **1**, with random velocities assigned to the atoms, and the structure has been equilibrated to 300 and 600 K, respectively, employing a Nosé-Hoover thermal bath, for 20 ps. Afterwards, 50 ps trajectories have been calculated.

18 M. J. Frisch, et. al., *Gaussian03 rev. D.02*, computational package, Gaussian Inc., Pittsburgh, PA, 2003.

19 A. P. Sergeeva and A. I. Boldyrev, *Comm. Inorg. Chem*. 2010, **31**, 2.

20 D. Y. Zubarev and A. I. Boldyrev, *J. Org. Chem.,* 2008, **73**, 9251.

21 (a) G. Merino, T. Heine and G. Seifert, *Chem. Eur. J.* 2004, **10**, 4367; (b) T. Heine, R. Islas and G. Merino, *J. Comput. Chem.* 2007, **28**, 302. (c) R. Islas, G. Martínez-Guajardo, G. Seifert, T. Heine and G. Merino, in *Aromaticity and Metal Clusters,* ed. P. K. Chattaraj, CRC Press, Taylor & Francis Group, New York, 2010, pp. 185-202.

22 W. N. Lipscomb, *Science,* 1966, **153**, 3734.

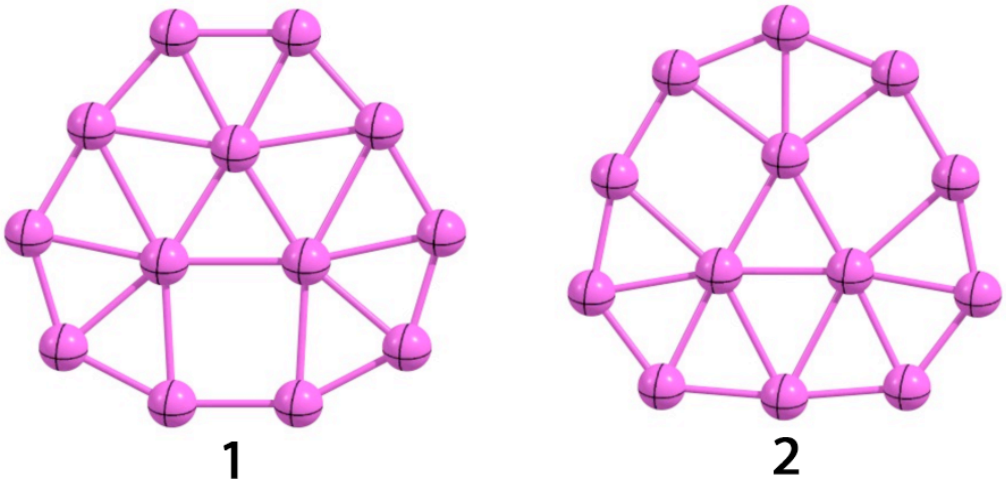

Figure 4-1. Structures of the global minimum of B_{13}^{+} (**1**) and the transition state for the internal rotation of inner triangle (**2**).

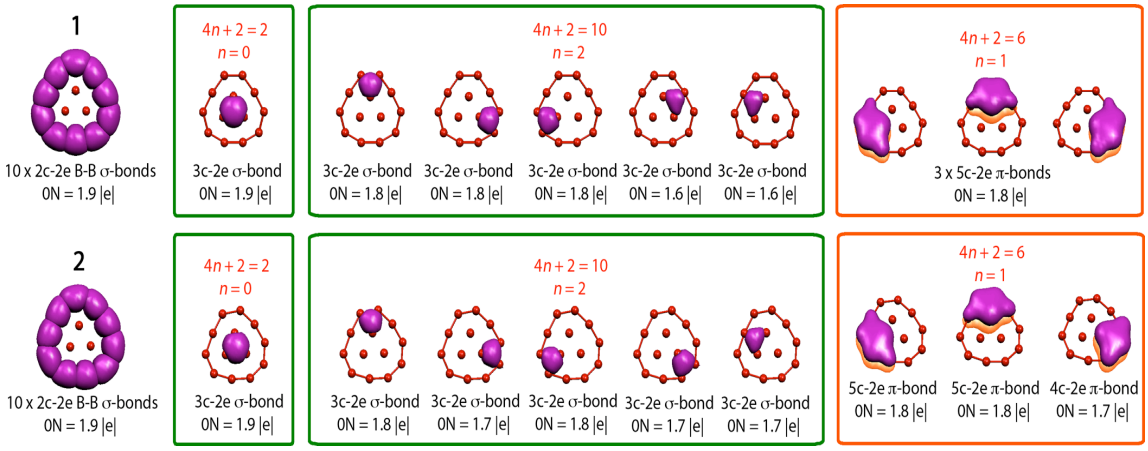

Figure 4-2. Chemical bonding pattern revealed for **1** and **2** using Adaptive Natural Density Partitioning method. The delocalized σ-bonds are enclosed in green rectangles, while the delocalized π-bonds are enclosed in orange rectangles.

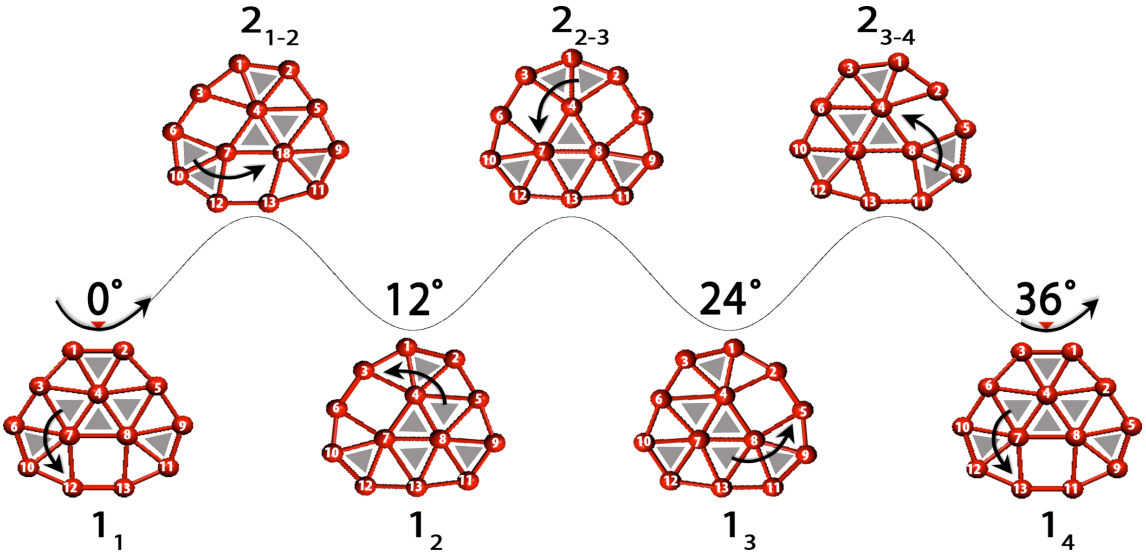

Figure 4-3. The schematic representation of the 3c-2e σ-bonds migration during the internal rotation of B_{13}^{+}. Note: the positions of the boron atoms in **1** (Figure 4-2) correspond to the $\mathbf{1_4}$ global minimum presented in this figure, whereas positions of the boron atoms in **2** (Figure 4-2) correspond to the $\mathbf{2_{3\text{-}4}}$ transition state.

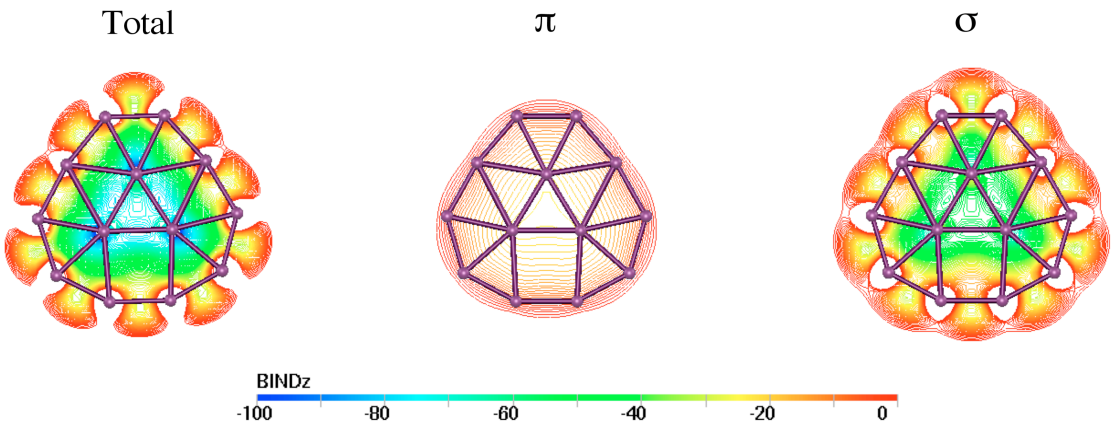

Figure 4-4. The diatropic region of B^{ind}_{z} for **1**.

CHAPTER 5

PLANARIZATION OF B_7^- AND B_{12}^- CLUSTERS BY ISOELECTRONIC SUBSTITUTION: AlB_6^- AND AlB_{11}^-[1]

Abstract

Small boron clusters have been shown to be planar from a series of combined photoelectron spectroscopy and theoretical studies. However, a number of boron clusters are quasi-planar, such as B_7^- and B_{12}^-. To elucidate the nature of the nonplanarity in these clusters, we have investigated the electronic structure and chemical bonding of two isoelectronic Al-doped boron clusters, AlB_6^- and AlB_{11}^-. Vibrationally-resolved photoelectron spectra were obtained for AlB_6^-, resulting in an accurate electron affinity (EA) for AlB_6 of 2.49 ± 0.03 eV. The photoelectron spectra of AlB_{11}^- revealed the presence of two isomers with EAs of 2.16 ± 0.03 and 2.33 ± 0.03 eV, respectively. Global minimum structures of both AlB_6^- and AlB_{11}^- were established from unbiased searches and comparison with the experimental data. The global minimum of AlB_6^- is nearly planar with a central B atom and an AlB_5 six membered ring, in contrast to that of B_7^-, which possesses a C_{2v} structure with a large distortion from planarity. Two nearly degenerate structures were found for AlB_{11}^- competing for the global minimum, in agreement with the experimental observation. One of these isomers with the lower EA can be viewed as substituting a peripheral B atom by Al in B_{12}^-, which has a bowl shape with a B_9 outer ring and an out-of-plane inner B_3 triangle. The second isomer of AlB_{11}^- can be viewed as an Al atom interacting with a B_{11}^- cluster. Both isomers of AlB_{11}^- are

[1] Coauthored by Constantin Romanescu, Alina P. Sergeeva, Wei-Li Li, Alexander I. Boldyrev, and Lai-Sheng Wang. Reproduced with permission from *J. Am. Chem. Soc.* **2011**, 133, 8646-8653. Copyright 2011, American Chemical Society

perfectly planar. It is shown that Al substitution of a peripheral B atom in B_7^- and B_{12}^- induces planarization by slightly expanding the outer ring due to the larger size of Al.

5-1. Introduction

Elemental boron possesses many complex crystal structures, consisting of B_{12} icosahedral or larger cage building blocks.[1,2] However, early theoretical calculations suggested that the cage structures are not stable as isolated units in the gas phase and planar or quasiplanar structures are more favored.[3-8] Over the past decade, we have combined photoelectron spectroscopy (PES) and theoretical calculations in a major research effort to elucidate the structure and bonding in small boron clusters.[9-21] We have found that the planarity of boron clusters is primarily due to two-dimensional electron delocalizations, which have given rise to concepts of σ- and π-aromaticity, σ- and π-antiaromaticity, or conflicting aromaticity–antiaromaticity.[11,12,22-24] One of the key structural and bonding features that have emerged from our joint experimental and computational investigations is that each planar boron cluster contains an outer boron ring with strong classical two-center two electron (2c-2e) B-B bonds and various inner B atom groups that are bonded to the outer ring via delocalized σ and π bonding.[9-21] Among the well characterized boron clusters, some are found to be perfectly planar, while others are quasi-planar with the inner atoms exhibiting some degree of nonplanarity. A question arises, what causes the nonplanarity?

Some nonplanarity has been traced to antiaromaticity, i.e. electronic in origin. One aspect that has not been addressed is if the nonplanarity can be mechanical in origin, i.e. the outer B ring is too small to fit the central atoms. Two quasi-planar clusters may

belong to this category, B_7^- and B_{12}^-. The global minimum of B_7^- is of C_{2v} symmetry with a central B atom significantly out of plane.[15] On the other hand, the B_8 cluster is a perfect planar cluster with a B_7 ring and a central B atom.[11] B_{12} is a highly stable and aromatic cluster with a large HOMO-LUMO gap, as revealed from the PES spectra of B_{12}^-.[12] Yet, the global minima of both B_{12} and B_{12}^- are non-planar and have bowl shapes with an outer B_9 ring and an inner out-of-plane B_3 triangle. In both B_7^- and B_{12}^-, there is a possibility that the outer B rings are simply too small to host the central atoms in a perfect planar arrangement, even though from an electronic point of view, planarity clearly favors electron delocalization in two dimensions. Thus, if the outer ring can be expanded to release the strain, we expect that both B_7^- and B_{12}^- should favor the perfect planar structures.

In this article, we set out to test the above hypothesis by substituting a B atom with Al in B_7^- and B_{12}^-. Because of the larger size of Al, it may induce planarity by slightly expanding the outer ring. We have obtained well-resolved photoelectron spectra of AlB_6^- and AlB_7^- at several detachment laser wavelengths. Unbiased global minimum searches are carried out for both clusters to locate their lowest energy structures, which are then compared with the experimental data. It is shown that indeed the Al atom can induce planarization in both clusters.

Relatively little is known about metal-doped boron clusters. The only experimental studies on metal-doped boron clusters reported prior to this study concern the structure of two Au-doped boron clusters, $Au_2B_7^-$ and AuB_{10}^-, in which the Au atoms are found to behave like H atoms.[25,26] A number of calculations on Al-B mixed clusters have been reported.[27-29] The most relevant work is the report,[27] which suggested that a

planar nona-coordinated structure with a central Al atom (D_{9h}) is the global minimum of AlB_9, while a deca-coordinated (D_{10h}) structure of AlB_{10}^+ corresponds to a local minimum on the potential energy surface. The current study shows that, for AlB_6^- and AlB_{11}^-, the aluminum atom avoids hyper-coordination and occupies a peripheral position, inducing planarization to the B_7^- and B_{12}^- parent clusters, respectively.

5-2. Experimental and Computational Methods

5-2.1. Photoelectron spectroscopy

The experiment was performed using a magnetic-bottle PES apparatus equipped with a laser vaporization cluster source, details of which have been published elsewhere.[30] Briefly, the aluminum-doped boron clusters were produced by laser vaporization of a target made of isotopically enriched ^{10}B or ^{11}B (~10% wt.), Al (~2.5% wt.), balanced by Bi or Au, which acted as binders for the targets and provided convenient intrinsic calibrants for the apparatus. The vaporization laser beam (~10 mJ/pulse, 7 ns pulse width at 532 nm) was focused onto the disk target inside the nozzle. The clusters were entrained by the helium carrier gas supplied by two pulsed valves and underwent a supersonic expansion to form a collimated cluster beam. The cluster composition and cooling were controlled by the time delay between the pulsed valves and the vaporization laser and the resident time of the clusters in the nozzle.[31] To achieve an even higher degree of cluster cooling, some experiments were carried out using a mixture of 5% Ar in He as a carrier gas. This approach has been shown recently to produce cold Au cluster anions.[32]

The anionic clusters were extracted from the cluster beam and analyzed with a time-of-flight mass spectrometer. The clusters of interest (AlB_6^- and AlB_{11}^-) were mass selected and decelerated before being intercepted by a photodetachment laser beam: 193 nm (6.424 eV), 266 nm (4.661 eV), or 355 nm (3.496 eV). Photoelectrons were collected at nearly 100% efficiency by a magnetic bottle and analyzed in a 3.5 m long electron flight tube. Photoelectron spectra were calibrated using the atomic spectra of Bi^- or Au^-.[33,34] The kinetic energy resolution of the magnetic bottle apparatus, $\Delta E/E$, was typically ~2.5%, *i.e.* ~ 25 meV for 1 eV electrons.

5-2.2. Computational Methods

The search for the global minimum structures of AlB_6^- and AlB_{11}^- was performed using the Coalescence Kick (CK) method.[35] The CK method subjects large populations of randomly generated structures to a coalescence procedure, in which all atoms are pushed gradually to the center of mass to avoid generation of fragmented structures, and then optimizes them to the nearest local minima. The initial CK global minimum search was performed using the hybrid DFT method known in the literature as B3LYP[36-38] with the small split-valence basis set 3-21G.[39] The structures of all the revealed low-lying isomers were then reoptimized with subsequent frequency calculations at the B3LYP level of theory using the 6-311+G* basis set.[40-43] Single point energy calculations for the lowest energy isomers of both AlB_6^- and AlB_{11}^- were performed using the restricted (unrestricted) coupled cluster method with single, double and non-iterative triple excitations [R(U)CCSD(T)][44-47] with the 6-311+G(2df) basis set at the geometries optimized at B3LYP/6-311+G*.

The vertical detachment energies (VDEs) were calculated using two levels of theory: 1) the time-dependent DFT method[48,49] utilizing the B3LYP functional with the 6-311+G(2df) basis set at the geometries optimized at B3LYP/6-311+G* (TD-B3LYP); 2) the restricted (unrestricted) CCSD(T) calculations with the 6-311+G(2df) basis set at the geometries optimized at B3LYP/6-311+G*. In the TD-B3LYP approach, the first VDE of the global minimum of AlB_6^- was calculated as the lowest transition from the singlet state of the AlB_6^- anion into the final lowest doublet state of neutral AlB_6 at the B3LYP/6-311+G(2df) level of theory at the geometry optimized for the AlB_6^- anion at B3LYP/6-311+G* (B3LYP/6-311+G(2df)//B3LYP/6-311+G*). Then the vertical excitation energies of neutral AlB_6 were calculated at the TD-B3LYP level at the optimized geometry of the AlB_6^- anion and were added to the first VDE to obtain the higher VDEs of AlB_6^-. The first two VDEs of AlB_{11}^- were calculated at the B3LYP/6-311+G(2df)//B3LYP/6-311+G* level of theory as the lowest transitions from the doublet ground state of the AlB_{11}^- anion into the final lowest singlet and triplet states of neutral AlB_{11} at the geometry optimized for the AlB_{11}^- anion. Then the vertical excitation energies calculated at the TD-B3LYP level for the singlet and triplet states of neutral AlB_{11} were added correspondingly to the two lowest VDEs to obtain the higher VDEs of the AlB_{11}^- anion. Core electrons were frozen in treating the electron correlation at the CCSD(T) level of theory.

Chemical bonding analysis was performed using the Adaptive Natural Density Partitioning (AdNDP) method[23,50,51] at B3LYP/3-21G level using the optimized B3LYP/6-311+G* geometries. It has been shown that the results of the AdNDP analysis do not depend much on the level of theory or basis set used.[23,52] All the calculations were

performed using the Gaussian 03 software package.[53] Molecular structure visualization was done using MOLDEN 3.4.[54] Molecular orbital visualization was performed using Molekel 4.3.[55]

5-3. Experimental Results

The photoelectron spectra of AlB_6^- and AlB_{11}^- are shown in Figures 5-1 and 5-2, respectively, each at three different photodetachment energies. The spectra measured at 193 nm reveal spectral features with binding energies up to 6.424 eV, whereas the spectra obtained at lower photon energies offer better spectral resolution. The electronic transitions are labeled with letters and the measured vertical detachment energies (VDE) are given in Tables 5-1 and 5-2. The band marked as X usually represents the transition from the ground electronic state of the anion to that of the neutral species, while the higher binding energy bands (A, B, ...) denote transitions to excited electronic states of the neutral cluster.

5-3.1. AlB_6^-

The 355 nm spectrum (Figure 5-1a) shows a vibrationally-resolved ground state transition. The short vibrational progression, with an average spacing of 480 ± 40 cm^{-1}, and the sharp onset of the X band suggest a minimal geometry change upon photodetachment of an electron from the highest occupied molecular orbital (HOMO) of the anion. The intense 0-0 vibrational peak of the X band defines an adiabatic detachment energy (ADE) of 2.49 ± 0.03 eV, which also represents the electron affinity (EA) of neutral AlB_6. Because of the small geometry change between the ground state of AlB_6^- and AlB_6, the VDE and the ADE are the same.

The 266 nm spectrum (Figure 5-1b) reveals two additional PES bands (A and B), corresponding to the two lowest-lying electronic excited states of AlB_6. The A band (ADE = 3.74 ± 0.03 eV) is sharp and intense with a very short vibrational progression, which yields a vibrational frequency of 400 ± 50 cm^{-1} for the first excited state of AlB_6. The A-X energy gap is similar to that observed for the main isomer of the B_7^- cluster (1.2 eV), as reported in ref. 15. The B band (VDE: 3.98 ± 0.05 eV) is relatively weak, but its intensity is enhanced in the 193 nm spectrum (Figure 5-1c). There is a weak feature around 4.3 eV (unmarked) in the 266 nm spectrum, whose relative intensity is also enhanced at 193 nm. A relatively intense band C is observed with a VDE of 4.61 ± 0.06 eV in the 193 nm spectrum (Figure 5-1c). There seem to be signals beyond 5 eV, but the signal-to-noise ratios in the higher binding energy side of the 193 nm spectrum are poor. Only one feature D is tentatively labeled at a VDE of 5.26 ± 0.05 eV.

5-3.2. AlB_{11}^-

At 355 nm (Figure 5-2a), two intense bands are observed for AlB_{11}^-. A very sharp band (X) is observed at the threshold with a discernible vibrational feature, yielding an ADE of 2.16 ± 0.03 eV. The second band (X′) with an ADE of 2.33 ± 0.03 eV exhibits a sharp rise and is rather broad. For both the X and X′ bands, their VDEs are the same as their ADEs because of the relatively small geometry changes between the anion and the neutral states, in particular for the X band. There are two weak, but sharp and well resolved features (unmarked) at 2.90 and 3.15 eV in the 355 nm spectrum. However, the relative intensities of these two features seem to decrease with the photon energies, and become negligible in the 193 nm spectrum (Figure 5-2c).

Following a large energy gap, the 266 nm spectrum (Figure 5-2b) displays two broad bands, A and B, with VDEs of 4.06 ± 0.05 eV and 4.38 ± 0.05 eV, respectively. At 193 nm (Figure 5-1c), one more band is observed at the high binding energy side (C, VDE = 5.57 ± 0.05 eV). The parent B_{12} cluster is a highly stable quasi-planar cluster with a large HOMO-LUMO, as revealed from the PES spectra of B_{12}^-.[12] The PES patterns of AlB_{11}^- are similar to those of B_{12}^-, except the fact that there are two strong features (X and X′) in the low binding energy range. These features suggest the presence of low-lying isomers, which are borne out from the theoretical calculations (*vide infra*). We note that the two unmarked weak features observed in the 355 nm (Figure 5-2a) occur in the HOMO-LUMO gap region, as will be shown later. We observe these features with both ^{10}B and ^{11}B isotopes, ruling out contributions from impurities. We attribute tentatively these weak features to multi-electron (shakeup) transitions.

5-4. Theoretical Results

5-4.1. AlB_6^-

Figure 5-3 presents the global minimum and all other isomers of AlB_6^-, which were initially found using the CK global minimum search at the B3LYP/3-21G level of theory. All the structures were reoptimized at the B3LYP/6-311+G* level of theory with subsequent frequency calculations. The global minimum of AlB_6^- was identified as **I** (C_s, $^1A'$), which has a nearly planar hexagonal structure (Figure 5-3). Four low-lying isomers ($\Delta E < 3$ kcal/mol) were found at the B3LYP/6-311+G* level of theory: **III** ($\Delta E = 0.2$ kcal/mol), **VII** ($\Delta E = 1.4$ kcal/mol), **VI** ($\Delta E = 1.6$ kcal/mol), and **V** ($\Delta E = 2.6$ kcal/mol). To determine the proper order of the isomers we performed single-point energy

calculations at a higher level of theory (CCSD(T)/6-311+G(2df) //B3LYP/6-311+G*) for all isomers lying within 20 kcal/mol of the global minimum at the B3LYP/6-311+G* level of theory. The isomers shown in Figure 3 are arranged and enumerated according to the relative energies calculated at the CCSD(T) level. The relative energies of **III**, **VII**, **VI**, and **V** increased considerably ($\Delta E > 5$ kcal/mol) at the CCSD(T) level as compared to the B3LYP/6-311+G* level, while the relative energy of **II** decreased from 7.5 kcal/mol (B3LYP) to 4.2 kcal/mol (CCSD(T)). The structures of AlB_6^- containing a planar tetra- (**VIII**), penta- (**X**), and hexa-coordinate (**XVI**) aluminum atom were found to be high-lying isomers.

5-4.2. AlB_{11}^-

Figure 5-4 shows all structures of AlB_{11}^- obtained from the CK global minimum search up to 42 kcal/mol above the global minimum. Again all the isomers of AlB_{11}^- were reoptimized at the B3LYP/6-311+G* level along with frequency calculations. There are only three low-lying isomers for AlB_{11}^- at the B3LYP/6-311+G* level of theory: **XX** ($\Delta E = 0.0$ kcal/mol), **XIX** ($\Delta E = 2.3$ kcal/mol), and **XXI** ($\Delta E = 4.4$ kcal/mol); all the other structures are much higher in energy by more than 14 kcal/mol above the lowest energy structure. The three low-lying isomers were further calculated at UCCSD(T)/6-311+G(2df)//B3LYP/6-311+G* and they are ordered accordingly in Figure 5-4. At the CCSD(T) level, isomer **XIX** is the global minimum, which has a perfect planar structure and can be viewed as replacing a peripheral B atom from the C_{3v} B_{12}.[12] Isomer **XX**, which can be viewed as an Al atom attached to one edge of the planar B_{11} cluster,[12] is only 1.0 kcal/mol higher in energy at the CCSD(T) level and is competing for the global

minimum. Isomer **XXI** is 3.9 kcal/mol higher in energy at the CCSD(T) level and it can be viewed as replacing a B atom from the peripheral of the C_{3v} B_{12}, but at a different position from that of the global minimum **XIX**. Isomers in which the Al is inside the planar structures are much higher in energy (see **XXII**, **XXVII**, and **XXIX** in Figure 5-4) and are not viable structures.

5-5. Comparison between Experimental and Theoretical Results

5-5.1. AlB_6^-

According to the relative energies calculated at the CCSD(T) level, the global minimum **I** of AlB_6^- is significantly more stable than the nearest low-lying isomer **II**. Since our cluster source is relatively cold, as evidenced by the absence of any measurable hot band transitions (Figure 5-1a), we can rule out any significant contributions to the PES spectra of AlB_6^- from low-lying isomers. As will be shown below, the main spectral features are in good agreement with the theoretical results from the lowest energy isomer **I**.

The global minimum of AlB_6^- is closed shell with a singlet ground state (C_s, $^1A'$). Thus, each occupied valence MO is expected to yield one PES band, resulting in a doublet final neutral state. The comparison with the calculated VDEs from the global minimum **I** is given in Table 5-1. The first VDE corresponds to electron detachment from the doubly occupied HOMO (5a″) to produce the final doublet state ($^2A''$) of neutral AlB_6. The calculated VDE at the CCSD(T) level (2.52 eV) is in excellent agreement with the experimental value of 2.49 eV. The first VDE calculated at TD-B3LYP is somewhat lower compared to the experimental data. The second, third, and fourth VDEs correspond

to electron detachment from HOMO-1 (6a′), HOMO-2 (4a″), and HOMO-3 (3a″) of the AlB_6^- anion into the final $^2A'$, $^2A''$, and $^2A''$ excited states of neutral AlB_6, respectively (Table 5-1). The calculated second VDE at the CCSD(T) level (3.80 eV), as well as at TD-B3LYP (3.79 eV), is in excellent agreement with the experimental value (3.74 eV) from the A band. We were not able to compute higher VDEs at the CCSD(T) level. However, the third and fourth VDEs (4.04 eV and 4.48 eV) from TD-B3LYP are in good agreement with the VDEs from the B band (3.98 eV) and the C band (4.51 eV), respectively. There are two more detachment channels with VDEs around 5.43 and 5.93 eV from TD-B3LYP (Table 5-1). Because of poor signal-to-noise ratios in the higher binding energy range in the 193 nm spectrum (Figure 5-1c), we cannot definitely assign these two transitions. But they are certainly consistent with the broad features in this spectral range. The unmarked weak feature observed around 4.3 eV does not correspond to any computed detachment channel and it is likely due to a multielectron (shakeup) transition.

We also calculated the VDEs of isomers **II** and **III** (Tables 5-3 and 5-4). The calculated VDEs of isomer **II** do not agree with the experimental values. Isomer **III** corresponds to the triplet excited state of the global minimum **I** and yields a slightly lower VDE (2.43 eV), as expected. However, our PES data are very clean in the low binding energy range (Figure 5-1), ruling out any contribution from isomer **III**. Hence, the excellent agreement between the experimental and theoretical data confirms unequivocally that isomer **I** is the global minimum of AlB_6^-.

5-5.2. AlB_{11}^-

As shown in Figure 5-4, isomers **XIX** and **XX** of AlB_{11}^- are within 1.0 kcal/mol of each other at the CCSD(T) level and should be considered degenerate within the accuracy of the theory. Thus, both isomers are expected to be present in our cluster beam and contribute to the observed PES spectra. Isomer **XXI** is 3.9 kcal/mol higher in energy at CCSD(T) and is not expected to have any significant population in the cluster beam.

The calculated VDEs for isomers **XIX** and **XX** are compared with the experimental data in Table 5-2. Both isomers give rise to rather low first VDEs, due to the fact that the corresponding neutral clusters are both closed-shell with large HOMO-LUMO gaps. The theoretical VDEs for the two isomers are in excellent agreement with the experimental observations. The first VDE calculated for **XIX** at CCSD(T) is 2.08 eV, is slightly smaller than that for **XX** at 2.24 eV. Thus, the lowest X band observed in the PES spectra should come from **XIX**. The experimental VDE of 2.16 eV agrees well with the calculated value of 2.08 eV (Table 5-2). The next detachment channel for the **XIX** isomer comes from the doubly occupied $9a_1$ orbital, yielding a triplet ($^3A_2$) excited state of the corresponding neutral AlB_{11}. The VDE calculated for this channel at CCSD(T) (4.14 eV) is in good agreement with the VDE of the A band (4.06 eV). The experimental HOMO-LUMO gap (1.90 eV) defined by the X-A VDE difference is also in reasonable agreement with the calculated value of 2.06 eV. There is a high density of detachment channels due to the large size of the AlB_{11}^- cluster and the fact that both triplet and singlet final states are produced. The calculated spectral pattern is in good agreement with the congested spectral features in the high binding energy side. We note that the VDE of **XIX** (2.16 eV) is very similar to that of the parent B_{12}^- (2.26 eV).[12] The HOMO-

LUMO gap of **XIX** (1.90 eV) is also similar to that of B_{12}^- (2.05 eV). However, the X band of **XIX** is very sharp in comparison to the first band in the PES spectra of B_{12}^-, suggesting the planar AlB_{12}^- is extremely rigid with little geometry change between the ground states of the anion and the neutral.

The calculated first VDE for **XX** at CCSD(T) is 2.24 eV, which agrees well with the VDE of the X′ band (2.33 eV). The next detachment channel should be from the doubly occupied $9a_1$ orbital, similar to **XIX**, leading to the first triplet excited state ($^3B_1$) of the corresponding neutral. The calculated VDE for this channel at CCSD(T) is 4.19 eV, which overlaps with the A band of **XIX**. There is also a relatively high density of detachment channels for **XX**, which all overlap with those of **XIX**. We further calculated the VDEs for **XXI**, as shown in Table 5-5. Its first VDE was calculated at 2.27 eV, which may contribute to the X′ band. The second and higher detachment channels for **XXI** all overlap with those of **XIX** and **XX**. Based on the energetics, however, we expect the contributions of **XXI** to the PES spectra of AlB_{11}^- to be small, if at all. The overall spectral patterns calculated from **XIX** and **XX** are in excellent agreement with the key features of the experimental spectra, confirming the presence of the two nearly degenerate isomers for AlB_{11}^-. The two weak features observed at 2.9 and 3.1 eV (Figure 5-2a) occur in the band gap region for all three low-lying isomers of AlB_{11}^- and cannot come from direct one-electron transitions from any of these isomers. They are likely from multielectron (shapeup) processes.

5-6. Chemical Bonding Analyses and Al-Induced Planarization

5-6.1. AlB_6^-

The chemical bonding of the global minimum structure of AlB_6^- was analyzed using the AdNDP method, as given in Figure 5-5. The occupation numbers (denoted as ON) of all the revealed chemical bonds are close to the ideal value of 2.0 |e|. The bonding in AlB_6^- can be explained by the formation of six peripheral 2c-2e σ-bonds: four B-B σ-bonds and two B-Al σ-bonds. The rest of the valence electron density is totally delocalized. There are six delocalized σ-electrons, rendering σ-aromaticity to AlB_6^-, according to the $4n+2$ rule for aromaticity ($n = 1$). There are four delocalized π-electrons in AlB_6^-, which indicate that AlB_6^- is π-antiaromatic according to the $4n$ rule for antiaromaticity. Therefore, the AlB_6^- cluster is an example of a system with conflicting aromaticity. The π-antiaromatic nature of AlB_6^- explains why this cluster is not perfectly planar, even though the distortion from planarity is very small. The chemical bonding of the global minimum of AlB_6^- is similar to that of the C_{2v} isomer of B_7^- ($^1A_1$).[15] However, AlB_6^- is much closer to a perfect planar structure than its valence isoelectronic B_7^-. Clearly, the large distortion from planarity in B_7^- is due to the fact that the B_6 ring is too small to fit a B atom in its center to from a planar hexagonal structure. Substitution of one B atom by Al at the periphery decreases the geometric strain for planarity because of the slightly bigger AlB_5 ring due to the larger size of Al.

5-6.2. AlB_{11}^-

We performed chemical bonding analyses using AdNDP for the two nearly degenerate isomers **XIX** and **XX** of AlB_{11}^-, as shown in Figure 5-6. The occupation

numbers of all the revealed chemical bonds range from 1.7 to 2.0 |e| for the doubly occupied bonds, and are 1.0 |e| for the singly occupied bonds. The current AdNDP method is applicable to closed shell systems only. Hence in order to obtain chemical bonding information for AlB_{11}^-, which has one unpaired electron, we performed AdNDP analyses for the closed shell AlB_{11}^{2-} and AlB_{11} at the geometry of the singly charged anion. The sets of chemical bonding elements for the doubly charged anion and the neutral species were found to be the same except for one bond, which is not occupied in the neutral species (ON = 0.0 |e|) and was doubly occupied in the doubly charged anion (ON = 2.0 |e|). Thus, we assumed that this bonding element of the singly charged anion should have an occupation number of 1.0 |e|, as shown in Figure 5-6.

According to the AdNDP analysis, the 19 canonical molecular orbitals for **XIX** can be transformed into the following bonding elements (Figure 5-6a): nine peripheral 2c-2e σ-bonds (seven B-B and two B-Al bonds); two sets of delocalized σ-bonds (one 3c-2e σ-bond delocalized over the inner B_3 triangle and five 3c-2e σ-bonds responsible for bonding between the inner B_3 triangle and the peripheral AlB_8 ring); four delocalized π-bonds (two being doubly occupied and delocalized over three centers, one doubly occupied 5c-2e π-bond, and one singly occupied 5c-1e π-bond). This cluster can be considered as doubly σ-aromatic because the $4n+2$ rule is satisfied for each set of the σ-bonds: 1) $4n+2 = 2$ ($n = 0$) for two σ-electrons delocalized over the inner B_3 triangle; 2) $4n+2 = 10$ ($n = 2$) for the three-center σ-electrons between the inner B_3 ring and the peripheral B atoms. The singly occupied 5c-1e π bond is derived from the extra electron in the anion. Thus, the neutral AlB_{11} corresponding to isomer **XIX** is a highly π-aromatic system with 6π electrons according to the $4n+2$ rule ($n = 1$). The large HOMO-LUMO

gap observed in the PES spectra for XIX suggests the neutral AlB_{11} cluster is a highly stable electronic system, consistent with its multiple aromaticity. It is interesting to note that the peripheral Al atom does not seem to participate in any of the delocalized bonding. Thus, in the structure **XIX** presented in Figure 5-4 it may be more appropriate to omit the bonds between the Al atom and the two inner B atoms.

The chemical bonding pattern of **XIX** is nearly identical to that of its valence isoelectronic B_{12}^- cluster.[12] The structures of these two clusters are similar: a B_3 triangle inside a nine-atom ring. The only difference is that the AlB_{11}^- cluster is perfectly planar, whereas in B_{12}^- the inner B_3 ring is slightly out of plane, giving rise to a bowl-shaped B_{12}^-. Clearly, the B_9 ring is too small to host comfortably the B_3 inner ring in B_{12}^-. Substitution of one B atom in the B_9 ring by the bigger Al atom in AlB_{11}^- gives rise to a slightly larger 9-atom outer ring and a perfectly planar AlB_{11}^- cluster.

The chemical bonding analysis for isomer **XX** of AlB_{11}^- (Figure 5-6b) revealed an Al lone pair, nine 2c-2e B-B σ-bonds, five delocalized 3c-2e σ-bonds, three totally delocalized 11c-2e π-bonds, and one 12c-2e singly occupied π-bond. The latter is derived from the extra electron in the AlB_{11}^- anion. The chemical bonding of **XX** suggests that it is basically an Al atom bonded ionically with a B_{11}^- cluster. We have shown previously that the B_{11}^- cluster is a highly aromatic planar cluster.[12] The B_{11}^- fragment in AlB_{11}^- has little change from the bare B_{11}^- in both its structural details and chemical bonding. Thus, the neutral AlB_{11} corresponding to **XX** can be viewed as $Al^+[B_{11}^-]$.

5-7. Conclusion

We have carried out a joint experimental and theoretical study on the structures and chemical bonding of AlB_6^- and AlB_{11}^- to test if isoelectronic substitution of a B atom by Al in the nonplanar B_7^- and B_{12}^- clusters can induce planarization. Well-resolved photoelectron spectra were obtained for AlB_6^- and AlB_{11}^- and were compared with theoretical calculations for the lowest energy structures found from unbiased global minimum searches. The photoelectron spectra of the Al-doped clusters are similar to those of the bare boron clusters, suggesting their structural similarity. Our global minimum search showed that AlB_6^- is a nearly planar and highly stable cluster in good agreement with the experimental data. Two nearly degenerate perfectly planar isomers were found for AlB_{11}^-, which were both present in the experiment. The one, which is slightly more favored, is the B_{12}^- analog, in which a peripheral B atom is replaced by an Al atom. The second isomer, which is only 1 kcal/mol higher in energy at CCSD(T), is a structure that can be viewed as an Al atom interacting with a B_{11}^- cluster. The current work shows that the nonplanarity in B_7^- and B_{12}^- is mechanical in nature. Thus, suitable isoelectronic substitution can be a powerful means to elucidate the structures and bonding of complex atomic clusters, as we have shown recently for Cu or Ag substituted Au clusters.[56]

References

(1) Cotton, F. A.; Wilkinson, G.; Murillo, C. A.; Bochmann, M. *Advanced Inorganic Chemistry*, 6 ed.; Wiley-Interscience: New York, 1999.

(2) (a) Fujimori, M.; Nakata, T.; Nakayama, T.; Nishibori, E.; Kimura, K.; Takata, M.; Sakata, M. *Phys. Rev. Lett*. **1999**, *82*, 4452. (b) Vast, N.; Baroni, S.; Zerah, G.; Besson, J. M.; Polian, A.; Grimsditch, M.; Chervin, J. C. *Phys. Rev. Lett*. **1997**, *78*, 693.

(3) Hanley, L.; Whitten, J. L.; Anderson, S. L. *J. Phys. Chem.* **1988**, *92*, 5803.

(4) (a) Kawai, R.; Weare, J. H. *J. Chem. Phys.* **1991**, *95*, 1151. (b) Kawai, R.; Weare, J. H. *Chem. Phys. Lett.* **1992**, *191*, 311.

(5) (a) Hernandez, R.; Simons, J. *J. Chem. Phys.* **1991**, *94*, 2961. (b) Martin, J. M. L.; François, J. P.; Gijbels, R. Chem. Phys. Lett. **1992**, *189*, 529. (c) Kato, H.; Yamashita, K.; Morokuma, K. *Chem. Phys. Lett.* **1992**, *190*, 361.

(6) (a) Boustani, I. *Int. J. Quantum Chem.* **1994**, *52*, 1081. (b) Boustani, I. *Phys. Rev. B* **1997**, *55*, 16426. (c) Boustani, I. *Surf. Sci.* **1997**, *370*, 355. (d) Boustani, I.; Quandt, A. *Comput. Mater. Sci.* **1998**, *11*, 132.

(7) Ricca, A.; Bauschlicher, C. W. *Chem. Phys.* **1996**, *208*, 233.

(8) (a) Niu, J.; Rao, B. K.; Jena, P. *J. Chem. Phys.* **1997**, *107*, 132. (b) Gu, F. L.; Yang, X.; Tang, A. C.; Jiao, H.; Schleyer, P. v. R. *J. Comput. Chem.* **1998**, *19*, 203.

(9) Zhai, H. J.; Wang, L. S.; Alexandrova, A. N.; Boldyrev, A. I. *J. Chem. Phys.* **2002**, *117*, 7917.

(10) Alexandrova, A. N.; Boldyrev, A. I.; Zhai, H. J.; Wang, L. S.; Steiner, E.; Fowler, P. W. *J. Phys. Chem. A* **2003**, *107*, 1359.

(11) Zhai, H. J.; Alexandrova, A. N.; Birch, K. A.; Boldyrev, A. I.; Wang, L. S. *Angew. Chem., Int. Ed. Engl.* **2003**, *42*, 6004.

(12) Zhai, H. J.; Kiran, B.; Li, J.; Wang, L. S. *Nat. Mater.* **2003**, *2*, 827.

(13) Zhai, H. J.; Wang, L. S.; Alexandrova, A. N.; Boldyrev, A. I. *J. Phys. Chem. A* **2003**, *107*, 9319.

(14) Alexandrova, A. N.; Zhai, H. J.; Wang, L. S.; Boldyrev, A. I. *Inorg. Chem.* **2004**, *43*, 3552.

(15) Alexandrova, A. N.; Boldyrev, A. I.; Zhai, H.-J.; Wang, L. S. *J. Phys. Chem. A* **2004**, *108*, 3509.

(16) Kiran, B.; Bulusu, S.; Zhai, H. J.; Yoo, S.; Zeng, X. C.; Wang, L. S. *Proc. Natl. Acad. Sci. U. S. A.* **2005**, *102*, 961.

(17) Alexandrova, A. N.; Boldyrev, A. I.; Zhai, H. J.; Wang, L. S. *J. Chem. Phys.* **2005**, *122*.

(18) Alexandrova, A. N.; Boldyrev, A. I.; Zhai, H. J.; Wang, L. S. *Coord. Chem. Rev.* **2006**, *250*, 2811.

(19) Sergeeva, A. P.; Zubarev, D. Y.; Zhai, H. J.; Boldyrev, A. I.; Wang, L. S. *J. Am. Chem. Soc.* **2008**, *130*, 7244.

(20) Pan, L. L.; Li, J.; Wang, L. S. *J. Chem. Phys.* **2008**, *129*, 024302.

(21) Huang, W.; Sergeeva, A. P.; Zhai, H. J.; Averkiev, B. B.; Wang, L. S.; Boldyrev, A. I. *Nat. Chem.* **2010**, *2*, 202.

(22) Zubarev, D. Y.; Boldyrev, A. I. *J. Comput. Chem.* **2007**, *28*, 251.

(23) Zubarev, D. Y.; Boldyrev, A. I. *Phys. Chem. Chem. Phys.* **2008**, *10*, 5207.

(24) Zubarev, D. Y.; Sergeeva, A. P.; Boldyrev, A. I. In *Chemical Reactivity Theory: A Density Functional View*; Chattaraj, P. K., Ed.; CRC Press: 2009, p 439.

(25) Zhai, H. J.; Wang, L. S.; Zubarev, D. Y.; Boldyrev, A. I. *J. Phys. Chem. A* **2006**, *110*, 1689.

(26) Zhai, H. J.; Miao, C. Q.; Li, S. D.; Wang, L. S. *J. Phys. Chem. A* **2010**, *114*, 12155.

(27) Averkiev, B. B.; Boldyrev, A. I. *Russ. J. Gen. Chem.* **2008**, *78*, 769.

(28) Averkiev, B. B.; Wang, L. M.; Huang, W.; Wang, L. S.; Boldyrev, A. I. *Phys. Chem. Chem. Phys.* **2009**, *11*, 9840.

(29) (a) Guo, J. C.; Yao, W. Z.; Li, Z.; Li, S. D. *Sci. China, Ser. B: Chem.* **2009**, *52*, 566. (b) Jiang, Z. Y.; Lou, X. M.; Li. S. T.; Chu, S. Y. *Int. J. Mass Spectrom*. **2006**, *252*, 197. (c) Kawamata, H.; Negishi, Y.; Nakajima, A.; Kaya, K. *Chem. Phys. Lett*. **2001**, *337*, 255. (d) Feng, X. J.; Luo, Y. H. *J. Phys. Chem. A* **2007**, *111*, 2420.

(30) (a) Wang, L. S.; Cheng, H. S.; Fan, J. *J. Chem. Phys.* **1995**, *102*, 9480. (b) Wang, L. S.; Li, X. In *Advances in Metal and Semiconductor Clusters. IV. Cluster Materials;* Duncan, M. A., Ed.; JAI Press: Greenwich, 1998; pp 299-343.

(31) (a) Akola, J.; Manninen, M.; Hakkinen, H.; Landman, U.; Li, X.; Wang, L. S. *Phys. Rev. B* **1999**, *60*, R11297. (b) Wang, L. S.; Li, X. In *Clusters and Nanostructure Interfaces*; Jena, P., Khanna, S. N., Rao, B. K., Eds.; World Scientific: River Edge, NJ, 2000; pp 293-300.

(32) (a) Huang, H.; Wang, L. S. *Phys. Chem. Chem. Phys*. **2009**, *11*, 2663. (b) Huang, W.; Wang, L. S. *Phys. Rev. Lett.* **2009**, *102*, 153401. (c) Huang, H.; Bulusu, S.; Pal, R.; Zeng, X. C.; Wang, L. S. *ACS Nano* **2009**, *3*, 1225.

(33) Bilodeau, R. C.; Haugen, H. K. *Phys. Rev. A* **2001**, *64*, 024501.

(34) Feigerle, C. S.; Corderman, R. R.; Bobashev, S. V.; Lineberger, W. C. *J. Chem. Phys.* **1981**, *74*, 1580.

(35) Averkiev, B. B., Ph.D. thesis, Utah State University, Logan, UT, 2009.

(36) Becke, A. D. *J. Chem. Phys.* **1993**, *98*, 5648.

(37) Vosko, S. H.; Wilk, L.; Nusair, M. *Can. J. Phys.* **1980**, *58*, 1200.

(38) Lee, C. T.; Yang, W. T.; Parr, R. G. *Phys. Rev. B* **1988**, *37*, 785.

(39) Binkley, J. S.; Pople, J. A.; Hehre, W. J. *J. Am. Chem. Soc.* **1980**, *102*, 939.

(40) Gordon, M. S.; Binkley, J. S.; Pople, J. A.; Pietro, W. J.; Hehre, W. J. *J. Am. Chem. Soc.* **1982**, *104*, 2797.

(41) Pietro, W. J.; Francl, M. M.; Hehre, W. J.; Defrees, D. J.; Pople, J. A.; Binkley, J. S. *J. Am. Chem. Soc.* **1982**, *104*, 5039.

(42) McLean, A. D.; Chandler, G. S. *J. Chem. Phys.* **1980**, *72*, 5639.

(43) Clark, T.; Chandrasekhar, J.; Spitznagel, G. W.; Schleyer, P. v. R. *J. Comput. Chem*. **1983**, *4*, 294.

(44) Cizek, J. *Adv. Chem. Phys.* **1969**, 14, 35.

(45) Purvis, G. D.; Bartlett, R. J. *J. Chem. Phys.* **1982**, *76*, 1910.

(46) Raghavachari, K.; Trucks, G. W.; Pople, J. A.; Headgordon, M. *Chem. Phys. Lett.* **1989**, *157*, 479.

(47) Knowles, P. J.; Hampel, C.; Werner, H. J. *J. Chem. Phys.* **1993**, *99*, 5219.

(48) Bauernschmitt, R.; Ahlrichs, R. *Chem. Phys. Lett.* **1996**, *256*, 454.

(49) Casida, M. E.; Jamorski, C.; Casida, K. C.; Salahub, D. R. *J. Chem. Phys.* **1998**, *108*, 4439.

(50) Zubarev, D. Y.; Boldyrev, A. I. *J. Org. Chem.* **2008**, *73*, 9251.

(51) Zubarev, D. Y.; Boldyrev, A. I. *J. Phys. Chem. A* **2009**, *113*, 866.

(52) Sergeeva, A. P.; Boldyrev, A. I. *Comments Inorg. Chem.* **2010**, *31*, 2.

(53) Frisch, M. J. et al., *Gaussian 03*, revision D.01; Gaussian, Inc.; Wallingford, CT, 2004.

(54) Schaftenaar, G. MOLDEN3.4, CAOS/CAMM Center, The Netherlands, 1998.

(55) Portmann, S. Molekel, Version 4.3. Swiss National Supercomputing Centre/Swiss Federal Institute of Technology, Zurich, 2002.

(56) (a) Huang, W.; Pal, R.; Wang, L. M.; Zeng, X. C.; Wang, L. S. *J. Chem. Phys*. **2010**, *132*, 054305. (b) Wang, L. M.; Pal, R.; Huang, W.; Zeng, X. C.; Wang, L. S. *J. Chem. Phys*. **2010**, *132*, 114306. (c) Pal, R.; Wang, L. M.; Huang, W.; Wang, L. S.; Zeng, X. C. *J. Chem*. *Phys*. **2011**, *134*, 054306.

Table 5-1. Comparison of the experimental VDEs with the calculated values for structure **I** (C_s, $^1A'$) of AlB_6^-. All energies are in eV.

Feature	VDE (exp.)[a]	Final State and Electronic Configuration	VDE (theor.)	
			TD-B3LYP[b]	CCSD(T)[c]
X	2.49(3)	$^2A''$, {...4a′^{2}5a′^{2}3a″^{2}4a″^{2}6a′^{2}5a″^{1}}	2.30	2.52
A	3.74(3)	$^2A'$, {...4a′^{2}5a′^{2}3a″^{2}4a″^{2}6a′^{1}5a″^{2}}	3.79	3.80
B	3.98(4)	$^2A''$, {...4a′^{2}5a′^{2}3a″^{2}4a″^{1}6a′^{2}5a″^{2}}	4.04	[e]
C	4.51(4)	$^2A''$, {...4a′^{2}5a′^{2}3a″^{1}4a″^{2}6a′^{2}5a″^{2}}	4.48	[e]
D	5.26(4)	$^2A'$, {...4a′^{2}5a′^{1}3a″^{2}4a″^{2}6a′^{2}5a″^{2}}	5.43[d]	[e]
		$^2A'$, {...4a′^{1}5a′^{2}3a″^{2}4a″^{2}6a′^{2}5a″^{2}}	5.93[d]	[e]

[a] Numbers in parentheses represent the uncertainty in the last digit.
[b] VDEs were calculated at the TD-B3LYP/6-311+G(2df)//B3LYP/6-311+G* level of theory.
[c] VDEs were calculated at the R(U)CCSD(T)/6-311+G(2df)//B3LYP/6-311+G* level of theory.
[d] VDE corresponds to transition of multiconfigurational nature.
[e] VDE value cannot be calculated at this level of theory.

Table 5-2. Comparison of the experimental VDEs with the calculated values for structures **XIX** (C_{2v}, $^2A_2$) and **XX** (C_{2v}, $^2B_1$) of AlB_{11}^-. All energies are in eV.

Feature	VDE (exp.)[a]	Final State and Electronic Configuration	VDE (theor.)	
			TD-B3LYP[b]	CCSD(T)[c]
Isomer XIX				
X	2.16(3)	$^1A_1$, {...$7a_1^2 5b_2^2 8a_1^2 1a_2^2 2b_1^2 6b_2^2 9a_1^2 2a_2^0$}	2.04	2.08
A	4.06(5)	$^3A_2$, {...$7a_1^2 5b_2^2 8a_1^2 1a_2^2 2b_1^2 6b_2^2 9a_1^1 2a_2^1$}	4.00	4.14
		$^1A_2$, {...$7a_1^2 5b_2^2 8a_1^2 1a_2^2 2b_1^2 6b_2^2 9a_1^1 2a_2^1$}	4.11	[e]
B	4.38(5)	$^3B_1$, {...$7a_1^2 5b_2^2 8a_1^2 1a_2^2 2b_1^2 6b_2^1 9a_1^2 2a_2^1$}	4.42	4.51
		$^3B_2$, {...$7a_1^2 5b_2^2 8a_1^2 1a_2^2 2b_1^1 6b_2^2 9a_1^2 2a_2^1$}	4.53	4.75
		$^1B_1$, {...$7a_1^2 5b_2^2 8a_1^2 1a_2^2 2b_1^2 6b_2^1 9a_1^2 2a_2^1$}	4.62	[e]
		$^3A_1$, {...$7a_1^2 5b_2^2 8a_1^2 1a_2^1 2b_1^2 6b_2^2 9a_1^2 2a_2^1$}	4.89	5.10
		$^1B_2$, {...$7a_1^2 5b_2^2 8a_1^2 1a_2^2 2b_1^1 6b_2^2 9a_1^2 2a_2^1$}	5.11	[e]
C	5.57(5)	$^3A_2$, {...$7a_1^2 5b_2^2 8a_1^1 1a_2^2 2b_1^2 6b_2^2 9a_1^2 2a_2^1$}	5.50	[e]
		$^1A_1$, {...$7a_1^2 5b_2^2 8a_1^2 1a_2^1 2b_1^2 6b_2^2 9a_1^2 2a_2^1$}	5.51[d]	[e]
		$^1A_2$, {...$7a_1^2 5b_2^2 8a_1^1 1a_2^2 2b_1^2 6b_2^2 9a_1^2 2a_2^1$}	5.65	[e]
		$^3B_1$, {...$7a_1^2 5b_2^1 8a_1^2 1a_2^2 2b_1^2 6b_2^2 9a_1^2 2a_2^1$}	5.95	[e]
		$^3A_2$, {...$7a_1^1 5b_2^2 8a_1^2 1a_2^2 2b_1^2 6b_2^2 9a_1^2 2a_2^1$}	5.97	[e]
		$^1B_1$, {...$7a_1^2 5b_2^1 8a_1^2 1a_2^2 2b_1^2 6b_2^2 9a_1^2 2a_2^1$}	6.10[d]	[e]
Isomer XX				
X′	2.33(3)	$^1A_1$, {...$8a_1^2 1a_2^2 6b_2^2 2b_1^2 9a_1^2 3b_1^0$}	2.20	2.24
		$^1B_1$, {...$8a_1^2 1a_2^2 6b_2^2 2b_1^2 9a_1^1 3b_1^1$}	4.02	[e]
		$^3B_1$, {...$8a_1^2 1a_2^2 6b_2^2 2b_1^2 9a_1^1 3b_1^1$}	4.08	4.19
		$^3A_1$, {...$8a_1^2 1a_2^2 6b_2^2 2b_1^1 9a_1^2 3b_1^1$}	4.18	4.34
		$^3A_2$, {...$8a_1^2 1a_2^2 6b_2^1 2b_1^2 9a_1^2 3b_1^1$}	4.23	4.30
		$^1A_1$, {...$8a_1^2 1a_2^2 6b_2^2 2b_1^1 9a_1^2 3b_1^1$}	4.75	[e]
		$^3B_2$, {...$8a_1^2 1a_2^1 6b_2^2 2b_1^2 9a_1^2 3b_1^1$}	5.27	-
		$^3B_1$, {...$8a_1^1 1a_2^2 6b_2^2 2b_1^2 9a_1^2 3b_1^1$}	5.55	[e]
		$^1B_1$, {...$8a_1^1 1a_2^2 6b_2^2 2b_1^2 9a_1^2 3b_1^1$}	5.69	[e]
		$^1B_2$, {...$8a_1^2 1a_2^1 6b_2^2 2b_1^2 9a_1^2 3b_1^1$}	6.06[d]	[e]

[a] Numbers in parentheses represent the uncertainty in the last digit.
[b] VDEs were calculated at TD-B3LYP/6-311+G(2df)//B3LYP/6-311+G* level of theory.
[c] VDEs were calculated at CCSD(T)/6-311+G(2df)//B3LYP/6-311+G* level of theory.
[d] VDE corresponds to transition of multiconfigurational nature.
[e] VDE value cannot be calculated at this level of theory.

Table 5-3. Comparison of the experimental VDEs with the calculated values of structure **II** (C_2, ^{1}A) of the B_6Al^- cluster. All energies are in eV.

Feature	VDE (exp.)[a]	Final State and Electronic Configuration	VDE (theo.)	
			TD-B3LYP[b]	CCSD(T)[c]
X	2.49(3)	^{2}B, {...4a^{2}3b^{2}4b^{2}5a^{2}6a^{2}5b^1}	2.74	3.05
A	3.74(3)	^{2}A, {...4a^{2}3b^{2}4b^{2}5a^{2}6a^{1}5b^2}	3.52	3.50
B	3.98(3)	^{2}A, {...4a^{2}3b^{2}4b^{2}5a^{1}6a^{2}5b^2}	4.58	[d]
C	4.51(3)	^{2}B, {...4a^{2}3b^{2}4b^{1}5a^{2}6a^{2}5b^2}	4.59	[d]
D	5.26(3)	^{2}B, {...4a^{2}3b^{1}4b^{2}5a^{2}6a^{2}5b^2}	4.96	[d]

[a] Numbers in parentheses represent the uncertainty in the last digit.
[b] VDEs were calculated at TD-B3LYP/6-311+G(2df)//B3LYP/6-311+G* level of theory.
[c] VDEs were calculated at CCSD(T)/6-311+G(2df)//B3LYP/6-311+G* level of theory.
[d] VDE value cannot be calculated at this level of theory.

Table 5-4. Comparison of the experimental VDEs with the calculated values of structure **III** (C_s, ^{3}A") of the B_6Al^- cluster. All energies are in eV.

Feature	VDE (exp.)[a]	Final State and Electronic Configuration	VDE (theo.)	
			TD-B3LYP[b]	CCSD(T)[c]
X	2.49(3)	^{2}A", {...4a'^{2}5a'^{2}3a"^{2}4a"^{2}6a'^{2}5a"^{1}7a'^{0}}	2.48	2.43
A	3.74(3)	^{4}A", {...4a'^{2}5a'^{2}3a"^{2}4a"^{2}6a'^{1}5a"^{1}7a'^{1}}	3.51	3.57
B	3.98(3)	^{4}A', {...4a'^{2}5a'^{2}3a"^{2}4a"^{1}6a'^{2}5a"^{1}7a'^{1}}	3.85	4.03
C	4.51(3)	^{2}A', {...4a'^{2}5a'^{2}3a"^{2}4a"^{2}6a'^{1}5a"^{2}7a'^{0}}	4.25	4.00
D	5.26(3)	^{2}A", {...4a'^{2}5a'^{2}3a"^{2}4a"^{1}6a'^{2}5a"^{2}7a'^{0}}	4.30	[d]
		^{4}A', {...4a'^{2}5a'^{2}3a"^{1}4a"^{2}6a'^{2}5a"^{1}7a'^{1}}	4.40	[d]
		^{2}A", {...4a'^{2}5a'^{2}3a"^{1}4a"^{2}6a'^{2}5a"^{2}7a'^{0}}	4.79	[d]

[a] Numbers in parentheses represent the uncertainty in the last digit.
[b] VDEs were calculated at TD-B3LYP/6-311+G(2df)//B3LYP/6-311+G* level of theory.
[c] VDEs were calculated at CCSD(T)/6-311+G(2df)//B3LYP/6-311+G* level of theory.
[d] VDE value cannot be calculated at this level of theory.

Table 5-5. Comparison of the experimental VDEs with the calculated values of structure **XXI** (C_1, ^{2}A) of the $B_{11}Al^-$ cluster. All energies are in eV.

Feature	VDE (exp.)[a]	Final State and Electronic Configuration	VDE (theo.)	
			TD-B3LYP[b]	CCSD(T)[c]
		^{1}A, {...14a^{2}15a^{2}16a^{2}17a^{2}18a^{2}19a^0}	2.30	2.27
		^{3}A, {...14a^{2}15a^{2}16a^{2}17a^{2}18a^{1}19a^1}	3.85	3.96
		^{3}A, {...14a^{2}15a^{2}16a^{2}17a^{1}18a^{2}19a^1}	4.22	[d]
		^{1}A, {...14a^{2}15a^{2}16a^{2}17a^{2}18a^{1}19a^1}	4.31	[d]
		^{1}A, {...14a^{2}15a^{2}16a^{2}17a^{1}18a^{2}19a^1}	4.52	[d]
		^{3}A, {...14a^{2}15a^{2}16a^{1}17a^{2}18a^{2}19a^1}	4.57	[d]

[a] Numbers in parentheses represent the uncertainty in the last digit.
[b] VDEs were calculated at TD-B3LYP/6-311+G(2df)//B3LYP/6-311+G* level of theory.
[c] VDEs were calculated at CCSD(T)/6-311+G(2df)//B3LYP/6-311+G* level of theory.
[d] VDE value cannot be calculated at this level of theory.

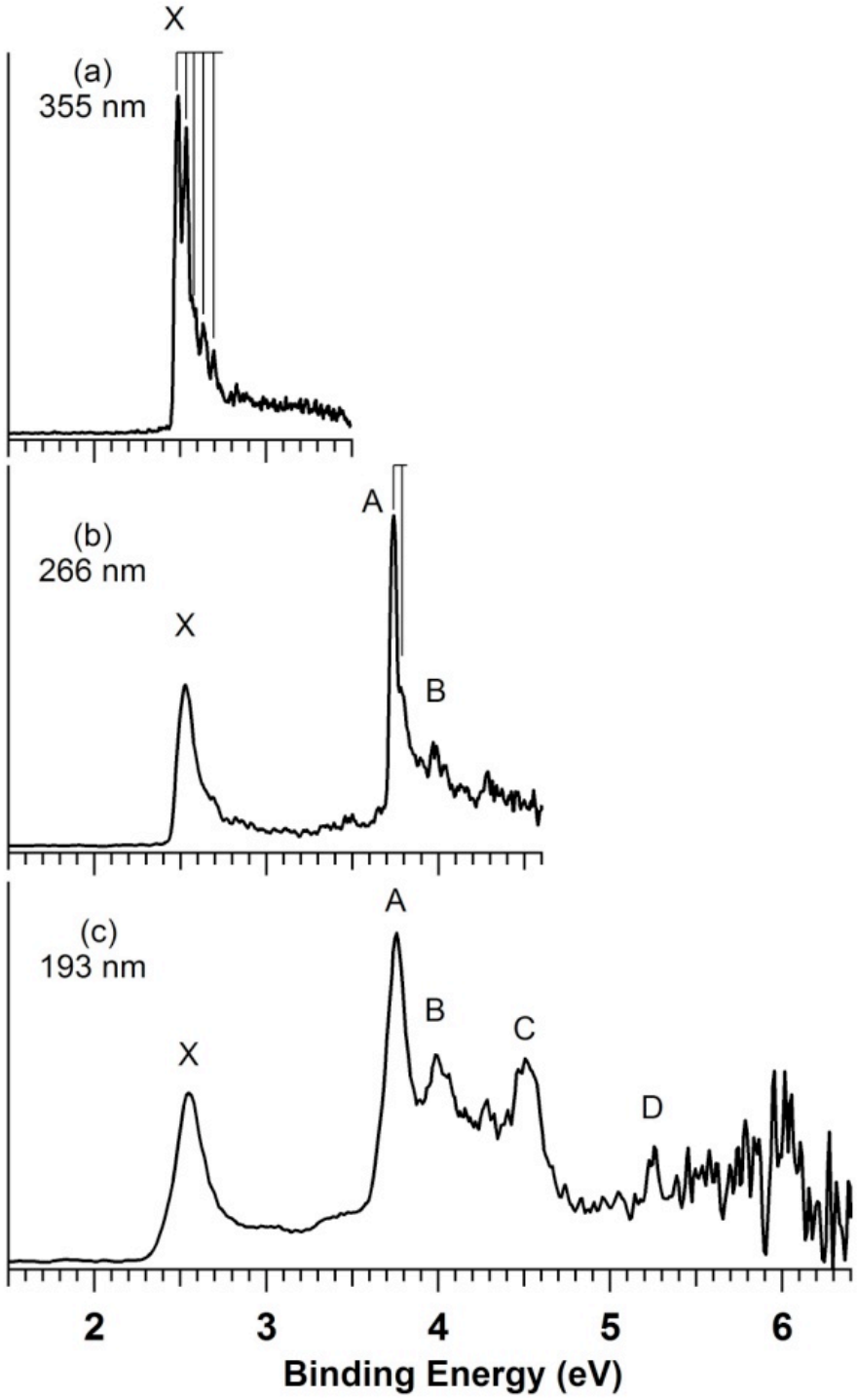

Figure 5-1. Photoelectron spectra of AlB_6^- at (a) 355 nm (3.496 eV), (b) 266 nm (4.661 eV), and (c) 193 nm (6.424 eV). Vertical lines in (a) and (b) represent resolved vibrational structures.

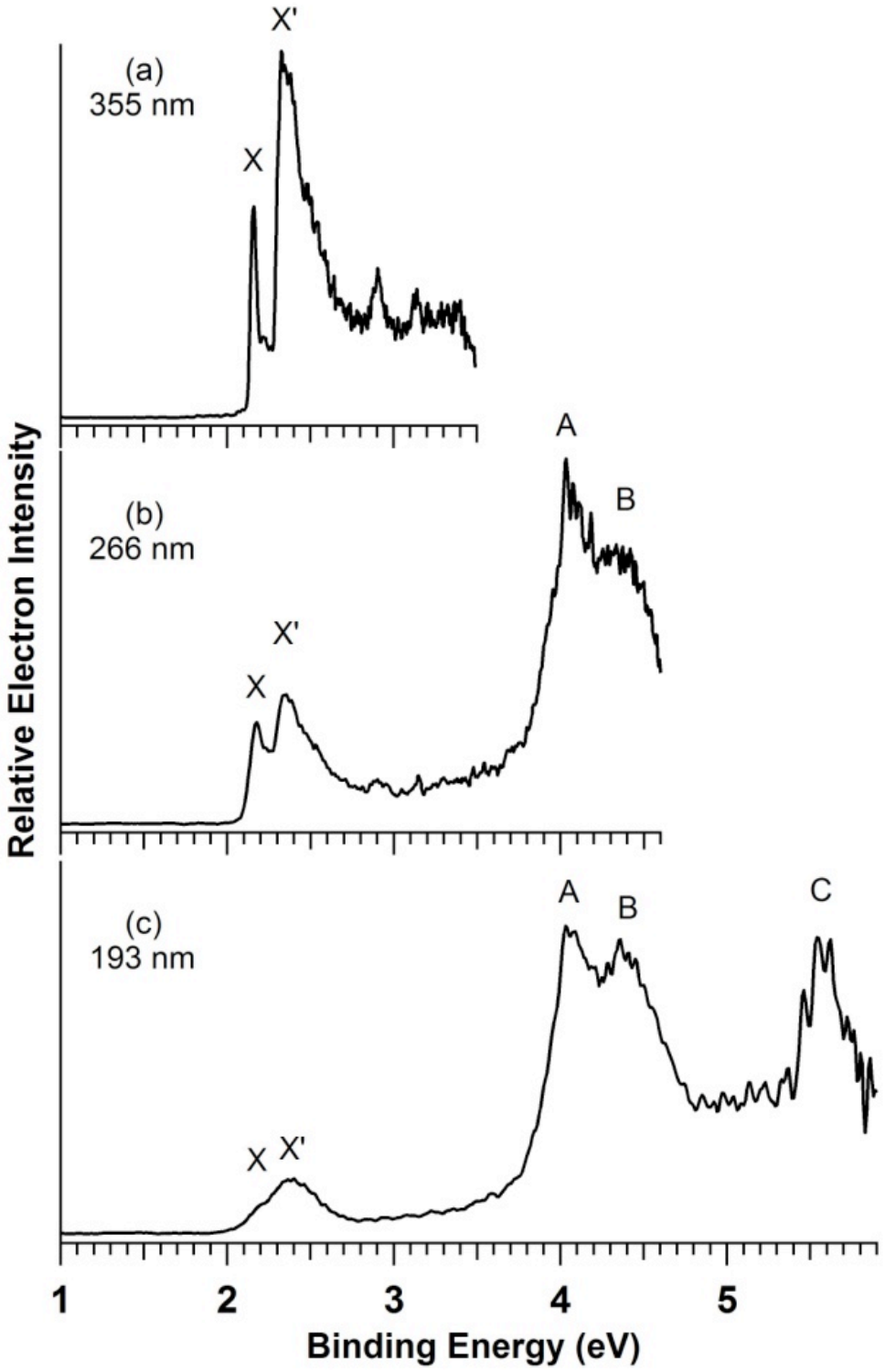

Figure 5-2. Photoelectron spectra of AlB_{11}^- at (a) 355 nm, (b) 266 nm, and (c) 193 nm.

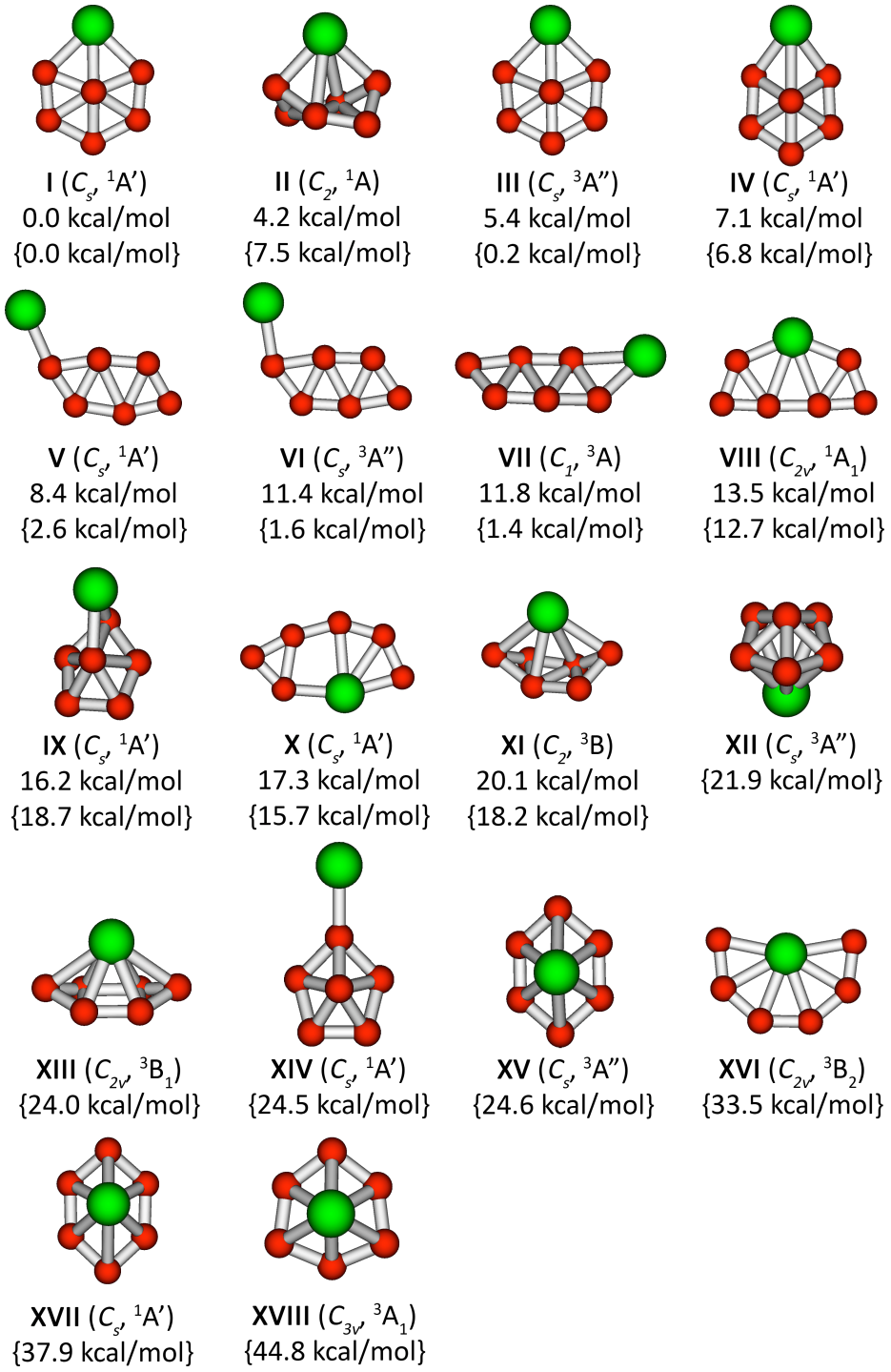

Figure 5-3. Optimized structures for AlB_6^-, their point group symmetries, spectroscopic states, and relative energies. Relative energies are given at CCSD(T)/6-311+G(2df)//B3LYP/6-311+G* and at B3LYP/6-311+G* (in curly brackets). All the relative energies have been corrected for zero-point energies calculated at the B3LYP/6-311+G* level.

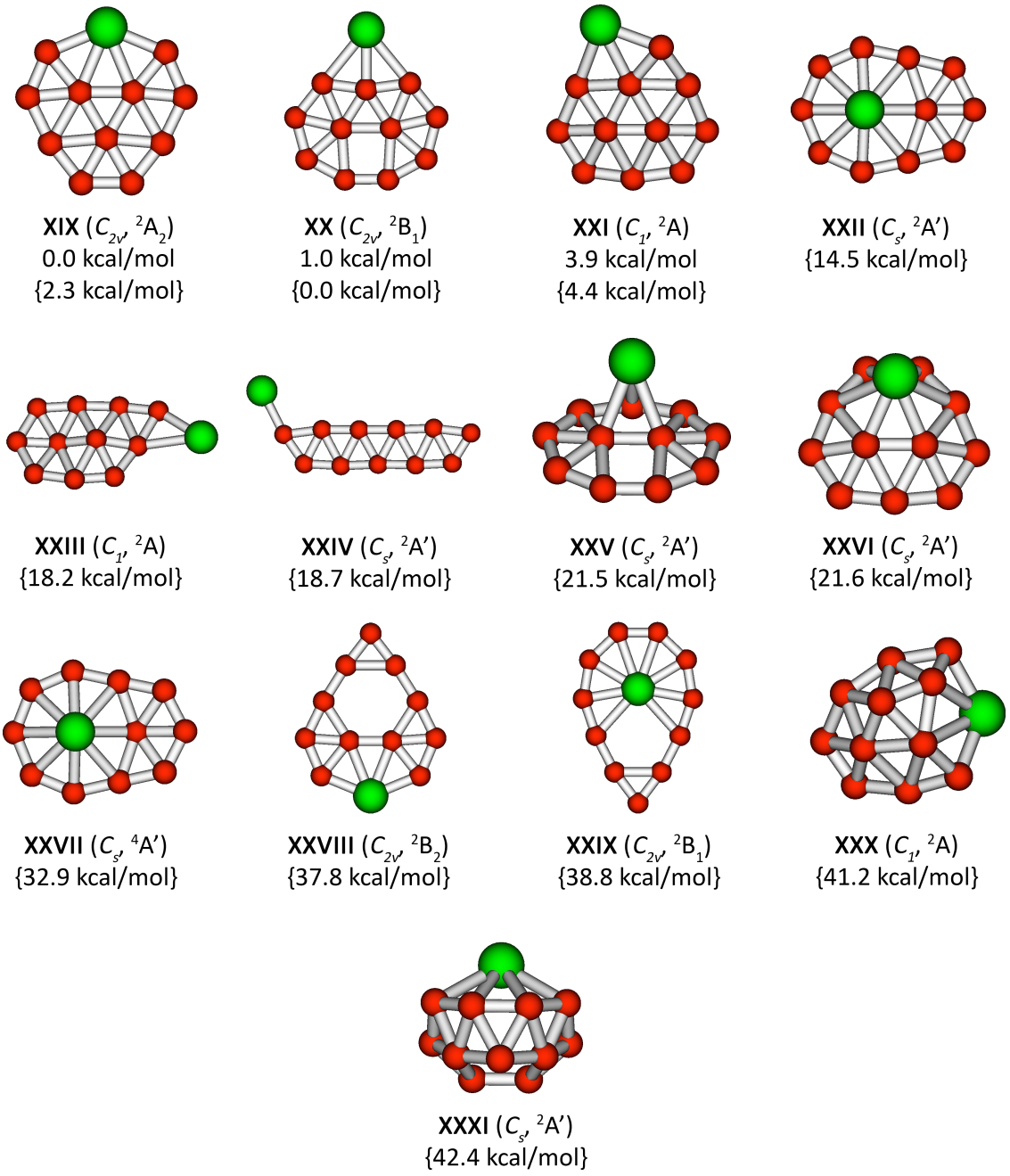

Figure 5-4. Optimized structures for AlB_{11}^-, their point group symmetries, spectroscopic states, and relative energies. Relative energies are given at CCSD(T)/6-311+G(2df)//B3LYP/6-311+G* and at B3LYP/6-311+G* (in curly brackets). All the relative energies have been corrected for zero-point energies calculated at the B3LYP/6-311+G* level.

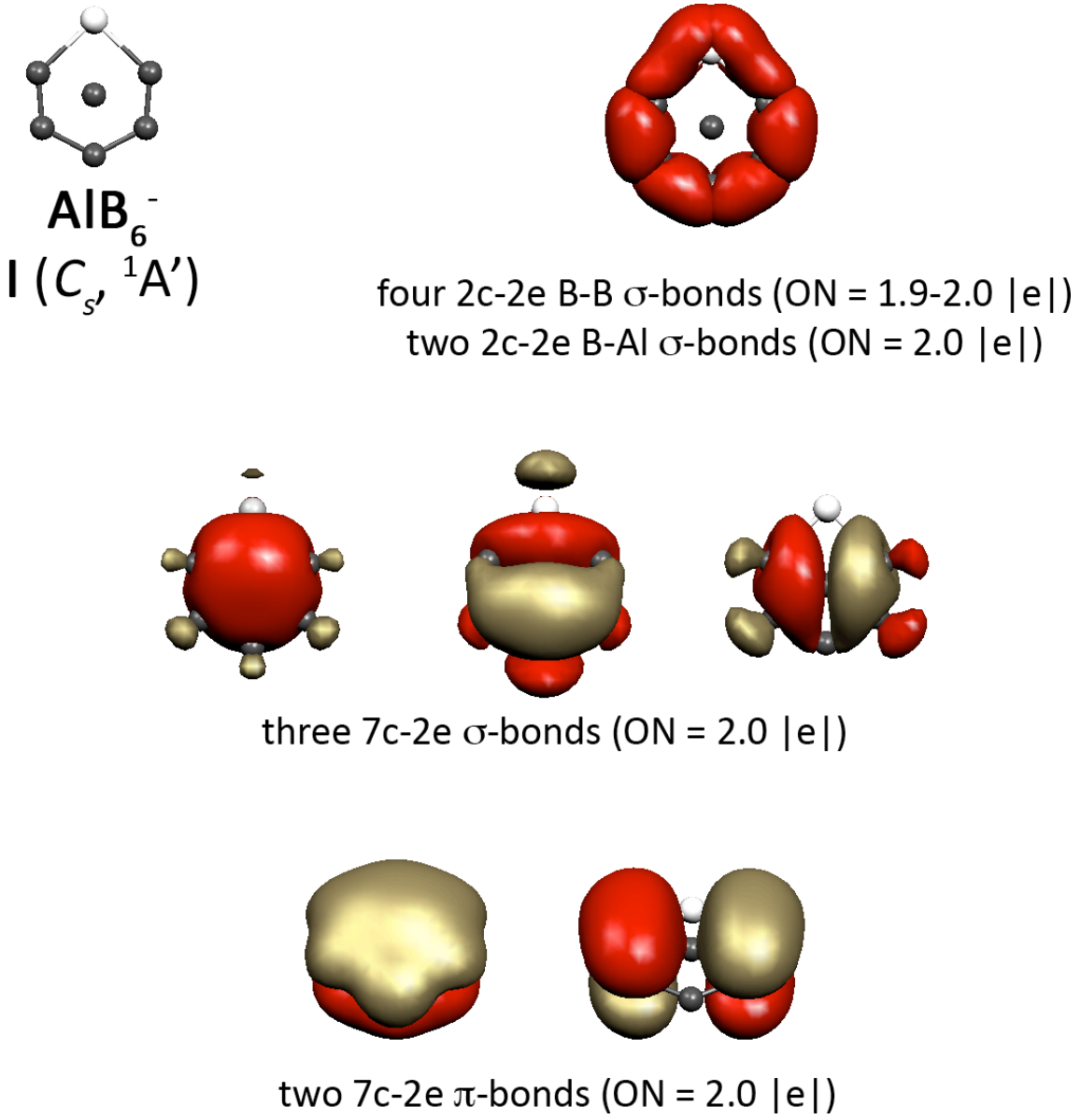

Figure 5-5. Chemical bonding analysis for the global minimum of AlB_6^- (isomer **I**, C_s, $^1A'$) at the AdNDP/B3LYP/3-21G//B3LYP/6-311+G* level.

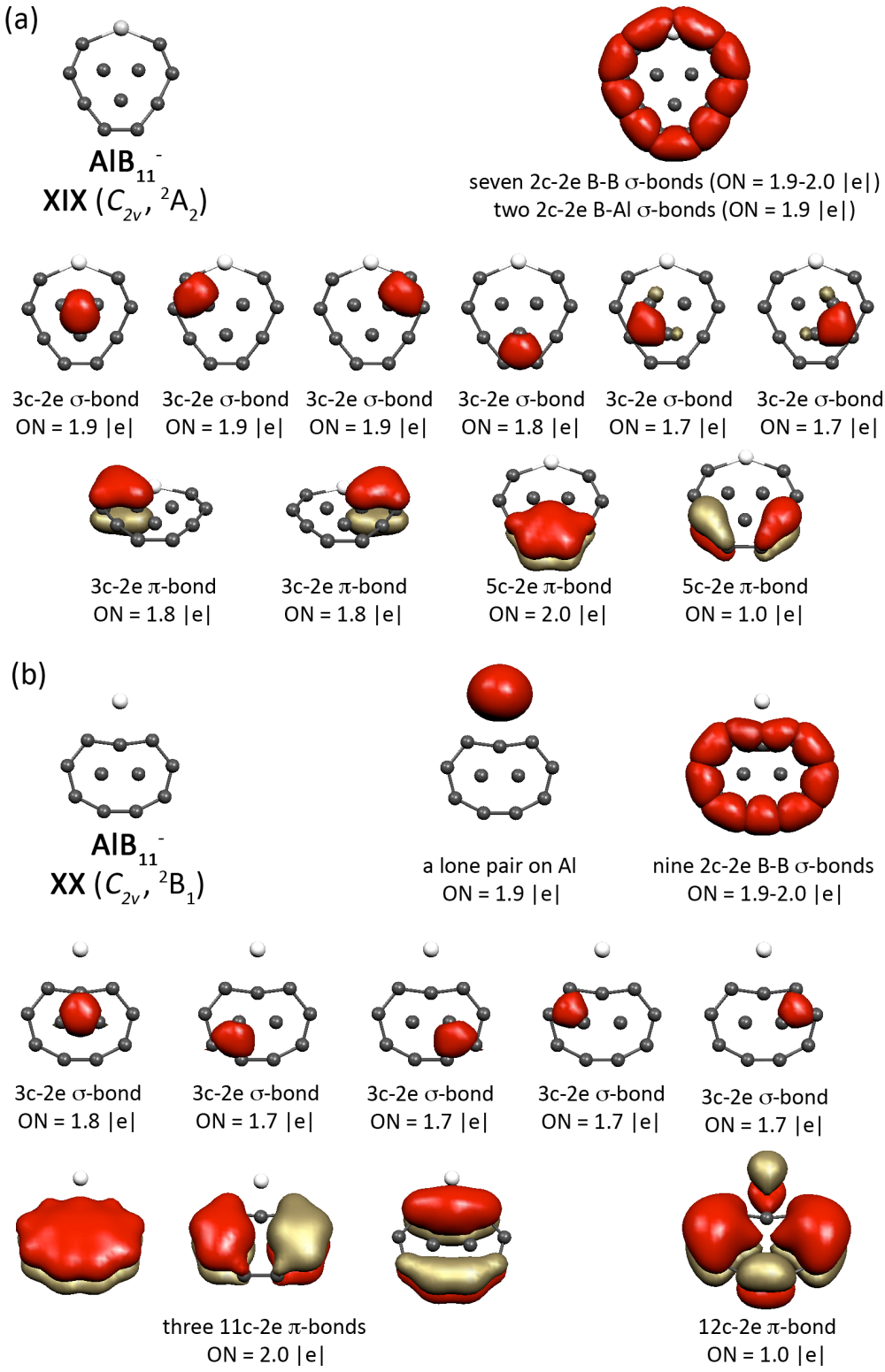

Figure 5-6. Chemical bonding analysis of the two lowest energy structures of AlB_{11}^- at the AdNDP/B3LYP/3-21G//B3LYP/6-311+G* level: (a) isomer **XIX** (C_{2v}, $^2A_2$); (b) isomer **XX** (C_{2v}, $^2B_1$).

CHAPTER 6

DECIPHERING THE MYSTERY OF HEXAGON HOLES IN ALL-BORON GRAPHENE α-SHEET[1]

Abstract

Boron could be the next element after carbon capable of forming 2D-materials similar to graphene. Theoretical calculations predict that the most stable planar all-boron structure is the so-called α-sheet. The mysterious structure of α-sheet with peculiar distribution of filled and empty hexagons is rationalized in terms of chemical bonding. We show that the hexagon holes serve as scavengers of extra electrons from the filled hexagons. This work could advance rational design of all-boron nanomaterials.

Recently discovered graphene,[1,2] a one-atom-thick planar sheet of carbon atoms densely packed in a honeycomb crystal lattice gave us the opportunity to probe properties of 2D-materials. The isolated layers of graphene were found to exhibit high carrier mobilities (>200 000 $cm^2\ V^{-1}\ s^{-1}$ at electron densities of 2 x 10^{11} cm^{-2}),[3-6] exceptional Young modulus values (>0.5-1 TPa), and large force constants (1-5 Nm^{-1}).[7-9] Due to these properties graphene is attractive for many potential commercial applications such as energy storage,[10] micro- and optoelectronics.[11]

Boron, the light neighbour of carbon in the Periodic Table, is an excellent next candidate for acquiring 2D-structures. Indeed, graphite-like material MgB_2, which possesses remarkable superconductivity near 40 K,[12] is composed of planar honeycomb

[1] Coauthored by Timur R. Galeev, Qiang Chen, Jin-Chang Guo, Hui Bai, Chang-Qing Miao, Hai-Gang Lu, Alina P. Sergeeva, Si-Dian Li, Alexander I. Boldyrev with permission from *Phys. Chem. Chem. Phys.* **2011**, 13, 11575-11578.

crystal lattices of boron atoms with magnesium atoms located above the center of the hexagons between the layers. Thus, each of the all-boron graphite-like sheets in MgB_2 is an example of a 2D-structure composed of boron atoms. However, boron atoms in MgB_2 have a charge of -1 and thus acquire electronic configuration similar to that of carbon. One can construct a honeycomb crystal lattice of neutral boron sheet assuming that every boron is sp^2-hybridized and forms three two-center-two-electron (2c-2e) σ-bonds. Such structure was shown to be less stable than the truly remarkable α-sheet structure (Fig. 6-1), computationally predicted by Tang and Ismail-Beigi[13,14] and Yang, Ding and Ni.[15] This structure is formed of two types of hexagons: empty hexagons and ones with an additional boron atom at the center. Similar pattern with hexagon holes and filled hexagons was predicted for boron nanotubes.[15,16] All-boron fullerenes with a similar network of filled hexagons and pentagon holes have also attracted significant attention[13,16-27] since Szwacki, Sadrzadeh and Yakobson predicted a highly spherical buckyball structure for B_{80}.[28]

The 2D-lattice with hexagon holes and filled hexagon motifs in the α-sheet is puzzling and understanding its chemical bonding pattern could be an important advancement towards future design of all-boron nanostructures. In order to address this issue we performed a chemical bonding analysis for the lattice. To date there is no computational tool capable of analyzing chemical bonding in terms of 2c-2e, 3c-2e or *n*c-2e bonds in general in infinite 2D-lattices, therefore we investigated chemical bonding in fragments of the all-boron α-sheet. For our analysis we chose three α-sheet fragments, which are shown in Fig. 6-2, 6-3, and 6-4. They were selected in a way to preserve electro neutrality when placed into the 2D-α-sheet. These fragments allowed us to trace

all bonding elements in the α-sheet and reduce the influence of the boundary conditions in our fragments upon extension of their size.

Since chemical bonding in the all-boron α-sheet was anticipated to involve delocalized bonding we selected the Adaptive Natural Density Partitioning (AdNDP) method as a tool for our chemical bonding analysis. This method was recently developed by Zubarev and Boldyrev[29] and used to analyze chemical bonding in boron clusters,[29-31] prototypical aromatic organic molecules[32] and gold clusters.[33] The AdNDP method analyzes the first-order reduced density matrix in order to obtain its local block eigenfunctions with optimal convergence properties for electron density description. The obtained local blocks correspond to the sets of *n* atoms (*n* ranging from one to the total number of atoms in the molecule) that are tested for presence of two-electron objects (*n*-center two electron (*n*c-2e) bonds, including core electrons and lone pairs as a special case of *n*=1) associated with this particular set of *n* atoms. AdNDP initially searches for core electron pairs and lone pairs (1c-2e), then 2c-2e, 3c-2e, … and finally *n*c-2e bonds. At every step the density matrix is depleted of the density corresponding to the appropriate bonding elements. User-directed form of the AdNDP analysis can be applied to specified molecular fragments and is analogous to the directed search option of the standard Natural Bond Orbital (NBO) code.[34,35] AdNDP accepts only those bonding elements, whose occupation numbers (ON) exceed the specified threshold values, which are usually chosen to be close to 2.00 |e|. When all recovered *n*c-2e bonding elements are superimposed onto the molecular frame the overall pattern always correspond to the point-group symmetry of the system. Thus, AdNDP recovers both Lewis bonding elements (1c-2e and 2c-2e objects, corresponding to the core electrons and lone pairs, and

two-center two-electron bonds) and delocalized bonding elements, which are associated with the concepts of aromaticity and antiaromaticity. From this point of view, AdNDP achieves seamless description of systems featuring both localized and delocalized bonding without invoking the concept of resonance. Essentially, AdNDP is a very efficient and visual approach to interpretation of the molecular orbital-based wave functions.

We performed the AdNDP analysis of the all boron α-sheet fragments with geometric parameters (B-B distance of 1.67Å) of the predicted lattice structure.[13,15] We used hybrid density functional method known in the literature as B3LYP with the 6-31G basis set. AdNDP is an extension of the NBO analysis[34,35] and it was shown before[29,36] that AdNDP is not sensitive to the level of theory or the basis set. All calculations were performed using the AdNDP program and the Gaussian 03 software package.[37] Molecular visualization was performed using Molekel 5.4.[38]

First, we analyzed the seven-atom (the filled hexagon) fragment of the α-sheet (Fig. 6-2a). The charge of +7 was selected for the bare B_7 cluster from a few trial AdNDP runs which allowed us to have a symmetric chemical bonding picture with bonding elements, which will be shown later to be present in the 2D α-sheet lattice. The AdNDP analysis revealed six 3c-2e σ-bonds and one 7c-2e π–bond in the B_7^{+7} fragment. In order to reduce external charge we ran AdNDP calculations for the $B_7H_6^+$ cluster. The analysis revealed the same chemical bonding pattern with additional six 2c-2e B-H σ-bonds (Fig. 6-2b), showing robustness of the chemical bonding picture.

The second model system was chosen in order to understand how the chemical bonding picture changes upon addition of three neighbouring filled hexagons to the B_7

motif (Fig. 6-3a). The AdNDP analysis of the B_{22}^{+16} cluster revealed a 3c-2e σ-bond in every peripheral triangle while a 4c-2e σ-bond was found in every rhombus motif at the junction of two hexagons (Fig. 6-3a). In addition, a 7c-2e π-bond on every filled hexagon was revealed using the user-directed form of the AdNDP method. It will be shown below that the newly found 4c-2e σ-bonds are present in the α-sheet at all junctions of the filled hexagons. Again, in order to test robustness of this chemical bonding pattern we performed the same analysis for the $B_{22}H_{12}^{+4}$ system (Fig. 6-3b). We found that the bonding picture is the same as that for the B_{22}^{+16} cluster with additional twelve 2c-2e B-H σ-bonds.

The B_{30}^{+16} cluster was chosen as a fragment of the all-boron α-sheet containing a hexagonal hole (Fig. 6-4). The AdNDP analysis revealed twenty-four 3c-2e σ-bonds at the peripheral triangles and triangles bordering upon the hole. Again, a 4c-2e σ-bond was found in every rhombus motif at the junction of two hexagons. Then a 7c-2e π-bond was revealed on every filled hexagon using the user directed AdNDP method as well as the new bonding element in this cluster: a 6c-2e π-bond over the hexagon hole at the center. The analysis of the largest studied fragment allowed us to recover the last missing bonding element – the 6c-2e π-bond over the hexagon hole.

From the chemical bonding analyses of the model fragments we now can propose the following chemical bonding picture (Fig. 1b) for the infinite all-boron α-sheet. On every filled hexagon we found three 3c-2e σ-bonds (solid triangles), which are bordering upon the holes, three 4c-2e σ-bonds (solid rhombi) at the junction of two filled hexagons, and one 7c-2e π-bond (circles). With this chemical bonding for each B_7 fragment we

have six valence electrons coming from three 3c-2e σ-bonds, three electrons coming from three 4c-2e σ-bonds and two electrons coming from the 7c-2e π-bond with the total number of eleven electrons. On the other hand, if we consider a filled hexagon as a part of the lattice we can calculate the total number of valence electrons as follows: each of the six peripheral boron atoms brings half of its valence electrons (9 electrons in total) and the central atom brings all its valence electrons (3 electrons) resulting in the total of twelve electrons per filled hexagon. Thus, there is one extra electron on each filled hexagon motif not involved in the bonding presented above. As one can see from the whole lattice picture the extra electron on a filled hexagon (an electronic donor) is shared by three hexagonal holes (three electronic acceptors) evenly distributed around it, while each hole is surrounded by six filled hexagons, resulting in two "extra" electrons per hole. Those two electrons form the 6c-2e π-bond (Fig. 6-1b, circles over hexagon holes), which was revealed in our B_{30}^{+16} model system. It is interesting to notice that, unlike graphene, which contains in-plane 2c-2e C-C σ-bonds, the all-boron graphene α-sheet studied in this work possesses no localized 2c-2e B-B σ-interactions.

Occupation numbers (ONs) revealed for every bonding element are very close to the ideal value of 2.00 |e| (see Fig. 6-2, 6-3, and 6-4) giving additional credibility to the presented chemical bonding picture for all-boron α-sheet.

The AdNDP method revealed a delocalized π-bond on every filled hexagon and every hexagon hole. Each π-bond is responsible for local π-aromaticity in the corresponding fragment. We further probed the revealed π-aromaticity using one of the most popular ways of evaluating aromaticity in planar species, the nuclear independent chemical shift ($NICS_{zz}$), which was introduced by Schleyer and co-workers.[39] In this

method negative $NICS_{zz}$ values indicate aromaticity and positive values indicate antiaromaticity. $NICS_{zz}$ calculations were performed above the center of the filled and empty hexagons in the B_{30}^{+16} model system using the B3LYP/6-311+G* level of theory. We also calculated the same set of the $NICS_{zz}$ values for the prototypical aromatic system, benzene, using the B3LYP/6-311++G** level of theory. Results of all the calculations are summarized in Table 6-1.

One can see that the $NICS_{zz}$ values above the filled hexagons and hexagon holes are significantly more negative than the corresponding values of benzene, thus, confirming the presence of local π-aromaticity in the hexagons.

From our overall chemical bonding picture we get a 1/3 ratio for the numbers of valence π- and σ-electrons in the all-boron α-sheet, which was obtained from the fact that out of total of twelve valence electrons on each filled hexagon motif (including the one it donates to the holes) three form π-bonds and nine form σ-bonds. We would like to stress that this ratio is close to that of the so far largest planar boron clusters studied both experimentally and theoretically: B_{16}^{2-} (the valence π- to σ- ratio is 0.25)[30] and B_{19}^{-} (the valence π- to σ- ratio is 0.26).[31] The presence of holes as well as their amount relative to the number of filled hexagons in the all-boron α-sheet is determined by this π- to σ-electrons ratio: the holes in the all-boron α-sheet absorb the third π-electron of each filled hexagon, which cannot be accepted by the motif. Interestingly, the ratio of 1/9 between the number of the donated π-electrons (1 electron) and the number of total σ-electrons (9 electrons) in a filled hexagon equals to the hexagon hole density of 1/9 in the infinite all-boron α-sheet.[13] This analysis agrees with the proposed chemical bonding pattern demonstrated in Fig. 6-1b for a building block of the α-sheet boron.

Now it is clear why the hypothetical honeycomb crystal lattice of neutral boron sheet where each boron atom acquires sp^2-hybridization and forms three 2c-2e σ-bonds but no π-bonds is not energetically favourable. In order for neutral all-boron 2D-structure to be energetically favourable it should have a certain amount of electron density in π-system. If we transfer some amount of electrons from the 2c-2e σ-bonds in the honeycomb crystal lattice to π-system it breaks the connectivity in the σ-framework and that makes the whole structure energetically unfavourable. The all-boron neutral 2D-structure composed of boron equilateral triangles (or of filled hexagons but with no holes), the so-called triangular sheet, also should be unstable. There are two ways to construct the triangular boron sheet in accordance with our bonding model. First, if one tried to build it with every triangle carrying a 3c-2e σ-bond, there would not be enough electrons even for such σ-bonding, since every boron atom belongs to six triangles and therefore it can give only 3x(1/6)=1/2 electrons to each 3c-2e σ-bond, which leads to 1.5 electrons per bond only. Alternatively, we can construct the neutral all-boron 2D-sheet of filled hexagons with presence of six 4c-2e σ-bonds (they are shared with the neighbouring hexagons) and six π-orbitals on each filled hexagon. This structure is also unfavourable since the ratio of π- to σ- electrons is 0.5, which was not observed for the lowest energy planar boron clusters.[30, 31, 40-42]

The unprecedented chemical bonding model presented in the current work widens our understanding of chemical bonding in general and we believe that the presented bonding picture could be an advance toward rational design of future all-boron nanomaterials.

References

1 K. S. Novoselov, A. K. Geim, S. V. Morozov, D. Jiang, Y. Zhang, S. V. Dubonos, I. V. Grigorieva and A. A. Firsov, *Science*, 2004, **306**, 666.

2 K. S. Novoselov, A. K. Geim, S. V. Morozov, D. Jiang, M. I. Katsnelson, I. V. Grigorieva, S. V. Dubonos and A. A. Firsov, *Nature*, 2005, **438**, 197.

3 S. Unarunotai, Y. Murata, C. E. Chialvo, N. Mason, I. Petrov, R. G. Nuzzo, J. S. Moore and J. A. Rogers, *Adv. Mater.*, 2010, **22**, 1072.

4 K. I. Bolotin, K. J. Sikes, Z. Jiang, M. Klima, G. Gudenberg, J. Hone, P. Kim and H. L. Stormer, *Solid State Commun.*, 2008, **16**, 351.

5 S. V. Morozov, K. S. Novoselov, M. I. Katsnelson, F. Schedin, D. C. Elias, J. A. Jaszcnak and A. K. Geim, *Phys. Rev. Lett*., 2008, **100**, 016602.

6 X. Du, I. Skachko, A. Barker and E. Y. Andrei, *Nat. Nanotechnol.*, 2008, **3**, 491.

7 I. W. Frank, D. M. Tanenbaum, A. M. van der Zanda and P. L. McEuen, *J. Vac. Sci. Technol. A*, 2007, **25**, 2558.

8 F. Scarpa, S. Adhikari and A. S. Phani, *Nanotechnology*, 2009, **20**, 065709.

9 R. Faccio, P. A. Denis, H. Pardo, C. Goyenola and A. W. Mombru, *J. Phys. Condens. Matter*, 2009, **21**, 285304

10 M. D. Stoller, S. Park, Y. Zhu, J. An and R. S. Ruoff, *Nano Lett*., 2008, **8**, 3498.

11 K. Mullen and J. P. Rabe, *Acc. Chem. Res*., 2008, **41**, 511.

12 J. Nagamatsu, N. Nakagawa, T. Muranaka, Y. Zenitani and J. Akimitsu, *Nature*, 2001, **410**, 63.

13 H. Tang and S. Ismail-Beigi, *Phys. Rev. Lett*., 2007, **99**, 115501.

14 H. Tang and S. Ismail-Beigi, *Phys. Rev. B*, 2009, **80**, 134113.

15 X. Yang, Y. Ding and J. Ni, *Phys. Rev. B*, 2008, **77**, 0414402.

16 N. G. Szwacki and C. J. Tymczak, *Chem. Phys. Lett.*, 2010, **494**, 80.

17 G. Gopakumar, M. T. Nguyen and A. Ceulemans, *Chem. Phys. Lett.*, 2008, **450**, 175.

18 T. Baruah, M. R. Pederson and R. R. Zope, *Phys. Rev. B*, 2008, **78**, 045408.

19 A. Sadrzadeh, O. V. Pupysheva, A. K. Singh and B. I. Yakobson, *J. Phys. Chem. A*, 2008, **112**, 13679.

20 S. Botti, A. Castro, N. N. Lathiotakis, X. Andrade and M. A. L. Marques, *Phys. Chem. Chem. Phys.*, 2009, **11**, 4523.

21 Q. B. Yan, Q. R. Zheng and G. Su, *Phys. Rev. B*, 2008, **77**, 224106.

22 A. Y. Liu, R. R. Zope and M. R. Pederson, *Phys. Rev. B*, 2008, **78**, 155422.

23 N. G. Szwacki, *Nanoscale Res. Lett.*, 2008, **3**, 80.

24 Q. B. Yan, X. L. Sheng, Q. R. Zheng, L. Zhang and G. Su, *Phys. Rev. B*, 2008, **78**, 201401R.

25 R. R. Zope, T. Baruah, K. C. Lau, A. Y. Liu, M. R. Pederson and B. I. Dunlap, *Phys. Rev. B*, 2009, **79**, 161403R.

26 J. Zhao, L. Wang, F. Li and Z. Chen, *J. Phys. Chem. A*, 2010, **114**, 9969.

27 P. Jin, C. Hao, Z. Gao, S. Zhang and Z. Chen, *J. Phys. Chem. A*, 2009, **113**, 11613.

28 N. G. Swacki, A. Sadrzadeh and B. I. Yakobson, *Phys. Rev. Lett.*, 2007, **98**, 166804.

29 D. Y. Zubarev and A. I. Boldyrev, *Phys. Chem. Chem. Phys.*, 2008, **10**, 5207.

30 A. P. Sergeeva, D. Y. Zubarev, H.-J. Zhai, A. I. Boldyrev and L. S. Wang, *J. Am. Chem. Soc.*, 2008, **130**, 7244.

31 W. Huang, A. P. Sergeeva, H.-J. Zhai, B. B. Averkiev, L. S. Wang and A. I. Boldyrev, *Nat. Chem.*, 2010, **2**, 202.

32 D. Y. Zubarev and A. I. Boldyrev, *J. Org. Chem.*, 2008, **73**, 9251.

33 D. Y. Zubarev and A. I. Boldyrev, *J. Phys. Chem.*, 2009, **13**, 866.

34 J. P. Foster and F. Weinhold, *J. Am. Chem. Soc.*, 1980, **102**, 7211.

35 F. Weinhold and C. Landis, *Valency and Bonding. A Natural Bond Orbital Donor-Acceptor Perspective*, Cambridge University Press, Cambridge, UK, 2005.

36 A. P. Sergeeva and A. I. Boldyrev, *Comm. Inorg. Chem.*, 2010, **31**, 2.

37 M. J. Frisch, G. W. Trucks, H. B. Schlegel, G. E. Scuseria, M. A. Robb, J. R. Cheeseman, J. A. Montgomery, Jr., T. Vreven, K. N. Kudin, J. C. Burant, J. M. Millam, S. S. Iyengar, J. Tomasi, V. Barone, B. Mennucci, M. Cossi, G. Scalmani, N. Rega, G. A. Petersson, H. Nakatsuji, M. Hada, M. Ehara, K. Toyota, R. Fukuda, J. Hasegawa, M. Ishida, T. Nakajima, Y. Honda, O. Kitao, H. Nakai, M. Klene, X. Li, J. E. Knox, H. P. Hratchian, J. B. Cross, V. Bakken, C. Adamo, J. Jaramillo, R. Gomperts, R. E. Stratmann, O. Yazyev, A. J. Austin, R. Cammi, C. Pomelli, J. W. Ochterski, P. Y. Ayala, K. Morokuma, G. A. Voth, P. Salvador, J. J. Dannenberg, V. G. Zakrzewski, S. Dapprich, A. D. Daniels, M. C. Strain, O. Farkas, D. K. Malick, A. D. Rabuck, K. Raghavachari, J. B. Foresman, J. V. Ortiz, Q. Cui, A. G. Baboul, S. Clifford, J. Cioslowski, B. B. Stefanov, G. Liu, A. Liashenko, P. Piskorz, I. Komaromi, R. L. Martin, D. J. Fox, T. Keith, M. A. Al-Laham, C. Y. Peng, A. Nanayakkara, M. Challacombe, P. M. W. Gill, B. Johnson, W. Chen, M. W. Wong, C. Gonzalez and J. A. Pople, *GAUSSIAN 03, (Revision D.01)*, Gaussian, Inc., Wallingford, CT, 2004.

38 U. Varetto, Molekel 5.4.0.8, Swiss National Supercomputing Centre, Manno (Switzerland).

39 P. v. R. Schleyer, C. Maerker, A. Dransfeld, H. Jiao and N. J. R. v. E. Hommes, *J. Am. Chem. Soc.*, 1996, **118**, 6317.

40 A. N. Alexandrova, A. I. Boldyrev, H. J. Zhai and L. S. Wang, *Coord. Chem. Rev*., 2006, **250**, 2811.

41 B. Kiran, S. Bulusu, H. J. Zhai, S. Yoo, X. C. Zeng and L. S. Wang, *Proc. Natl. Acad. Sci. U. S. A.*, 2005, **102**, 961.

42 H. J. Zhai, B. Kiran, J. Li and L. S. Wang, *Nature Materials*, 2003, **2**, 827.

Table 6-1 Calculated NICSzz values (ppm)

R_z (Å)[a]	Filled hexagon[b]	Hexagon hole[b]	Benzene[c]
0.0	-	-51.5	-14.5
0.2	-100.4	-53.0	-16.3
0.4	-75.3	-56.9	-20.6
0.6	-70.8	-61.7	-25.2
0.8	-66.3	-66.1	-28.3
1.0	-60.8	-68.9	-29.2
1.2	-55.2	-69.9	-28.2
1.4	-49.9	-69.0	-26.0
1.6	-45.2	-66.8	-23.2
1.8	-41.0	-63.6	-20.2
2.0	-37.3	-59.8	-17.4

[a] Distance from hexagon centre
[b] Calculated at B3LYP/6-311+G*
[c] Calculated at B3LYP/6-311++G**

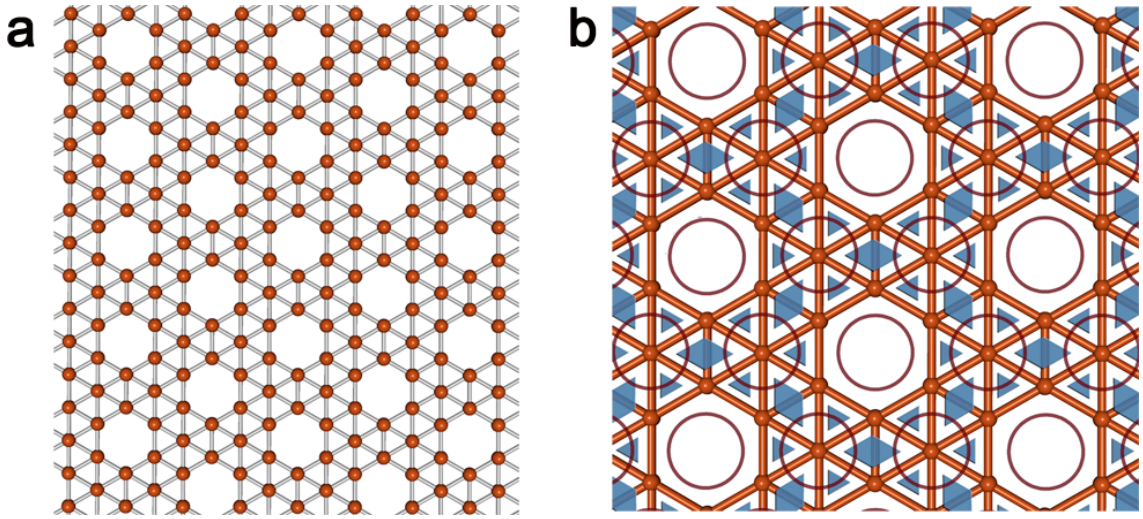

Fig. 6-1 (a) Geometric structure of all-boron α-sheet. (b) The proposed bonding pattern for all-boron α-sheet: 3c-2e σ-bonds (solid triangles), 4c-2e σ-bonds (solid rhombi) and delocalized π-bonds (circles).

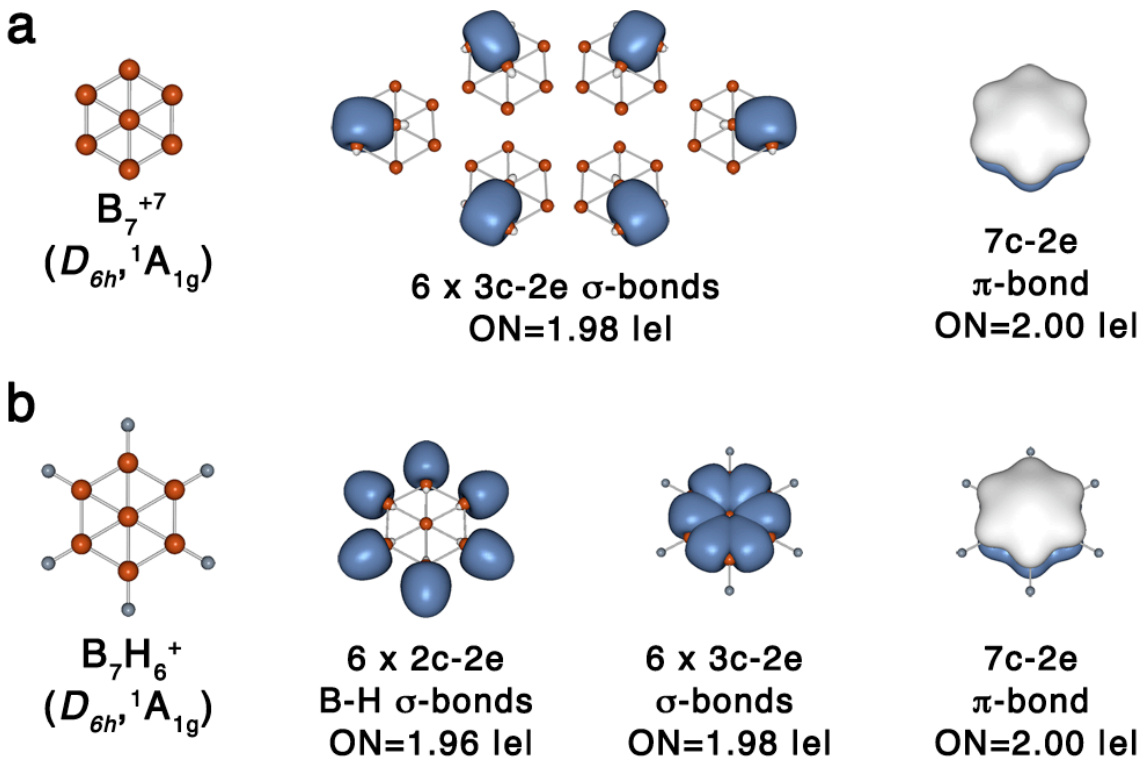

Fig. 6-2 (a) Geometric structure of the B_7^{+7} fragment, six 3c-2e σ-bonds, and one 7c-2e π-bond. (b) Geometric structure of the $B_7H_6^+$ fragment, six 2c-2e B-H σ-bonds superimposed on a single framework, six 3c-2e σ-bonds superimposed on a single framework, and one 7c-2e π-bond.

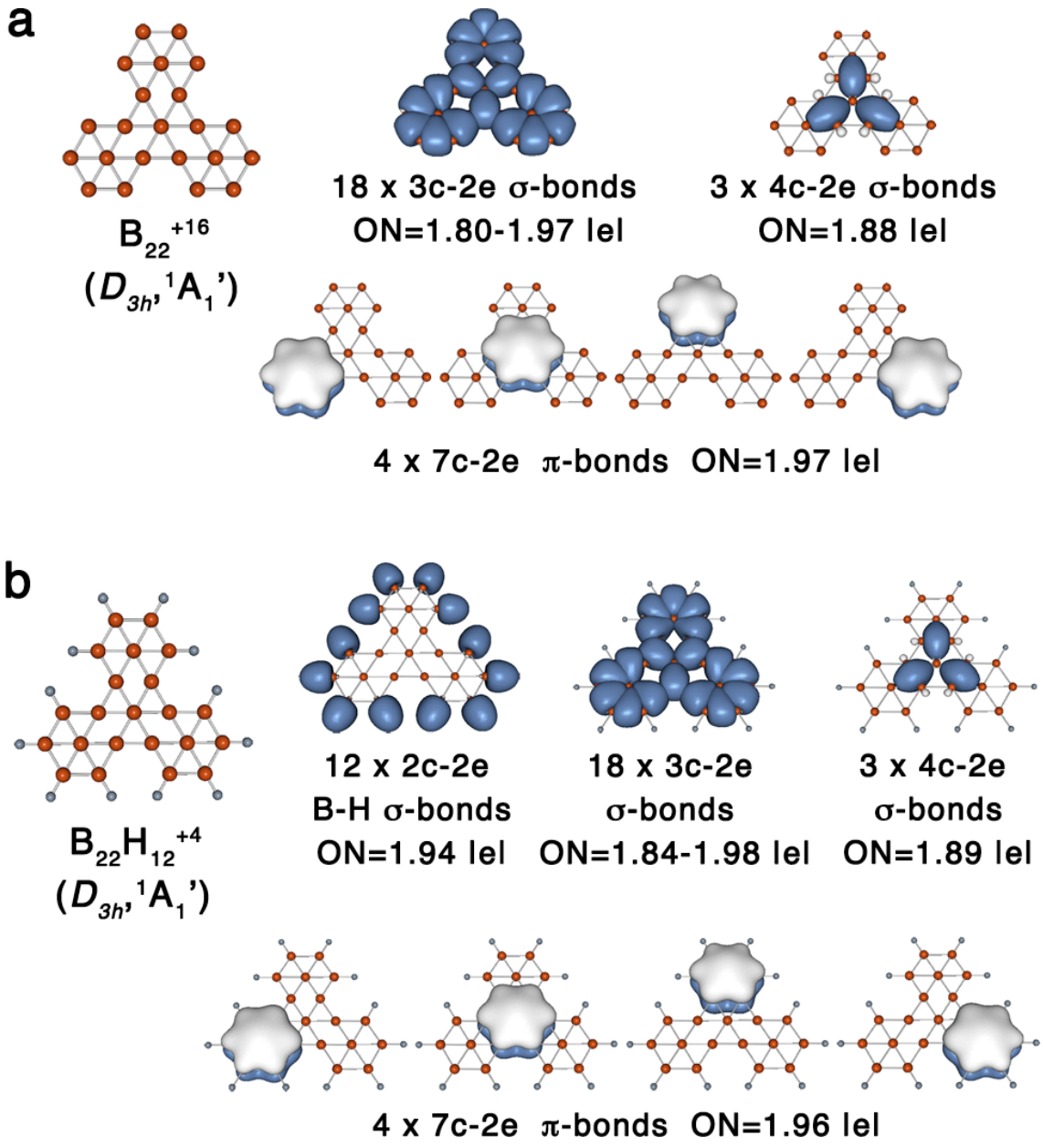

Fig. 6-3 (a) Geometric structure of the B_{22}^{+16} fragment, eighteen 3c-2e σ-bonds (inside of peripheral triangles) superimposed on a single framework, three 4c-2e σ-bonds (inside of rhombus motifs) superimposed on a single framework, and four 7c-2e π-bonds located on filled hexagons. (b) Geometric structure of the $B_{22}H_{12}^{+4}$ fragment, twelve 2c-2e B-H σ-bonds, eighteen 3c-2e σ-bonds superimposed on a single framework, three 4c-2e σ-bonds superimposed on a single framework, and four 7c-2e π-bonds.

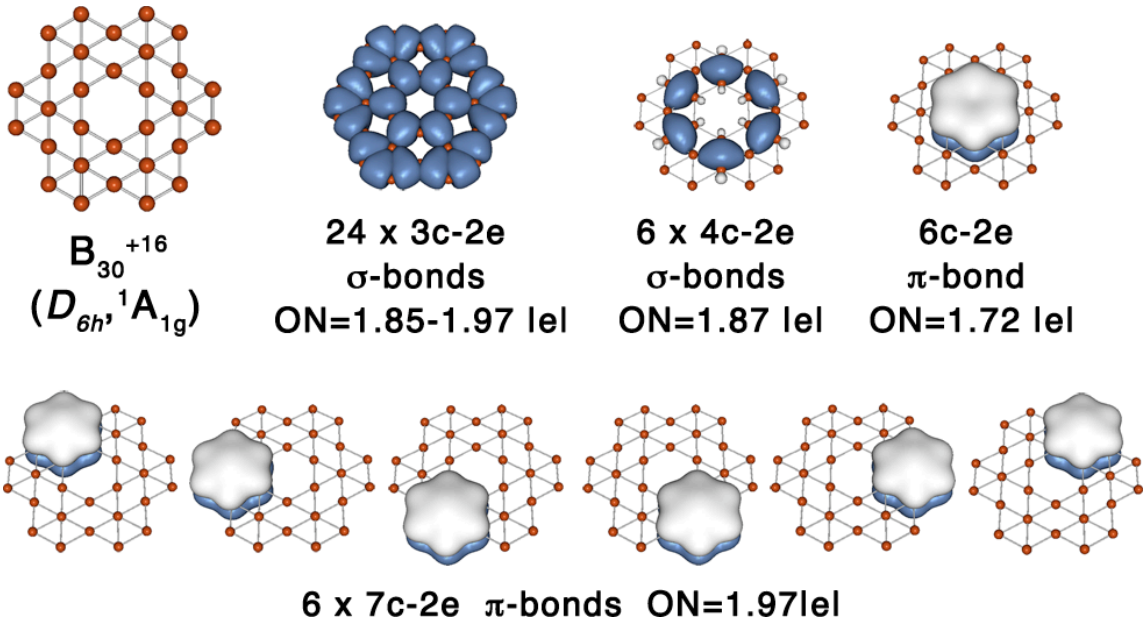

Fig. 6-4. Geometric structure of the B_{30}^{+16} fragment of the α-sheet, twenty-four 3c-2e σ-bonds (inside of peripheral triangles and triangles bordering upon the hole) superimposed on single framework, six 4c-2e σ-bonds (inside of rhombus motifs) superimposed on a single framework, one 6c-2e π-bond located on the hexagon hole, and six 7c-2e π-bonds located on filled hexagons.

CHAPTER 7

δ-BONDING IN THE $[Pd_4(\mu_4\text{-}C_9H_9)(\mu_4\text{-}C_8H_8)]^+$ SANDWICH COMPLEX[1]

Abstract

A remarkable triple-decker sandwich complex $[Pd_4(\mu_4\text{-}C_9H_9)(\mu_4\text{-}C_8H_8)][BAr^f_4]$ (BAr^f_4 = B{3,5-$(CF_3)_2(C_6H_3)$}$_4$) composed out of cyclononatetraenyl anion and cyclooctatetraene as "bread pieces" and square tetrapalladium dication as "meat" (Figure 7-1a) has been synthesized recently.[1] This complex attracted our attention because of the presence of an almost perfect square sheet composed out of four palladium atoms. Such a structure could be a sign of aromatic nature of chemical bonding as it was shown to be present in the square Al_4^{2-} cluster.[2] In this work we show that according to our chemical bonding analysis the bonding in the Pd_4^{2+} unit of $[Pd_4(\mu_4\text{-}C_9H_9)m_4\text{-}C_8H_8)]^+$ is of δ-character among four palladium atoms, making the triple-decker sandwich complex the first synthesized compound identified as having δ-bonding in its cyclic building block when it is in solution or in a crystalline state.

We performed the chemical bonding analysis for the $[Pd_4(\mu_4\text{-}C_9H_9)(\mu_4\text{-}C_8H_8)]^+$ unit of the recently synthesized $[Pd_4(\mu_4\text{-}C_9H_9)(\mu_4\text{-}C_8H_8)][BAr^f_4]$ solid state compound[1] containing a square of four metals atoms, which raises a question of possible aromaticity similar to the Al_4^{2-} cluster.[2] For our chemical bonding analysis we used the Adaptive Natural Density Partitioning method recently developed in our lab by Zubarev and

[1] Coauthored by Alina P. Sergeeva and Alexander I. Boldyrev. Reproduced with permission from *Phys. Chem. Chem. Phys.* **2010**, 12, 12050-12054. Copyright 2010, The Owner Societies.

Boldyrev, which has been successfully applied for the analysis of chemical bonding in boron clusters,[3] prototypical aromatic organic molecules,[4] and gold clusters.[5] The AdNDP method performs analysis of the first-order reduced density matrix with the purpose of obtaining its local block eigenfunctions with optimal convergence properties for describing the electron density. The local blocks of the first-order reduced density matrix correspond to the sets of *n* atoms (from one to all the atoms of the molecule) that are tested for the presence of a two-electron object (*n*-center *two* electron (*n*c-*2*e) bonds, including core electrons and lone pairs as a special case of $n = 1$) associated with this particular set of *n* atoms. The AdNDP search starts with core electron pairs and lone pairs (*1*c-*2*e), then *2*c-*2*e, *3*c-*2*e, … and finally *n*c-*2*e bonds. On each step the density matrix is depleted for the density corresponding to the appropriate bonding elements. The AdNDP procedure can also be applied to specified molecular fragments. This user-directed form of the AdNDP analysis is analogous to the directed search option of the standard NBO code. The recovered *n*c-*2*e bonding elements always correspond to the point-group symmetry of the system after these bonding elements are superimposed onto the molecular frame. For the given *n*-atomic block those eigenvectors are accepted whose occupation numbers (eigenvalues) exceed the established threshold value, and which usually are chosen to be close to 2.00 |e|. Thus, Lewis's idea of an electronic pair as the essential element of bonding is preserved. We consider a molecule as being aromatic if a delocalized bonding is encountered in a planar cyclic system by means of the AdNDP analysis and the number of electrons occupying the delocalized bonds satisfies the $4n+2$ rule. We selected the monomeric unit of $[Pd_4(\mu_4\text{-}C_9H_9)(\mu_4\text{-}C_8H_8)]^+$ shown in Figure 7-1a for our chemical bonding analysis. Calculations were performed using hybrid and

nonhybrid density functional methods known in the literature as B3LYP[6-8] and BPW91,[9-10] respectively, as well as the Hartree-Fock method all with the LANL2DZ[11] pseudo potential and basis set at the experimentally reported geometry.[1] The results of the chemical bonding analysis recovered by the AdNDP method are presented in Figure 7-1b-e. All the calculations were done using Gaussian 03 software package.[12] Molecular visualization was performed using MOLEKEL 4.3.[13]

The results of our AdNDP analysis were independent of the choice of the method used (B3LYP, BPW91, or HF), that is why we present all the data at the B3LYP/LANL2DZ level of theory.

We initially performed the general AdNDP search for lone pairs and *2*c-*2*e bonds in the whole complex. After depleting the total density for the lone pairs and *2*c-*2*e bonds, we then performed user-directed search of bonding elements on each of the building blocks of the sandwich complex ($C_9H_9^-$, C_8H_8, and Pd_4^{2+}) separately.

As one would expect, the AdNDP analysis revealed nine *2*c-*2*e C-C σ-bonds and nine *2*c-*2*e C-H σ-bonds in $C_9H_9^-$ as a part of the sandwich complex (with occupation numbers (ON) lying within the 1.97-1.99 |e| and 1.95-1.97 |e| range, respectively (Figure 7-1b). There are also five completely delocalized π-bonds occupation of which satisfy the 4*n*+2 Huckel rule for π-aromaticity in $C_9H_9^-$, according to the direct AdNDP search. The totally bonding π-bond of the $C_9H_9^-$ unit has ON = 1.89 |e|, the two π-bonds with one nodal plane have ON = 1.93-1.94 |e|, and two π-bonds with two nodal planes have ON = 1.58-1.59 |e|.

The direct AdNDP search on the C_8H_8 unit recovered eight *2*c-*2*e C-C σ-bonds and eight *2*c-*2*e C-H σ-bonds (with ON lying within the 1.98 |e| and 1.96 |e|, respectively)

(Figure 7-1c). There are also four completely delocalized π-bonds occupation of which satisfy the 4*n* Huckel rule for π-antiaromaticity in C_8H_8. The totally bonding π-bond of the C_8H_8 unit has ON = 1.88 |e|, the two π-bonds with one nodal plane have ON = 1.92 |e|, and one π-bond with two nodal planes has ON = 1.34 |e|. The antiaromaticity of the C_8H_8 is consistent with the experimentally observed distance alternation of single and double bonds. The alternative description of the π-bonding in C_8H_8 based on the formation of four conjugated *2*c-*2*e C-C π-bonds with ON = 1.66 |e| can also be recovered by the AdNDP method (Figure 7-1e). However, we believe it is more appropriate to accept the *8*c-*2*e π-bonds (Figure 7-1c) mentioned above due to higher ON values.

The AdNDP search recovered four lone pairs on each of the palladium atoms based on 4d atomic orbitals (AOs) with ON = 1.76-2.00 |e| (during the general AdNDP search) and three *4*c-*2*e δ-bonds (ON = 1.85-1.97 |e|) (during the user-directed AdNDP search on the Pd_4^{2+} building block), see Fig. 7-1d.

Strictly speaking, one can apply the notation of σ-, π-, δ-, ϕ- etc. irreducible representations, when explaining chemical bonding, only to molecules of the linear point groups ($C_{\infty v}$ and $D_{\infty h}$). Thus, a σ-bond is most clearly defined for diatomic molecules as symmetrical with respect to rotation about the bond axis with no nodal planes between the bonded atoms. In a π-bond of a diatomic molecule, two lobes of one involved atomic orbital overlap with two lobes of the other involved atomic orbital with one nodal plane passing through both of the involved nuclei. The definition of a δ-bond in diatomics varies depending on the shape of δ-atomic orbitals (d-AOs) involved in a formation of a

δ-bond. d-AOs can be of two shapes: 1) d_{xy}, d_{yz}, d_{xz}, $d_{x^2-y^2}$ – each with four pear-shaped lobes tangent to two others with a pair of nodal planes perpendicular to the plane comprising the four lobes; 2) the unique d_{z^2} atomic orbital that consists of three regions of high probability density: a torus with two pear-shaped regions placed symmetrically on its *z* axis. Hence, a δ-bond in diatomics can be formed by combinations of either the first or the second type of d-AOs. In the first case, a δ-bond consists of four lobes of one involved atomic orbital that overlap with four lobes of the other involved atomic orbital (both of the first type, e.g. combination of d_{xy}-d_{xy}) with two nodal planes going through both nuclei. In the second case, a δ-bond is that comprised of two d_{z^2}-shaped atomic orbitals (combination of d_{z^2}-d_{z^2}), which both lie perpendicular to the axis of a diatomic molecule and overlap within their tori and the two lobes. If one draws a cycle in the plane perpendicular to the axis of a diatomic molecule, there's a four-fold change in the sign – this holds for both representative d_{xy}-d_{xy} and d_{z^2}-d_{z^2} combinations and offers a criterion for assigning such bonds to δ-type in linear molecules.

Nevertheless, chemists transfer the σ-, π-, δ-, ϕ- etc. notation to explain bonding in molecules of non-linear point groups. The most prominent example would be the prototypic hydrocarbons such as benzene (D_{6h} point group) or toluene (C_s point group), which are attributed to π-aromatic species. The first δ-bond between two rhenium atoms in the $K_2[Re_2Cl_8]\cdot 2H_2O$ compound (with the $Re_2Cl_8^{2-}$ core of nearly D_{4h} point group symmetry) was identified in a milestone work of Cotton and co-workers.[14] Since then, a new branch of inorganic chemistry has been developed involving multiple metal-metal bonding with bond orders higher than three, the maximum allowed for main group molecules.[15] One of the most representative works was by Power and co-workers who

synthesized a non-linear complex having a quintuply-bonded Cr(I)-Cr(I) fragment.[16] In the follow-up computational studies by Brynda et al. it was shown that one of those bonds was *2*c-*2*e δ-bond comprised out of two d_{z^2}-AOs.[17] Similarly, the σ-, π-, δ-, etc. notation is used to describe multiple bonding in main-group (only σ-, π-) and transition metal (σ-, π-, δ-, ϕ-) compounds. Double aromaticity involving in-plane σ- and π-delocalization was introduced by Chandrasekhar et al.[18] Averkiev and Boldyrev[19] reported the first theoretical example of the triple (σ-, π-, and δ-) aromaticity: the triangular Hf_3 cluster in the lowest singlet state. Tsipis et al.[20] demonstrated that the delocalized σ-, π-, δ-, and φ-electron density in the rings of planar isocyclic and heterocyclic uranium clusters could be associated with cyclic electron delocalization, which is a characteristic feature of multiple aromaticity. Martin-Santamaria and Rzepa[21] in their theoretical study were the first to recognize double antiaromaticity in the cyclic C_{12} cluster. Comπλιχατed nature of aromaticity in cyclic systems composed out of transition metal atoms was understood on simplified models – cyclic triatomic and tetratomic systems.[22] The reader can consult reference 22 for the counting rules derived for σ-, π-, δ-, and ϕ-aromaticity and antiaromaticity for both singlet/triplet coupled triatomic and tetratomic systems as depended on the nature of atomic orbitals involved in the formation of corresponding bonding/antibonding molecular orbitals.

Returning to the chemical bonding picture of the sandwich complex $[Pd_4(\mu_4\text{-}C_9H_9)(\mu_4\text{-}C_8H_8)][BAr^f_4]$ (BAr^f_4 = B{3,5-$(CF_3)_2(C_6H_3)$}$_4$), there are three *4*c-*2*e δ-bonds recovered on the Pd_4^{2+} building block (Fig. 7-1d). These three δ-bonds are formed out of $4d_z2$ AOs of four palladium atoms. Similarly to the δ-bond in diatomics comprised of two d_{z^2}-shaped atomic orbitals (combination of d_{z^2}-d_{z^2}), the $4d_{z^2}$ AOs of four palladium atoms,

which form the three bonds, all lie perpendicular to the plane of the Pd_4^{2+} core and overlap within their tori and the two lobes. If one draws a cycle in the plane perpendicular to the plane of the Pd_4^{2+} core, there's a four-fold change in the sign. Therefore, these three bonds formed out of $4d_{z^2}$ AOs are of a δ type.

One can construct four distinct *4*c-*2*e δ-bonds out of d_{z^2} AOs:[22] a completely bonding δ-bond (a_{1g}), a pair of doubly degenerate nonbonding δ-bonds (e_u), and a completely antibonding δ-bond (b_{1g}), see Figure 7-2. In the case of the Pd_4^{2+} system as a part of the sandwich complex there are three of those δ-bonds being occupied with six electrons that satisfy the $4n + 2$ rule for δ-aromaticity. The $4n + 2$ rule was originally developed by Huckel for π-systems of planar monocyclic [*n*]annulenes. This rule is based on the symmetry of π-MOs in a cyclic system, which has one non-degenerate completely bonding MO (responsible for 2 in the $4n + 2$ formula of the rule), and pairs of degenerate partially bonding-antibonding MOs (responsible for $4n$ in the $4n + 2$ formula of the rule). Similar rules have been developed for σ-, δ-, and ϕ- MOs in cyclic systems.[22] In particular, it was shown that due to symmetry of δ-MOs one should use the same $4n + 2$ counting rule in the case of a cyclic transition metal clusters.[22]

The possibility of δ-aromaticity in transition metal systems was initially predicted by Boldyrev and Wang.[23] Zhai et al.[24] presented theoretical and experimental evidence on the presence of δ-aromaticity in $Ta_3O_3^-$ cluster. Since then a few more systems with δ-aromaticity have been reported in the literature,[19,25] but all of these systems were gas-phase clusters. There is a temptation to claim the $[Pd_4(\mu_4\text{-}C_9H_9)(\mu_4\text{-}C_8H_8)][BAr^f{}_4]$ compound to be the first example containing a δ-aromatic Pd_4^{2+} unit in a condense phase.

We would like to point out that the obtained chemical bonding picture of the $[Pd_4(\mu_4\text{-}C_9H_9)(\mu_4\text{-}C_8H_8)]^+$ sandwich complex with 62 pairs of valence electrons comprising 62 recovered by the AdNDP bonds: 1) 23 bonds being responsible for the bonding in the $C_9H_9^-$ unit (9 C-C, 9 C-H, and 5 totally delocalized π-bonds making it π-aromatic); 2) 20 bonds being responsible for the bonding in the C_8H_8 unit (8 C-C, 8 C-H, and 4 totally delocalized π-bonds making it π-antiaromatic); and finally 3) 3 *4*c-*2*e δ-bonds exclusively responsible for the bonding in the Pd_4^{2+} unit with four lone pairs on each of the palladium atoms (16 in total) – is a zero-order chemical bonding model, since the occupation numbers for some of the recovered bonding elements have significant deviation from the ideal value of 2.00 |e|.

According to the NBO analysis of the $[Pd_4(\mu_4\text{-}C_9H_9)(\mu_4\text{-}C_8H_8)]^+$ sandwich complex at the B3LYP/LANL2DZ level of theory the bonding is partially ionic and partially covalent, since the overall NBO charges are 1) + 1.65 |e| (on the Pd_4 unit); 2) – 0.37 |e| (on the $C_9H_9^-$ unit); and 3) -0.28 (on the C_8H_8 unit). Thus, appreciable charge transfer occurs.

To improve the zero-order chemical bonding model, we need to accept all bonding elements which have ON close to 2.00 |e| and allow the bonding elements with low occupation numbers to be delocalized over larger number of atoms. In other words, the user-directed AdNDP search has to be performed not just on the $C_9H_9^-$, C_8H_8, and Pd_4^{2+} building blocks of the sandwich complex separately. Since the bonding elements with significant deviation from the ideal value of the ON = 2.00 |e| are located on the $C_9H_9^-$ and C_8H_8 units, next we performed the user-directed AdNDP search on the ($C_9H_9^-$ + Pd_4^{2+}) fragment, and on the (C_8H_8 + Pd_4^{2+}) fragment. Results of the new searches are

presented in Figure 7-3. The ON of one of the two π-bonds of $C_9H_9^-$ with two nodal planes increases from ON = 1.59 |e| to ON = 2.00 |e| upon allowing this bond to be delocalized over the $C_9H_9^-$ together with the Pd_4^{2+} unit (Fig. 7-3ab, the first row). That indicates that this bond is responsible for the partial covalent bonding between $C_9H_9^-$ and Pd_4^{2+}. The ON of the other π-bond of the $C_9H_9^-$ unit with two nodal planes increases only from ON = 1.58 |e| to 1.69 |e| (Fig. 7-3ab, the second row), thus, indicating, that this bond is delocalized even further: over the ($C_9H_9^-$ + Pd_4^{2+} + C_8H_8) fragment. Upon this expansion, this bond acquires the ON of 2.00 |e| (Fig. 7-3c, the second row). This bond is partially responsible for the direct covalent bonding between the $C_9H_9^-$ and C_8H_8 rings even though the distance between those is about 4.2 Å. This is far not the first example of covalent bonding encountered at such as long distance. Novoa, Miller and co-workers have published a series of articles on such an exceptionally long multicenter-two-electron covalent bonding interactions.[26-28] We would like to stress that approximately 0.3 |e| is participating in such a bonding. This bond has a remarkable δ-appearance (Figure 7-3c, the second row) consisting of four lobes with two nodal planes going through the axis perpendicular to the both $C_9H_9^-$ and C_8H_8 ligands and the Pd_4^{2+} core. It is similar to the δ-bond in diatomics of the first type, e.g. combination of d_{xy}-d_{xy}. If the π-bond of C_8H_8 with two nodal planes is allowed to be delocalized over the (C_8H_8 + Pd_4^{2+}) fragment, the ON of the bond increases from ON = 1.34 |e| to ON = 2.00 |e| (Fig. 7-3de), thus, indicating that this bond is responsible for the partial covalent bonding between C_8H_8 and Pd_4^{2+}. Partial covalent bonding between C_8H_8 and Pd_4^{2+} (Figure 7-3e), and between $C_9H_9^-$ and Pd_4^{2+} (Figure 7-3b, the first row) results in the effective occupation of the totally antibonding δ-bond (b_{1g}) over the palladium square by 1.1 |e| (Figure 7-2). That should

lead to the deviation from the $4n+2$ (n = 1) number of electrons in the palladium square, but we still believe that bonding is of δ-delocalized nature. In case of the occupation of all four *4*c-*2*e δ-bonds (a_{1g}, e_u, b_{1g}) (Figure 7-2), one should obtain four lone pairs on the palladium atoms of $4d_{z^2}$-AO appearance. And, indeed the latter four lone pairs in addition to the 16 being revealed during the general AdNDP search, can be recovered, though their occupation numbers are just 1.66 |e|, and, therefore, cannot be accepted. Thus, for the accurate chemical bonding picture in assigning the density associated with Pd_4^{2+} core we can accept neither four *4*c-*2*e δ-bonds, nor four $4d_{z^2}$ lone pairs, but rather the three *4*c-*2*e δ-bonds (Fig. 7-1d) and the bonds responsible for the partial covalent bonding of the Pd_4^{2+} building block with $C_9H_9^-$, and C_8H_8 (Fig. 7-3b, the first row; and Fig. 7-3e). We would like to compare the obtained result with the works of V. M. Rayon and G. Frenking[29] as well as P. L. Diaconescu et al.[30] Similarly to their examples of metal-ligand interactions in bis(benzene)chromium[29] and an inverted (μ-C_6H_6)[$U(NH_2)_2$]$_2$ sandwich complex,[30] respectively, we consider the covalent bonding between the Pd_4^{2+} building block and the two $C_9H_9^-$ and C_8H_8 ligands as δ-back-donation.

To sum up, we are presenting a chemical bonding picture in the [Pd_4(μ_4-C_9H_9)(μ_4-C_8H_8)]$^+$ sandwich complex as 62 pairs of valence electrons comprising 62 recovered by the AdNDP bonds: 1) 23 bonds being responsible for the bonding in the $C_9H_9^-$ unit (9 C-C, 9 C-H, and 3 totally delocalized π-bonds); + another two π-bonds, which are delocalized over ($C_9H_9^-$ + Pd_4^{2+}), and ($C_9H_9^-$ + Pd_4^{2+} + C_8H_8), respectively, and represent the partial covalent bonding of $C_9H_9^-$ with Pd_4^{2+}, as well as the direct interaction of two rings: $C_9H_9^-$ and C_8H_8; 2) 20 bonds being responsible for the bonding in the C_8H_8 unit (8 C-C, 8 C-H, and 3 totally delocalized π-bonds) + the 4th π-bond, which is delocalized

over (C_8H_8 + Pd_4^{2+}), thus, indicating the partial covalent bonding of C_8H_8 with Pd_4^{2+}; and finally 3) 3 4c-2e δ-bonds, satisfying the $4n$+2 rule (n = 1) and being exclusively responsible for the bonding and square geometry of the Pd_4^{2+} unit with additional four lone pairs on each of the palladium atoms (16 in total).

Having attributed the Pd_4^{2+} block of the $[Pd_4(\mu_4\text{-}C_9H_9)(\mu_4\text{-}C_8H_8)][BAr^f_4]$ sandwich complex to δ-aromatic species, we would like to stress that there are various aromaticity descriptors now-a-days.[31-34] The latter have been tested recently to evaluate their performance by Sola and co-workers.[35-38] We propose a new criterion of aromaticity in planar species: a chemical species should be considered aromatic if there is a delocalized bonding encountered in a cyclic planar system by means of the AdNDP analysis that satisfies the $4n$ + 2 rule. The key feature of AdNDP is to recover first all the localized bonding elements, such as 1c-2e (lone pairs) and 2c-2e bonds, and only then rationalize the residual density in terms of delocalized objects. This procedure assures that the recovered delocalized objects cannot be localized. The AdNDP method has proven itself as the right tool in determining such delocalization in organic molecules,[4] boron clusters,[3,39] and transition metal compounds,[40] and, as shown in the current work, in the Pd_4^{2+} building block of the $[Pd_4(\mu_4\text{-}C_9H_9)(\mu_4\text{-}C_8H_8)][BAr^f_4]$ sandwich complex. We would like to stress that applicability of AdNDP to probe aromaticity in twisted (half twist) systems and double twist systems requires further studies.

The existence of the $[Pd_4(\mu_4\text{-}C_9H_9)(\mu_4\text{-}C_8H_8)][BAr^f_4]$ sandwich compound is an excellent demonstration of the importance of delocalized δ-bonding in inorganic and organometallic chemistry.

The detailed description of the AdNDP method can be found in the original article by Zubarev and Boldyrev.[3] The user-friendly version of the AdNDP method is currently under development and will be soon available upon request to the authors.

References

1 T. Murahashi, R. Inoue, K. Usui and S. Ogoshi, *J. Am. Chem. Soc*. 2009, **131**, 9888.

2 X. Li, A. E. Kuznetsov, H. F. Zhang, A. I. Boldyrev and L. S. Wang, *Science* 2001, **291**, 859.

3 D. Y. Zubarev and A. I. Boldyrev, *Phys. Chem. Chem. Phys.* 2008, **10**, 5207.

4 D. Y. Zubarev and A. I. Boldyrev, *J. Org. Chem.* 2008, **73**, 9251.

5 D. Y. Zubarev and A. I. Boldyrev, *J. Phys. Chem.* 2009, **13**, 866.

6 A. D. Becke, *J. Chem. Phys*. 1993, **98**, 5648.

7 S. H. Vosko, L. Wilk and M. Nusair, *Can. J. Phys.* 1980, **58**, 1200.

8 C. Lee, W. Yang and R. G. Parr, *Phys. Rev. B*. 1988, **37**, 785.

9 J. P. Perdew, J. A. Chevary, S. H. Vosko, K. A. Jackson, M. R. Pederson, D. J. Singh and C. Fiolhais, *Phys. Rev. B* 1992, **46**, 6671.

10 J. P. Perdew, J. A. Chevary, S. H. Vosko, K. A. Jackson, M. R. Pederson, D. J. Singh and C. Fiolhais, *Phys. Rev. B* 1993, **48**, 4978.

11 P. J. Hay and W. R. Wadt, *J. Chem. Phys.* 1985, **82**, 299.

12 M. J. Frisch, G. M. Trucks, H. B. Schlegel, G. E. Scuseria, M. A. Robb, J. R. Cheeseman, J. A. Montgomery, T. Vreven, K. N. Kudin, J. C. Burant, J. M. Millam, S. S. Iyengar, J. Tomasi, V. Barone, B. Mennucci, M. Cossi, G. Scalmani, N. Rega, G. A. Petersson, H. Nakatsuji, O. Kitao, H. Nakai, M. Klene, X. Li, J. E. Knox, H. P.

Hratchian, J. B. Cross, C. Adamo, J. Jaramillo, R. Gomperts, R. E. Stratmann, O. Yazyev, A. J. Austin, R. Cammi, C. Pomelli, J. W. Ochterski, P. Y. Ayala, K. Morokuma, G. A. Voth, P. Salvador, J. J. Dannenberg, V. G. Zakrzewski, S. Dapprich, A. D. Daniels, M. C. Strain, O. Farkas, D. K. Malick, A. D. Rabuck, K. Raghavachari, J. B. Foresman, J. V. Ortiz, Q. Cui, A. G. Baboul, S. Clifford, J. Cioslowski, B. B. Stefanov, G. Liu, A. Liashenko, P. Piskorz, I. Komaromi, R. L. Martin, D. J. Fox, T. Keith, M. A. Al-Laham, C. Y. Peng, A. Nanayakkara, M. Challacombe, P. M. W. Gill, B. G. Johnson, W. Chen, M. W. Wang, C. Gonzales and J. A. Pople, *Gaussian 03 (revision D.01)*, Gaussian, Inc., Wallington, CT, 2004.

13 MOLEKEL, Version 4.3. S. Portmann, CSCS/ETHZ, 2002.

14 F. A. Cotton, N. F. Curtis, C. B. Harris, B. F. G. Johnson, S. J. Lippard, J. T. Mague, W. R. Robinson and J. S. Wood, *Science* 1964, **145**, 1305.

15 F. A. Cotton, C. A. Murillo and R. A. Walton, *Multiple Bonds Between Metal Atoms*, Springer, New York, 3rd edn, 2005.

16 T. Nguyen, A. D. Sutton, M. Brynda, J.C. Fettinger, G. J. Long and P. P. Power, *Science* 2005, **310**, 844.

17 M. Brynda, L. Gagliardi, P.-O. Widmark, P. P. Power and B. O. Roos, *Angew. Chem. Int. Ed.* 2006, **45**, 3804.

18 J. Chandrasekhar, E. D. Jemmis and P.v. R. Schleyer, *Tetrahedron Lett.*, 1979, **39**, 3707.

19 B. B. Averkiev and A. I. Boldyrev, *J. Phys. Chem. A*, 2007, **111**, 12864.

20 A. C. Tsipis, C. E. Kefalidis and C. A. Tsipis, *J. Am. Chem. Soc.*, 2008, **130**, 9144.

21 S. Martin-Santamaria and H. S. Rzepa, *Chem. Commun.*, 2000, **16**, 1503.

22 A. P. Sergeeva, B. B. Averkiev and A. I. Boldyrev, in *Metal-Metal Bonding. Structure and Bonding book series,* ed. G. Parkin, Springer, Berlin/Heidelberg, 2010, vol. 136, pp. 275-306.

23 A. I. Boldyrev and L. S. Wang, *Chem. Rev.* 2005, **105**, 3716.

24 H. J. Zhai, B. B. Averkiev, D. Y. Zubarev, L. S. Wang, A. I. Boldyrev, *Angew. Chem. Int. Ed.* 2007, **46**, 4277.

25 B. Wang, H. J. Zhai, X. Huang and L. S. Wang, *J. Phys. Chem. A.* 2008, **112**, 10962.

26 R. E. Del Sesto, J. S. Miller, P. Lafuente, J. J. Novoa, *Chem. Eur. J.* 2002, **8**, 4894.

27 J. S. Miller, J. J. Novoa, *Acc. Chem. Res.*, 2007, **40**, 189.

28 I. Garcia-Yoldi, J. S. Miller, J. J. Novoa, *Phys. Chem. Chem. Phys*. 2008, **10**, 4106.

29 V. M. Rayon and G. Frenking, *Organometallics*, 2003, **22**, 3304.

30 P. L. Diaconescu, P. L. Arnold, T. A. Baker, D. J. Mindiola and C. C. Cummins, *J. Am. Chem. Soc.* 2000, **122**, 6108.

31 V. I. Minkin, M. N. Glukhovtsev and B. Y. Simkin, *Aromaticity and Antiaromaticity*. Wiley, New York, 1994.

32 ed. P. v. R. Schleyer, *Chem. Rev.*, 2005, **105**, No. 10.

33 ed. P. v. R. Schleyer, *Chem. Rev.*, 2001, **101**, No. 5.

34 P. v. R. Schleyer, C. Maerker, A. Dransfeld, H. Jiao and N. J. R. v. E. Hommes, *J. Am. Chem. Soc.* 1996, **118**, 6317.

35 F. Feixas, J. O. C. Jimenez-Halla, E. Matito, J. Poater and M. Sola, *J. Chem. Theory Comp.*, 2010, **6**, 1118.

36 R. Islas, G. Martinez-Guajardo, J. O. C. Jimenez-Halla, M. Sola and G. Merino, *J. Chem. Theory Comp.*, 2010, **6**, 1131.

37 F. Feixas, M. Sola and M. Swart, *Can. J. Chem*., 2009, **87**, 1063.

38 E. Matito and M. Sola, *Coord. Chem. Rev.*, 2009, **253**, 647.

39 W. Huang, A. P. Sergeeva, H. J. Zhai, B. B. Averkiev, L. S. Wang and A. I. Boldyrev, *Nat. Chem.,* 2010, **2**, 202.

40 A. P. Sergeeva and Alexander I. Boldyrev, *Comments Inorg. Chem*. 2010, **31**, 2.

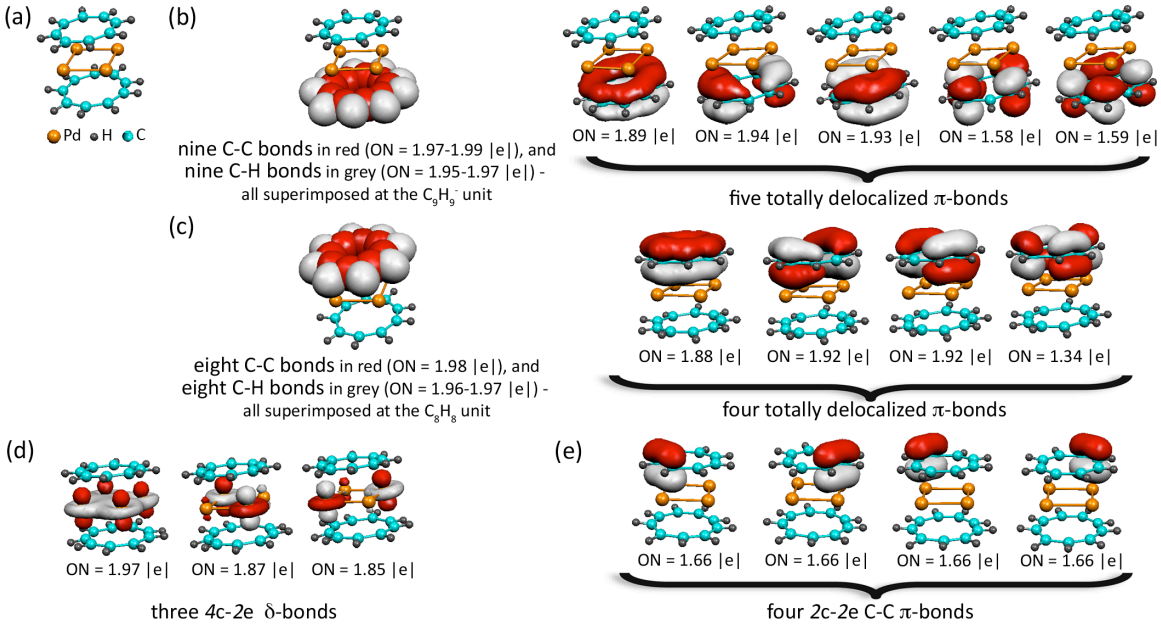

Fig. 7-1. Experimental structure of the $[Pd_4(\mu_4\text{-}C_9H_9)\mu_4\text{-}C_8H_8)]^+$ sandwich complex (a). The chemical bonding picture of the complex obtained via the AdNDP method: (b) bonds recovered on the $C_9H_9^-$ unit; (c) bonds recovered on the C_8H_8 unit; (d) bonds recovered on the Pd_4^{2+} unit; (e) alternative representation of the π-bonding of the C_8H_8 unit presented in (c) in terms of four *2*c-*2*e C-C π-bonds.

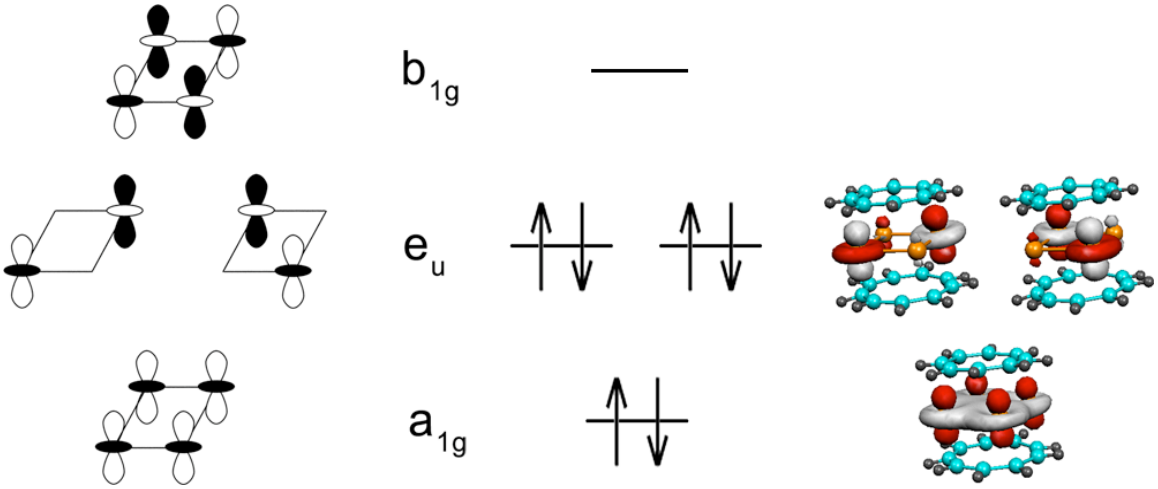

Fig. 7-2. Schematic representation of d_z^2 AO-based *4*c-*2*e δ-bonds and their symmetry, as well as three doubly occupied *4*c-*2*e δ-bonds of the Pd_4^{2+} unit as a part of the sandwich complex recovered by the AdNDP analysis.

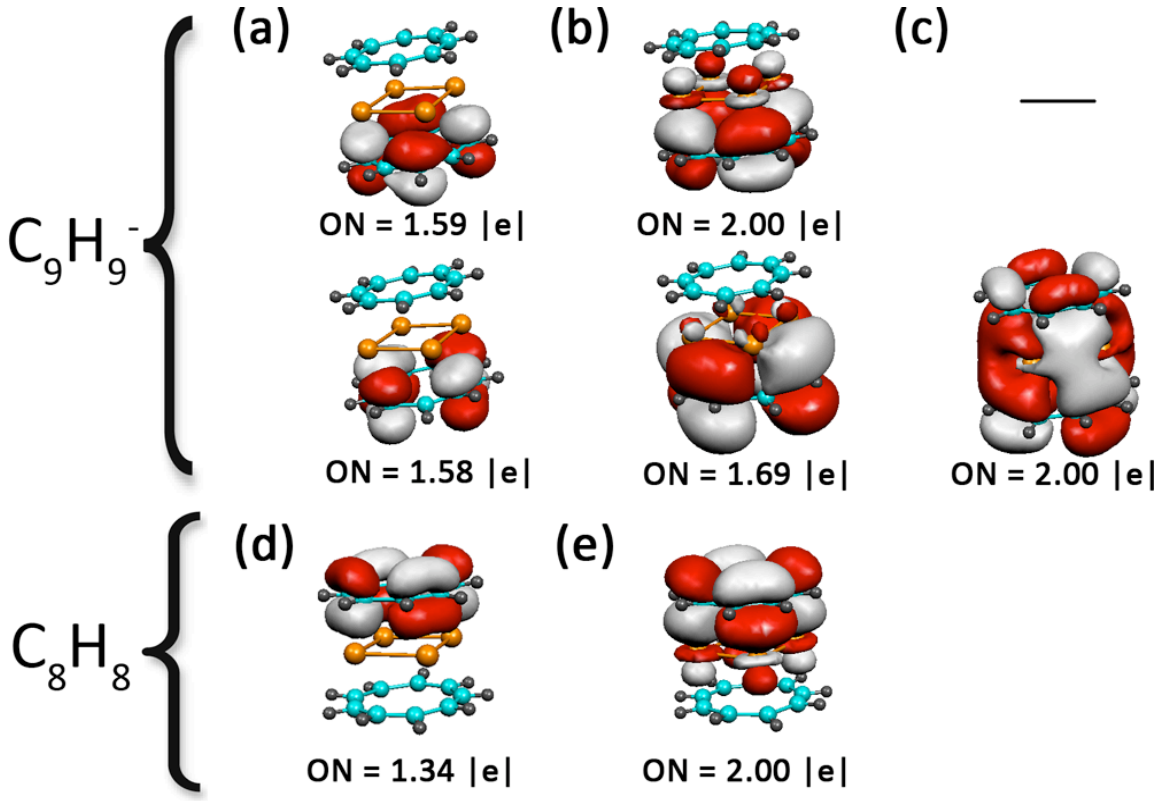

Fig. 7-3. Variance of occupation numbers in the π-bonds with two nodal planes of the $C_9H_9^-$ (a,b,c) and C_8H_8 (d,e) building blocks of the sandwich complex in accordance with the number of centers a bond is allowed to be delocalized over. Delocalization is over: (a) $C_9H_9^-$; (b) ($C_9H_9^-$ + Pd_4^{2+}); (c) ($C_9H_9^-$ + Pd_4^{2+} + C_8H_8); (d) C_8H_8; (e) (C_8H_8 + Pd_4^{2+}).

CHAPTER 8

THE CHEMICAL BONDING OF Re_3Cl_9 AND $Re_3Cl_9^{2-}$ REVEALED BY THE ADAPTIVE NATURAL DENSITY PARTITIONING ANALYSES[1]

Chemical bonding of neutral rhenium trichloride Re_3Cl_9 and doubly charged $Re_3Cl_9^{2-}$ has been brought into question in the current work. Despite recently reported propositions of π-aromaticity of neutral Re_3Cl_9 based on negative nuclear independent chemical shift (NICS) values,[1,2] to the contrary, it is shown to be a purely classical chemical molecule, according to the results of the recently developed Adaptive Natural Density Partitioning (AdNDP) analysis.[3-5] The formation of three consecutive double bonds in a triatomic cycle formed by rhenium atoms that was initially predicted by Cotton et al.[6-8] is confirmed. The chemical bonding picture changes dramatically upon addition of two excess electrons to Re_3Cl_9. The rhenium atoms of the resulting doubly charged cluster are shown to be held together via three single Re-Re σ-bonds, three Re-Cl-Re σ-bonds, and a totally delocalized π-bond based on valence d atomic orbitals (d-AO) of rhenium atoms with minor contributions coming from the density associated with six apical chlorine atoms, which makes $Re_3Cl_9^{2-}$ π-aromatic.

The polymeric rhenium chloride $[Re_3(\mu\text{-}Cl)_3Cl_6]$ when dissolved[6] or in the gas phase[9] features a Re_3Cl_9 metal cluster in which three rhenium atoms form an equilateral triangle with three chlorine atoms (μ) acting as bridging groups along the edges of the triangle and the remaining six apical chlorine atoms out of the plane forming a trigonal prism. Cotton and co-workers[6-8] proposed that each rhenium atom in Re_3Cl_9 possessed

[1] Coauthored by Alina P. Sergeeva and Alexander I. Boldyrev. Reproduced with permission from *Comments Inorg. Chem.* **2010**, 31, 2-12. Copyright 2010, Taylor & Francis Group, LLC.

homophilicity, or a tendency to form bonds to one or more other atoms of the same chemical identity, based on a valence bond approach by use of certain limiting, generally quite symmetrical, hybridization schemes. There exist two different chemical bonding languages in contemporary chemistry. The first is the well-known Lewis chemical bonding model,[10] which he had developed as a generalization of numerous experimental data well before the formulation of quantum mechanics. It is a "pencil and paper" approach based on the octet rule to predict structure of a given system knowing its chemical formula, where chemical bonding objects are thought to be comprised of two electrons localized over one (a lone pair, or *one*-center—*two*-electron (*1*c-*2*e) bond), or two atoms (*two*-center—*two*-electron (*2*c-*2*e) bond). The second language was introduced by quantum chemistry on the basis of canonical Hartree−Fock or Kohn−Sham molecular orbitals. The key difference of the second language is that *two*-electron chemical bonding objects called canonical molecular orbitals (CMOs) are now delocalized over the entire molecule. Since 1960s, a few schemes have been proposed for obtaining localized orbitals from completely delocalized ones,[11-15] with the Natural Bonding Orbital (NBO) procedure being the most popular, and incorporated into most of the computational chemistry software packages such as Gaussian. While reproducing intuitively expected Lewis bonding pictures for classical chemical molecules in terms of *1*c-*2*e (lone pairs) and *2*c-*2*e bonds, and a single resonance Kekule structure, when it comes to typical aromatic organic systems,[4] the NBO analysis gives a non-interpretive chemical bonding picture for non-classical systems with delocalized bonding such as boron clusters.[3] This issue arises due to the fact that NBO is restricted for dividing the total electron density into two electron objects delocalized over no more than three atoms. To reconcile this

problem the AdNDP analysis was developed,[3-5] which represents the electronic structure in terms of *n*-center–*two*-electron (*n*c-*2*e) bonds, with *n* spanning from one to the total number of atoms of the system of interest (see detailed description of the method elsewhere). The development of such a unified chemical bonding theory tool was most essential for deciphering chemical bonding in metal clusters, which often feature both localized Lewis bonding elements and delocalized bonding objects, with the latter being interpreted from the view of aromaticity concepts, since 2001.[16]

In the present study, we performed the AdNDP analysis of the molecular orbital (MO) wave function of both neutral and doubly charged rhenium chloride species. All the calculations were carried out using the hybrid density functional method, known in the literature as B3LYP,[17-19] with a pseudo core LANL2DZ potential and basis-set.[20] In order to test if the obtained results depend on the method used, we repeated all the calculations at Hartree-Fock, BPW91,[21-24] and PBE1PBE[25-26] levels with the same LANL2DZ potential and basis-set. All the calculations were performed using the Gaussian 03 software package.[27] It is shown that the results of the AdNDP analysis, similar to those of NBO, do not depend on the quality of the basis set used,[3,4] so the choice of the level of theory for the AdNDP application is adequate. The visualization of the AdNDP results are done using MOLEKEL 4.3 program.[28] The experimental X-ray parameters of Re_3Cl_9 were reported by Cotton and co-workers,[29] whereas the theoretical structural parameters of Re_3Cl_9, and $Re_3Cl_9^{2-}$ calculated using Amsterdam Density Functional with spin orbit and scalar relativistic effects incorporated via the zero order regular approximation were reported by Alvarado-Soto et al.[1,2]

The results of the AdNDP analysis of Re_3Cl_9 and $Re_3Cl_9^{2-}$ clusters are presented in Figure 8-1 (a) and (b), respectively. The occupation numbers and the visualized AdNDP-obtained bonds do not depend on the choice of the theoretical method. Occupation numbers for all the bonds are given at B3LYP/LANL2DZ, HF/LANL2DZ (in parenthesis), BPW91/LANL2DZ (in square brackets), PBE1PBE/LANL2DZ (in squiggle brackets) levels (see Figure 8-1) and differ by no more than 0.1 |e|.

There are 84 and 86 valence electrons, which form 42 and 43 *two*-electron elements in Re_3Cl_9 and $Re_3Cl_9^{2-}$, respectively. In both cases, 27 lone pairs (three on each of the chlorine atoms) are deleted from Figure 8-1, thus, leaving only 15 and 16 chemical bonding objects in (a) and (b), respectively. According to the AdNDP analyses, both neutral and doubly charged anion have six *2*c-*2*e p-d-hybridized σ-bonds between each apical chlorine atom and the neighboring rhenium atom; bridging chlorine atoms are bound to the triangular Re_3 core via *3*c-*2*e p-d-hybridized Re-Cl-Re σ-bonds with the major electron density contribution of 74 % coming from lone pairs on bridging μ-chlorine atoms (in other words if these three *3*c-*2*e p-d-hybridized Re-Cl-Re σ-bonds are reduced to just lone pairs on the three bridging μ-chlorine atoms their occupation numbers drops to 1.46 |e|); and, finally, there are three *2*c-*2*e Re-Re d-AO based σ-bonds. For all the recovered chemical bonding elements the occupation numbers (ON), which indicate how many electrons there are per bond are close to the ideal limit of 2.00 |e|. The difference in the chemical bonding picture of Re_3Cl_9 and $Re_3Cl_9^{2-}$ is rooted in the AdNDP bonds formed out of d-AO based canonical π-MOs. There are six symmetry-adapted combinations of d-AOs that one can construct to form π-MOs in a model triatomic system: totally bonding radial, totally antibonding tangential, and two sets of doubly

degenerate π-MOs of bonding-antibonding characters built out of both tangential and radial d-AOs.

In the case of Re_3Cl_9, there are three occupied π-CMOs with the main electron density contribution coming from d-AOs of rhenium atoms, namely: highest occupied doubly degenerate MO (HOMO) of e" symmetry and a totally bonding radial HOMO-1 of a_2" symmetry (Figure 8-2a). If one were to exclude the contribution of electron density associated with chlorine atoms, the resulting MOs would resemble a model triatomic system (Figure 8-2b). According to the AdNDP analysis, the occupation of 6e" HOMO, and $5a_2$" HOMO-1 results in the formation of three consecutive *2*c-*2*e Re-Re π-bonds of ON = 1.99 |e| (Figure 8-2c) as predicted by Cotton and co-workers.[6,8,9] In the neutral Re_3Cl_9 a pair of doubly degenerate LUMO+2 of e" symmetry are not occupied. These orbitals lie higher in energy than the totally antibonding tangential π-CMO of a_1" symmetry due to the contribution of electron density from the six apical chlorine atoms, which increases the antibonding nature of these doubly degenerate π-CMOs compared to that of LUMO ($2a_1$").

Addition of two excess electrons to the totally antibonding π-tangential $2a_1$" lowest unoccupied MO (LUMO) of Re_3Cl_9 to produce doubly charged $Re_3Cl_9^{2-}$ changes the chemical bonding picture distinctly (Figure 8-3).

The totally bonding $5a_2$" MO is the major contributor to the bonding between rhenium atoms. If only this orbital were occupied out of the whole set of π-canonical molecular orbitals with the main electron density contribution coming from d-AOs of rhenium atoms ($5a_2$", 6e", 7e", and $2a_1$" π-CMOs), the system would be π-aromatic (a model $Re_3Cl_9^{4+}$ system). The occupation of a pair of doubly degenerate 6e" MOs by four

electrons brings antibonding character to the bonding between rhenium atoms and results in the formation of three 2c-2e Re-Re π-bonds (as revealed by the AdNDP method for neutral Re_3Cl_9). The subsequent occupation of the antibonding π-tangential $2a_1$" MO by two electrons to yield the $Re_3Cl_9^{2-}$ cluster brings even more antibonding character to the Re-Re bonding and increases electron "crowding" in the Re_3 triangle. The AdNDP method showed that in the case of the $Re_3Cl_9^{2-}$ cluster, the density associated with these four CMOs can be considered as three lone pairs (ON = 1.90 |e|) on rhenium atoms and a totally bonding π-radial (π_r) *3*c-*2*e bond of ON=1.62 |e|. The loss of three double 2c-2e Re-Re π-bonds is now partially compensated by the formation of a totally bonding π-radial (π_r) *3*c-*2*e bond, and formation of three lone pairs allows the electron "crowding" in Re_3 triangle to diminish. The $Re_3Cl_9^{2-}$ cluster is, thus, π-aromatic with the two electrons of the *3*c-*2*e π_r-bond satisfying the 4n+2 rule for aromaticity (n=0). The low value of the ON for the d-AO based π_r-bond means that this bond is delocalized over more than just three rhenium atoms. If we allow the AdNDP method to increase the number of atoms on which the π_r-bond can be delocalized, this bond can be found as a *9*c-*2*e π_r-bond with ON=2.00, now also involving electron density coming from apical chlorine atoms (Figure 8-4).

The major contribution of 81% of the electron density of the *9*c-*2*e π_r-bond still comes from rhenium atoms. Again, in the doubly charged $Re_3Cl_9^{2-}$ a pair of doubly degenerate LUMO+2 of e" symmetry is not occupied. These two orbitals lie higher in energy than the totally antibonding tangential π-CMO of a_1" symmetry due to the contribution of electron density coming from the six apical chlorine atoms, which

increases the antibonding nature of these doubly degenerate π-CMOs compared to that of HOMO ($2a_1$").

To summarize, in the neutral Re_3Cl_9 cluster each rhenium atom is bound by double (*2*c-*2*e σ- and π-) bonds to the two neighboring rhenium atoms, exactly as Cotton and co-workers predicted 45 years ago; while in the doubly charged $Re_3Cl_9^{2-}$ cluster rhenium atoms are bound together by three single d-AO based *2*c-*2*e σ-bonds and a completely delocalized *9*c-*2*e (which can be reduced to a *3*c-*2*e) π_r-bond responsible for the aromaticity in the $Re_3Cl_9^{2-}$ cluster.

The erroneous proposition of aromatic nature of neutral Re_3Cl_9 has been deduced on the basis of negative NICS values only. It should be kept in mind that NICS does not always give a correct evaluation of aromaticity. The most spectacular failure is assigning cyclopropane (C_3H_6) to the family of aromatic species on the basis of negative NICS values. Indeed, $NICS_{zz}$ values for C_3H_6 (-29.82 ppm (0.0 Å), -30.87 ppm (0.4 Å), and -24.15 ppm (1.0 Å)) are comparable to those of benzene, a prototypical aromatic hydrocarbon (-14.49 ppm (0.0 Å), -20.57 ppm (0.4 Å), and -29.25 ppm (1.0 Å)), all calculated at the B3LYP/6-311++G** level of theory. Though there has been a long discussion on whether cyclopropane is σ-aromatic or not, Schleyer and co-workers, who developed the NICS criteria, have concluded:[30] "there is no need to invoke σ-aromaticity in cyclopropane energetically" because "the extra σ-stabilization energy (at most 3.5 kcal mol^{-1}) is far too small to explain the small difference in strain energy between cyclopropane (27.5 kcal mol^{-1}) and cyclobutane (26.5 kcal mol^{-1}) by σ-aromaticity."

There are various criteria for aromaticity that have been proposed in the literature[31-34] such as enhanced stability, high symmetry, low reactivity, bond length equalization, enhanced anisotropy of diamagnetic susceptibility, diatropic (low-field) ^{1}H NMR shifts, large negative nucleus independent chemical shift (NICS) values, and high electron detachment energies in photoelectron spectra. We propose a new criterion of aromaticity: a chemical molecule should be considered as being aromatic if there is a delocalized bonding encountered in a cyclic system by means of the AdNDP analysis that satisfies the 4*n*+2 rule. The key feature of AdNDP is to recover first all the localized bonding elements, such as lone pairs and 2*c*-2*e* bonds, and only then rationalize the residual density in terms of delocalized objects. This procedure assures that the recovered delocalized objects cannot be localized. The AdNDP method has proven itself as the right tool in determining such delocalization in organic molecules,[4] boron clusters,[3] and transition metal compounds, as shown in the current work, as an example of doubly charged rhenium trichloride.

References

1. Alvarado-Soto, L., R. Ramirez-Tagle, and R. Arratia-Perez, 2008. Spin–orbit effects on the aromaticity of the Re_3Cl_9 and Re_3Br_9 clusters. *Chem. Phys. Lett.,* **467**: 94-96.

2. Alvarado-Soto, L., R. Ramirez-Tagle, and R. Arratia-Perez, 2009. Spin−orbit effects on the aromaticity of the $Re_3X_9^{2-}$ (X = Cl, Br) cluster ions. *J. Phys. Chem. A.,* **113**: 1671-1673.

3. Zubarev, D. Y. and A. I. Boldyrev. 2008. Developing paradigms of chemical bonding: adaptive natural density partitioning. *Phys. Chem. Chem. Phys.,* **10**: 5207-5217.

4. Zubarev, D. Y. and A. I. Boldyrev. 2008. Revealing intuitively assessable chemical bonding patterns in organic aromatic molecules via Adaptive Natural Density Partitioning. *J. Org. Chem.,* **73**: 9251-9258.

5. Zubarev, D. Y. and A. I. Boldyrev. 2009. Deciphering chemical bonding in golden cages. *J. Phys. Chem.,* **13**: 866-868.

6. Cotton, F. A. and T. Haas. 1964. A molecular orbital treatment of the bonding in certain metal atom clusters. *Inorg. Chem.,* **3**: 10-17.

7. Cotton, F. A., N. F. Curtis, C. B. Harris, B. F. G. Johnson, S. J. Lippard, J. T. Mague, W. R. Robinson, and J. S. Wood. 1964. Mononuclear and polynuclear chemistry of rhenium (III): its pronounced homophilicity. *Science,* **145**: 1305-1307.

8. Bursten, B. E., F. A. Cotton, J. C. Green, E. A. Seddon, and G. G. Stanley. 1980. Electronic structures and photoelectron spectra of the metal atom cluster species Re_3Cl_9, Re_3Br_9, $[Re_3Cl_{12}]^{3-}$. *J. Am. Chem. Soc.,* **102**: 955-968.

9. Trogler, W. C., D. E. Ellis, and J. Berkowitz. 1979. Spectroscopic and theoretical studies of metal cluster complexes. 1. The He(I) photoelectron spectrum of Re_3Cl_9. Calculations by the SCC DV Xa method of Re_3Cl_9 and $Re_2Cl_8^{2-}$. *J. Am. Chem. Soc.,* **101**: 5896-5901.

10. Pauling, L. 1931. The nature of the chemical bond. Application of results obtained from the quantum mechanics and from a theory of paramagnetic susceptibility to the structure of molecules. *J. Am. Chem. Soc*., **53**: 1367-1400.

11. Foster, J. M. and S. F. Boys. 1960. Canonical configurational interaction procedure. *Rev. Mod. Phys.,* **32**: 300-302.

12. Edmiston, C. and K. Ruedenberg. 1963. Localized atomic and molecular orbitals. *Rev. Mod. Phys.,* **35**: 457-464.

13. Pipek, J. and P. G. Mezey. 1989. A fast intrinsic localization procedure applicable for ab initio and semiempirical linear combination of atomic orbital wave functions. *J. Chem. Phys.,* **90**: 4916-4926.

14. Foster, J. P. and F. Weinhold. 1980. Natural hybrid orbitals. *J. Am. Chem. Soc.,* **102**: 7211-7218.

15. Reed, A. E., L. A. Curtiss, and F. Weinhold. 1988. Intermolecular interactions from a natural bond orbital, donor-acceptor viewpoint. *Chem. Rev.,* **88**: 899-926.

16. Li, X., A. E. Kuznetsov, H. F. Zhang, A. I. Boldyrev, and L. S. Wang. 2001. Observation of all-metal aromatic molecules. *Science,* **291**: 859-861.

17. Becke, A. D. 1993. Density-functional thermochemistry. III. The role of exact exchange. *J. Chem. Phys*., **98**: 5648-5652.

18. Vosko, S. H., L. Wilk, and M. Nusair. 1980. Accurate spin-dependent electron liquid correlation energies for local spin density calculations: a critical analysis. *Can. J. Phys.,* **58**: 1200-1211.

19. Lee, C., W. Yang, and R. G. Parr. 1988. Development of the Colle-Salvetti correlation-energy formula into a functional of the electron density. *Phys. Rev. B*., **37**: 785-789.

20. Hay, P. J. and W. R. Wadt. 1985. Ab initio effective core potentials for molecular calculations. Potentials for K to Au including the outermost core orbitals. *J. Chem. Phys.,* **82**: 299-310.

21. Becke, A. D. 1988. Density-functional exchange-energy approximation with correct asymptotic behavior. *Phys. Rev. A,* **38**: 3098-3100.

22. Perdew, J. P., J. A. Chevary, S. H. Vosko, K. A. Jackson, M. R. Pederson, D. J. Singh, and C. Fiolhais. 1992. Atoms, molecules, solids, and surfaces: applications of the generalized gradient approximation for exchange and correlation. *Phys. Rev. B,* **46**: 6671-6687.

23. Perdew, J. P., J. A. Chevary, S. H. Vosko, K. A. Jackson, M. R. Pederson, D. J. Singh, and C. Fiolhais. 1993. Erratum: atoms, molecules, solids, and surfaces: Applications of the generalized gradient approximation for exchange and correlation. *Phys. Rev. B,* **48**: 4978-4978.

24. Perdew, J. P., K. Burke, and Y. Wang. 1996. Generalized gradient approximation for the exchange-correlation hole of a many-electron system. *Phys. Rev. B,* **54**: 16533-16539.

25. Perdew, J. P., K. Burke, and M. Ernzerhof. 1996. Generalized gradient approximation made simple. *Phys. Rev. Lett.,* **77**: 3865-3868.

26. Perdew, J. P., K. Burke, and M. Ernzerhof. 1997. Generalized gradient approximation made simple [Phys. Rev. Lett. 77, 3865 (1996)]. *Phys. Rev. Lett.,* **78**: 1396-1396.

27. Frisch, M. J., et al. 2003. The Gaussian 03 program (revision D.01), Gaussian, Inc., Pittsburgh, PA.

28. Portmann, S. 2002. MOLEKEL, Version 4.3., CSCS/ETHZ.

29. Bertrand, J. A., F. A. Cotton, and W. A. Dollase. 1963. The crystal structure of cesium dodecachlorotrirhenate-(III), a compound with a new type of metal atom cluster. *Inorg. Chem.,* **2**: 1166-1171.

30. Wu, W., B. Ma, J. I. C. Wu, P. v. R. Schleyer, and Y. Mo. 2009. Is cyclopropane really the σ-aromatic paradigm? *Chem. Eur. J.,* **15**: 9730-9736.

31. Minkin, V. I., M. N. Glukhovtsev, and B. Y. Simkin. 1994. *Aromaticity and Antiaromaticity,* Wiley, New York.

32. Schleyer, P. v. R., ed. 2005. *Chem. Rev.*, **105**: 10.

33. Schleyer, P. v. R., ed. 2001. *Chem. Rev.*, **101**: 5.

34. Schleyer, P. v. R., Maerker, C., Dransfeld, A., Jiao, H., and Hommes, N. J. R. v. E. 1996. Nucleus-independent chemical shifts: a simple and efficient aromaticity probe. *J. Am. Chem. Soc.,* **118**: 6317-6318.

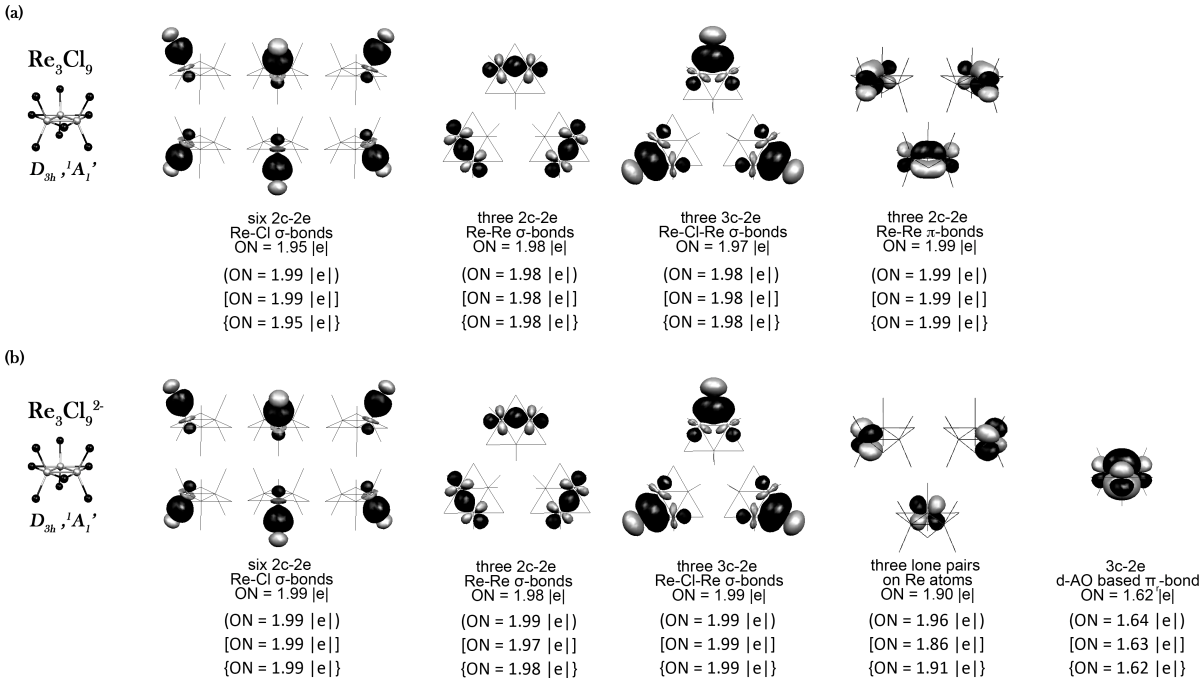

Figure 8-1. Chemical bonding elements revealed by the AdNDP analyses of (a) neutral Re_3Cl_9; (b) doubly charged $Re_3Cl_9^{2-}$. Occupation numbers (ON) are reported at B3LYP/LANL2DZ, HF/LANL2DZ (in parenthesis), BPW91/LANL2DZ (in square brackets), PBE1PBE/LANL2DZ (in squiggle brackets) levels.

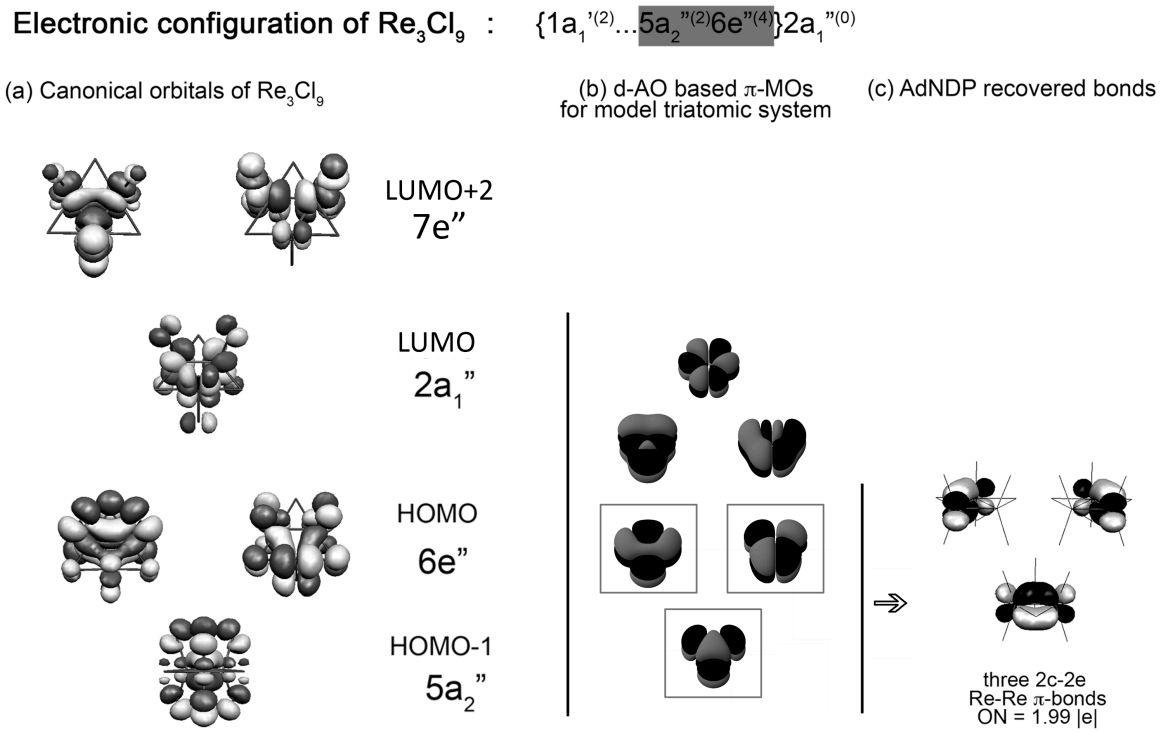

Figure 8-2. (a) Canonical molecular orbitals (CMOs) of Re_3Cl_9; (b) d-AO based π-molecular orbitals for model triatomic system (with the occupied ones enclosed in rectangles); (c) three Re-Re π-bonds recovered by the AdNDP analysis.

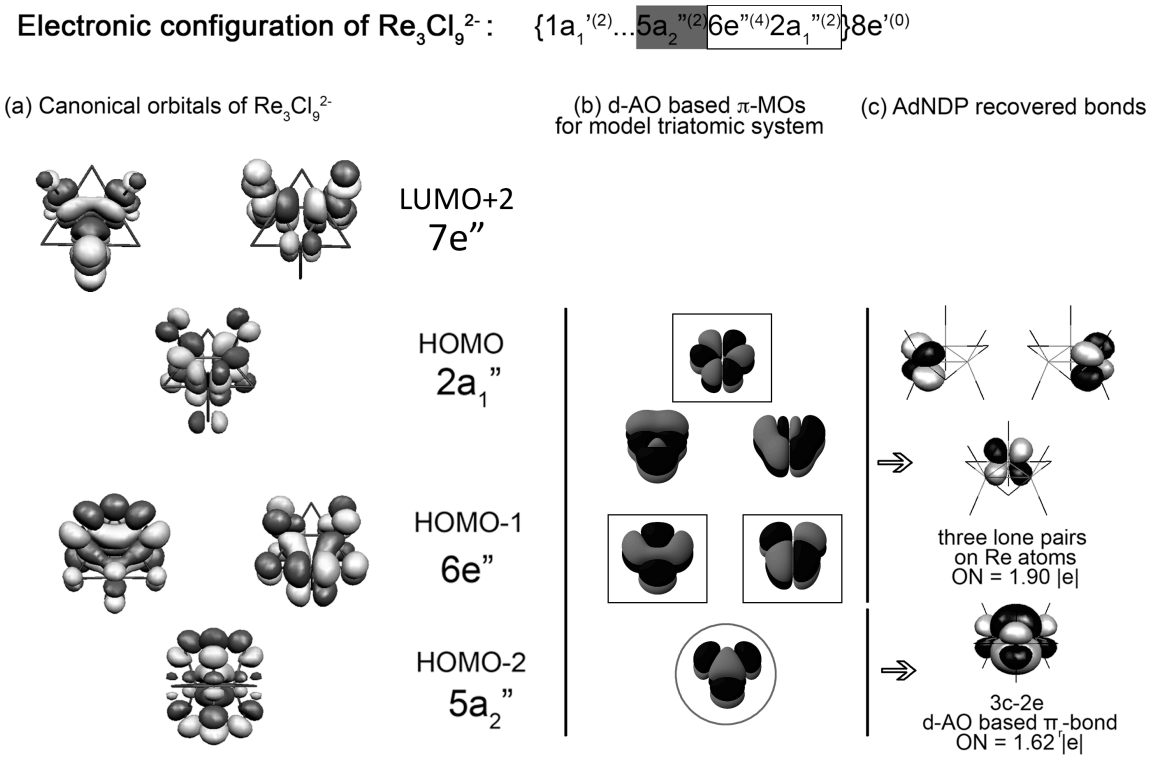

Figure 8-3. (a) CMOs of $Re_3Cl_9^{2-}$; (b) d-AO based π-molecular orbitals for model triatomic system; (c) three lone pairs on rhenium atoms formed out of three CMOs (HOMO and doubly degenerate HOMO-1), and totally delocalized d-AO based radial π-bond recovered by the AdNDP analysis.

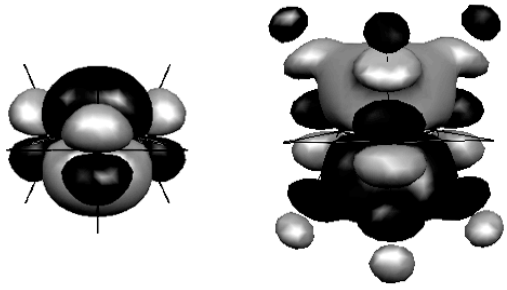

3c-2e	9c-2e
ON = 1.62 |e|	ON = 2.00 |e|
(ON = 1.64 |e|)	(ON = 2.00 |e|)
[ON = 1.63 |e|]	[ON = 2.00 |e|]
{ON = 1.62 |e|}	{ON = 2.00 |e|}

Figure 8-4. Variation of the occupation number of the d-AO based π_r-bond of $Re_3Cl_9^{2-}$ upon changing the number of centers (atoms) it is allowed to be delocalized on. Occupation numbers (ON) are given at B3LYP/LANL2DZ, HF/LANL2DZ (in parenthesis), BPW91/LANL2DZ (in square brackets), PBE1PBE/LANL2DZ (in squiggle brackets).

CHAPTER 9

RATIONAL DESIGN OF SMALL 3D GOLD CLUSTERS[1]

Abstract

We designed a series of small 3D gold clusters using a four-atomic tetrahedron with a four center – two electron (4c-2e) bond inside as a building block. The follow-up results of the unbiased global minimum searches proved that indeed the designed 3D structures containing small tetrahedral building blocks with a 4c-2e bond inside are either global minimum structures or low-lying isomers. We believe that the proposed way of building 3D clusters could be used for rational design of other 3D gold clusters.

9-1. Introduction

Gold clusters attracted lots of attention since Haruta and co-workers discovered that nanoscale gold particles have unusual catalytic properties for selective oxidation of CO [1]. There is a significant body of experimental and theoretical data concerning structure of gold clusters [2-22]. Comprehensive reviews on gold clusters have been published recently [23, 24]. One of the important questions is where the transition from 2D to 3D occurs in gold clusters. According to the recent ion mobility measurements [3], photoelectron experiments [6], and electron diffraction data [12], as well as theoretical calculations [18] it is known that anionic gold clusters assume a planar structure for $n \leq 11$, while at $n = 12$ there is a point with both 2D and 3D structures being present. According to Gilb at el., the 2D-3D transition in cationic gold clusters occurs between seven and eight atoms [4]. Walker identified the 2D-3D transition in cationic gold

[1] Coauthored by Alina P. Sergeeva and Alexander I. Boldyrev. Reproduced with permission from *J. Clust. Sci*. **2011**, 22, 321-329. Copyright 2011, Springer Science+Business Media, LLC 2011.

clusters as occurring between eight and nine atoms though [5]. The planar to three-dimensional transition in neutral gold clusters occurs at 11 atoms [5]. The remarkable system tetrahedral Au_{20} golden cage was discovered in molecular beams by Li et al [7]. The chemical bonding model for this species was first conjectured by King, Chen, and Schleyer [25]. Zubarev and Boldyrev [26] have recently confirmed that the Au_{20} cluster can be rationalized in terms of ten four center two electron (*4*c-*2*e) bonds located at the center of every small tetrahedra comprising Au_{20} cluster. Thus, there is an opportunity to use gold tetrahedron with a 4c-2e bond inside as a building block of 3D gold clusters. In this article we first build small 3D clusters composed of one, two or three tetrahedral building blocks. We then perform unbiased global minimum searches, which confirm that indeed clusters containing gold tetrahedra with a 4c-2e bond inside are either global minimum structures or low-lying isomers. We thoroughly study the chemical bonding of all the designed structures and explain why global minima assume the particular geometries. On the basis of the gained knowledge of the chemical bonding patterns and stability of these 3D clusters we propose a rational design for small gold clusters (built of more than three Au_4^{2+} tetrahedral blocks). Unlike all the previous works where people analyzed the 2D-3D transition in gold clusters in a series of the species having the same charge: anionic (Au_x^-), neutral (Au_x), or cationic (Au_x^+), we want to design 3D gold structures containing tetrahedral blocks since Corbett and co-workers demonstrated that gold tetrahedra serve as building blocks in the crystalline structures of K_3Au_5Tr (Tr = In, Tl) [27], Rb_2Au_3Tl [28], $K_{12}Au_{21}Sn_4$ [28].

9-2. Theoretical Results

In the current article we show that understanding of chemical bonding in 3D gold clusters, which is based on formation of *4*c-*2*e bonds, can help us to rationally design small (n < 10) clusters with 3D global minimum structure, which could be building blocks of solid materials. Each gold atom has one valence 6s electron (if we treat 5d electrons as core ones). We are presenting our results for design of gold clusters with one, two, three and four pairs of valence electrons.

9-3. One Electron Pair Cluster

The smallest 3D gold cluster can be constructed of four atoms. In order to have a single *4*c-*2*e bond, the tetratomic cluster should have a tetrahedral structure with the external charge +2. In order to test this conjecture we performed Coalescence Kick (CK) global minimum search, recently developed by Boris Averkiev in our group [29] at the B3LYP/LANL2DZ [30-33] level of theory (we used this level of theory for all our CK seaches). The lowest structures found by the CK method were further reoptimized with the calculation of frequencies at the B3LYP/ Stuttgart_rsc_1997_ecp [34] + 2f1g [35] or PBE1PBE/Stuttgart_rsc_1997_ecp [36, 37] + 2f1g (α(f)=0.448, α(f)=1.464, α(g)=1.218) ([8s6p5d2f1g/7s3p4d2f1g]) levels of theory. Relativistic effects are taken into account through the use of effective core potentials (LANL2DZ and Stuttgart_rsc_1997_ecp). The CK method subjects large populations of randomly generated structures to a coalescence procedure with all atoms gradually pushed to the molecular center of mass to avoid generation of fragmented structures and then optimizes them to the nearest local minima. The CK search revealed only one non-fragmented structure, which is a

tetrahedral Au_4^{2+} cluster of T_d symmetry in the $^1A_1$ singlet state (Figure 9-1a), in accordance with our conjecture.

The electronic structure of the Au_4^{2+} cluster was analyzed using the Adaptive Natural Density Partitioning (AdNDP) method developed by Dmitry Zubarev in our lab [38, 39]. The AdNDP analysis is based on the concept of an electron pair as the main element of chemical bonding. It represents the electronic structure in terms of *n*-center–two-electron (*n*c-*2*e) bonds. With *n* ranging from one to the total number of atoms in the whole cluster, AdNDP recovers both Lewis bonding elements (*1*c-*2*e or *2*c-*2*e objects, i.e., lone pairs or two-center two-electron bonds) and delocalized bonding elements (*n*c-*2*e bonds, $n>2$). The AdNDP analysis confirmed the presence of a pair of electrons located inside of the gold tetrahedron being delocalized over all four gold atoms (Figure 9-1b). The occupation number (ON), which represents number of electrons per a bond, of the recovered *4*c-*2*e bond is equal to the ideal value of 2.00 |e|. Relativistic effects have no effect on the formation of the 4c-2e bonds. Since Au_4^{2+} is a doubly charged cation, it is not thermodynamically stable. Dissociation energy towards Au_3^+ and Au^+ is -37.0 kcal/mol, and towards two Au_2^+ is equal to -11.2 kcal/mol, here and thereafter the numerical data are given at B3LYP/Stuttgart_rsc_1997_ecp + 2f1g and at PBE1PBE/Stuttgart_rsc_1997_ecp + 2f1g (the data calculated at this level is given throughout the text in parenthesis). Thus, transition from 2D to 3D occurs at $n = 4$ if we select the appropriate external charge. Therefore, if Au_4^{2+} were made in a molecular beam or found as a building block in solids, it would possess a tetrahedral structure.

9-4. Two Electron Pairs Clusters

The next type of clusters of interest is that having two electron pairs comprising two *4*c-*2*e bonds. One may think of three possible structures: Au_5^+ where two gold tetrahedra have mutual face (Figure 9-2a, see the D_{3h} structure), Au_6^{2+} where two gold tetrahedra have mutual edge (Figure 9-2b, see the D_{2h} structure), and finally Au_7^{3+} where they have mutual vertex (Figure 9-2c, see the D_{3d} structure).

The trigonal bipyramidal cluster of Au_5^+ (D_{3h}, $^1A_1$') is not a minimum (Figure 9-2a). The optimized structure has two imaginary frequencies ($\omega_{1,2}$(e") = -23.3 cm^{-1}). Geometry optimization following imaginary normal modes leads to two structures: D_{2h} (^1A_g) and D_{2d} ($^1A_1$), with the latter being a first order saddle point in transition into the D_{2h} (^1A_g) structure (Figure 9-2a). The global minimum of the Au_5^+ cluster is the D_{2h} structure in agreement with the previous calculations [4, 5]. We performed the AdNDP analysis for all these structures and found out that there are two *4*c-*2*e bonds in the trigonal bypiramidal structure and two 3c-2e bonds in each D_{2h} and D_{2d} structures (Figure 9-2a). We believe, that the trigonal bipyramidal structure is not stable due to the fact that two pairs of electrons comprising *4*c-*2*e bonds in Au_5^+ are too close to each other. Indeed, if we assume that the centers of electron density of *4*c-*2*e bonds and *3*c-*2*e bonds are located at the centers of tetrahedrons or triangles, respectively, the distances between those centers in the D_{3h} structure (~1.3 Å) are much smaller than there in the D_{2h} structure (~3.1 Å).

We found two non-fragmented structures for the Au_6^{2+} cluster: the first one being the D_{2h} (^1A_g) structure (comprised out of two gold tetrahedra sharing an edge), and the C_s (^1A') structure (which is composed of a tetrahedron and a triangle of gold atoms merged

through a vertex (Figure 9-2b)). Both structures are true isomers (all frequencies are positive) with isomer C_s being the global minimum. Isomer D_{2h} is 9.4 (7.5) kcal/mol higher in energy. The AdNDP analysis reveals that two valence pairs of electrons form either a *4*c-*2*e bond and a *3*c-*2*e bond (in the case of the C_s structure), or two *4*c-*2*e bonds (D_{2h}), see Figure 9-2b. Like in the case of Au_5^+, the repulsion between electron pairs in the D_{2h} structure is greater than there in the C_s structure, which is again due to the shorter distance between centers of bonds (2.2 Å vs. 3.3 Å). Though, the D_{2h} isomer is not a global minimum, the lowest C_s isomer is a 3D structure.

There are two structures of Au_7^{3+} with a mutual vertex: D_{3h} ($^1A_1$') and D_{3d} ($^1A_{1g}$) (Figure 9-2c). According to our calculations, the D_{3d} structure is a minimum, whereas the D_{3h} structure is the first order saddle point in rearrangement of one D_{3d} structure into another. The AdNDP analysis confirmed the expected two *4*c-*2*e bonds inside both of the tetrahedra comprising the D_{3d} structure (Figure 9-2c). We then performed the CK search to reveal the most stable non-fragmented structure, which has been proved to have D_{3d} symmetry.

Therefore, the most stable 3D structure formed of two tetrahedra is such that when two tetrahedra share a vertice for the two electron pairs comprising the 4c-2e bonds to account for the least repulsion.

9-5. Three Electron Pairs Clusters

Considering clusters having three electron pairs that may comprise three *4*c-*2*e bonds, one may think of three possible structures: Au_7^+ where three gold tetrahedra have

mutual face (Figure 9-3a), Au_8^{2+} where three gold tetrahedra have mutual edges (Figure 9-3b), and finally Au_9^{3+} where they have mutual vertices (Figure 9-3c).

The geometry optimization of the Au_7^+ cluster (C_{3v}, $^1A_1$) with three gold tetrahedra having mutual face leads to the structure, which is a second order saddle point (Figure 9-3a). Optimization along the imaginary frequency modes leads to two isomers having no imaginary frequencies: C_{2v}, I ($^1A_1$) and C_{2v}, II ($^1A_1$). The global minimum structure of Au_7^+ was previously reported to be a centered planar hexagon structure of D_{6h} ($^1A_{1g}$) symmetry [4, 5]. We found this structure to be the global minimum at the both levels of theory in agreement with the previous reports [4, 5]. The high stability of the Au_7^+ centered planar hexagon can be easily rationalized on the basis of the σ-aromaticity. Indeed, the AdNDP analysis revealed (Figure 9-3a) that this structure has three completely delocalized σ-bonds, thus satisfying the 4n+2 rule (n=1) for σ-aromaticity in ring- and wheel-type structures [40]. Still, we would like to point out that the most stable 3D-structure C_{2v}, I with one 4c-2e and two 3c-2e bonds is only 1.7 (1.8) kcal/mol higher in energy than the aromatic planar one.

In Figure 9-3b the optimized D_{2d} ($^1A_1$) structure of Au_8^{2+}, comprised out of three gold tetrahedra sharing edges, is presented. It is not a minimum but rather a third order saddle point. Geometry optimization along the imaginary frequencies leads to two isomers: C_s ($^1A'$) and C_2 (^1A). The CK global minimum search performed for this cluster revealed the global minimum to be a C_{2v} ($^1A_1$) structure. As in the previous case of Au_6^{2+}, the structure with gold tetrahedra having mutual edges is not favorable, because electron pairs inside of tetrahedra (according to our AdNDP analysis, see Figure 9-3b) are too

close to each other (2.4 Å) compared to the same distance in global minimum structure (3.5 Å) where the two tetrahedra and the triangle are connected to each other via vertices.

The optimized Au_9^{3+} D_{3h} ($^1A_1$') structure with tetrahedra connected to each other through vertices is a minimum with three 4c-2e bonds located inside of every tetrahedra recovered by the AdNDP method (Figure 9-3c). However, there are two more competitive isomers revealed by the CK global minimum search: C_{2v} ($^1A_1$) and C_s (^1A'). At the B3LYP/Stuttgart_rsc_1997_ecp + 2f1g level of theory all three structures are close in energy (Figure 9-3c). The D_{3h} ($^1A_1$') isomer has three 4c-2e bonds inside of every small tetrahedra, the C_{2v} ($^1A_1$) isomer has two 4c-2e bonds located inside of each of the tetrahedra, and one 3c-2e bond located inside of the triangle, and the C_s (^1A') isomer has two 3c-2e bonds located inside of each of the tetrahedron, and one 4c-2e bond located inside of the triangle.

We again see that the most favorable 3D structures built of Au_4^{2+} building blocks (global minima or low-lying isomers) have electron pairs located in tetrahedra sharing a vertice. Therefore, the strategy for designing the 3D gold clusters should be based on this idea.

9-6. Four Electron Pairs Clusters

Now that we learnt that the 3D structures containing Au_4^{2+} building blocks are only stable when tetrahedra share vertices, we can construct the most favorable structural arrangement for the gold clusters composed of four tetrahedral units. Four tetrahedra each having a *4*c-*2*e bond inside can be assembled into a tetrahedral T_d ($^1A_1$) structure of the neutral Au_8 cluster (Figure 9-4a), or the T_d ($^1A_1$) structure of Au_{10}^{2+} (Figure 9-4b).

The Au_8 cluster has been thoroughly studied by Olson and Gordon [13] and Walker [5]. Olson and Gordon showed that the global minimum structure at their highest level of theory (CCSD(T)/cc-pVTZ-PP+CV) of Au_8 is the planar structure D_{4h} ($^1A_{1g}$) (Figure 9-4a), which is lower in energy than the T_d ($^1A_1$) structure by about 6 kcal/mol. According to our calculations, the D_{4h} structure is also lower in energy by 19.5 (11.5) kcal/mol than the T_d structure in a qualitative agreement with results reported by Olson and Gordon [13] and Walker [5]. The AdNDP analysis revealed that there is a 4c-2e bond inside every of four tetrahedra in the T_d structure, whereas there is a 3c-2e bond inside of every outer triangle in the D_{4h} structure. On one hand, one could think that the tetrahedral Au_8 cluster is more stable due to the fact that each electron pair is stabilized by four Au^+ cations compared to three Au^+ cations in the planar Au_8 cluster (if one consider a gold cluster as formed of Au^+ cations and electron pairs). Though, the D_{4h} structure is the global minimum and we again attribute this phenomena to the difference in distances between the centers of two closest electron pairs: 3.1 Å (D_{4h}) > 1.8 Å (T_d).

From the gained experience, it is clear that if one wants to design a stable cluster composed out of tetrahedral building blocks, one needs to assemble them in a way that all tetrahedra are connected to each other through vertices. We can achieve that for the T_d ($^1A_1$) structure of Au_{10}^{2+} with four electron pairs located inside of each tetrahedron with no electron density in the central octahedral unit. Our CK global minimum search confirmed that it is a global minimum structure. The T_d ($^1A_1$) structure of Au_{10}^{2+} together with a few other alternative structures found by the CK search are presented in Figure 9-4b. The AdNDP analysis (Figure 9-4b) revealed that indeed every small tetrahedron hosts

a 4c-2e bond inside and those tetrahedra are connected to each other through common vertices. It is interesting to note that the doubly charged cation Au_{10}^{2+} is thermodynamically stable (ΔE = + 9.4 kcal/mol) towards dissociation into two Au_5^+ (D_{2h}, ^1A_g).

9-7. Discussion

We showed that one could construct the 3D gold clusters containing tetrahedral building blocks by choosing the appropriate charge for the cluster. In this article we demonstrated that the smallest 3D gold cluster is Au_4^{2+}. The tetrahedral structure of this cluster is based on the formation of a 4c-2e bond inside of the tetrahedron. We further showed that this tetrahedral unit could be used as a building block of other small 3D gold clusters, such as the Au_6^{2+} (C_s, $^1A'$), Au_7^{3+}(D_{3d}, $^1A_{1g}$), Au_7^+(C_{2v}, I, $^1A_1$), Au_8^{2+} (C_{2v}, $^1A_1$), Au_9^{3+} (C_{2v}, $^1A_1$), Au_9^{3+} (C_s, $^1A'$), Au_9^{3+} (D_{3h}, $^1A_1'$), and Au_{10}^{2+} (T_d, $^1A_1$). We found that in the most stable structures tetrahedral units are always connected through the vertices. Structures where tetrahedra share edges, or faces are either higher in energy, or are not even local minima. Analyses of structure and chemical bonding revealed that the two latter types of structures are less stable due to the repulsion between electron pairs inside of the tetrahedra. Thus, in the rational design of stable gold clusters one needs to use the following construction principle: build the gold clusters in a way that all tetrahedral units are connected to each other through common vertices. We demonstrated such a design on an example of Au_{10}^{2+} where four tetrahedra merged together through vertices are forming a super tetrahedron. The previously discussed Au_{20} cluster is also constructed in the same

manner. In that case ten small tetrahedra merged together through the vertices comprise a beautiful tetrahedral Au_{20} structure.

The gold tetrahedra were shown to be building blocks in a solid state. In particular, Corbett and co-workers demonstrated that the crystalline structures K_3Au_5Tr (Tr = In, Tl) [26], Rb_2Au_3Tl [26], $K_{12}Au_{21}Sn_4$ [27] consisted of infinite puckered sheets of vertex-sharing gold tetrahedra, which is consistent with our findings.

We believe that the proposed construction principle can be used for rational design of gold clusters, solids containing gold clusters, and gold nanoparticles.

References

1. M. Haruta, T. Kobayashi, H. Sano, and N. Yamada (1987). *Chem. Lett.* **16**, 405.
2. M. A. Omary, M. A. Rawashdeh-Omary, C. C. Chusuei, J. P. Fackler Jr., and P. S. Bagus (2001). *J. Chem. Phys.* **114**, 10695.
3. F. Furche, R. Ahlrichs, P. Weis, C. Jacob, S. Gilb, T. Bierweiler, and M. M. Kappes (2002). *J. Chem. Phys.* **117**, 6982.
4. S. Gilb, P. Weis, F. Furche, R. Ahlrichs, and M. M. Kappes (2002). *J. Chem. Phys.* **116**, 4094.
5. A. V. Walker (2005). *J. Chem. Phys.* **122**, 094310.
6. H. Hakkinen, B. Yoon, U. Landman, X. Li, H. J. Zhai, and L. S. Wang (2003). *J. Phys. Chem. A.* **107**, 6168.
7. J. Li, X. Li, H. J. Zhai, and L. S. Wang (2003). *Science* **299**, 864.
8. H. F. Zhang, M. Stender, R. Zhang, C. M. Wang, J. Li, and L. S. Wang (2004). *J. Phys. Chem. B* **108**, 12259.

9. M. Ji, X. Gu, X. Li, X. G. Gong, J. Li, and L. S. Wang (2005). *Angew. Chem. Int. Ed.* **44**, 7119.

10. S. Bulusu, X. Li, L. S. Wang, and X. C. Zeng (2006). *Proc. Natl. Acad. Sci.* (USA) **103**, 8326.

11. M. F. Bertino, Z. M. Sun, R. Zhang, and L. S. Wang (2006). *J. Phys. Chem. B* **110**, 21416.

12. X. Xing, B. Yoon, U. Landman, and J. H. Parks (2006). *Phys. Rev. B: Condens. Matter Mater. Phys.* **74**, 165423.

13. R. M. Olson and M. S. Gordon (2007). *J. Phys. Chem.* **126**, 214310.

14. S. Bulusu, X. Li, L. S. Wang, and X. C. Zeng (2007). *J. Phys. Chem. C* **111**, 4190.

15. X. Gu, S. Bulusu, X. Li, X. C. Zeng, J. Li, X. G. Gong, and L. S. Wang (2007). *J. Phys. Chem. C* **111**, 8228.

16. W. Huang, M. Ji, C. D. Dong, X. Gu, L. M. Wang, X. G. Gong, and L. S. Wang (2008). *ACS Nano* **2**, 897.

17. M. P. Johansson, A. Lechtken, D. Schooss, M. M. Kappess, and F. Furche (2008). *Phys. Rev. A: At. Mol. Opt. Phys.* **77**, 053202.

18. M. Mantina, R. Valero, and D. G. Truhlar (2009). *J. Chem. Phys.* **131**, 064706.

19. L. Ferrighi, B. Hammer, and G. K. H. Madsen (2009). *J. Am. Chem. Soc*. **131**, 10605.

20. W. Huang and L. S. Wang (2009). *Phys. Chem. Chem. Phys.* **11**, 2663.

21. W. Huang and L. S. Wang (2009). *Phys. Rev. Lett*. **102**, 153401.

22. W. Huang, S. Bulusu, R. Pal, X. C. Zeng, and L. S. Wang (2009). *ACS Nano* **3**, 1225.

23. P. Pyykko (2004). *Angew. Chem. Int. Ed*. **43**, 4412.

24. H. Hakkinen (2008). *Chem. Soc. Rev.* **37**, 1847.

25. R. B. King, Z. Chen, and P. v. R. Schleyer (2004). *Inorg. Chem.* **43**, 4564.

26. D. Y. Zubarev and A. I. Boldyrev (2009). *J. Phys. Chem. A* **113**, 866.

27. B. Li, S. J. Kim, G. J. Miller, and J. D. Corbett (2009). *Inorg. Chem.* **48**, 6573.

28. Q. Lin and J. D. Corbett (2010). *J. Am. Chem. Soc*. **132**, 5662.

29. B. B. Averkiev (2009). Geometry and electronic structure of doped clusters via the Coalescence Kick Method. PhD Dissertation. Utah State University, Logan, Utah.

30. A. D. Becke (1993). *J. Chem. Phys*. **98**, 5648.

31. S. H. Vosko, L. Wilk, and M. Nusair (1980). *Can. J. Phys.* **58**, 1200.

32. C. Lee, W. Yang, and R. G. Parr (1988). *Phys. Rev. B* **37**, 785.

33. P. J. Hay and W. R. Wadt (1985). *J. Chem. Phys.* **82**, 299.

34. M. Dolg, U. Wedig, H. Stoll, and H. Preuss (1987). *J. Chem. Phys*. **86**, 866.

35. J. M. L. Martin and A. Sundermann (2001). *J. Chem. Phys*. **114**, 3408.

36. J. P. Perdew, K. Burke, and M. Ernzerhof (1996). *Phys. Rev. Lett*. **77**, 3865.

37. J. P. Perdew, K. Burke, and M. Ernzerhof (1997). *Phys. Rev. Lett*. **78**, 1396.

38. D. Y. Zubarev and A. I. Boldyrev (2008). *Phys. Chem. Chem. Phys.* **10**, 5207.

39. D. Y. Zubarev, N. Robertson, D. Domin, J. McClean, J. Wang, W. A. Lester, Jr., R. Whitesides, X. You, and M. Frenklah (2010). *J. Phys. Chem. C* **114**, 5429.

40. A. P. Sergeeva, B. B. Averkiev, and A. I. Boldyrev, in G. Parkin (ed.), *Metal-Metal Bonding.* Structure and Bonding book series. vol. 136 (Springer, Berlin/Heidelberg, 2010), pp. 275-306.

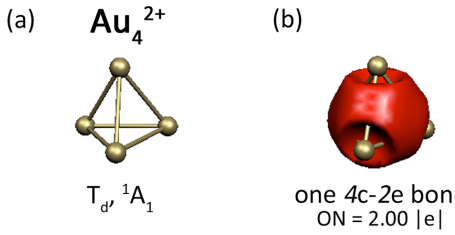

Fig. 9-1. Structure, symmetry, and spectroscopic state of the Au_4^{2+}cluster (a); the *4*c-*2*e valence bond based on σ-atomic orbitals as recovered by the AdNDP analysis (b).

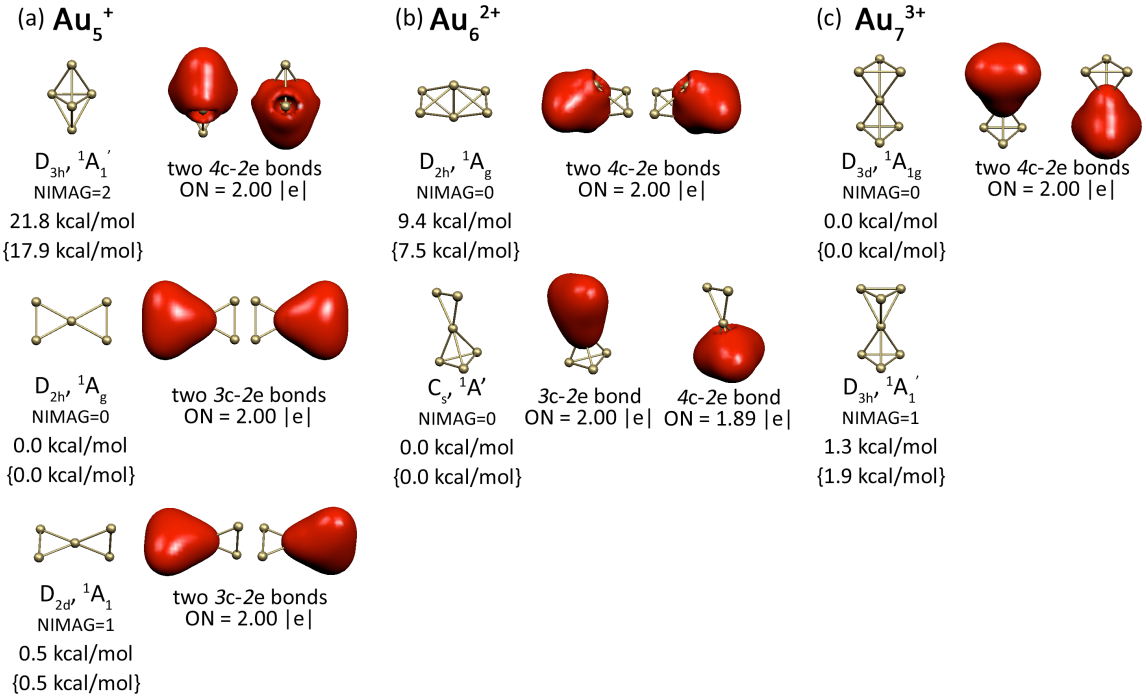

Fig. 9-2. Structures, symmetries, and spectroscopic states and the chemical bonding picture recovered by the AdNDP analyses for alternative isomers of the Au_5^+cluster (a); the Au_6^{2+} cluster (b); and the Au_7^{3+} cluster (c). Relative energies are given at B3LYP/Stuttgart_rsc_1997_ecp + 2f1g and at PBE1PBE/Stuttgart_rsc_1997_ecp + 2f1g (in curly brackets).

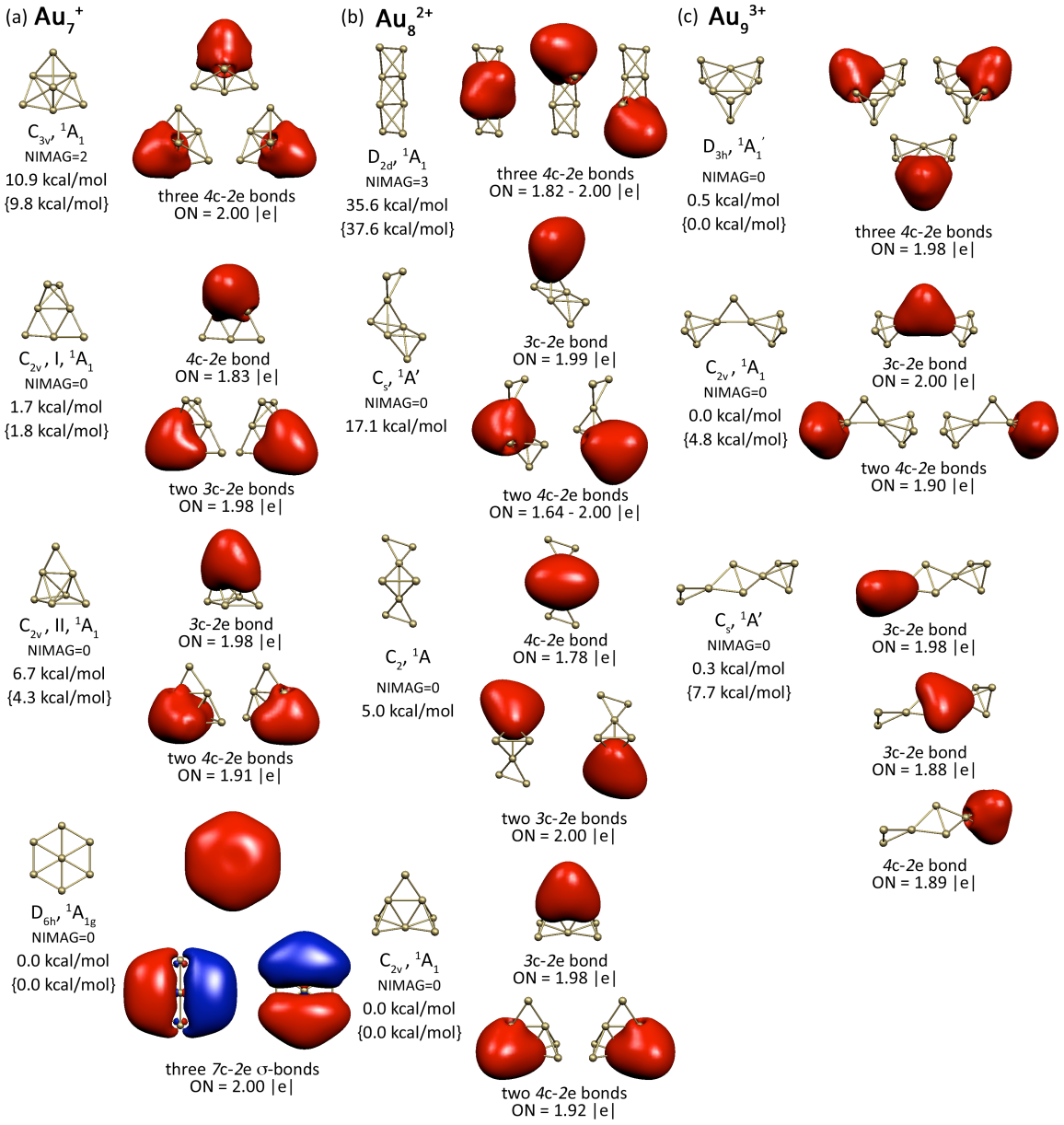

Fig. 9-3. Structures, symmetries, and spectroscopic states and the chemical bonding picture recovered by the AdNDP analysis for alternative isomers of the Au_7^+cluster (a); the Au_8^{2+} cluster (b); and the Au_9^{3+} cluster (c). Relative energies are given at B3LYP/Stuttgart_rsc_1997_ecp + 2f1g and at PBE1PBE/Stuttgart_rsc_1997_ecp + 2f1g (in curly brackets).

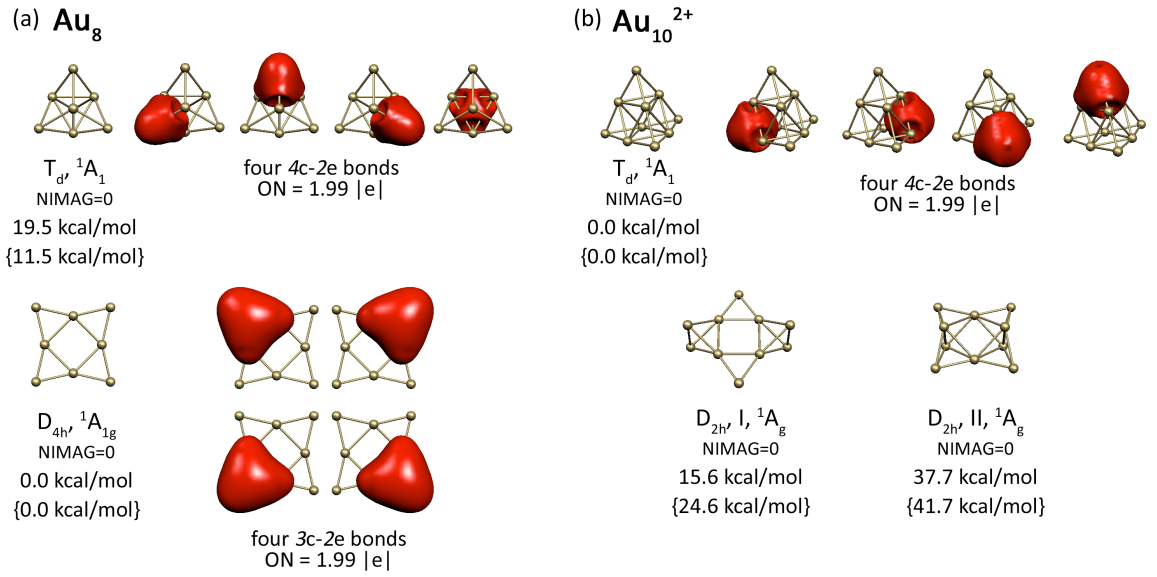

Fig. 9-4. Structures, symmetries, and spectroscopic states and the chemical bonding picture recovered by the AdNDP analysis for two low-lying isomers of the Au_8 cluster (a); and the Au_{10}^{2+} cluster (b). Relative energies are given at B3LYP/Stuttgart_rsc_1997_ecp + 2f1g and at PBE1PBE/Stuttgart_rsc_1997_ecp + 2f1g (in curly brackets).

CHAPTER 10

PROBING THE ELECTRONIC STABILITY OF MULTIPLY CHARGED ANIONS: THE SULFONATED PYRENE TRI- AND TETRA-ANIONS[1]

Abstract

The strong intramolecular Coulomb repulsion in multiply charged anions (MCAs) creates a potential barrier that provides dynamic stability to MCAs and allows electronically metastable species to be observed. The 1-hydroxy-3,6,8-pyrene-trisulfonate {$[Py(OH)(SO_3)_3]^{3-}$ or $HPTS^{3-}$} was recently observed as a long-lived metastable MCA with a large negative electron binding energy of –0.66 eV. Here we use Penning trap mass spectrometry to monitor the spontaneous decay of $HPTS^{3-} \rightarrow HPTS^{\bullet 2-} + e^-$ and have determined the half-life of $HPTS^{3-}$ to be 0.1 s. To explore the limit of electronic metastability, we tried to make the related quadruply charged pyrene-1,3,6,8-tetrasulfonate {$[Py(SO_3)_4]^{4-}$}. However, only its decay product — the triply charged radical anion $[Py(SO_3)_4]^{\bullet 3-}$, as well as the triply charged ion-pairs $[Py(SO_3)_4H]^{3-}$ and $[Py(SO_3)_4Na]^{3-}$, were observed, suggesting that the tremendous intramolecular Coulomb repulsion makes the $[Py(SO_3)_4]^{4-}$ anion extremely short-lived. Photoelectron spectroscopy data showed that $[Py(SO_3)_4]^{\bullet 3-}$ is an electronically stable species with electron binding energies of +0.5 eV, whereas $[Py(SO_3)_4H]^{3-}$ and $[Py(SO_3)_4Na]^{3-}$ possess electron binding energies of 0.0 eV and –0.1 eV, respectively. Ab initio calculations confirmed the stability of these triply charged species and further predicted a large

[1] Coauthored by Xue-Bin Wang, Alina P. Sergeeva, Xiao-Peng Xing, Maria Massaouti, Tatjana Karpuschkin, Oliver Hampe, Alexander I. Boldyrev, Manfred M. Kappes, and Lai-Sheng Wang. Reproduced with permission from *J. Am. Chem. Soc.* **2009**, 131, 9836-9842. Copyright 2009, American Chemical Society

negative electron binding energy (–2.78 eV) for $[Py(SO_3)_4]^{4-}$ consistent with its short lifetime.

10-1. Introduction

Although multiply charged anions (MCAs) are common in solution and solids, they cannot be easily studied in the gas phase,[1-14] because of the strong intramolecular Coulomb repulsion that renders these species unstable against either autodetachment or charge-separation fragmentation outside the condensed media. The electrospray ionization technique has made it possible to produce intense beams of MCAs in the gas phase and allowed their first spectroscopic characterization by photoelectron spectroscopy (PES).[15-21] The electron detachment dynamics of MCAs are strongly influenced by the so-called repulsive Coulomb barriers (RCB) originated from the superposition of the long-range Coulomb repulsion between the remaining anion and the outgoing electron and the short-range polarization attraction / chemical binding of this electron. The RCB prevents slow photoelectrons from being emitted from MCAs, giving rise to a cutoff in photoelectron spectra, which has become a hallmark of PES of MCAs.[15-21] More interestingly, the RCB provides dynamic stability for unstable or metastable MCAs, allowing such exotic species to be observed experimentally.[17,22,23] As a corollary, metastable MCAs store excess electrostatic energies, which are released upon electron detachment. Therefore, metastable MCAs can produce photoelectrons with kinetic energies (KE) *higher* than the detachment laser energy ($h\nu$), resulting in negative electron binding energies (BE) according to Einstein's photoelectric equation: $h\nu$ = BE + KE.

The lifetimes of metastable MCAs can be qualitatively estimated[22,24] using the Wentzel-Kramers-Brillouin (WKB) tunneling formalism through a Coulomb potential developed for a-decay in nuclear physics. The lifetimes depend exponentially on the tunneling distance (molecular size) and the magnitude of the negative electron binding energy. Many small MCAs with large negative electron binding energies are too shorted-lived to allow experimental observation, which is typically on the order of tens of microseconds. The first MCA directly observed to possess a negative electron binding energy was the copper phthalocyanine tetrasulfonate $[CuPc(SO_3)_4]^{4-}$ with a negative electron binding energy of –0.9 eV.[17,23] The relatively small $PtCl_4^{2-}$ dianion was observed to possess a negative electron binding energy of –0.25 eV.[22] The lifetimes of both $[CuPc(SO_3)_4]^{4-}$ and $PtCl_4^{2-}$ have been measured at room temperature in a Fourier-transform ion cyclotron resonance (FT-ICR) mass spectrometer as 275 and 2.5 s, respectivly.[25,26] The long lives of several quadruply charged phthalocyanine systems, $[MPc(SO_3)_4]^{4-}$ (M = Cu, Ni, H_2), have been exploited for electronic spectroscopy in the gas phase.[27] Furthermore, femtosecond pump-probe experiments have shown that electron tunneling from excited states is a major relaxation channel in $[H_2Pc(SO_3)_4]^{4-}$.[28] Very recently, a long-lived metastable triply-charged anion, 1-hydroxy-3,6,8-pyrene-trisulfonate ($HPTS^{3-}$) (see Scheme 10-1a), was observed with a relatively high negative electron binding energy of –0.66 eV and a high RCB of ~3.3 eV.[29]

In the current work, we explore a general question, that is, how much excess energy can be stored in an MCA of a given charge state such that its lifetime is still long enough to allow experimental observation and interrogation? The pyrene system (Scheme 10-1) provides an opportunity to address this question because by varying the R group the

charge states of the system can be changed while maintaining similar molecular size. We are particularly interested in the R = SO_3^- case to see if the quadruply charged $[Py(SO_3)_4]^{4-}$ species can be observed and how much excess energy it stores. We first measured the lifetime of $HPTS^{3-}$ using Penning trap FT-ICR mass spectrometry and determined its room temperature half-life to be 0.1 s. However, we were not able to observe $[Py(SO_3)_4]^{4-}$, consistent with its large estimated negative electron binding energy of –2.78 eV. We were able to observe its decay product, $[Py(SO_3)_4]^{\bullet 3-}$, and the quadruply charged anions stabilized by H^+ and Na^+. All these triply charged species, $[Py(SO_3)_4]^{\bullet 3-}$, $[Py(SO_3)_4H]^{3-}$, and $[Py(SO_3)_4Na]^{3-}$ have been shown to be stable by FT-ICR measurements. PES data showed that $[Py(SO_3)_4]^{\bullet 3-}$ possesses a surprisingly high positive electron binding energy of 0.6 eV, whereas the ion-pairs, $[Py(SO_3)_4H]^{3-}$ and $[Py(SO_3)_4Na]^{3-}$, both possess much lower electron binding energies of 0.0 and –0.1 eV, respectively. Ab initio calculations were further carried out to help understand the electronic structures and stability of the pyrene multianions.

10-2. Experimental and Theoretical Methods

10-2.1. Photoelectron Spectroscopy

The PES experiments were carried out with a low-temperature magnetic-bottle PES apparatus equipped with an electrospray ion source and a cryogenically-controlled ion trap. Details of this instrument have been published[30] and only a brief description is given here. The radical $[Py(SO_3)_4]^{\bullet 3-}$ trianion was observed via electrospray of a 1 mMol solution of pyrene-1,3,6,8-tetrasulfonic tetrasodium salt dissolved in a water/acetonitrile solvent mixture (1/1 volume ratio) that was aimed to produce $[Py(SO_3)_4]^{4-}$, but no trace

of the intended quadruply charged anions was observed due to its high instability. It was found that adding acetonitrile, instead of methanol, in the solvent makes the electrospray more stable without the complication of introducing a proton source. The monoprotonated and sodiumated triply-charged anions, $[Py(SO_3)_4H]^{3-}$ and $[Py(SO_3)_4Na]^{3-}$ were produced from a water/methanol solvent mixture (1/3 volume ratio). The $[Py(SO_3)_4]^{\bullet 3-}$ autodetachment product was also observed in this condition and could not be resolved from $[Py(SO_3)_4H]^{3-}$ in the time-of-flight mass spectrum due to their close *m/z* ratios.

Anions from the electrospray source were guided by a radio-frequency quadrupole and octopole and then bent 90º into the temperature-controlled ion trap, where they were accumulated and collisionally cooled before being pulsed out into the extraction zone of a time-of-flight mass spectrometer. The ion trap was attached to the cold head of a closed-cycle helium refrigerator to allow ion temperatures to be controlled between 10 and 350 K via collisional cooling with ~1 mTorr helium background gas containing 20% H_2. The ion trap was operated at 70 K in the current experiment. The desired anions were mass selected and decelerated before detachment by a laser beam in the interaction zone of a magnetic-bottle photoelectron analyzer. Two detachment photon energies were used in the current study: 193 nm (6.424 eV) from an ArF excimer laser and 266 nm (4.661 eV) from a Nd:YAG laser. Both lasers were operated at a 20 Hz repetition rate with the ion beam off on alternating laser shots for background subtraction. Photoelectrons were collected at nearly 100% efficiency by the magnetic-bottle and analyzed in a 5.2-meter long electron flight tube. Time-of-flight photoelectron spectra were collected and converted to kinetic energy spectra calibrated with the known spectra

of I^- and ClO_2^-. The energy resolution (ΔKE/KE) of the magnetic-bottle electron analyzer was about 2%, i.e., ~20 meV for 1 eV electrons.

10-2.2. Unimolecular Decay and Lifetime Measurements

Lifetime measurements were performed on a FT-ICR mass spectrometer employing a passively shielded 7T magnet. Gas-phase anions were generated using an electrospray ionization source (Analytica of Branford) with an on-axis sprayer as previously described.[31] The sprayed solutions comprised, respectively, 1-hydroxy-3,6,8-pyrene-trisulfonic acid (for $HPTS^{3-}$) and tetrasodium pyrene-1,3,6,8-tetrasulfonate hydrate (both Sigma-Aldrich, >98% purity) {for $[Py(SO_3)_4]^{4-}$} at concentrations of ~10^{-5} mol/L in methanol/water mixtures (3:1). The generated ions were trapped in an ICR cell, whose temperature can be controlled over a range of 90-400 K at typical base pressures <$2x10^{-10}$ mbar. The resolution of the FT-ICR mass spectrometer (M/ΔM) was ~10^5, allowing unequivocal assignments of all relevant anions. For the lifetime studies, the parent MCAs were mass-selected in the ICR cell and mass spectra were taken after variable time delays of up to 100 s. Decay kinetics was obtained by integrating and normalizing the parent and fragment ion intensities.

10-2.3. Ab Initio Calculations

Theoretical calculations were performed to obtain the optimal structures and vertical detachment energies (VDEs) for comparison with the experimental data. Geometry optimization and vibrational frequency calculations for $HTPS^{3-}$, $[Py(SO_3)_4]^{4-}$, $[Py(SO_3)_4]^{\bullet 3-}$, $[Py(SO_3)_4H]^{3-}$ and $[Py(SO_3)_4Na]^{3-}$ were carried out using the hybrid density functional theory (DFT) method known in the literature as B3LYP[32-34] with

augmented correlation-consistent polarized double-ζ valence basis sets (aug-cc-pVDZ) for O and Na atoms[35] and correlation-consistent polarized double-ζ valence basis sets (cc-pVDZ) for C, H, and S atoms.[35,36] The VDE for all the species was calculated at the B3LYP/O/aug-cc-pVDZ/H,C,S/cc-pVDZ//B3LYP/O/aug-cc-pVDZ/H,C,S/cc-pVDZ level of theory as the lowest energy transition from the ground state of the optimized M^{n-} species to the state of $M^{(n-1)-}$ at the frozen geometry of M^{n-}. Higher VDEs were obtained using the time-dependent DFT method (TD-B3LYP/O/aug-cc-pVDZ/H,C,S/cc-pVDZ) by adding the vertical excitation energies in $M^{(n-1)-}$ at the optimized geometry of M^{n-} to the first VDE. Natural Bond Orbital analysis was performed at the B3LYP/O/aug-cc-pVDZ/H,C,S/cc-pVDZ//B3LYP/O/aug-cc-pVDZ/H,C,S/cc-pVDZ level of theory to show the natural charge distribution in all the species and how the net charge in the peripheral groups affects the energy of the HOMO and thus the stability of the MCAs. The B3LYP calculations and NBO analysis were performed using the Gaussian 03 program.[37] Molecular orbital visualization was done using the MOLDEN 3.4 program.[38]

10-3. Experimental results

10-3.1. Lifetime measurements for $HPTS^{3-}$

The PES spectra of $HPTS^{3-}$ were recently reported, revealing a comparatively large negative electron binding energy of –0.66 eV.[29] During the PES experiment, the $HPTS^{3-}$ anions were stored and cooled in an ion trap for about 50 ms without visible signal loss, suggesting that it is quite long-lived. In the current study, we have directly measured the lifetime of $HPTS^{3-}$ using FT-ICR mass spectrometry. The metastability of $HPTS^{3-}$ was immediately confirmed by the appearance of the $HPTS^{\bullet 2-}$ daughter ion in the

FT-ICR mass spectra. Figure 10-1 displays the autodetachment kinetics of $HPTS^{3-}$ at room temperature. An exponential decay was observed, for which a half-life of 0.1 s is deduced from a single-exponential fit. Note that on the time scale of the decay experiment, the collisional mass loss in the ICR cell was negligible at the UHV pressure. In order to shed some light on the autodetachment mechanism, we have calculated thermionic emission rate constants corresponding to a classical "over-the-barrier" process using statistical unimolecular rate theory as recently outlined.[39,40] Figure 10-2 shows the rate constants obtained as a function of internal energy for three different values of RCB (note the RCB was previously determined to be ~3.3 eV[29]). From these data we conclude that at room temperature (~0.7 eV average internal energy) the detached electron must indeed be *tunneling* through the RCB, because the *classical* thermionic process is orders of magnitude slower than the experimental observation for any conceivable internal energy or barrier height.

10-3.2. Attempt to observe the $[Py(SO_3)_4]^{4-}$ quadruply charged anion

We electrosprayed a pyrene-1,3,6,8-tetrasulfonic acid tetrasodium salt solutions, but did not observe any quadruply charged anion $[Py(SO_3)_4]^{4-}$, as intended. We were only able to observe triply-charged anions (Figure 10-3), including the autodetachment product of the tetraanion, $[Py(SO_3)_4]^{\bullet 3-}$, and two ion-pairs, $[Py(SO_3)_4Na]^{3-}$ and $[Py(SO_3)_4H]^{3-}$, in which the parent tetraanion was stabilized by Na^+ and H^+. High resolution FT-ICR mass spectra indicated that the trianions formed depended somewhat on the solvent. $[Py(SO_3)_4]^{\bullet 3-}$ and $[Py(SO_3)_4Na]^{3-}$ were generated by electrospray from a pure aqueous solution of the pyrene-1,3,6,8-tetrasulfonic acid tetrasodium salt. When a

water-methanol solution was used, the protonated species, $[Py(SO_3)_4H]^{3-}$ was also observed, as shown in the inset of Figure 10-3. The protonated tetraanion was likely formed through ion-molecule reactions with methanol during the electrospray or ion transport processes. An analogous variation of ionic products upon addition of methanol was recently observed from electrospray of amino acids.[41,42] Lifetime measurements showed that all the trianions, $[Py(SO_3)_4]^{\bullet 3-}$, $[Py(SO_3)_4H]^{3-}$, and $[Py(SO_3)_4Na]^{3-}$, displayed no measurable decays on a time scale of 100 s, suggesting that all these species are either electronically stable or possess half-lives of at least 100 s.

10-3.3. Photoelectron spectra of $[Py(SO_3)_4]^{\bullet 3-}$.

The time-of-flight mass spectrometer in the low-temperature PES apparatus[30] was not sufficient to resolve $[Py(SO_3)_4]^{\bullet 3-}$ and $[Py(SO_3)_4H]^{3-}$. The FT-ICR mass spectrometric results were used to help identify source conditions to distinguish the two trianions. Figure 10-4 displays the 70 K PES spectra of $[Py(SO_3)_4]^{\bullet 3-}$ at two photon energies obtained by electrospray of a H_2O/CH_3CN solution. The FT-ICR study mentioned above suggested that only $[Py(SO_3)_4]^{\bullet 3-}$ with negligible $[Py(SO_3)_4H]^{3-}$ was produced under this condition. The 193 nm spectrum (Figure 10-4b) shows a weak broad feature (X) at low binding energy with a VDE of ~0.6 eV, and a strong band (A) spanning the range from 1.5 to 2.8 eV. At 266 nm, the X feature became dominant while only the low binding energy part of the A band was observed due to the RCB cutoff. From this cutoff, we estimated a RCB of ~3.0 eV, which is quite close to the previously estimated RCB of 3.3 eV for $HPTS^{3-}$. The weak feature around 3.5 eV in the 266 nm spectrum (Figure 10-4a) was likely due to detachment of the product dianion

$[Py(SO_3)_4]^{\bullet 2-}$ from the same detachment laser pulse. The adiabatic detachment energy (ADE) of $[Py(SO_3)_4]^{\bullet 3-}$ was evaluated from the onset of the 266 nm spectrum by drawing a straight line along the leading edge and adding the instrumental resolution to the intersection with the binding energy axis. We obtained an ADE of 0.5 eV for $[Py(SO_3)_4]^{\bullet 3-}$ (Table 10-1), which is surprisingly high in comparison to the negative electron binding energy of –0.66 eV for $HPTS^{3-}$, considering their very similar molecular compositions and structures.

10-3.4. Photoelectron spectra of $[Py(SO_3)_4H]^{3-}$ and $[Py(SO_3)_4Na]^{3-}$

Figure 10-5 shows the spectra of $[Py(SO_3)_4H]^{3-}$ at two photon energies, produced using a water/methanol solution. As shown by the high-resolution FT-ICR study above, a mixture of $[Py(SO_3)_4]^{\bullet 3-}$ and $[Py(SO_3)_4H]^{3-}$ was produced when spraying a water/methanol solution. Thus, the PES spectra in Figure 10-5a and 10-5b should contain contributions from both $[Py(SO_3)_4]^{\bullet 3-}$ and $[Py(SO_3)_4H]^{3-}$ because they could not be separated in the time-of-flight mass spectra during the PES experiment. Indeed, the spectral features coming from $[Py(SO_3)_4]^{\bullet 3-}$ can be readily recognized, specifically the X band. The weaker, lower binding energy feature (X') should come from $[Py(SO_3)_4H]^{3-}$. The higher binding energy features from both species overlap with each other. The threshold of the X' band yielded an ADE of 0.0 eV for $[Py(SO_3)_4H]^{3-}$ (Table 10-1), which is considerably less stable than $[Py(SO_3)_4]^{\bullet 3-}$.

The PES spectra of $[Py(SO_3)_4Na]^{3-}$ at 266 and 193 nm are shown in Figure 10-5c and 10-5d, respectively. Three broad features X, A, and B centered at 0.15, 1.7, and 3.3 eV, respectively, were resolved at 193 nm. The sharp falloff on the high binding energy

side of the B band is due to the RCB cutoff effect, allowing the RCB barrier height to be determined as ~3 eV. At 266 nm, some fine structures were observed around the X band region (Figure 10-5c), which might suggest the existence of conformers or isomers. The A band was cut off due to the RCB. The ADE (–0.1 eV, Table 1) determined from the threshold of the X band for $[Py(SO_3)_4Na]^{3-}$ is slightly negative, suggesting that this trianion is weakly electronically metastable.

10-4. Theoretical Results and Discussions

Ab initio calculations were performed to optimize the MCAs structures, sort out possible isomers, and compute the VDEs to compare with the experimental spectra. Figure 10-6 displays the optimized structures along with the computed first VDE for each species. The top few molecular orbitals for each species are shown in Figure 10-7.

10-4.1. $[Py(SO_3)_4]^{4-}$

This quadruply-charged anion is closed-shell (^1A_g) with D_{2h} symmetry (Figure 10-6a). The calculated first VDE lies at –2.78 eV, followed by a transition at –2.09 eV. In fact, the first twenty VDEs were all calculated to be negative. Therefore, $[Py(SO_3)_4]^{4-}$ was predicted to be a very unstable species in agreement with the experimental observations or lack thereof. As in the case of $HTPS^{3-}$,[29] the HOMO of $[Py(SO_3)_4]^{4-}$ is also found to be on the center part of the molecule, consisting of an antibonding π orbital associated with the pyrene rings (Figure 10-7a). The center part of the molecule experiences the strongest Coulomb repulsion from the peripheral negatively charged SO_3^- groups, resulting in the large negative electron binding energies for this tetraanion. This is similar to $CuPc(SO_3)_4^{4-}$, the first MCA to be observed with a large negative electron

binding energy.[17,23] The HOMO of $CuPc(SO_3)_4^{4-}$ was also found to be on the center part of the molecule because of the enormous Coulomb repulsions from the peripheral negative charges. However, $CuPc(SO_3)_4^{4-}$ is bigger than $[Py(SO_3)_4]^{4-}$, resulting in a comparatively smaller negative electron binding energy (–0.9 eV) and a much longer life time.

10-4.2. $[Py(SO_3)_4]^{\bullet 3-}$

$[Py(SO_3)_4]^{\bullet 3-}$ is a radial anion with an unpaired electron ($^2B_{3g}$ ground electronic state) and D_{2h} symmetry (Figure 10-6b). The first VDE was calculated to be 0.64 eV in excellent agreement with the experimental data of 0.6 eV (Table 10-1 and Figure 10-4). We computed the VDEs up to ~2.9 eV and compared them with the experimental PES spectra in Figure 10-8a. Because of the large size of the molecule, the density of electronic state is quite high. The computed VDEs (displayed as solid bars) are in good agreement with the observed PE spectra. The molecular orbitals of the radical trianion are nearly the same as for the quadruply charged parent anion (Figure 10-7a).

10-4.3. $[Py(SO_3)_4H]^{3-}$

Two low-lying isomers were found for the $[Py(SO_3)_4H]^{3-}$ anion both of C_1 symmetry and ^1A ground state (Figure 10-6c). The proton is attached to one of four equivalent SO_3^- groups thus neutralizing one charge, which significantly reduced the intramolecular Coulomb repulsion and stabilized the trianion. Isomer II, which is only 2.83 kcal/mol higher in energy, can be obtained from isomer I by rotating the $–SO_3H$ group by 120º along the C-S bond. We computed the VDEs up to ~3.5 eV for both isomers. They compare well with the PES spectra, as shown in Figure 10-8b. Since our

PES experiment was taken at 70 K, the contributions from isomer II were expected to be minor. The calculated first VDEs (0.09 eV of isomer I) is in excellent accord with the X' feature in Figure 10-5a, lending further support to the assignment of this feature to $[Py(SO_3)_4H]^{3-}$. It is also worth noting that the calculated VDEs show no transitions around 0.6 eV from the protonated trianions (Figure 10-8b), consistent with the assignment of the main X peak in Figure 10-5a to the radical trianion $[Py(SO_3)_4]^{\bullet 3-}$.

Figure 10-7b displays the top four highest occupied molecular orbitals for the two isomers of the protonated trianions. The HOMO in each case is similar to the parent tetraanion, coming from the pyrene-based antibonding π orbital.

10-4.4. $[Py(SO_3)_4Na]^{3-}$

Two nearly degenerate isomers were identified for this species both with C_s symmetry and a $^1A'$ closed-shell ground state (Figure 10-6d). Isomer II was found to be only higher in energy than isomer I by 0.64 kcal/mol. The calculated first VDE was 0.00 eV for isomer I and –0.10 eV for isomer II, which both agree well with the PES spectra in Figure 10-5c, suggesting the presence of isomer II experimentally. VDEs were calculated up to 3.2 eV, as compared with the PES spectra in Figure 10-8c. The top three molecular orbitals for both isomers of $[Py(SO_3)_4Na]^{3-}$ are shown in Figure 10-7c. The HOMO of both isomers is again the pyrene-based antibonding π orbitals, similar to the parent tetraanion, followed by the orbitals from oxygen lone-pairs on the two peripheral sulfonate groups that are not attached with the Na^+ cation. It is interesting to note that the oxygen lone-pair orbitals derived from the sulfonate groups directly interacting with the Na^+ cation are significantly stabilized, becoming HOMO-8 for isomer I and HOMO-11

for isomer II (Figure 10-7c).

10-4.5. Factors controlling electronic stability of MCAs

Despite the same total charges as well as similar molecular structures, compositions, and HOMOs, the electron binding ability of the four triply-charged anions is found to vary over a range of 1.2 eV from a significantly negative value of –0.66 eV for $HTPS^{3-}$ → –0.1 eV for $[Py(SO_3)_4Na]^{3-}$ → 0.0 eV for $[Py(SO_3)_4H]^{3-}$ → +0.5 eV for $[Py(SO_3)_4]^{\bullet 3-}$. For each triply-charged anion, the detachment product corresponds to the respective dianion and a free electron. Thus, the electron binding ability or detachment energy is defined as the energy difference between the ground state of the initial triply-charged anion and such final detachment product.

It appears that the electronic stability of this series of trianions is very sensitive to the peripheral groups. The OH-group in $HTPS^{3-}$ is relatively compact and close to the pyrene ring. Consequently, any negative charge located on its oxygen atom is expected to have a more significant effect to the HOMO, which is centered on the pyrene rings. According to our NBO analysis, each of the three SO_3-groups in $HTPS^{3-}$ contributes a charge of ~ –0.75 |e|, whereas the OH-group carries a charge of –0.28 |e|. In comparison, in $[Py(SO_3)_4H]^{3-}$ each of the three SO_3-groups carries a charge of –0.73 |e|, while the fourth protonated sulfonate group is effectively charge neutral due to the screening of the proton. Therefore, a simple electrostatic argument would predict that $HTPS^{3-}$ should be much less stable than $[Py(SO_3)_4H]^{3-}$ consistent with experimental observations.

Why is the radical trianion $[Py(SO_3)_4]^{\bullet 3-}$ so much more stable? The net charge on each of the four SO_3-groups in $[Py(SO_3)_4]^{\bullet 3-}$ is –0.67 |e|, giving rise to a total charge

carried by the peripheral groups as –2.68 |e|, the highest among the trianions. Yet, the electron binding energy of $[Py(SO_3)_4]^{\bullet 3-}$ is +0.5 eV. This noticeable conflict may be reconciled by considering the radical nature of the $[Py(SO_3)_4]^{\bullet 3-}$ species in comparison to the closed-shell molecules of both $HTPS^{3-}$ and $[Py(SO_3)_4H]^{3-}$. The HOMO of the radical trianion is singly occupied, and therefore the Coulomb repulsion is smaller than for the doubly occupied HOMO in the closed shell trianions, enhancing the electron binding energy. In addition, the extra charges in $[Py(SO_3)_4]^{\bullet 3-}$ are completely delocalized among the four peripheral $–SO_3$ groups, thus enhancing the electron binding ability via delocalization, as suggested recently.[43] Alternatively, the radical trianion, $[Py(SO_3)_4]^{\bullet 3-}$, may be formally viewed as a zwitterion with a positive hole on the pyrene rings and four peripheral $–SO_3^-$ groups. The positive hole is expected to provide a major stabilizing effect to the remaining electron in the SOMO, thus enhancing the electronic stability of the radical trianion relative to the closed shell trianions.

The measured electron binding energy/half-life of –0.66 eV/0.1 s for $HTPS^{3-}$, along with those reported previously for $PtCl_4^{2-}$ (–0.25 eV/2.5 s) [25] and $[CuPc(SO_3)_4]^{4-}$ (–0.9 eV/~275 s)[26] provides a series of benchmarks to predict electronic metastability in doubly, triply, and quadruply charged anions. Given the comparatively long lifetimes of these MCAs, it is conceivable that even higher negative binding energies can be observed in suitably designed doubly, triply or quadruply charged anions.

10-5. Conclusion

We report a combined study on the electronic metastability and lifetimes of a series of triply charged anions consisting of a central pyrene scaffold and peripheral

sulfonate groups as charge carriers. Autodetachment of $HTPS^{3-}$ to $HTPS^{\bullet 2-} + e^-$ was measured in a FT-ICR cell and was used to measure a half-life of 0.1 s for this metastable trianion, which carries 0.66 eV excess energy. The quadruply charged $[Py(SO_3)_4]^{4-}$ anion estimated to possess a –2.78 eV negative electron binding energy was shown to be too unstable to be observed experimentally. Instead, its autodetachment product, $[Py(SO_3)_4]^{\bullet 3-}$, as well as ion-pairs stabilized by H^+ and Na^+, were observed and studied both experimentally and computationally. Photoelectron spectroscopy study showed that the $[Py(SO_3)_4]^{\bullet 3-}$ trianion is very stable with an electron binding energy of 0.5 eV, whereas $[Py(SO_3)_4H]^{3-}$ and $[Py(SO_3)_4Na]^{3-}$ are less stable with electron binding energies of 0.0 and –0.1 eV, respectively.

References

(1) Scheller, M. K.; Compton, R. N.; Cederbaum, L. S. *Science* **1995**, *270*, 1160.

(2) Freeman, G.R.; March, N. H. *J. Phys. Chem.* **1996**, *100*, 4331.

(3) Schauer, S. N.; Williams, P.; Compton, R. N. *Phys. Rev. Lett*. **1990**, *65*, 625.

(4) Boldyrev, A. I.; Gutowski, M.; Simons, J. *Acc. Chem. Res*. **1996**, *29*, 497.

(5) Dreuw, A.; Cederbaum, L. S. *Chem. Rev*. **2002**, *102*, 181.

(6) Weikert, H. G.; Cederbaum, L. S.; Tarantelli, F.; Boldyrev, A. I. *Z. Phys. D* **1991**, *18*, 299.

(7) Scheller, M. K.; Cederbaum, L. S. *J. Chem. Phys.* **1994**, *100*, 8934.

(8) Boldyrev, A. I.; Simons, J. *J. Chem. Phys.* **1993**, *98*, 4745.

(9) Zakrzewski, V. G.; Ortiz, J. V. *J. Chem. Phys*. **1995**, *102*, 294.

(10) Gnaser, H.; Oechsner, H. *Nucl. Instr, Methods Phys. Res*. B **1993**, *82*, 518.

(11) Middleton, R.; Klein, J. *Nucl. Instr, Methods Phys. Res*. B **1997**, *123*, 532.

(12) Hettich, R. L.; Compton, R. N.; Rotchie, R. H. *Phys. Rev. Lett*. **1991**, *67*, 1242.

(13) (a) Boldyrev, A. I.; Simons, J. *J. Phys. Chem*. **1994**, *98*, 2298. (b) Simons, J.; Skurski, P.; Barrios, R. *J. Am. Chem. Soc*. **2000**, *122*, 11893.

(14) Blades, A. T.; Kebarle, P. *J. Am. Chem. Soc*. **1994**, *116*, 10761.

(15) Wang, X. B.; Ding, C. F.; Wang, L. S. *Phys. Rev. Lett*. **1998**, *81*, 3351.

(16) Wang, L. S.; Ding, C. F.; Wang, X. B.; Nicholas, J. B. *Phys. Rev. Lett*. **1998**, *81*, 2667.

(17) Wang, X. B.; Wang, L. S. *Nature* **1999**, *400*, 245.

(18) Wang, L. S.; Wang, X. B. *J. Phys. Chem. A* **2000**, *104*, 1978.

(19) Wang, X. B.; Yang, X.; Wang, L. S. *Int. Rev. Phys. Chem*. **2002**, *21***,** 473.

(20) Ehrler, O. T.; Weber, J. M.; Furche, F.; Kappes, M. M. *Phys. Rev. Lett*. **2003**, *91*,113006.

(21) Wang, X. B.; Wang, L. S. *Annu. Rev. Phys. Chem.* **2009**, *60*, 105.

(22) Wang, X. B.; Wang, L. S. *Phys. Rev. Lett*. **1999**, *83*, 3402.

(23) Wang, X. B.; Ferris, K.; Wang, L. S. *J. Phys. Chem. A* **2000**, *104*, 25.

(24) Wang, X. B.; Ding, C. F.; Wang, L. S. *Chem. Phys. Lett*. **1999**, *307*, 391.

(25) Weis, P.; Hampe, O.; Gilb, S.; Kappes, M. M. *Chem. Phys. Lett*. **2000**, *321*, 426.

(26) Arnold, K.; Balaban, T. S.; Blom, M. N.; Ehrler, O. T.; Gilb, S.; Hampe, O.; van Lier, J. E.; Weber, M.; Kappes, M. M. *J. Phys. Chem. A* **2003**, *107*, 794.

(27) Kordel, M.; Schooss, D.; Gilb, S.; Blom, M. N.; Hampe, O.; Kappes, M. M. *J. Phys. Chem. A* **2004**, *108*, 4830.

(28) Ehrler, O. T.; Yang, J.-P.; Sugiharto, A. B.; Unterreiner, A. N.; Kappes, M. M. *J. Chem. Phys.* **2007**, *127*, 184301.

(29) Yang, J.; Xing, X. P.; Wang, X. B.; Wang, L. S.; Sergeeva, A. P.; Boldyrev, A. I. *J. Chem. Phys.* **2008**, *128*, 091102.

(30) Wang, X. B.; Wang, L. S. *Rev. Sci. Instrum.* **2008**, 79, 073108.

(31) Blom, M.; Hampe,O.; Gilb, S.; Weis, P.; Kappes, M. M. *J. Chem. Phys.* **2001**, *115*, 3690.

(32) Becke, A. D. *J. Chem. Phys.* **1993**, *98*, 5648.

(33) Vosko, S. H.; Wilk, L.; Nusair, M. *Can. J. Phys*. **1980**, *58*, 1200.

(34) Lee, C.; Yang, W.; Parr, R. G. *Phys. Rev. B*, **1988**, *37*, 785.

(35) Dunning, T. H. Jr. *J. Chem. Phys*. **1989**, *90*, 1007.

(36) Woon, D. E.; Dunning, T. H. Jr. *J. Chem. Phys*. **1993**, *98*, 1358.

(37) Frisch, M. J.; et al. *Gaussian 03*, Revision C.02; Gaussian, Inc.: Wallingford CT, 2004.

(38) MOLDEN3.4. Schaftenaar, G. MOLDEN3.4, CAOS/CAMM Center, The Netherlands (1998).

(39) Concina, B.; Neumaier, M.; Hampe, O.; Kappes, M. M. *J. Chem. Phys.* **2008**, *128*, 134306.

(40) Concina, B.; Neumaier, M.; Hampe, O.; Kappes, M. M. *Int. J. Mass Spectrom.* **2006**, *252*, 110.

(41) Tian, Z.; Kass, S. R. *J. Am. Chem. Soc*. **2008**, *130*, 10842.

(42) Tian, Z.; Wang, X. B.; Wang, L. S.; Kass, S. R. *J. Am. Chem. Soc*. **2009**, *131*, 1174.

(43) Tian, Z. ; Chan, B. ; Sullivan, M. B. ; Radom, L. ; Kass, S. R. *Proc. Natl. Acad. Sci. (USA)* **2008**, *105*, 7647.

Table 10-1. Experimental Adiabatic (ADE) and Vertical (VDE) Detachment Energies, and the Estimated Repulsive Coulomb Barriers (RCB) for $[Py(SO_3)_4]^{3-}$, $[Py(SO_3)_4H]^{3-}$, and $[Py(SO_3)_4Na]^{3-}$.[a]

Species	ADE (expt)[b]	VDE (expt)[c]	VDE (theor)	RCB[d]
$Py(SO_3)_4^{3-}$	0.50 ± 0.05	0.60 ± 0.05	0.64	3.0
$Py(SO_3)_4H^{3-}$	0.0 ± 0.1	0. 0 ± 0.1	0.09(I); -0.01 (II)[e]	3.0
$Py(SO_3)_4Na^{3-}$	-0.1 ± 0.1	-0.1 ± 0.1	0.00(I); -0.10 (II)[e]	3.0
$Py(SO_3)_4^{4-}$			-2.78	
$HTPS^{3-}$[f]	-0.66 ± 0.05	-0.62 ± 0.05	-0.70	3.3

[a] Calculated VDEs Are Included for Comparison. All Energies are in eV.

[b] The ADE was estimated by drawing a straight line at the leading edge of the 266 nm spectral band at 70 K and then adding the instrumental resolution to the intersection with the binding energy axis. The uncertainty is largely due to the fact that the rising edge is not perfectly smooth.

[c] Measured from the maximum of the first band from the 266 nm spectra at 70 K. For the triply charged ion-pairs, the listed VDEs should be regarded as rough estimates due to existence of two isomers and multiple transitions (see Figure 10-8).

[d] Estimated from the 266 nm spectral cutoff compared to the 193 nm spectra (see text).

[e] (I) and (II) refer structure I and II for each species (see Figure 10-6)

[f] Data from Reference 29.

Scheme 10-1

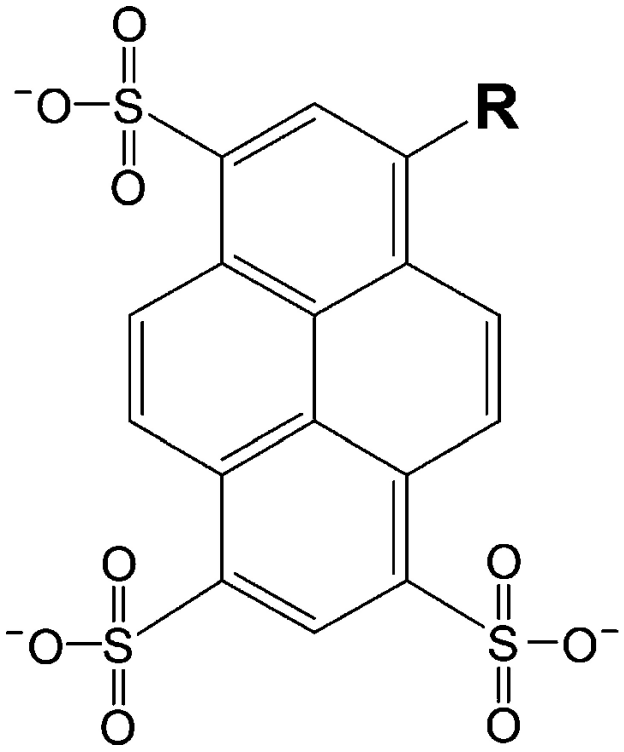

R = OH (a),

$SO_3^{\bullet}$ (b),

SO_3H (c),

SO_3Na (d)

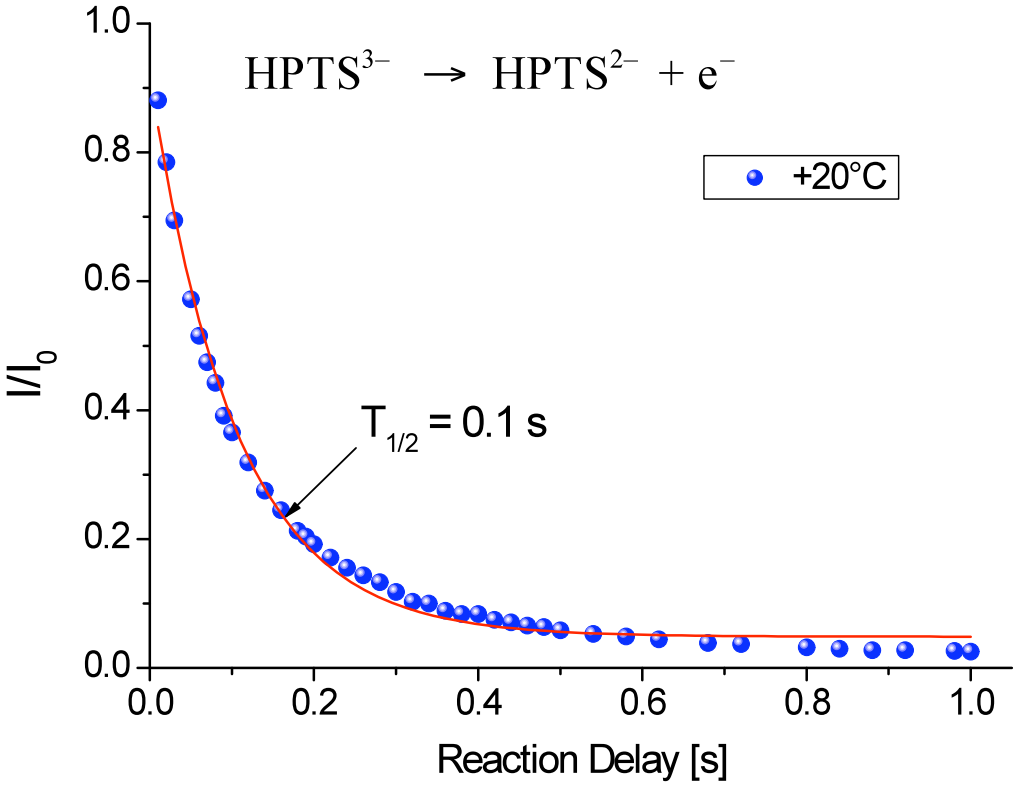

Figure 10-1. Unimolecular decay of the metastable $HPTS^{3-}$ trianion (via autodetachment of the unbound electron). The half-life is measured to be 0.1 seconds from the single exponential fit (solid red curve).

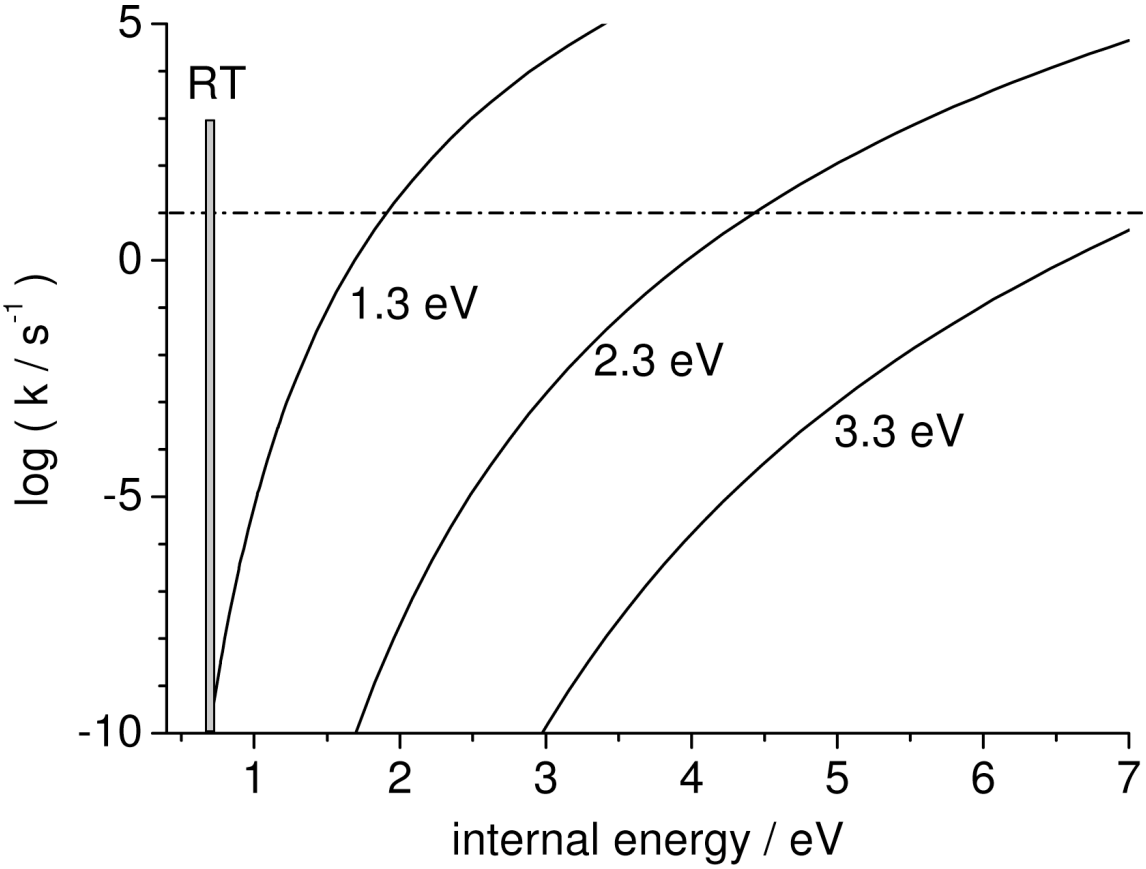

Figure 10-2. Unimolecular rate constants calculated for electron loss from metastable $HPTS^{3-}$ ions as a function of their internal energies - assuming an over-the-barrier mechanism (i.e. thermionic emission process). The three curves given are for different values of the repulsive Coulomb barrier (RCB) height. The horizontal dashed line marks the experimentally determined rate constant and the vertical bar gives the average ion energy at room temperature.

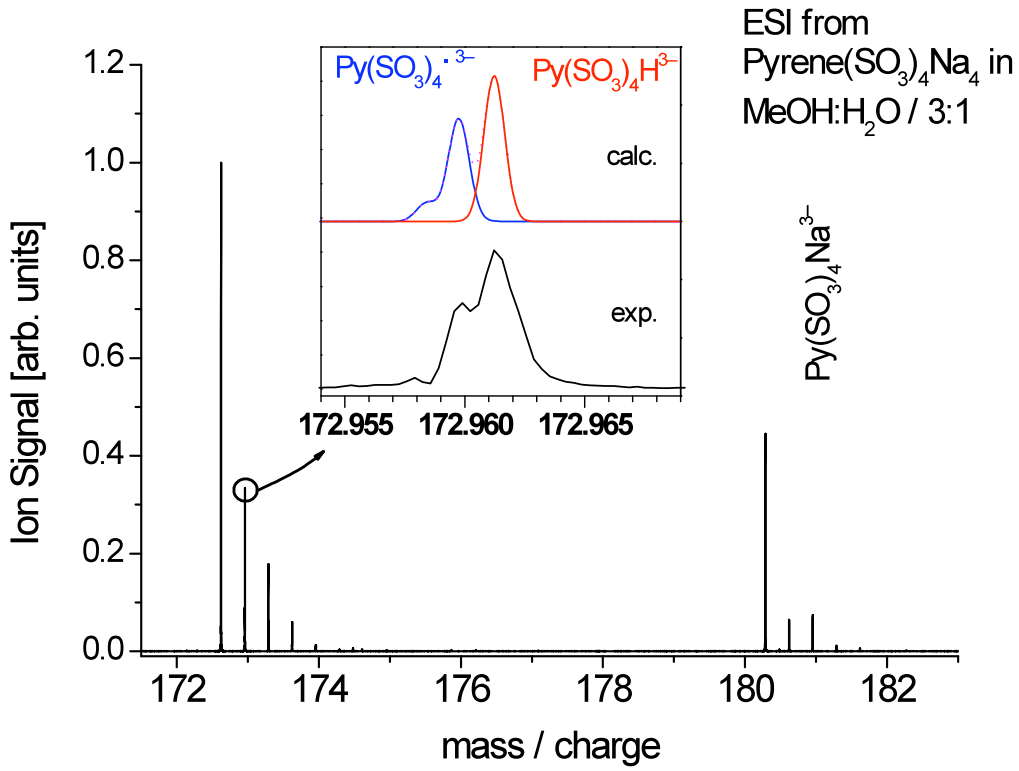

Figure 10-3. Negative-ion electrospray FT-ICR mass spectrum showing the region around the isotopomer-resolved triply charged species. The inset shows an enlarged view (around m/z = 172.96), revealing contributions from $[Py(SO_3)_4]^{\bullet 3-}$ and $[Py(SO)_4H]^{3-}$ in comparison with simulations.

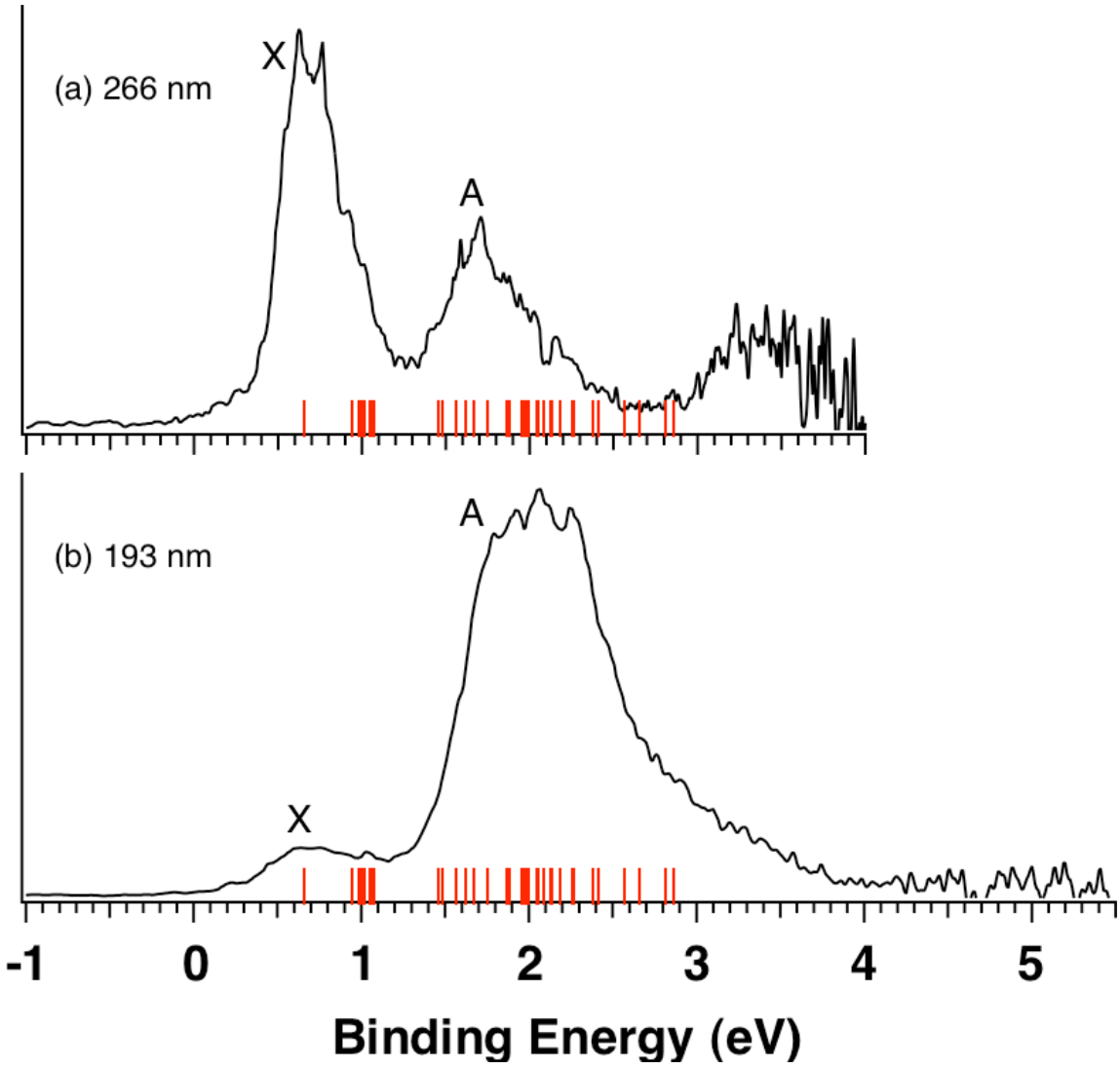

Figure 10-4. Photoelectron spectra of $[Py(SO_3)_4]^{\bullet 3-}$ at (a) 266 nm (4.661 eV), and (b) 193 nm (6.424 eV).

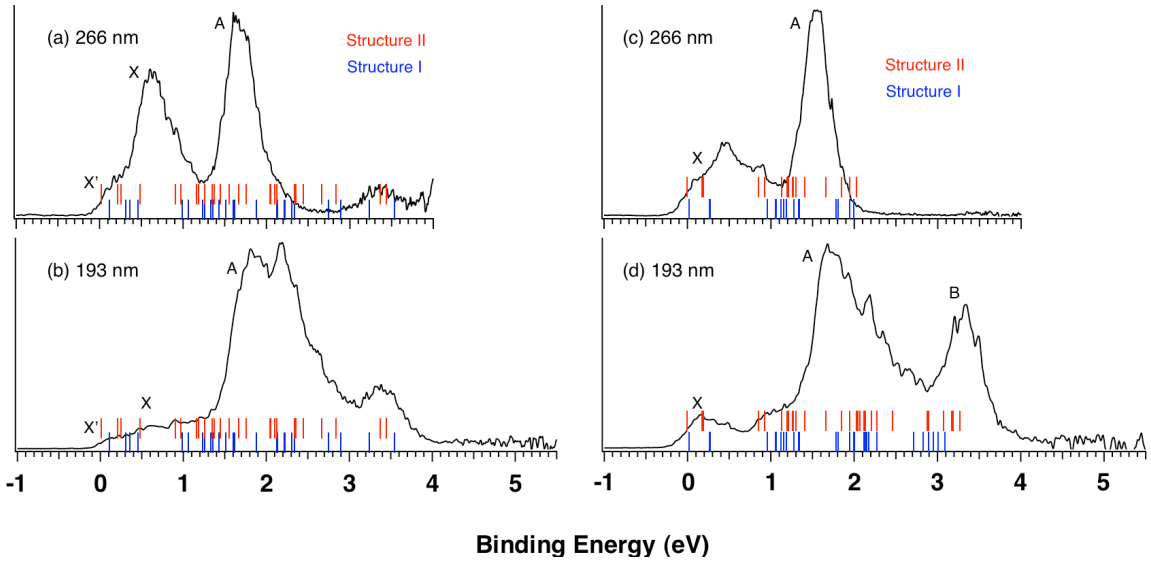

Figure 10-5. Photoelectron spectra of a mixture of $[Py(SO_3)_4H]^{3-}$ and $[Py(SO_3)_4]^{\bullet 3-}$ at 266 nm (a) and 193 nm (b), and of $[Py(SO_3)_4Na]^{3-}$ at 266 nm (c) and 193 nm (d).

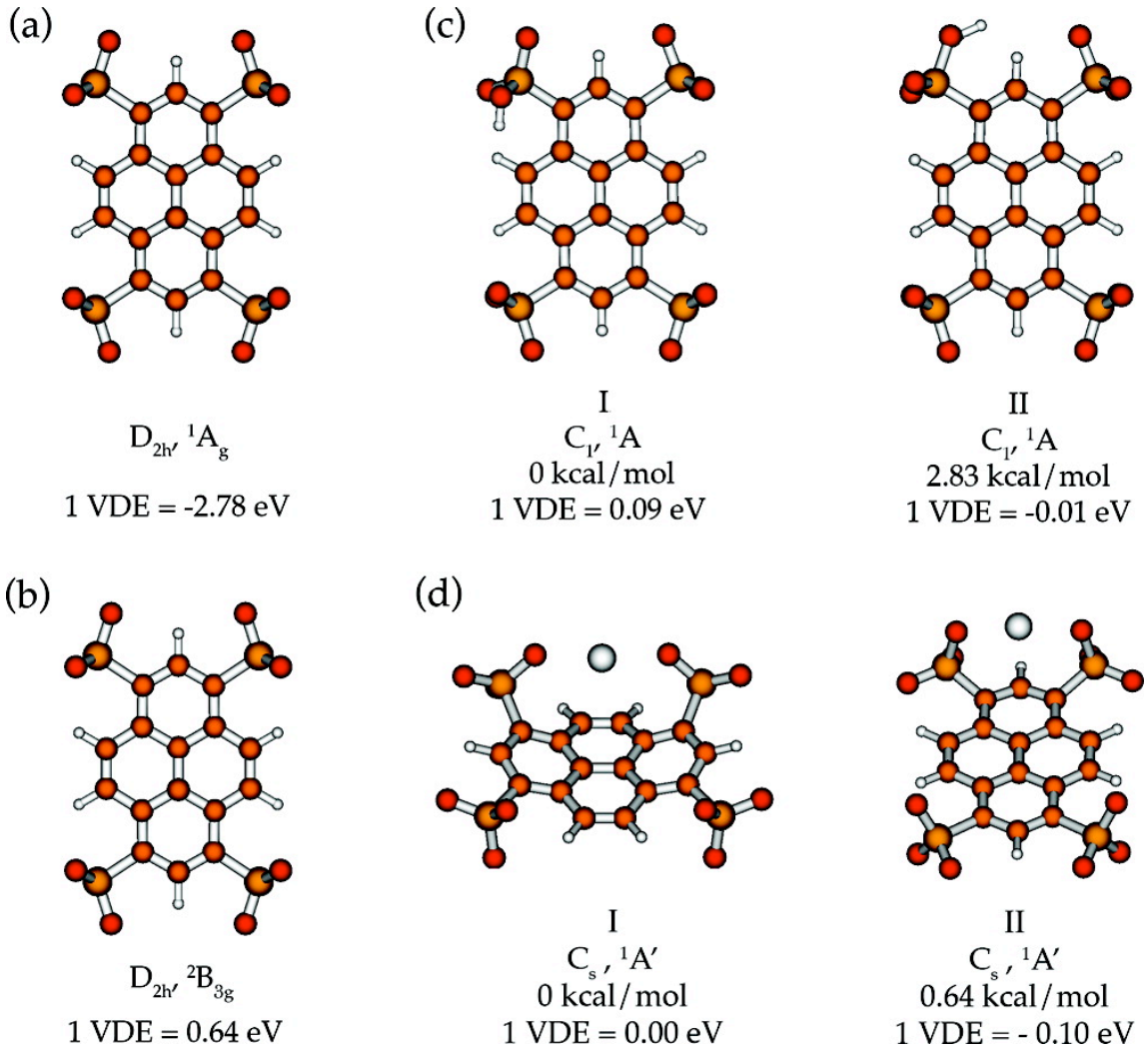

Figure 10-6. The optimized structures, symmetries, spectroscopic states, and the first VDEs for (a) $[Py(SO_3)_4]^{4-}$; (b) $[Py(SO_3)_4]^{\bullet 3-}$; (c) two low-lying isomers (I and II) of $[Py(SO_3)_4H]^{3-}$; (d) two low-lying isomers (I and II) of $[Py(SO_3)_4Na]^{3-}$. Relative energies are given at the B3LYP/O/aug-cc-pVDZ/H,C,S/cc-pVDZ level of theory and are corrected for zero-point vibrational energy.

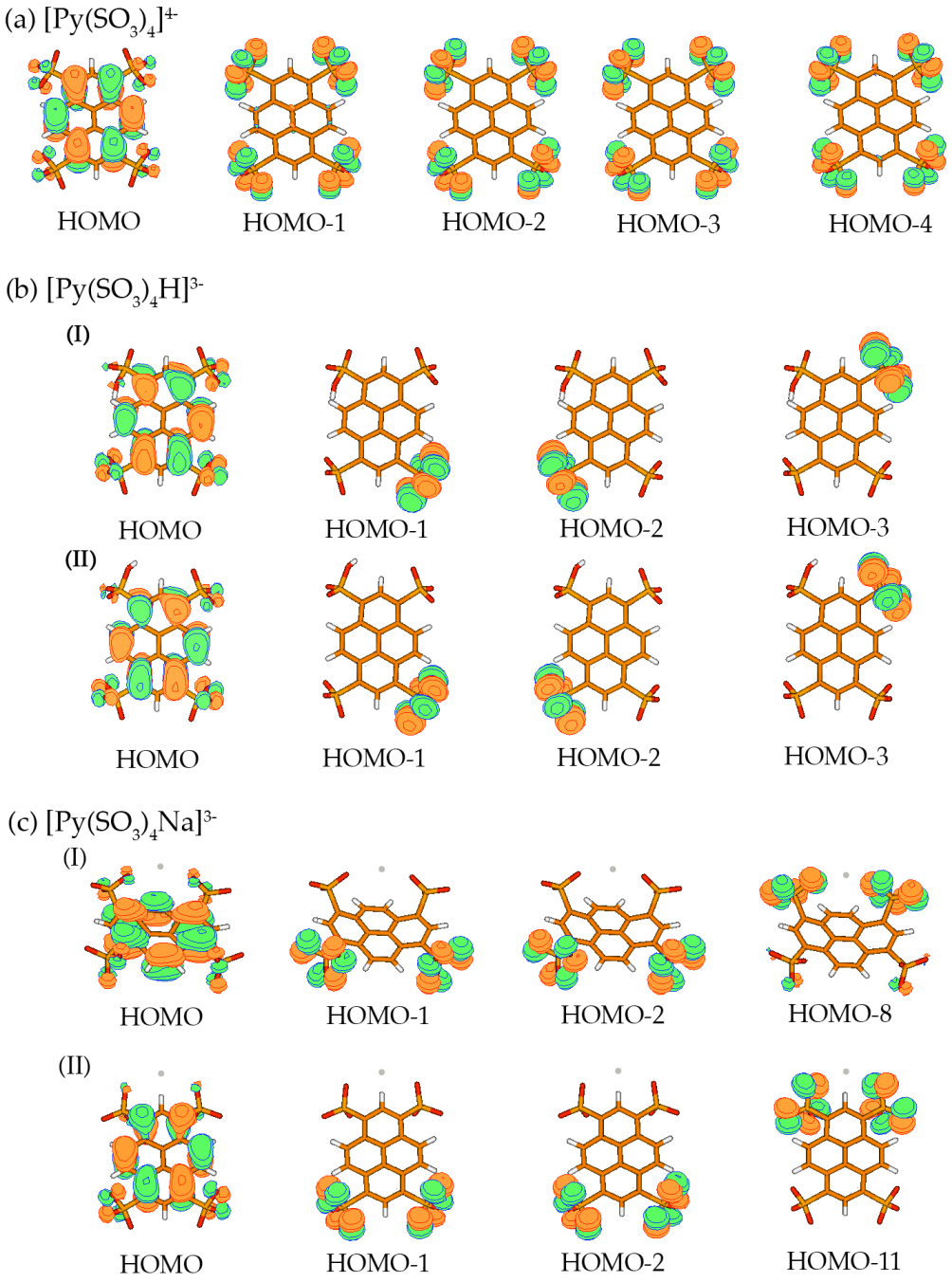

Figure 10-7. Selected top molecular orbitals for (a) $[Py(SO_3)_4]^{4-}$ (similar molecular orbitals were obtained for $[Py(SO_3)_4]^{\bullet 3-}$); (b) two low-lying isomers (I and II) of $[Py(SO_3)_4H]^{3-}$; (c) two low-lying isomers (I and II) of $[Py(SO_3)_4Na]^{3-}$.

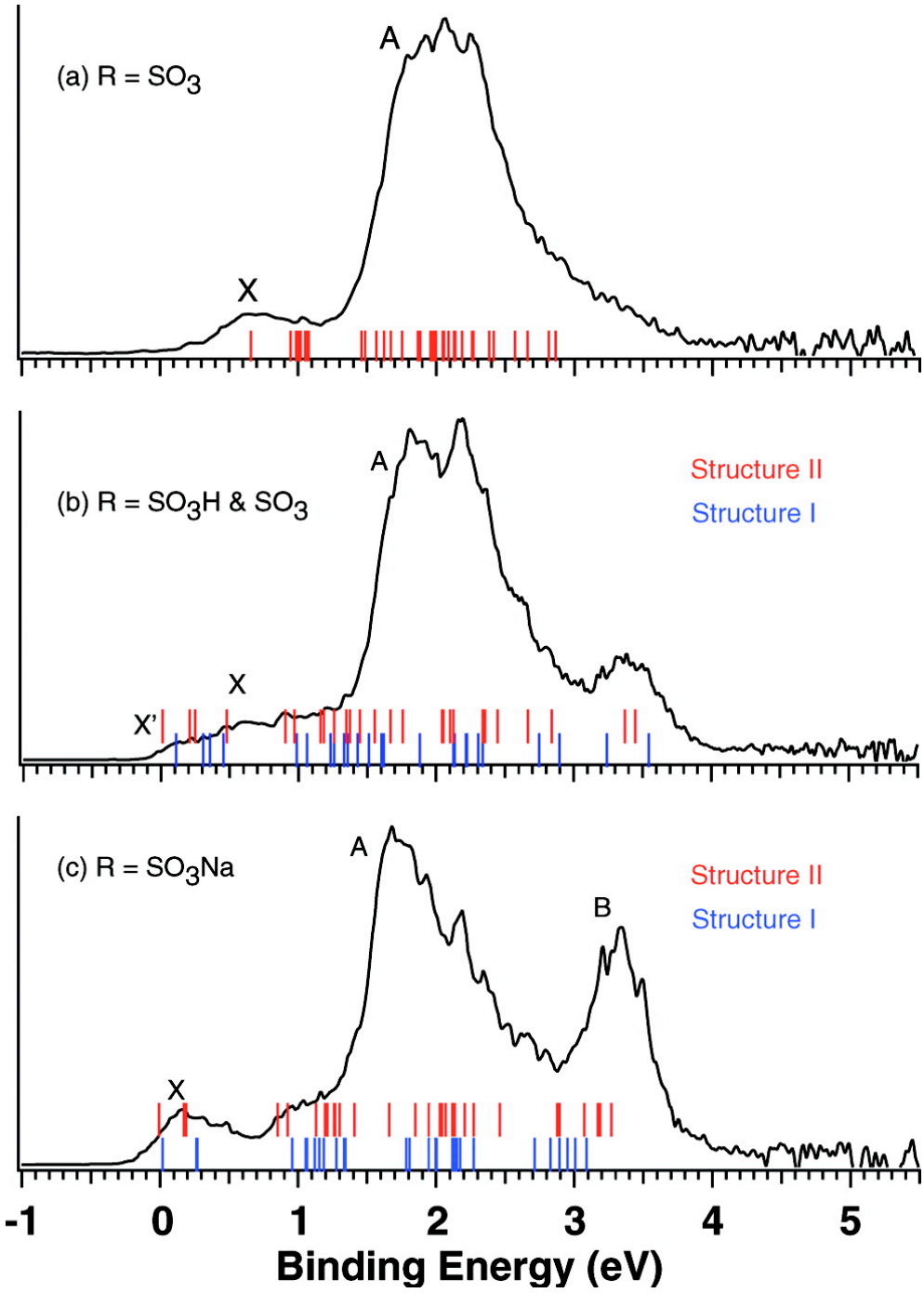

Figure 10-8. Comparison of the 193 nm photoelectron spectra of $[Py(SO_3)_3R]^{3-}$ [R = SO_3 (a), SO_3H and SO_3 (b), and SO_3Na (c)] with calculated VDEs (solid vertical bars). In (b) and (c), the bottom bars (blue) represent calculated VDEs for structure I, whereas the top bars (red) represent calcucated VDEs for structure II (see Figure 10-5). In (b), only the calculated VDEs for R = SO_3H are shown; those for R = SO_3 can be seen in (a).

CHAPTER 11

FLATTENING A PUCKERED PENTASILACYCLOPENTADIENIDE RING BY SUPPRESSION OF THE PSEUDO JAHN-TELLER EFFECT[1]

Abstract

We report theoretical prediction of flattening the puckered Si_5 ring by suppression of the pseudo Jahn-Teller effect through coordination of two Mg^{2+} cations to the $Si_5H_5^-$ anion to make an inverse $[Mg^{2+}Si_5H_5^-Mg^{2+}]$ sandwich complex. The pseudo Jahn-Teller (PJT) effect was suppressed through the OMO-UMO gaps increase in the resultant $[Mg^{2+}Si_5H_5^-Mg^{2+}]$ sandwich complex, as compared to the initial $Si_5H_5^-$ anion. It was the influence of two Mg^{2+} cations to cause the OMO-UMO gaps increase that made this type of PJT effect suppression work for in the three other complexes under the current computational study, namely $[Li^+Si_5H_5^-Li^+]$, $[Na^+Si_5H_5^-Na^+]$, and $[Be^{2+}Si_5H_5^-Be^{2+}]$, the $Si_5H_5^-$ moiety remains non-planar. We believe that if the $Mg(Si_5H_5)_2$ compound were synthesized it could have planar $Si_5H_5^-$ building blocks.

11-1. Introduction

The cyclic systems such as benzene (C_6H_6), cyclopentadienyl anion ($C_5H_5^-$) and recently synthesized cyclotetrabutadiene dianion derivative $((Me_3Si)_4C_4^{2-})$[1-3] are planar due to π-aromaticity, since they all have 6 π-electrons. These three cyclic systems are prototypical aromatic systems according to the $4n + 2$ Huckel rule where $n = 1$. Out of three silicon analogs, only the tetrasiliconcyclobutadiene dianion derivative $[(^tBu_2MeSi)_4Si_4]^{2-}$, as a part of the $[K(thf)_2]_2$ $[(^tBu_2MeSi)_4Si_4]$ salt, was synthesized[4] and

[1] Coauthored by Alina P. Sergeeva and Alexander I. Boldyrev. Reproduced with permission from *Organometallics* **2010**, 29, 3951-3954. Copyright 2010, American Chemical Society

shown to have the planar tetraatomic cyclic structure at the core using x-ray diffraction. The Si_6H_6 and $Si_5H_5^-$ species have not been made experimentally yet. Theoretical calculations of Si_6H_6 and $Si_5H_5^-$ showed that both of these molecules are non-planar.[5,6] The deviation from planarity in Si_6H_6 and $Si_5H_5^-$ species is caused by the only source of instability of high-symmetry configurations of polyatomic systems, namely the Jahn-Teller vibronic effects,[7-9] pseudo Jahn-Teller (PJT) effect to be precise. We have demonstrated recently[10] that the PJT effect can be suppressed by flattening the non-planar "chair" structure of Si_6X_{12} (X=Cl, Br) upon addition of two X^- ions to form the $[Si_6Cl_{14}]^{2-}$ dianion. The resultant $[Si_6Cl_{14}]^{2-}$ dianion was shown to have the restored planar Si_6 hexagon ring "sandwiched" between two apical chlorides.[10] The comprehensive computational analysis of the Si_6Cl_{12} electronic structure allowed us to identify the main cause of the PJT effect suppression originating from filling in the initially empty unoccupied molecular orbitals (UMOs) of Si_6Cl_{12} with electrons of the adduct (i.e., Cl^-). In the current article we show that there is an alternative mechanism of suppression of the PJT effect through extending the gap between interacting occupied and empty MOs, which participate in the PJT effect. We also demonstrate that the $Si_5H_5^-$ structure, which is non-planar in the isolated state, becomes planar in the $[MgSi_5H_5Mg]^{3+}$ sandwich complex through the OMO-UMO gaps increase caused by positive charge influence of the two extra Mg^{2+} cations.

11-2. Computational Results

We initially calculated the planar pentagonal D_{5h} ($^1A_1$') structure of $Si_5H_5^-$ (Figure 11-1, structure I) at two levels of theory: B3LYP/6-311++G** and CCSD(T)/6-311++G**.

All calculations were performed using Gaussian 03 program.[11] Geometry and molecular orbital visualization was done using MOLEKEL 4.3 package.[12] We found that the D_{5h} ($^1A_1$') structure I is not a minimum in agreement with the previously reported computational results for $Si_5H_5^-$ by Korkin et al.[6] It was found to have two doubly degenerate imaginary frequencies ($\omega_{1,2}(e_2$") and $\omega_{3,4}(e_1$")) leading to out-of-plane distortions, according to the B3LYP/6-311++G** and the CCSD(T)/6-311++G** levels of theory. Geometry optimization (at B3LYP/6-311++G**) following these imaginary frequency modes leads to one isomer: C_1 (^1A) (Figure 11-1, structure II). We also repeated geometry optimization for the two isomers, which were previously reported by Korkin et al.[6] The authors found two degenerate non-planar isomers of $Si_5H_5^-$ of C_s and C_2 symmetry, respectively, according to their calculations performed at the MP2(full)/6-31G* level of theory. We found that these two isomers reported by Korkin et al. are not minima at the B3LYP/6-311++G** level of theory, which is used in the current work. Geometry optimization following imaginary frequency modes of C_s and C_2 isomers leads again to structure II. Hence, there's only one isomer of $Si_5H_5^-$ at B3LYP/6-311++G**, which is of C_1 symmetry in the ^1A electronic state (Figure 11-1, structure II). The planar D_{5h} ($^1A_1$') structure I is only 7.2 kcal/mol higher in energy that the puckered C_1 (^1A) structure II at the B3LYP/6-311++G** level of theory with zero point energy correction.

The planar D_{5h} ($^1A_1$') structure I is not a minimum due to the pseudo Jahn-Teller (PJT) effect that forces puckering of the Si_5 ring and leads to out-of-plane distortions along the imaginary freguency modes. The PJT effect in the D_{5h} ($^1A_1$', $1a_1'^2 1e_1'^4 1e_2'^4 2a_1'^2 2e_1'^4 2e_2'^4 1a_2''^2 1e_1''^4 3a_1'^0 3e_1'^0 3e_2'^0$) structure of $Si_5H_5^-$ is a consequence of vibronic coupling of pairs of occupied molecular orbitals (OMO) and unoccupied molecular orbitals (UMO). The symmetry rule for the PJT effect is that the symmetry of the reaction coordinate (symmetry of one of the three imaginary frequency modes) should be the same as the direct product of the OMO and UMO states[13] as follows (Eq. 1):

$$\psi_{OMO} \otimes \psi_{UMO} = \Gamma_{RctnCoord} \tag{1}$$

Thus, the deformation of the D_{5h} ($^1A_1$') structure I of $Si_5H_5^-$ along the $\omega_{1,2}(e_2'')$ imaginary frequency mode can be caused by interaction between HOMO ($1e_1''$) and LUMO+1 ($3e_1'$) (see Eq. 2 and Figure 11-2a) and/or by interaction between HOMO ($1e_1''$) and LUMO+2 ($3e_2'$) (see Eq. 3 and Figure 11-2b):

$$e_1'' \otimes e_1' = a_1'' \oplus a_2'' \oplus e_2'' \tag{2}$$

$$e_1'' \otimes e_2' = e_1'' \oplus e_2'' \tag{3}$$

The deformation of the D_{5h} ($^1A_1$') structure I of $Si_5H_5^-$ along the $\omega_{3,4}(e_1'')$ imaginary frequency mode can be caused by interaction between HOMO ($1e_1''$) and LUMO ($3a_1'$) (see Eq. 4 and Figure 11-2c) and/or by interaction between HOMO ($1e_1''$) and LUMO+2 ($3e_2'$) (see Eq. 3 and Figure 11-2b):

$$1e_1'' \otimes a_1 = e_1'' \tag{4}$$

The orbital energies of the orbitals involved in pseudo Jahn-Teller Effect are the following: ε(HOMO, $1e_1''$) = - 0.078 a.u.; ε(LUMO, $3a_1'$) = 0.164 a.u.; ε(LUMO+1, $3e_1'$)

= 0.165 a.u.; and ε(LUMO+2, $3e_2$') = 0.172 a.u. Thus, the orbital energy difference in the $Si_5H_5^-$ anion between HOMO and LUMO is 6.58 eV, while the gap between HOMO and LUMO+1 is 6.60 eV, which are both somewhat smaller than the energy difference between HOMO and LUMO+2 (6.80 eV). All the above values are given at the RHF/6-311++G** level of theory since our most reliable data were obtained at the CCSD(T)/6-311++G** level, which is based on RHF/6-311++G**.

In order to test if the PJT effect can be suppressed by external charges we then calculated four inverse sandwich complexes, namely: $Li^+Si_5H_5^-Li^+$ (Figure 11-3a), $Na^+Si_5H_5^-Na^+$ (Figure 11-3b), $Be^{2+}Si_5H_5^-Be^{2+}$ (Figure 11-3c) and $Mg^{2+}Si_5H_5^-Mg^{2+}$ (Figure 11-3d) at the B3LYP/6-311++G** level of theory.

In the following text the reader can find the results of the testing whether electrostatic field from the pair of Li^+, Na^+, Be^{2+} or Mg^{2+} cations is enough to suppress the PJT effect in the $Si_5H_5^-$ anion by shifting apart occupied molecular orbitals (OMO) and unoccupied molecular orbitals (UMO). The addition of two Li^+ or Na^+ cations to make $M^+Si_5H_5^-M^+$ (M = Li, Na) complex or a pair of Be^{2+} or Mg^{2+} dications to make $M^{2+}Si_5H_5^-M^{2+}$ (M = Be, Mg) does not increase the number of valence electrons in the resultant inverse sandwich complex, as compared to the initial $Si_5H_5^-$ anion. Though, this coordination of the two positively charged ions to $Si_5H_5^-$ affects the gap between occupied and unoccupied molecular orbitals responsible for the PJT effect, which manifests itself in the increased stability of the $M^{n+}Si_5H_5^-M^{n+}$ complexes. According to our calculations $Li^+Si_5H_5^-Li^+$ and $Na^+Si_5H_5Na^+$ complexes have one doubly degenerate imaginary frequency of e_2" symmetry. Thus, the presence of two extra Li^+ or Na^+ cations does not suppress the PJT effect completely, though reduces the number of imaginary

frequency modes by one. Both $Be^{2+}Si_5H_5^-Be^{2+}$ and $Mg^{2+}Si_5H_5^-Mg^{2+}$ complexes were found to be minima at the B3LYP/6-311++G** level of theory. However, when we reoptimized the geometry of the $Be^{2+}Si_5H_5^-Be^{2+}$ complex and calculated its frequency modes at the CCSD(T)/6-311++G** level of theory, it was found to have one doubly degenerate imaginary frequency of e_2" symmetry. Thus, Be^{2+} cations cannot suppress the PJT effect either. Meanwhile, the $Mg^{2+}Si_5H_5^-Mg^{2+}$ complex was found to be a minimum at both levels of theory with the lowest $\omega_{1,2}(e_2")$ frequency mode being 90.0 cm^{-1} (B3LYP/6-311++G**) and 78.8 cm^{-1} (CCSD(T)/6-311++G**), which indicates that only the electrostatic field of Mg^{2+} causes the suppression of the PJT effect. The orbital energies of the orbitals of $Mg^{2+}Si_5H_5^-Mg^{2+}$, which correspond to those involved in pseudo Jahn-Teller Effect of $Si_5H_5^-$, are the following: ε(HOMO, $1e_1"$) = - 0.737 a.u.; ε(LUMO, $3a_1'$) = - 0.474 a.u.; ε(LUMO+4, $3e_1'$) = - 0.350 a.u.; and ε(LUMO+5, $3e_2'$) = - 0.335 a.u. Hence, the gap between HOMO ($1e_1"$) and LUMO ($3a_1'$) is increased from 6.58 eV in $Si_5H_5^-$ to 7.16 eV in $Mg^{2+}Si_5H_5^-Mg^{2+}$. The gaps between other UMO and OMO pairs, which participate in the PJT effect, are increased by more than 0.60 eV in $Mg^{2+}Si_5H_5^-Mg^{2+}$: from 6.60 eV to 10.52 eV (in the case of $1e_1"$ and $3e_1'$), and from 6.80 eV to 10.94 eV (in the case of $1e_1"$ and $3e_2'$). Apparently this extension of UMO-OMO gaps is large enough to restore planarity of $Si_5H_5^-$ in the inverse sandwich structure of $Mg^{2+}Si_5H_5^-Mg^{2+}$. As one of the reviewers recommended we performed additional calculations at B3LYP/6-311++G** to study the planarity or lack of planarity of the underlying 5-membered ring in $Mg^{2+}Si_5H_5^-Mg^{2+}$ as the distance between the magnesium cations and the ring is varied. We performed frequency calculations of $Mg^{2+}Si_5H_5^-Mg^{2+}$ at longer (with two Mg^{2+} cations moved farther from the center of mass by 0.1 Å) and shorter

(with two Mg^{2+} cations moved closer to the center of mass by 0.1 Å) cation-ring distances, as well as with one Mg^{2+} cation moved farther from the center of mass by 0.1 Å and the other Mg^{2+} cation moved closer to the center of mass by 0.1 Å. In the two latter cases the $Mg^{2+}Si_5H_5^-Mg^{2+}$ retained no imaginary frequencies while the $Mg^{2+}Si_5H_5^-Mg^{2+}$ with longer cation-ring distances has two imaginary frequencies. This elucidates the fact that the cation-ring interactions are mainly Coulombic and that there is a delicate balance between external field of cations and the geometry.

The PJT effect is a qualitative model of chemical bonding and it is not capable of predicting to what extent the OMO-UMO gaps should be increased in order to suppress its distortive nature. However, it can provide the direction of the search for the species where the high symmetry can be restored. In our case we studied four types of counter cations and it was enough to find the appropriate combination of cations to suppress the PJT effect.

11-3. Aromaticity in $Si_5H_5^-$ and $Mg^{2+}Si_5H_5^-Mg^{2+}$

The $Si_5H_5^-$ anion is aromatic in the planar form according to the molecular orbital chemical bonding analysis and the Si-Si bond equalization. We performed the nuclear independent chemical shit (NICS) analysis[14] for both $Si_5H_5^-$ and its planar carbon analog, $C_5H_5^-$. The calculated $NICS_{zz}$ values of the $Si_5H_5^-$ anion were found to be -11.5 ppm (Z = 0.0 Å, where Z represents the distance from the center of the $Si_5H_5^-$ moiety along the *z*-axis), -12.1 ppm (Z = 0.2 Å), -13.5 ppm (Z = 0.4 Å), -15.6 ppm (Z = 0.6 Å), -17.7 ppm (Z = 0.8 Å), and -19.3 ppm (Z = 1.0 Å) at the B3LYP/6-311++G** level of theory at the optimized B3LYP/6-311++G** geometry. The above $NICS_{zz}$ values of the $Si_5H_5^-$ anion

can be compared to those of the $C_5H_5^-$ anion at the same level of theory: -16.2 ppm (Z = 0.0 Å, where Z represents the distance from the center of the $C_5H_5^-$ moiety along the *z*-axis), -18.7 ppm (Z = 0.2 Å), -24.6 ppm (Z = 0.4 Å), -30.3 ppm (Z = 0.6 Å), -33.5 ppm (Z = 0.8 Å), and -33.7 ppm (Z = 1.0 Å). It is clear that $Si_5H_5^-$ is less aromatic than $C_5H_5^-$, according to the calculated $NICS_{zz}$ values. Since, the global minimum structure of $Si_5H_5^-$ anion is non-planar, the PJT effect overwhelms the stabilization due to aromaticity. When the planarity of the $Si_5H_5^-$ anion is restored in the sandwich $Mg^{2+}Si_5H_5^-Mg^{2+}$ structure, aromaticity in the $Si_5H_5^-$ anion as a part of the inverse sandwich complex is also restored. The $NICS_{zz}$ values calculated for the $Mg^{2+}Si_5H_5^-Mg^{2+}$ complex are -15.1 ppm (Z = 0.0 Å), -15.9 ppm (Z = 0.2 Å), -18.2 ppm (Z = 0.4 Å), -21.7 ppm (Z = 0.6 Å), -26.3 ppm (Z = 0.8 Å), and -32.1 ppm (Z = 1.0 Å).

11-4. Conclusion

In this article we have shown that the non-planarity of $Si_5H_5^-$ caused by the pseudo Jahn-Teller (PJT) effect can be eliminated through coordination of two Mg^{2+} cations to it to make the $Mg^{2+}Si_5H_5^-Mg^{2+}$ inverse sandwich complex. The PJT effect was suppressed in the $Si_5H_5^-$ anion through the OMO-UMO gaps increase in the $Mg^{2+}Si_5H_5^-Mg^{2+}$ complex because of the charge influence of two Mg^{2+} cations. We also presented the data on the $[Li^+Si_5H_5^-Li^+]$, $[Na^+Si_5H_5^-Na^+]$, and $[Be^{2+}Si_5H_5^-Be^{2+}]$ complexes. None of them was shown to contain a planar $Si_5H_5^-$ moiety. It was concluded that out of all the studied cations only two Mg^{2+} ions are able to increase the OMO-UMO gaps in the appreciable extent to suppress the PJT effect and restore the planarity of $Si_5H_5^-$. We believe that the way of suppression the PJT effect through coordination of extra cations

can be a useful tool in restoring high symmetry structures of numerous molecular species with otherwise distorted cyclic geometries.

The salts containing $C_5H_5^-$ anions are known to form stacking structures, where $C_5H_5^-$ anions together with counterions are forming "infinite" piles of sandwich type structures.[15] We hope that our theoretical prediction of planarization of the $Si_5H_5^-$ anion in the $Mg^{2+}Si_5H_5^-Mg^{2+}$ complex would stimulate synthesis of the first compounds containing the planar $Si_5H_5^-$ anion.

References

(1) Sekiguchi, A.; Matsuo, T.; H. Watanabe, H. *J. Am. Chem. Soc*. **2000**, *122*, 5652.

(2) Matsuo, T.; Sekiguchi, A. *Bull. Chem. Soc. Jpn*. **2004**, *77*, 211.

(3) Sekiguchi, A.; Matsuo, T. *Synlett.* **2006**, 2683.

(4) Lee, V. Ya.; Takanashi, K.; Matsuno, T.; Ichinohe, M.; Sekiguchi, A. *J. Am. Chem. Soc*. **2004**, *126*, 4758.

(5) (a) Baldrige, K. K.; Uzan, O.; Martin, J. M. L. *Organometallics*, **2000**, *19*, 1477; (b) Sax, A.; Janoschek, R. *Angew. Chem. Int. Ed*. **2003**, *25*, 651; (c) Sax, A.; Janoschek, R. *J. Comput. Chem*. **2004**, *9*, 564; (d) Grassi, A.; Lombardo, G. M.; Pucci, R.; Anglilella, G. G. N; Bartha, F.; March, N. H. *Chem. Phys.* **2004**, *297*, 13.

(6) Korkin, A.; Glukhovtsev, M.; Schleyer, P. v. R. *Int. J. Quant. Chem*. **1993**, *46*, 137.

(7) Bersuker, I. B. *Chem. Rev*. **2001**, *101*, 1067.

(8) Bersuker, I. B. *The Jahn-Teller Effect*; Cambridge University Press: New York, 2006.

(9) Boggs, J. E.; Polinger, V. Z.; Eds., *The Jahn-Teller Effect and Beyond: Selected Works of Isaac Bersuker with Commentaries;* The Academy of Sciences of Moldova: Chişinău, Moldova, 2008.

(10) Pokhodnya, K.; Olson, C.; Dai, X.; Schulz, D. L.; Boudjouk, P.; Sergeeva, A. P.; Boldyrev, A. I. *J. Chem. Phys.* **2011**, *134*, 014105.

(11) Frisch, M. J.; et al. *Gaussian 03* (revision D.01); Gaussian, Inc.: Pittsburgh, PA, 2003.

(12) Portmann, S. *MOLEKEL*, Version 4.3., CSCS/ETHZ, **2002**.

(13) Pearson, R. G. *Proc. Nat. Acad. Sci. U. S. A.* **1975**, *72*, 2104

(14) Schleyer, P. v. R., Maerker, C., Dransfeld, A., Jiao, H., and Hommes, N. J. R. v. E. *J. Am. Chem. Soc.* **1996**, *118*, 6317.

(15) Jutz, P.; Burford, N. *Chem. Rev*. **1999**, *99,* 969.

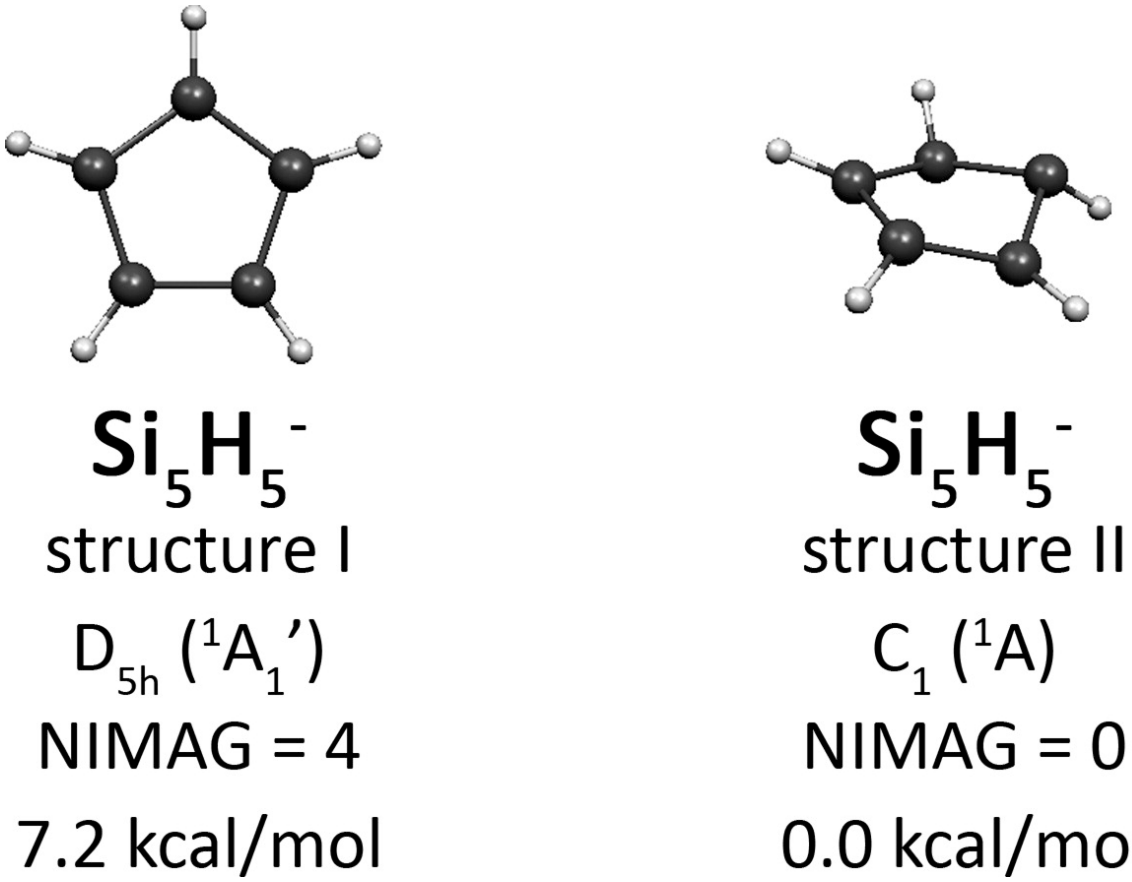

Figure 11-1. Alternative structures of $Si_5H_5^-$ (structure I and structure II), their symmetry, spectroscopic states, number of imaginary frequency modes (NIMAG), relative energies corrected for zero point energy, all calculated at the B3LYP/6-311++G** level of theory.

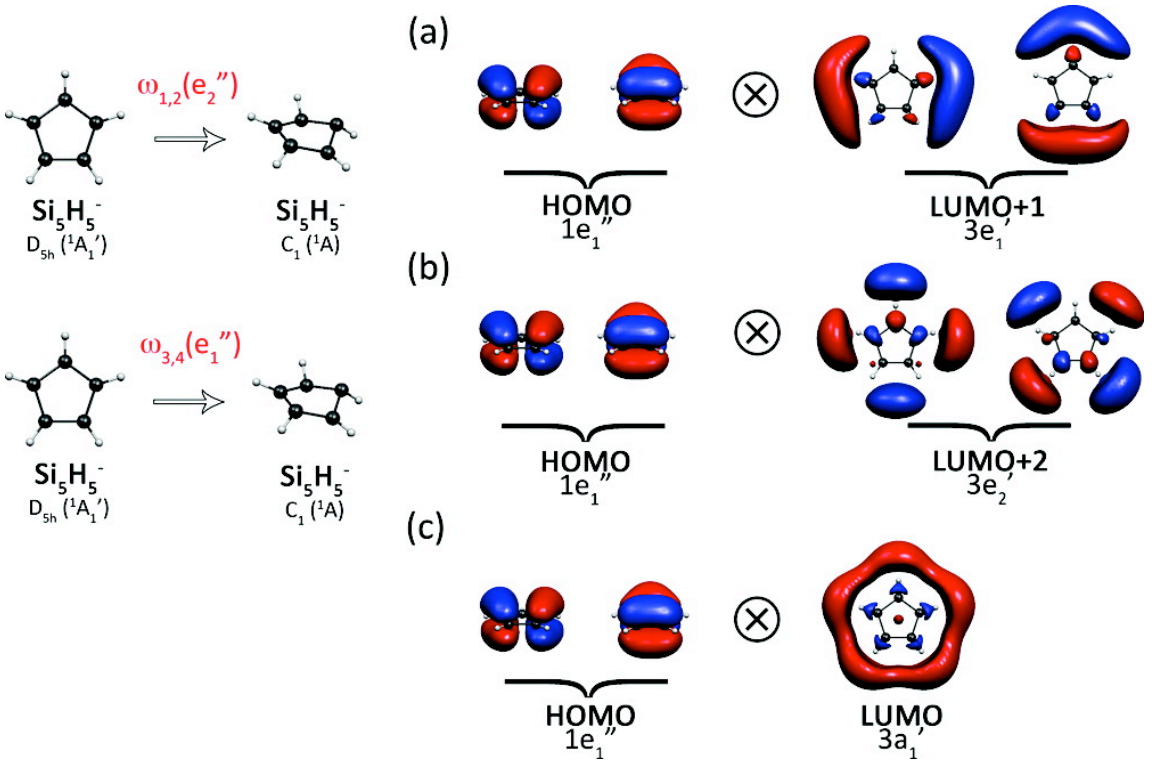

Figure 11-2. Interaction of the pairs of occupied and unoccupied molecular orbitals of the D_{5h} ($^1A_1$') structure I of $Si_5H_5^-$ responsible for the PJT effect: (a) and (b) interactions cause distortion towards the C_1 (^1A) structure upon following the doubly degenerate $\omega_{1,2}(e_2")$ imaginary frequency mode; (b) and (c) interactions cause distortion towards the the C_1 (^1A) structure upon following the doubly degenerate $\omega_{3,4}(e_1")$ imaginary frequency mode.

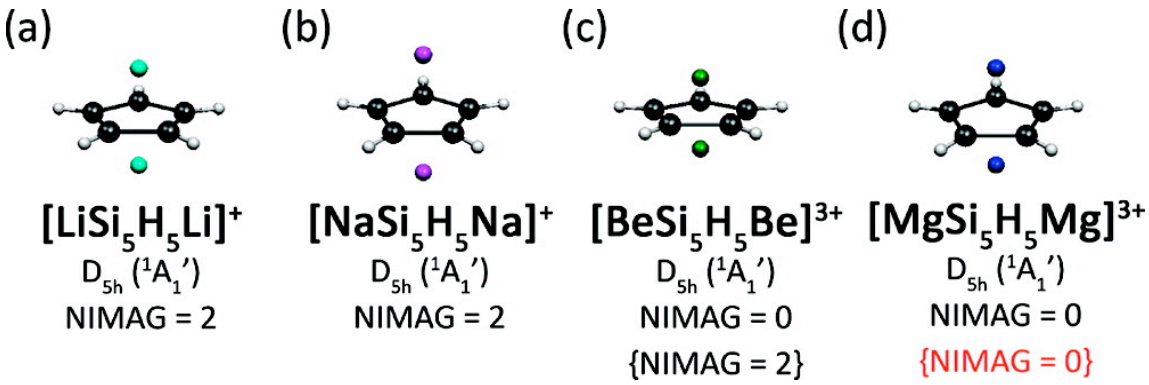

Figure 11-3. Optimized structures, point group symmetry, spectroscopic states, and number of imaginary frequency modes (NIMAG) of (a) $Li^{+}Si_5H_5^{-}Li^{+}$; (b) $Na^{+}Si_5H_5^{-}Na^{+}$; (c) $Be^{2+}Si_5H_5^{-}Be^{2+}$; and (d) $Mg^{2+}Si_5H_5^{-}Mg^{2+}$; at the B3LYP/6-311++G** level of theory, and at the CCSD(T)/6-311++G** level of theory (in squiggle brackets).

CHAPTER 12

FLATTENING A PUCKERED CYCLOHEXASILANE RING BY SUPPRESSION OF THE PSEUDO JAHN-TELLER EFFECT[1]

Abstract

We report the experimental and theoretical characterization of neutral Si_6X_{12} (X = Cl, Br) molecules that contain D_{3d} distorted six-member silicon rings due to a pseudo Jahn-Teller (PJT) effect. Calculations show that filling the intervenient molecular orbitals with electron pairs of adduct suppresses the PJT effect in Si_6X_{12}, with the Si_6 ring becoming planar (D_{6h}) upon complex formation. The stabilizing role of electrostatic and covalent interactions between positively charged silicon atoms and chlorine atoms of the subject $[Si_6Cl_{14}]^{2-}$ dianionic complexes is discussed. The reaction of Si_6Cl_{12} with a Lewis base (e.g. Cl^-) to give planar $[Si_6Cl_{14}]^{2-}$ dianionic complexes presents an experimental proof that suppression of the PJT effect is an effective strategy in restoring high Si_6 ring symmetry. Additionally, the proposed pathway for the PJT suppression has been proved by the synthesis and characterization of novel compounds containing planar Si_6 ring, namely: $[^nBu_4N]_2[Si_6Cl_{12}I_2]$, $[^nBu_4N]_2[Si_6Br_{14}]$, and $[^nBu_4N]_2[Si_6Br_{12}I_2]$. This work represents the first demonstration that PJT effect suppression is useful in the rational design of materials with novel properties.

---

[1] Coauthored by Konstantin Pokhodnya, Christopher Olson, Xuliang Dai, Douglas L. Schulz, Philip Boudjouk, Alina P. Sergeeva, Alexander I. Boldyrev. Reproduced with permission from *J. Chem. Phys.* **2011**, 134, 014105. Copyright 2011, American Institute of Physics.

12-1. Introduction

Symmetry breaking in polyatomic molecules due to degeneracy of their electronic states or sufficiently close in energy electronic states remains a focus of modern chemistry. According to Bersuker, the Jahn-Teller vibronic effects (Jahn-Teller, pseudo Jahn-Teller, and Renner-Teller) are the only source of instability of high-symmetry configurations of polyatomic systems.[1-3] Upon the study of amine-promoted oligomerization of trichlorosilane, a novel inverse sandwich $[Si_6Cl_{14}]^{2-}$ dianion was unexpectedly isolated.[4] The six silicon atoms in the $[Si_6Cl_{14}]^{2-}$ dianion form a planar hexagon "sandwiched" between two apical chlorides equally disposed from each Si_6 ring atom. The planarity of the Si_6 ring is highly unusual, since cyclohexane (C_6H_{12}) (Ref. 5) and its silicon-based analogs (cyclohexasilane, Si_6H_{12}) (Ref. 6) both adopt a non-planar "chair" structure.

Recently it was shown by symmetry-restricted complete-active-space self-consistent-field *(*CASSCF*)* calculations that ring puckering of cyclohexane is caused by the pseudo Jahn-Teller effect due to the coupling between the ground (π, σ^*) and excited (σ, σ^*) states.[7] Our X-ray diffraction studies of Si_6X_{12} (X = Cl, Br) compounds have shown that they both possess a "chair" structure similar to hexane, thus exemplifying the structures distorted due to the PJT effect.

In this study we have shown that coordination of two halide anions to Si_6Cl_{12} results in an inverse sandwich type $[Si_6Cl_{12}X_2]^{2-}$ dianion (X = Br, similarly to the previously reported case of Si_6Cl_{12} coordinated by two chloride anions[4]) with the planar Si_6 ring suggesting a total suppression of the PJT effect. The suppression of the ring puckering in the $[Si_6Cl_{14}]^{2-}$ dianion is shown to be due to filling of the empty orbitals of

Si_6Cl_{12} involved in the PJT effect. The restoration of high symmetry in distorted structures by the filling of empty orbitals involved in vibronic PJT coupling could be viewed as a new strategy toward design of novel high-symmetry compounds.

12-2. Experimental Methods

Both Si_6Cl_{12} and Si_6Br_{12} were synthesized according to the method described elsewhere.[8] Unpolarised Raman spectra were obtained in 75-3100 cm^{-1} spectral range with ~1 cm^{-1} resolution with a LabRAM Aramis Horiba Jobin Yvon confocal Raman microscope equipped with a CCD using 532 and 785 nm coherent excitation sources. A linear baseline was fitted directly to the corrected Raman spectra. To avoid air exposure the powder samples were placed between two glass slides glued inside the N_2 glove box (<1 ppm H_2O and O_2). To prevent the sample decomposition laser power should be below 50 mW/cm^2.

12-3. Theoretical methods

Quantum chemical calculations have been performed at the hybrid density functional method theory (DFT) method known in the literature as B3LYP (Refs. 9 and 10) utilizing 6-311+G(3df) basis set[11-13] for geometry optimization and frequency calculations. All calculations are performed using Gaussian 03 program.[14,15] Molecular orbital pictures are made using MOLEKEL 4.3 program.[16]

12-4. Results and Discussion

To understand the nature of ring puckering, we optimized the symmetrical Si_6Cl_{12} (D_{6h}, $^1A_{1g}$) conformer, which was found to be a third order saddle point with three

imaginary frequencies: one of b_{2g} symmetry (ω_1 = -30.70 cm^{-1}) and one degenerate pair of e_{2u} symmetry ($\omega_{2,3}$ = - 22.73 cm^{-1}). Geometry optimization following the first imaginary frequency mode (reaction coordinate) of the D_{6h} structure of Si_6Cl_{12} gives the global minimum structure of D_{3d} symmetry ("chair" structure) (Figure 12-1a) that is 49.8 kJ/mol lower in energy than D_{6h} structure (after zero-point energy correction). The geometry optimization along the other two degenerate imaginary frequency modes leads to the C_{2v} ("boat") and D_2 ("twist" or "twist-boat") structures (Figure 12-1b). The C_{2v} ("boat") structure has one imaginary frequency, while the D_2 ("twist" or "twist-boat") structure is a minimum. Following the imaginary frequency of the "boat" structure leads to the previously determined "twist-boat" structure. The PJT effect in the D_{6h} structure of Si_6Cl_{12} that forces non-planarity is a consequence of vibronic coupling of pairs of occupied molecular orbitals (OMO) and unoccupied molecular orbitals (UMO). The symmetry rule for the PJT effect is that the symmetry of the reaction coordinate (one of the three imaginary frequencies) should be the same as the direct product of these OMO and UMO states[17] as follows (Eq. 1):

$$\psi_{OMO} \otimes \psi_{UMO} = \Gamma_{RctnCoord} \tag{1}$$

Furthermore, the reaction coordinate must be totally symmetric in the point group of the new (distorted) structure.

The deformation resulting in the "chair" global minimum of Si_6Cl_{12} along the b_{2g} normal mode is caused by interaction between HOMO-3 ($3b_{2g}$) and LUMO+1 ($5a_{1g}$) of the D_{6h} structure of Si_6Cl_{12} (Figure 12-1a):

$$b_{2g} \otimes a_{1g} = b_{2g} \tag{2}$$

The b_{2g} mode of the planar D_{6h} structure becomes a totally symmetric a_{1g} mode in the new distorted D_{3d} "chair" structure.

Deformation along the degenerate e_{2u} normal modes leads to HOMO ($2b_{2u}$) / LUMO+4 ($5e_{1g}$) and HOMO-4 ($4e_{1g}$) / LUMO+3 ($6e_{1u}$) interaction within the Si_6Cl_{12} D_{6h} structure resulting in "boat" and "twist-boat" structures, respectively (Figure 12-1b):

$$b_{2u} \otimes e_{1g} = e_{2u} \tag{3}$$

$$e_{1g} \otimes e_{1u} = a_{1u} \oplus a_{2u} \oplus e_{2u} \tag{4}$$

Both e_{2u} modes of the planar D_{6h} structure become totally symmetric in the new distorted structures: the a_1 mode in C_{2v} "boat" structure and the a mode in D_2 "twist-boat" structure.

The single crystal x-ray diffraction confirms that the six silicon atoms adopt a chair conformation in Si_6Cl_{12} (Figure 12-2a) with Si-Si bond distances ~2.34 Å, Si-Cl bond distances ~2.03 Å, and Si-Si-Si angles ranging from 112 to 115° – all in good agreement with the calculated values for Si_6Cl_{12} (Table 12-1). Single crystal x-ray diffraction experiments also revealed that the substitution of chlorine atoms with bromine does not perturb the favored conformation, and Si_6Br_{12} is also a "chair" in the solid state (Figure 12-2b).[8]

To demonstrate the validity of the strategy of suppressing Si_6 ring puckering in Si_6X_{12} by adding two halide anions, we synthesized a series of $[^nBu_4N]_2[Si_6X_{12}Y_2]$ compounds containing $[Si_6X_{12}Y_2]^{2-}$ (X = Cl, Br; Y = Cl, Br, I) dianions. These compounds were studied by x-ray diffraction (Figure 12-2c-f) and Raman spectroscopy. In all these complexes the $[Si_6X_{12}Y_2]^{2-}$ dianions were found to possess the planar Si_6 ring.

Quantum mechanical calculations were performed for an isolated $[Si_6Cl_{14}]^{2-}$ moiety and compared with the experimental data for crystals of this dianion (Table 12-1).

There is a satisfactory agreement between the experimental and calculated parameters for $[Si_6Cl_{14}]^{2-}$ dianion, although calculated values are overestimated by ~3 %. When compared to Si_6Cl_{12}, the average calculated Si-Si bond length in $[Si_6Cl_{14}]^{2-}$ is ~0.01 Å shorter and the Si-Cl bond lengths are ~0.04 Å longer. Calculations also show that the Si_6 ring shape undergoes dramatic alteration when two chloride ions are added resulting in symmetry change from D_{3d} in Si_6Cl_{12} to D_{6h} in $[Si_6Cl_{14}]^{2-}$. The average Si-Si-Si angle in the ring increases from ~113° in Si_6Cl_{12} to ~120° in $[Si_6Cl_{14}]^{2-}$, while the Cl-Si-Cl angle decreases from ~110° to ~101°. We also calculated two model $[Si_6Cl_{12}H_2]^{2-}$ and $[Si_6H_{14}]^{2-}$ systems in which two negative hydrogen ions were positioned equidistantly above and below the center of the Si hexagon. It was found that the $[Si_6Cl_{12}H_2]^{2-}$ cluster has eight modes with imaginary frequencies, and the $[Si_6H_{14}]^{2-}$ cluster has five modes. All three modes of $\omega(b_{2g})$ and $\omega(e_{2u})$ symmetries, that are responsible for PJT distortion of the Si_6Cl_{12}, are imaginary in the both model systems. Not surprisingly, the PJTE is not suppressed in the $[Si_6Cl_{12}H_2]^{2-}$ and $[Si_6H_{14}]^{2-}$ model dianions.

Raman spectroscopy was performed on the polycrystalline samples Si_6Cl_{12} and $[TBA^+]_2[Si_6Cl_{14}]^{2-}$ to examine the effects of planarization in the Si_6 core. To aid in the characterization of Raman spectra, normal coordinate analysis was performed on the neutral Si_6Cl_{12} structure. It is found that under the D_{3d} symmetry point group, the normal modes are distributed as

$$\Gamma = 6A_{1g}(R) + 2A_{2g}(IA) + 16E_g(R) + 3A_{1u}(IA) + 5A_{2u}(IR) + 16E_u(IR) \quad (5)$$

(R, IR, and IA signify Raman, infared and inactive modes, respectively). Of the six predicted Raman active modes of A_{1g} symmetry, an intense band located at 267 cm^{-1} (Figure 12-3) is observed in the calculated Raman spectrum and assigned to a totally symmetric ring "breathing" mode of Si-Si stretching character. Experimental Raman spectroscopic studies show that structural perturbations of the Si_6 ring become more relaxed upon complexation with a softening of the totally symmetric Si-Si stretching frequency mode from 279 cm^{-1} in Si_6Cl_{12} to 257 cm^{-1} in $[Si_6Cl_{14}]^{2-}$ (Figure 12-4).

It should be noted that no elongation of the Si-Si bonds was observed or predicted by calculations (Table 12-1). However, the calculated frequency for the totally symmetric Si-Si stretching mode of $[Si_6Cl_{14}]^{2-}$ also exhibits a red shift with respect to that in Si_6Cl_{12} in accord with the experiment. To elucidate the mechanism for the observed redshift, a Raman spectrum was generated for neutral, planar (D_{6h},$^1A_{1g}$) Si_6Cl_{12}. This calculation reproduces the softening of the Si-Si stretching band, and indicates that the character of this vibration is very different in D_{6h} (pure breathing mode) versus D_{3d} (Si-Si stretching + ring deformation). These results suggest that structural planarity leads to a significant reduction in deformation potential, and plays a primary role in the softening of the symmetric Si-Si stretching band.

As mentioned above, several canonical UMOs of Si_6Cl_{12} with a planar Si_6 ring (LUMO+1, LUMO+3, and LUMO+4) are responsible for the PJT effect in Si_6Cl_{12} due to mixing with the HOMO-3, HOMO-4, and HOMO, respectively (Figure 12-1). Molecular orbital analysis (Figure 10-5) showed that molecular orbitals corresponding to the empty ones in the neutral Si_6Cl_{12} (i.e., LUMO+1, LUMO+3, and LUMO+4) are now occupied in the $[Si_6Cl_{14}]^{2-}$ dianion (i.e., HOMO-1, HOMO-2, and HOMO-3). Electron density of

the aforementioned occupied MOs of the $[Si_6Cl_{14}]^{2-}$ dianion comes primarily from $3p_z$, $3p_x$ and $3p_y$ electron pairs of the Cl^- ions (Figure 10-5). Consequently, the PJT effect was suppressed when empty orbitals responsible for the PJT effect were occupied in a larger dianion due to the ring interaction with halogen adducts. In contrast, when hydrogen H^- ions were used in the $[Si_6H_{14}]^{2-}$ model system (only one electron pair per ion), the corresponding conformer was found to be the 5th order saddle point, which supports our claim that the additional ligands must be halogens. Therefore, to suppress the PJT effect, all unoccupied orbitals engaged in its occurrence in Si_6Cl_{12} must become occupied in the resultant $[Si_6Cl_{14}]^{2-}$ dianion. It should be noted that by emphasizing that the PJT effect is attributed to the occupation of the intervenient molecular orbitals we do not imply a direct charge transfer of the valence electron pairs from Cl^- to LUMO+1, LUMO+3 and LUMO+4 of Si_6Cl_{12}, while a slight mixing of their orbitals does exist (*vide infra*). Thus, the proposed approach could be a very general tool in restoring high symmetry in structures otherwise distorted owing to the PJT effect.

Our calculations also show that isolated $[Si_6Cl_{14}]^{2-}$ dianion is an energy minimum, while the isoelectronic $[C_6Cl_{14}]^{2-}$ species tends to spontaneously dissociate into C_6Cl_{12} and two Cl^- anions. Therefore, the interaction between Cl^- and Si_6Cl_{12} is rather unique due to the ability of silicon to stabilize the $[Si_6Cl_{14}]^{2-}$ dianion. There are two effects favoring the stability of this dianion: first, electrostatic interactions between the positively charged silicon atoms of Si_6 core and two negatively charged chlorine adducts; second, covalent interactions between two apical chloride anions and Si_6Cl_{12} in the $[Si_6Cl_{14}]^{2-}$ dianion. Electrostatic potential mapped over total DFT electron density (Figure 10-6) shows the presence of a significant positive charge on both sides of Si_6 ring suggesting

that the appreciable electron density withdrawn by terminal Cl atoms plays an important role in forming Lewis-acid sites available for adduct formation. Indeed, addition of $^{n}Bu_4NCl$ to a CH_2Cl_2 solution of Si_6X_{12} at room temperature leads to immediate formation of the $[^{n}Bu_4N]_2[Si_6Cl_{14}]$ as a colorless precipitate. Natural charges of the $[Si_6Cl_{14}]^{2-}$ (D_{6h}, $^1A_{1g}$) calculated using Natural Bond Orbital analysis are +0.806 |e| at each ring silicon atoms, -0.694 |e| at each of the two apical chloride ions, and -0.454 |e| at the twelve chlorine atoms. Hence, Cl^- ligands donate ~0.3 |e| to Si_6Cl_{12}.

It was shown that sufficient OMO-UMO gaps increase may suppress the PJT effect.[18] In the current case the stabilizing interactions between positively charged silicon atoms and apical chloride ions in the $[Si_6Cl_{14}]^{2-}$ dianion do exist, but it is the occupation of the intervenient molecular orbitals that is predominantly responsible for killing the PJT effect of Si_6Cl_{12} resulting in planar cyclohexasilane rings. To verify this hypothesis we performed calculations with the two apical chloride atoms in $[Si_6Cl_{14}]^{2-}$ dianion substituted by Coulomb charges. Indeed, the gap between the OMO and UMO responsible for the PJT effect increases due to the external charges (Table 12-2). However, we have found that this model structure (i.e., Si_6Cl_{12} with two point charges located in positions identical to the apical chlorides in $[Si_6Cl_{14}]^{2-}$) still has three imaginary frequencies. Thus, the interaction of Si_6Cl_{12} with two Coulomb charges does not sufficiently increase OMO-UMO gaps and, therefore, does not suppress the PJT effect in the Si_6 ring.

It should be emphasized that calculations for $[Si_6Cl_{14}]^{2-}$ indicate that some covalent interaction between two extra Cl^- anions and Si_6Cl_{12} of $[Si_6Cl_{14}]^{2-}$ exists on the basis of charge transfer (about 0.30 |e|) from chloride anions to the Si_6Cl_{12} of $[Si_6Cl_{14}]^{2-}$.

It contributes to the stability of the $[Si_6Cl_{14}]^{2-}$ dianion against dissociation into Si_6Cl_{12} and two Cl^- anions. The PJT effect originates from formation of new covalency by distortion,[2] and the population of the corresponding unoccupied orbitals quenches this effect, like the population of antibonding orbitals diminishes the bonding effect.

12-5. Conclusion

We have shown that adding two chloride anions to perchlorocyclohexasilane results in planarization of the distorted Si_6 ring due to the suppression of the PJT effect. The comprehensive computational analysis of Si_6Cl_{12} electronic structure allowed us to identify the main cause of the PJT effect suppression originating from filling in the initially empty UMOs of Si_6Cl_{12} with electrons of the adduct (i.e., Cl^-). A number of new "inverse sandwich" compounds were isolated (i.e., $[^nBu_4N]_2[Si_6Cl_{12}I_2]$, $[^nBu_4N]_2[Si_6Br_{14}]$ and $[^nBu_4N]_2[Si_6Br_{12}I_2]$), where the Si_6 ring becomes planar upon coordination of the perhalocyclohexasilane, thus illustrating the predictive power of our strategy toward suppressing the PJT effect. While our calculations specify the interaction of Si_6X_{12} with halide adducts, we have also observed planarization of Si_6 rings when Si_6X_{12} (X=Cl, Br) was reacted with neutral coordinating species (such as nitriles and azides). This observation points out to the generality of this approach. The proposed strategy toward suppressing the PJT effect allows contemplation of synthetic routes to high symmetry in otherwise distorted structures and offers the community a tool for rational design of new materials.

References

[1] I. B. Bersuker, Chem. Rev. **101**, 1067 (2001).

[2] I. B. Bersuker, *The Jahn-Teller Effect* (Cambridge University Press, Cambridge, UK, 2006).

[3] *The Jahn-Teller Effect and Beyond: Selected Works of Isaac Bersuker with Commentaries,* edited by J. E. Boggs and V.Z. Polinger (The Academy of Sciences of Moldova, Chişinău, Moldova, 2008).

[4] S. B. Choi, B. K. Kim, P. Boudjouk, and D. G. Grier, J. Am. Chem. Soc. **123***,* 8117 (2001).

[5] M. B. Smith, J. March *March's Advanced Organic Chemistry: Reactions, Mechanisms, and Structure,* 6th ed. (Wiley-Interscience, New York, 2007).

[6] Z. Smith, A. Almenningen, E. Hengge, and D. Kovar, J. Am. Chem. Soc. **104**, 4362 (1982).

[7] L. Blancafort, M. J. Bearpark, and M. A. Robb, Molec. Phys. **104**, 2007 (2006).

[8] X. Dai, D. L. Schulz, C. W. Braun, A. Ugrinov, and P.Boudjouk, Organometallics **29**, 2203 (2010).

[9] A. D. Becke, J. Chem. Phys. **98**, 5648 (1993).

[10] S. H. Vosko, L. Wilk, and M. Nusair, Can. J. Phys. **58**, 1200 (1980).

[11] C. Lee, W. Yang, and R. G. Parr, Phys. Rev. B **37**, 785 (1988).

[12] J. S. Binkley, J. A. Pople, and W. J. Hehre, J. Am. Chem. Soc. **102**, 939 (1980); M. S. Gordon, J. S. Binkley, J. A. Pople, W. J. Pietro, and W. J. Hehre, J. Am. Chem. Soc. **104**, 2797 (1982); W. J. Pietro, M. M. Francl, W. J. Hehre, D. J. Defrees, J. A. Pople, and J. S. Binkley, J. Am. Chem. Soc. **104**, 5039 (1982).

[13] A. D. McLean and G. S. Chandler, J. Chem. Phys. **72**, 5639 (1980).

[14] T. Clark, J. Chandrasekhar, G. W. Spitznagel, and P. v. R. Schleyer, J. Comput. Chem. **4**, 294 (1983).

[15] M. J. Frisch, G. W. Trucks, H. B. Schlegel *et al*. GAUSSIAN 03, Revision D.01, Gaussian, Inc., Pittsburgh, PA, 2003.

[16] S. Portmann, MOLEKEL, Version 4.3., (CSCS/ETHZ, 2002)

[17] R.G. Pearson. Proc. Nat. Acad. Sci. USA. **72**, 2104 (1975).

[18] A. P. Sergeeva and A. I. Boldyrev Organometallics **29**, 3951 (2010).

TABLE 12-1. Comparison of the Averaged Experimental and Calculated parameters for Si_6X_{12} (X = Cl, Br) and $[Si_6Cl_{14}]^{2-}$ Dianion.

	Si-Si	**Si-X {ring}**	**Si-X {axial}**	**X-X**	**∠ {Si-Si-Si}**	**∠ {X-Si-X}**	**∠ {X-Si-Si}**	**$\angle_{Dihed}$ {ring}**
Si_6Cl_{12}[a]	2.38 Å	2.06 Å	—	—	113.0°	110.1°	108.4°	135.0°
Si_6Cl_{12}[b]	2.34 Å	2.03 Å	—	—	112.9°	110.4°	108.4°	134.8°
Si_6Br_{12}[b]	2.34 Å	2.20 Å	—	—	113.2°	110.7°	108.2°	135.0°
$[Si_6Cl_{14}]^{2-}$ [b]	2.29 Å	2.07 Å	3.00 Å	3.81 Å	119.9°	102.1°	108.3°	0.0°
$[Si_6Cl_{14}]^{2-}$ [a]	2.36 Å	2.11 Å	3.06 Å	3.90 Å	120.0°	101.4°	108.5°	0.0°

[a] Calculations at B3LYP/6-311+G(3df).
[b] Experimentally observed.

TABLE 12-2. The energies of OMOs and UMOs involved in the PJTE distortion in the neutral Si_6Cl_{12} and $[Si_6Cl_{12}]^{(q=-2)}$.

HOMO-3 ($3b_{2g}$) and LUMO+1 ($5a_{1g}$)						
E_{OMO}, Hartree◊	E_{UMO}, Hartree◊◊	ΔE_1, eV◊◊◊	$E_{OMO}^{q(-2)}$, Hartree◊◊◊◊	$E_{UMO}^{q(-2)}$, Hartree◊◊◊◊◊	ΔE_2, eV◊◊◊◊◊◊	$\Delta E_2 - \Delta E_1$, eV
-0.34010	-0.10950	6.28	-0.11129	+0.13125	6.60	0.32
HOMO ($2b_{2u}$) and LUMO+4 ($5e_{1g}$)						
E_{OMO}, Hartree◊	E_{UMO}, Hartree◊◊	ΔE_1, eV◊◊◊	$E_{OMO}^{q(-2)}$, Hartree◊◊◊◊	$E_{UMO}^{q(-2)}$, Hartree◊◊◊◊◊	ΔE_2, eV◊◊◊◊◊◊	$\Delta E_2 - \Delta E_1$, eV
-0.28177	-0.06351	5.94	-0.06566	0.16226	6.20	0.26
HOMO-4 ($4e_{1g}$) and LUMO+3 ($6e_{1u}$)						
E_{OMO}, Hartree◊	E_{UMO}, Hartree◊◊	ΔE_1, eV◊◊◊	$E_{OMO}^{q(-2)}$, Hartree◊◊◊◊	$E_{UMO}^{q(-2)}$, Hartree◊◊◊◊◊	ΔE_2, eV◊◊◊◊◊◊	$\Delta E_2 - \Delta E_1$, eV
-0.34236	-0.06504	7.55	-0.11647	+0.16250	7.59	0.04

◊ E_{OMO} – energy of the OMO of Si_6Cl_{12} (D_{6h}, $^1A_{1g}$);

◊◊ E_{UMO} – energy of the UMO of Si_6Cl_{12} (D_{6h}, $^1A_{1g}$);

◊◊◊ $\Delta E_1 = E_{UMO} - E_{OMO}$;

◊◊◊◊ $E_{OMO}^{q(-2)}$ – energy of the same OMO of Si_6Cl_{12} (D_{6h}, $^1A_{1g}$) with the artificial charges above (q = -1) and below (q = -1) the plane of the molecule;

◊◊◊◊◊ $E_{UMO}^{q(-2)}$ – energy of the same UMO of Si_6Cl_{12} (D_{6h}, $^1A_{1g}$) with the artificial charges above (q = -1) and below (q = -1) the plane of the molecule;

◊◊◊◊◊◊ $\Delta E_2 = E_{UMO}^{q(-2)} - E_{OMO}^{q(-2)}$.

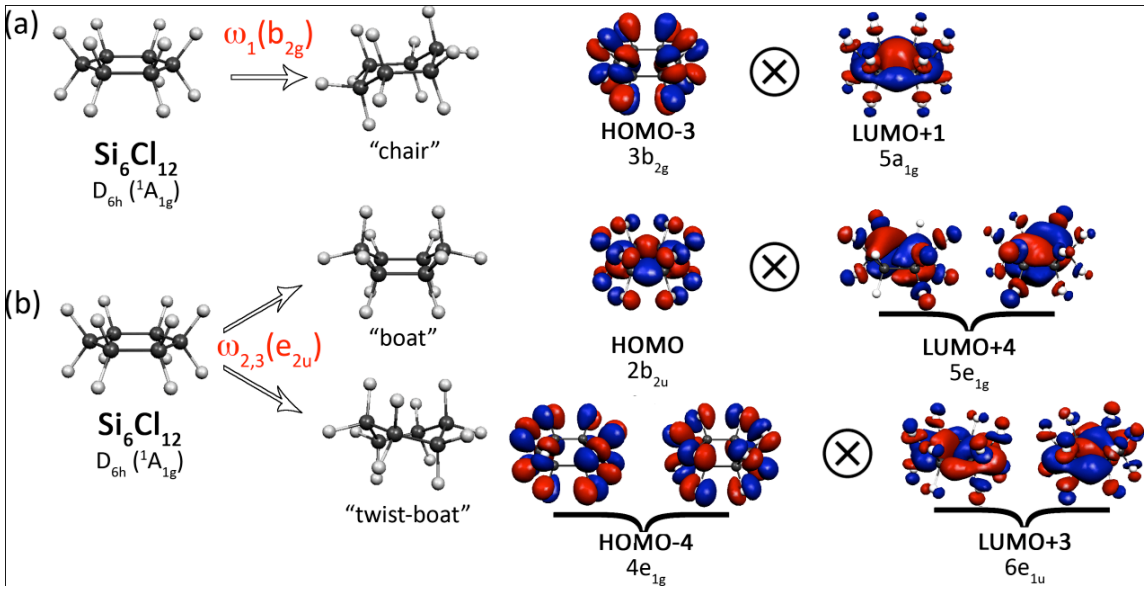

FIG. 12-1. Interaction of the pairs of occupied and unoccupied molecular orbitals of Si_6Cl_{12} (D_{6h}, $^1A_{1g}$) responsible for the PJT effect: (a) distortion towards the "chair" structure upon following the $\omega_1(b_{2g})$ imaginary frequency mode; (b) distortion towards the "boat" and "twist-boat" structures upon following the doubly degenerate $\omega_{2,3}(e_{2u})$ imaginary frequency modes.

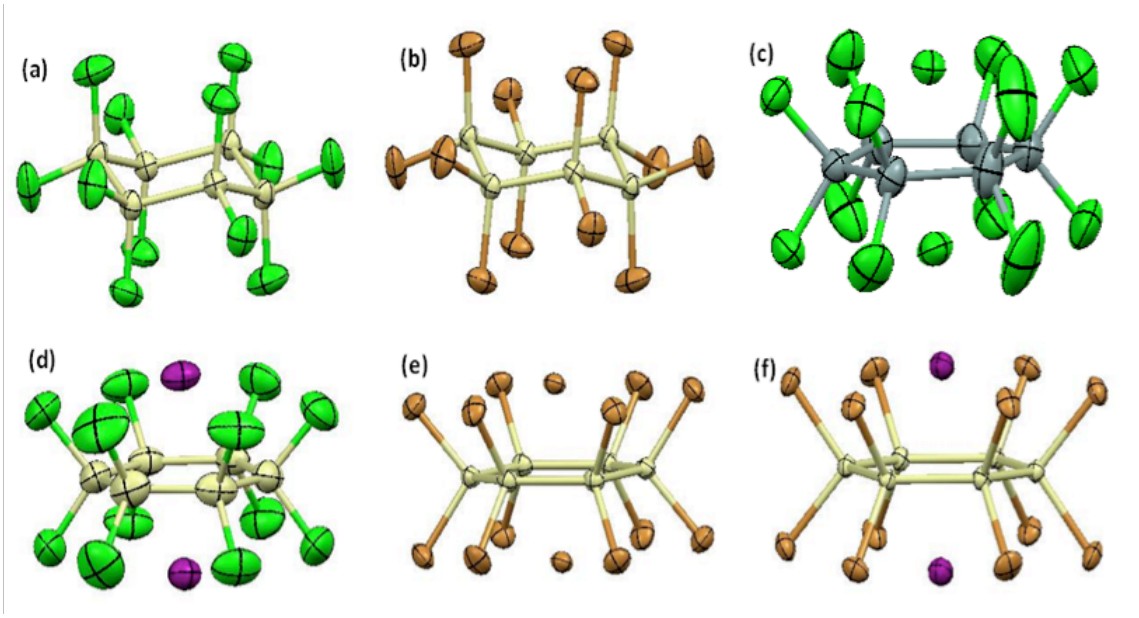

FIG. 12-2. Crystal structures of (a) Si_6Cl_{12}; (b) Si_6Br_{12}; (Ref.8) (c) $[Si_6Cl_{14}]^{2-}$ fragment in $[^nBu_4N]_2[Si_6Cl_{14}]$; (d) $[Si_6Cl_{12}I_2]^{2-}$ fragment in $[^nBu_4N]_2[Si_6Cl_{12}I_2]$; (e) $[Si_6Br_{14}]^{2-}$ fragment in $[^nBu_4N]_2[Si_6Br_{14}]$; and (f) $[Si_6Br_{12}I_2]^{2-}$ fragment in $[^nBu_4N]_2[Si_6Br_{12}I_2]$.

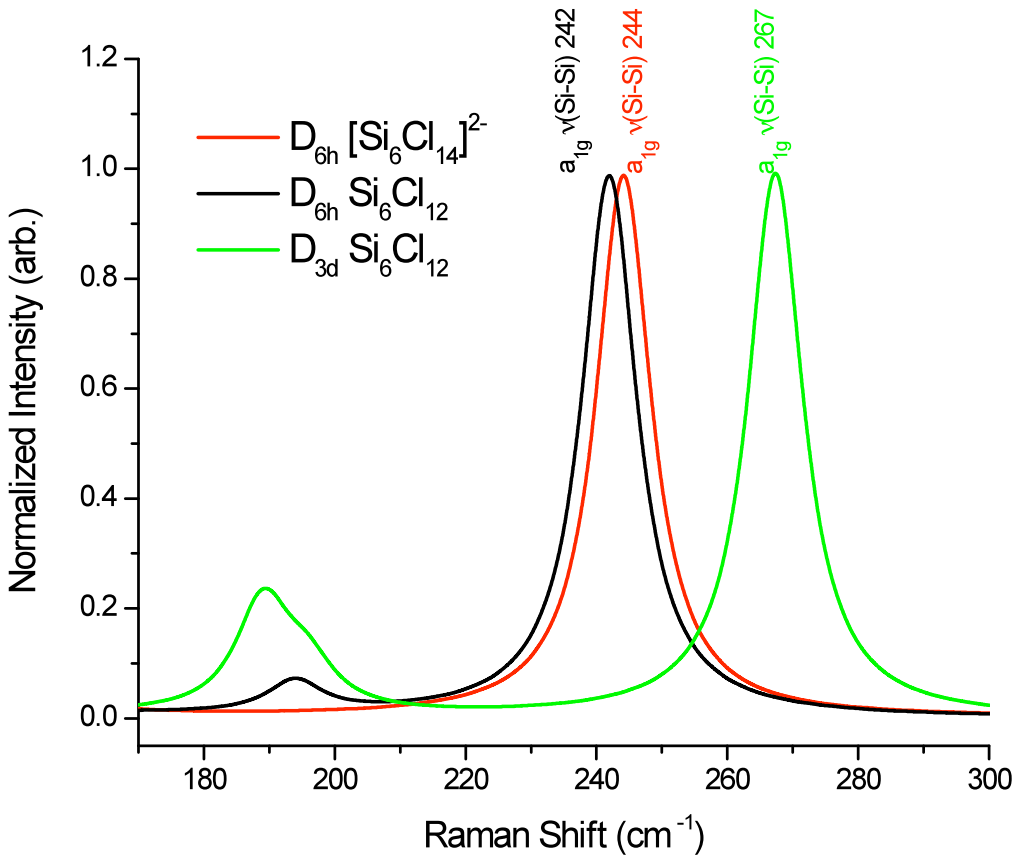

FIG. 12-3. Calculated Raman spectrum of "chair" (D_{3d}, $^1A_{1g}$) Si_6Cl_{12} (green), planar (D_{6h},$^1A_{1g}$) Si_6Cl_{12} (black), and (D_{6h},$^1A_{1g}$) $Si_6Cl_{14}^{2-}$ (red), simulated at B3LYP/6-311+G(3df) . All spectra are normalized to the dominant ν(Si-Si) modes. These calculations reproduce the ν(Si-Si) mode softening observed in the experimental Raman. Further, comparison of the ν(Si-Si) mode in planar and "chair" configurations of Si_6Cl_{12} confirm that the observed softening is due almost entirely to planarization of the Si_6 ring.

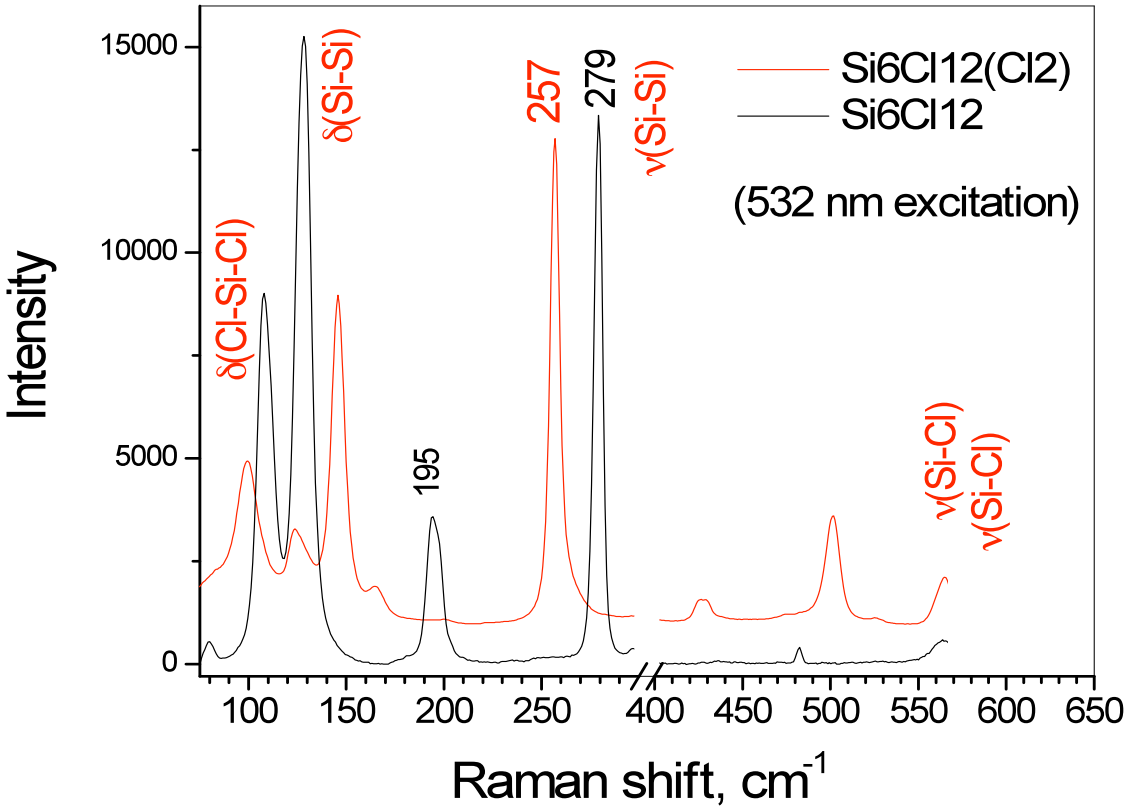

FIG. 12-4. Raman spectra of polycrystalline samples of Si_6Cl_{12} (black) and $[Si_6Cl_{14}]^{2-}$ (red) obtained with 532 nm laser excitation.

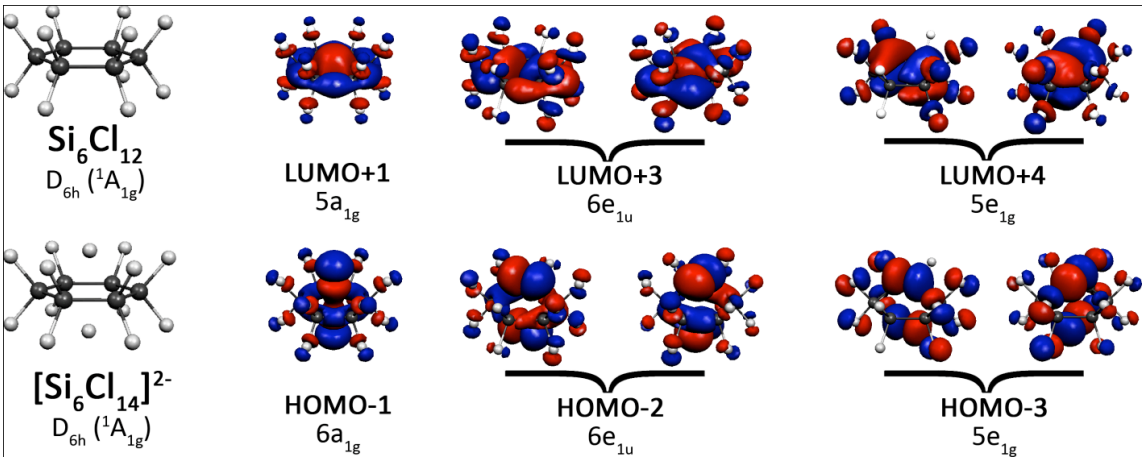

FIG. 12-5. One-to-one correspondence of unoccupied canonical molecular orbitals of Si_6Cl_{12} (D_{6h}, $^1A_{1g}$) to those of $[Si_6Cl_{14}]^{2-}$ (D_{6h}, $^1A_{1g}$), where occupation in the latter results in the suppression of PJT effect by adding two singly-charged chloride anions.

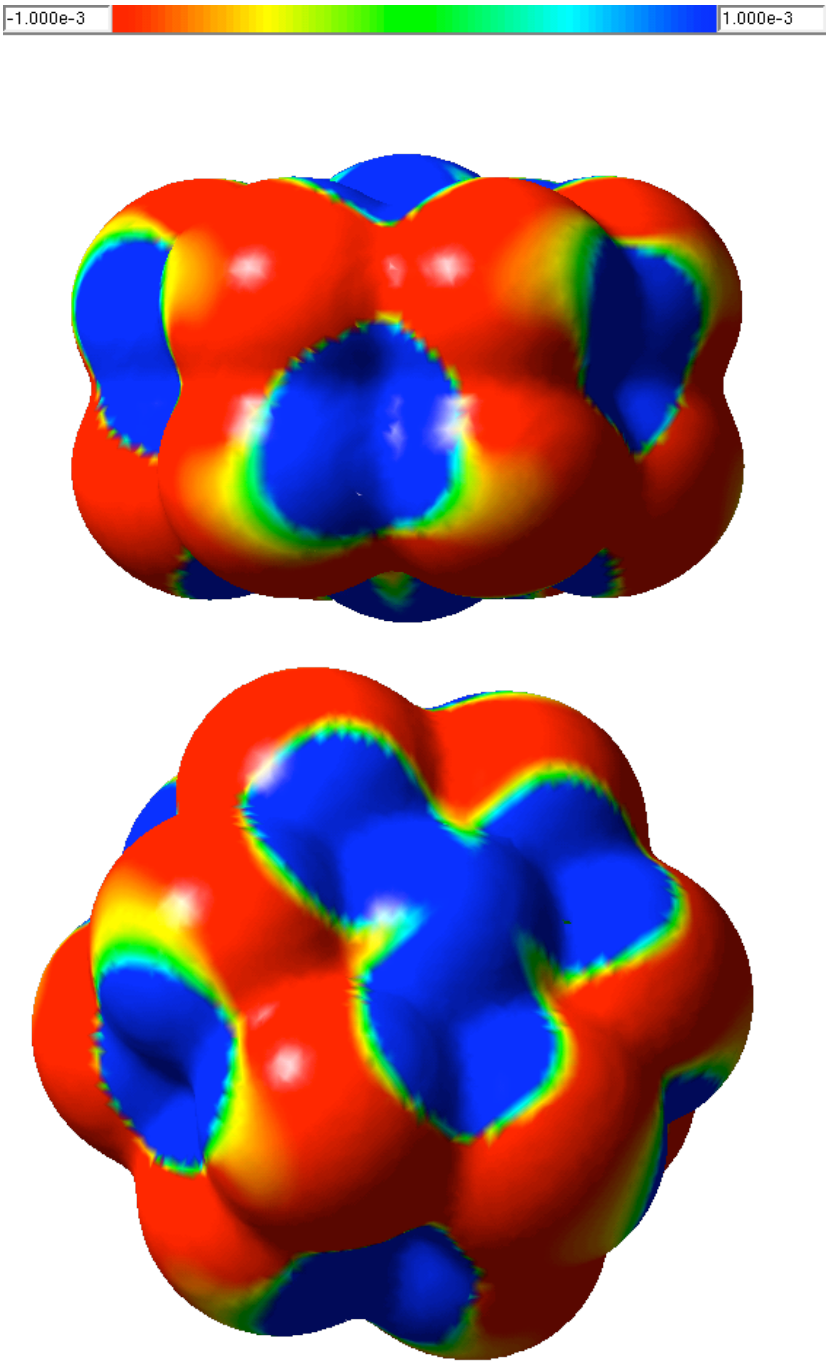

FIG. 12-6. Electrostatic potential map of Si_6Cl_{12}.

CHAPTER 13

SUMMARY AND CONCLUDING REMARKS

In chemistry, a cluster is an ensemble of bound atoms intermediate in size between a diatomic molecule and a bulk solid.[1] At first, people thought that clusters are simply small pieces of solids possessing the same structures like that of a corresponding solid with a lot of dangling bonds. The breakthrough in understanding peculiarities of clusters occurred in mid 80s of the last century, when Smalley and co-workers realized that C_{60} is not a piece of graphite, diamond or carbine, but it had a so-called "buckyball" structure.[1] Thus, the C_{60} cluster was shown to be a high symmetry structure with no dangling bonds at all. Moreover, this discovery opened a new direction in chemistry, so-called "Chemistry of Fullerenes." Another spectacular example is the Au_{20} cluster which was shown to possess a beautiful tetrahedral structure[2] with unexpected chemical bonding based on ten four center two electron bonds[3] located at the center of every small tetrahedra comprising Au_{20} cluster. For gold was considered as most inert metal over the centuries, it was used as coinage material as well as to make jewelry. Surprisingly, in 1987 Haruta and co-workers discovered that nanoscale gold particles have unusual catalytic properties for selective oxidation of CO.[4] Started from that it was clear that clusters are neither molecules nor crystals but unique chemical species with yet unknown structures, peculiar chemical bonding, and unexpected chemical reactivity. Since clusters are frequently composed of just a few atoms, their properties, such as structure, stability

[1] The next three paragraphs are coauthored by Alina P. Sergeeva and Alexander I. Boldyrev. Reproduced with permission from *Aromaticity and Metal clusters*. *Atoms, Molecules, and Clusters*. *Structure, Reactivity, and Dynamics book series*, ed. P. K. Chattaraj, CRC Press, Taylor & Francis Group, Boca Raton, 2011, pp. 55-68.. Copyright 2011, Taylor and Francis Group, LLC.

and reactivity can be studied computationally using high-levels of theory. Experimentally isolated clusters are generated in a molecular beam, where they are free from environmental influence such as solvent, or counterions in a crystalline lattice. That allows one to study their intrinsic properties.

Understanding chemical bonding of pure clusters may have significantly more profound effect in chemistry even though clusters are very exotic species being generated in a molecular beam for a short period of time. In order to facilitate chemical bonding analysis of cluster species, we used a tool recently developed in our lab: the Adaptive Natural Density Partitioning (AdNDP) method.[5] This method leads to partitioning of the charge density into elements with the highest possible degree of localization of electron pairs. If some part of the density cannot be localized in this manner, it is represented as completely delocalized objects, similar to canonical molecular orbitals, naturally incorporating the idea of delocalized bonding, i.e., *n* center - *two* electron (*n*c-*2*e) bonds. If one encounters a molecule or a cluster in which AdNDP analysis reveals that σ- or π-electrons cannot be localized into lone pairs or 2c-2e bonds, such a species is considered from the aromaticity/antiaromaticity point of view. If delocalization occurs over the whole molecule and corresponding bonds satisfy the 4n+2 rule we consider such species to be globally aromatic. Thus, we assess aromaticity in a particular chemical species on the basis of the presence of delocalized bonding recovered by the AdNDP analysis in a cyclic structure.

In the introduction we stated that clusters are neither molecules nor solids but unique chemical species with yet unknown structures, peculiar chemical bonding, and unexpected chemical reactivity. Despite a few decades of theoretical and experimental

studies of clusters they continue to be mysterious chemical species that are still poorly understood. Nevertheless, understanding chemical bonding of clusters can be useful for deciphering chemical bonding of solids, nanoparticles, novel materials, catalysts, active sites of enzymes, etc. We still do not have a simple chemical bonding model for clusters similar to the Lewis chemical bonding model for organic molecules capable of rationalizing and predicting their structure. While in recent years some progress has been made in developing such a chemical bonding model we still discover almost every day remarkable unexpected novel structures of clusters with surprising chemical bonding and reactivity. The development of a comprehensive chemical bonding model for clusters would be an important step towards a unified chemical bonding theory in chemistry.

One can find analogues of organic molecules among inorganic clusters. The π-bonding of the B_{19}^- cluster is similar to that of coronene,[6] while the B_{16}^{2-} and B_{17}^- clusters can be considered all-boron analogues of naphthalene.[7,8] The stability and chemical reactivity of pure boron cations can be also rationalized in terms of aromaticity and antiaromaticity.[9] The absence of localized bonds within pure boron clusters enables concentric boron clusters to have fluxional behavior with the inner fragment rotating with respect to the outer ring.[10] The B_{19}^- and B_{13}^+ clusters are shown to be the first two examples of molecular Wankel motors.[10,11]

Isoelectronic clusters may possess similar chemical bonding and yet different structures. B_7^- and B_{12}^- clusters were shown to become planar upon substitution of one boron atom by an isoelectronic aluminum atom.[12] The most stable structures of nitrogen-doped gallium clusters were shown to be similar to those of their isoelectronic aluminum congeners.[13] The unexpected presence of $Ga_xN_2^-$ species was reported; though, one might

well imagine that due to the strength of the nitrogen-nitrogen bond any attempts to add more than one nitrogen atom to gallium clusters would simply result in the formation of N_2 and its escape.[13] It is conceivable that nitrogen gallium clusters could be a good platform for understanding how the second (after C≡O) strongest chemical bond in diatomic molecules can be broken upon interaction with atomic clusters.

If one considers two-dimensional materials it becomes clear why boron-based materials are so different in structure compared to the carbon-based ones. The difference in one valence electron plays a huge role: one-atom-thick planar sheets of sp^2-bonded carbon atoms in graphene are densely packed in a honeycomb crystalline lattice (all the hexagons are empty),[14,15] while the similar crystalline lattice of boron is not stable at all.[16-18] If the electron deficiency of boron is compensated by accepting an extra electron from some metal (e.g. Mg, Al, Ti, V, Cr, etc.), the boron atoms undergo transmutation into a 'carbon' atom and all the resulting MB_2 borides[19] start possessing honey comb boron lattices. The electron deficiency of boron also explains why the most stable two-dimensional boron material, the so-called α-sheet, has some hexagons centered and some hexagons empty.[20] The extra boron atoms bring the needed electrons for the all-boron α-sheet to possess a chemical bonding picture similar to that of graphene: the delocalized σ-bonds in the all-boron α-sheet[20] mimic the localized 2c-2e C-C σ-bonds of graphene,[21] while the bonding pattern of local π-aromaticity is exactly the same in both graphene and the boron α-sheet.[20,21] In other words, electronic transmutation can guide experimentalists to synthesize new materials.

Though multiple bonding in transition metal compounds had been discussed in the literature for more than four decades, the discovery of aromaticity in all transition

metal systems (cyclic systems composed out of transition metal atoms)[22,23] was made only few years ago. In the compounds composed out of main group elements one may expect sigma-(σ-) and pi- (π-) aromaticity only. In all transition metal systems one may expect two new types of aromaticity: delta-(δ-) and fi-(φ-) in addition to σ- and π-aromaticity. The first δ-delocalized bond and δ-aromaticity was discovered in the $Ta_3O_3^-$ cluster.[22] The triangular Hf_3 cluster in its lowest singlet state was theoretically predicted to be the first example of triple (σ-, π-, and δ-) aromaticity.[23] We showed that the bonding in the Pd_4^{2+} unit of $[Pd_4(\mu_4\text{-}C_9H_9)(\mu_4\text{-}C_8H_8)]^+$ was of δ-character among four palladium atoms, making the triple-decker sandwich complex the first synthesized compound identified as having δ-bonding in its cyclic building block when it is in solution or in a crystalline state.[24] The existence of the $[Pd_4(\mu_4\text{-}C_9H_9)(\mu_4\text{-}C_8H_8)][BAr^f_4]$ sandwich compound is an excellent demonstration of the importance of delocalized δ-bonding in inorganic and organometallic chemistry.

Rhenium trichloride was proposed to have d-AO based π-aromaticity on the basis of the negative nuclear independent chemical shift values.[25,26] On the contrary, we confirmed the prediction of Cotton and co-workers[27-29] stating that neutral Re_3Cl_9 was a purely classical chemical molecule with three consecutive double bonds in a triatomic cycle formed by rhenium atoms.[30] The chemical bonding picture was shown to change dramatically upon addition of two excess electrons to Re_3Cl_9 with the resulting dianion being π-aromatic.[30] The isoelectronic neutral and dianionic technetium halides were shown to have chemical bonding pictures similar to those of rhenium trichlorides.[31]

The language of aromaticity is gradually entering the vocabulary of contemporary chemists. To facilitate easier identification of aromatic species we derived the counting

rules for σ-, π-, δ-, and ϕ-aromaticity and antiaromaticity for both singlet/triplet coupled triatomic and tetratomic systems as depended on the nature of atomic orbitals involved in the formation of corresponding bonding/antibonding molecular orbitals.[32] We have also shown that one can rationalize chemical bonding of crystals and alloys by performing the chemical bonding analysis of the constituent building blocks.[33] The main challenge of this approach is the proper choice of the charge to be imposed on the building block of interest.

Finally, if enough knowledge is accumulated one can try and use it for rational design of chemical species. We proposed rational design of small three-dimensional gold clusters based on the fact that gold atoms tend to form tetrahedra connected through vertices due to formation of a 4c-2e bond inside of each tetrahedron.[34]

The dissertation also provided the insight into the properties of multiply charged anions and the pseudo Jahn-Teller effect and its suppression.

Multiply charged anions (MCAs) are not thermodynamically stable due to the presence of intramolecular Coulomb repulsions. Metastable MCAs store excess electrostatic energies, which are released upon photodetachment. We discovered and characterized the first long-lived triply charged anion ($HPTS^{3-}$), which possesses negative electron binding energy of -0.66 eV.[35] One of the most interesting and unusual features of multiply charged anions is the repulsive Coulomb barrier, which prevents slow electrons from being emitted and therefore provides dynamic stability for MCAs, allowing metastable species to be observed experimentally.[36-42] We explored the limits of electron metastability by changing chemical identity of the substituent groups of the $HPTS^{3-}$ ion.[43] MCAs can be stabilized in the condensed phase by solvent in solution or counterions in

crystals. We explored the interactions of an important inorganic MCA, sulfate, with a fixed number of water molecules: $SO_4^{2-}(H_2O)_n$ (n = 4–7).[44] We found that different structural isomers were populated as a function of temperature. The work revealed the complexity of the water-sulfate potential energy landscape and the importance of temperature control in studying the solvent-solute systems and in comparing calculations with experiment.[44]

Jahn-Teller effects cause the deviation from high symmetry and planarity of ring structures. We reported theoretical prediction of flattening the puckered Si_5 ring by suppression of the pseudo Jahn-Teller (PJT) effect through coordination of two Mg^{2+} cations to the $Si_5H_5^-$ anion to make an inverse $[Mg^{2+}Si_5H_5^-Mg^{2+}]$ sandwich complex.[45] The PJT effect was suppressed through the OMO-UMO gaps increase in the resultant $[Mg^{2+}Si_5H_5^-Mg^{2+}]$ sandwich complex, as compared to the initial $Si_5H_5^-$ anion. We believe that the way of suppressing the PJT effect through coordination of extra cations can be a useful tool in restoring high symmetry structures in otherwise distorted cyclic geometries. The salts containing $C_5H_5^-$ anions are known to form stacking structures, where $C_5H_5^-$ together with counterions form “infinite” piles of sandwich type structures.[46] We hope that our theoretical prediction of planarization of the $Si_5H_5^-$ anion in the $Mg^{2+}Si_5H_5^-Mg^{2+}$ would stimulate synthesis of the first compounds containing the planar $Si_5H_5^-$ anions. The second way to suppress PJT effect was shown on an example of the chemical reaction of the puckered Si_6Cl_{12} molecule with a Lewis base (e.g. Cl^-) to give a planar $[Si_6Cl_{14}]^{2-}$ dianionic complex.[47] We proposed that the PJT effect in Si_6X_{12} was suppressed by filling the intervenient molecular orbitals with electron pairs of adduct.[47] Additionally, the proposed pathway for the PJT suppression has been proved by the synthesis and

characterization of novel compounds containing planar Si_6 ring, namely: $[^nBu_4N]_2[Si_6Cl_{12}I_2]$, $[^nBu_4N]_2[Si_6Br_{14}]$, and $[^nBu_4N]_2[Si_6Br_{12}I_2]$. This work demonstrated for the first time that PJT effect suppression is useful in the rational design of materials with novel properties.

References

1 H. W. Kyoto, J. R. Heath, S. C. O'Brien, R. F. Curl and R. E. Smalley, *Nature*, 1985, **318**, 162.

2 J. Li, X. Li, H. J. Zhai and L. S. Wang, *Science*, 2003, **299**, 864.

3 D. Y. Zubarev and A. I. Boldyrev, *J. Phys. Chem. A*., 2009, **113**, 866.

4 M. Haruta, T. Kobayashi, H. Sano and N. Yamada, *Chem. Lett.*, 1987, **16**, 405.

5 D. Y. Zubarev and A. I. Boldyrev, *Phys. Chem. Chem. Phys*., 2008, **10**, 5207.

6 W. Huang, A. P. Sergeeva, H. J. Zhai, B. B. Averkiev, L. S. Wang and A. I. Boldyrev, *Nature Chem.,* 2010, **2**, 202.

7 A. P. Sergeeva, D. Y. Zubarev, H. J. Zhai, A. I. Boldyrev and L. S. Wang, *J. Am. Chem. Soc.,* 2008, **130**, 7244.

8 A. P. Sergeeva, B. B. Averkiev, H. J. Zhai, A. I. Boldyrev and L. S. Wang, *J. Chem. Phys.,* 2011, **134**, 224304.

9 D. Y. Zubarev, A. P. Sergeeva and A. I. Boldyrev, in *Chemical Reactivity Theory. A Density Functional View,* ed. P. K. Chattaraj, CRC Press. Taylor & Francis Group, New York, 2009, pp. 439-452.

10 G. Martínez-Guajardo, A. P. Sergeeva, A. I. Boldyrev, T. Heine, J. M. Ugalde, G. Merino, *Chem. Commun*., 2011, **47**, 6242.

11 J. O. C. Jimenez-Halla, R. Islas, T. Heine and G. Merino, *Angew. Chem. Int. Ed*. 2010, **49**, 5668.

12 C. Romanescu, A. P. Sergeeva, W. L. Li, A. I. Boldyrev and L. S. Wang, *J. Am. Chem. Soc.,* 2011, **133**, 8646.

13 H. Wang, Y. J. Ko, K. H. Bowen, A. P. Sergeeva, B. B. Averkiev and A. I. Boldyrev, *J. Phys. Chem. A,* 2010, **114**, 11070.

14 K. S. Novoselov, A. K. Geim, S. V. Morozov, D. Jiang, Y. Zhang, S. V. Dubonos, I. V. Grigorieva and A. A. Firsov, *Science,* 2004, **306**, 666.

15 K. S. Novoselov, A. K. Geim, S. V. Morozov, D. Jiang, M. I. Katsnelson, I. V. Grigorieva, S. V. Dubonos and A. A. Firsov, *Nature*, 2005, **438**, 197.

16 H. Tang and S. Ismail-Beigi, *Phys. Rev. Lett*., 2007, **99**, 115501.

17 H. Tang and S. Ismail-Beigi, *Phys. Rev. B*, 2009, **80**, 134113.

18 X. Yang, Y. Ding and J. Ni, *Phys. Rev. B*, 2008, **77**, 0414402.

19 M. E. Jones and R. E. Marsh, *J. Am. Chem. Soc.*, 1954, **76**, 1434.

20 T. R. Galeev, Q. Chen, J. Guo, H. Bai, C. Q. Miao, H. G. Lu, A. P. Sergeeva, S. D. Li and A. I. Boldyrev, *Phys. Chem. Chem. Phys*., 2011, **13**, 11575.

21 I. A. Popov, K. V. Bogenko and A. I. Boldyrev, *Nano Res.*, 2011, DOI: 10.1007/s12274-011-0192-z.

22 H. J. Zhai, B. B. Averkiev, D. Y. Zubarev, L. S. Wang and A. I. Boldyrev, *Angew. Chem. Int. Ed*., 2007, **46**, 4277.

23 B. B. Averkiev and A. I. Boldyrev, *J. Phys. Chem. A*, 2007, **111**, 12864.

24 A. P. Sergeeva and A. I. Boldyrev, *Phys. Chem. Chem. Phys*., 2010, **12**, 12050.

25 L. Alvarado-Soto, R. Ramirez-Tagle and R. Arratia-Perez, *Chem. Phys. Lett*., 2008, **467**, 94.

26 L. Alvarado-Soto, R. Ramirez-Tagle and R. Arratia-Perez, *J. Phys. Chem. A*, 2009, **113**, 1671.

27 F. A. Cotton and T. Haas, *Inorg. Chem*., 1964, **3**, 10.

28 F. A. Cotton, N. F. Curtis, C. B. Harris, B. F. G. Johnson, S. J. Lippard, J. T. Mague, W. R. Robinson and J. S. Wood, *Science*, 1964, **145**, 1305.

29 B. E. Bursten, F. A. Cotton, J. C. Green, E. A. Seddon and G. G. Stanley, *J. Am. Chem. Soc*., 1980, **102**, 955.

30 A. P. Sergeeva and A. I. Boldyrev, *Comments Inorg. Chem*., 2010, **31**, 2.

31 P. F. Weck, A. P. Sergeeva, E. Kim, A. I. Boldyrev and K. R. Czerwinski, *Inorg. Chem*., 2011, **50**, 1039.

32 A. P. Sergeeva, B. B. Averkiev and A. I. Boldyrev, in *Metal-Metal Bonding. Structure and Bonding book series,* ed. G. Parkin, Volume 136, Springer, Berlin/Heidelberg, 2010, pp. 275-306.

33 A. P. Sergeeva and A. I. Boldyrev, in *Aromaticity and Metal clusters. Atoms, Molecules, and Clusters. Structure, Reactivity, and Dynamics book series*, ed. P. K. Chattaraj, CRC Press, Taylor & Francis Group, Boca Raton, 2010, pp. 55-68.

34 A. P. Sergeeva and A. I. Boldyrev, *J. Clust. Sci.*, 2011, **22**, 321.

35 J. Yang, X. P. Xing, X. B. Wang, L. S. Wang, A. P. Sergeeva and A. I. Boldyrev, *J. Chem. Phys*., 2008, **128**, 091102-1-4.

36 X. B. Wang and L. S. Wang, *Nature*, 1999, **400**, 245.

37 X. B. Wang and L. S. Wang, *Phys. Rev. Lett*., 1999, **83**. 3402.

38 X. B. Wang, K. Ferris and L. S. Wang, *J. Phys. Chem. A*, 2000, **104**, 25.

39 X. B. Wang and L. S. Wang, *J. Am. Chem. Soc.*, 2000, **122**, 2339.

40 P. Weis, O. Hampe, S. Gilb and M. M. Kappes, *Chem. Phys. Lett*., 2000, **321**, 426.

41 M. N. Blom, O. Hampe, S. Gilb, P. Weis and M. M. Kappes, *J. Chem. Phys*., 2001, **115**, 3690.

42 K. Arnold, T. S. Balaban, M. N. Blom, O. T. Ehrler, S. Gilb, O. Hampe, J. E. v. Lier, J. M. Weber and M. M. Kappes, *J. Phys. Chem. A,* 2003, **107**, 794.

43 X. B. Wang, A. P. Sergeeva, X. P. Xing, M. Massaouti, T. Karpuschkin, O. Hampe, A. I. Boldyrev, M. M. Kappes and L. S. Wang, *J. Am. Chem. Soc.,* 2009, **131**, 9836.

44 X. B. Wang, A. P. Sergeeva, J. Yang, X. P. Xing, A. I. Boldyrev and L. S. Wang, *J. Phys. Chem. A,* 2009, **113**, 5567.

45 A. P. Sergeeva and A. I. Boldyrev, *Organometallics*, 2010, **29**, 3951.

46 P. Jutz and N. Burford, *Chem. Rev*. 1999, **99***,* 969.

47 K. Pokhodnya, C. Olson, X. Dai, D. L. Schulz, P. Boudjouk, A. P. Sergeeva and A. I. Boldyrev, *J. Chem. Phys*., 2011, **134**, 014105.

APPENDIX

PERMISSIONS

Title: A Photoelectron Spectroscopic and Theoretical Study of $B16^-$ and $B162^-$: An All-Boron Naphthalene

Author: Alina P. Sergeeva et al.

Publication: Journal of the American Chemical Society

Publisher: American Chemical Society

Date: Jun 1, 2008

Quick Price Estimate

Permission for this particular request is granted for print and electronic formats at no charge. Figures and tables may be modified. Appropriate credit should be given. Please print this page for your records and provide a copy to your publisher. Requests for up to 4 figures require only this record. Five or more figures will generate a printout of additional terms and conditions. Appropriate credit should read: "Reprinted with permission from {COMPLETE REFERENCE CITATION}. Copyright {YEAR} American Chemical Society." Insert appropriate information in place of the capitalized words.

I would like to...	reuse in a Thesis/Dissertation
Requestor Type	Author (original work)
Portion	Full article
Format	Print and Electronic
Will you be translating?	No
Select your currency	USD – $
Quick Price	Click Quick Price

QUICK PRICE CONTINUE

This service provides permission for reuse only. If you do not have a copy of the article you are using, you may copy and paste the content and reuse according to the terms of your agreement. Please be advised that obtaining the content you license is a separate transaction not involving Rightslink.

To request permission for a type of use not listed, please contact the publisher directly.

Title: A concentric planar doubly π-aromatic B19− cluster

Author: Wei Huang, Alina P. Sergeeva, Hua-Jin Zhai, Boris B. Averkiev, Lai-Sheng Wang, Alexander I. Boldyrev

Publication: Nature Chemistry

Publisher: Nature Publishing Group

Date: Jan 24, 2010

Permission Request Submitted

Your request is now under review.
You will be notified of the decision via email.
Please print this request for your records.

Get the printable order details.

Order Number	500648127
License date	Jan 07, 2012
Licensed content publisher	Nature Publishing Group
Licensed content publication	Nature Chemistry
Licensed content title	A concentric planar doubly π-aromatic B19− cluster
Licensed content author	Wei Huang, Alina P. Sergeeva, Hua-Jin Zhai, Boris B. Averkiev, Lai-Sheng Wang, Alexander I. Boldyrev
Licensed content date	Jan 24, 2010
Type of Use	reuse in a thesis/dissertation
Volume number	2
Issue number	3
Requestor type	academic/educational
Format	print and electronic
Portion	Full article
Circulation/distribution	>50,000
Author of this NPG article	yes
Your reference number	
Title of your thesis / dissertation	RATIONALIZING STRUCTURE, STABILITY, AND CHEMICAL BONDING OF PURE AND DOPED CLUSTERS, ISOLATED AND SOLVATED MULTIPLY CHARGED ANIONS, AND SOLID STATE MATERIALS
Expected completion date	Mar 2012
Estimated size (number of pages)	400
Total	Not Available

ORDER MORE... CLOSE WINDOW

NATURE PUBLISHING GROUP ORDER TERMS AND CONDITIONS

Jan 07, 2012

This is an Agreement between Alina P. Sergeeva ("You") and Nature Publishing Group ("Nature Publishing Group"). It consists of your order details, the terms and conditions provided by RFPTest, and the payment terms and conditions.

Order Number	500648127
Order date	Jan 07, 2012
Licensed content publisher	Nature Publishing Group
Licensed content publication	Nature Chemistry
Licensed content title	A concentric planar doubly π-aromatic B19− cluster
Licensed content author	Wei Huang, Alina P. Sergeeva, Hua-Jin Zhai, Boris B. Averkiev, Lai-Sheng Wang, Alexander I. Boldyrev
Licensed content date	Jan 24, 2010
Volume number	2
Issue number	3
Type of Use	reuse in a thesis/dissertation
Requestor type	academic/educational
Format	print and electronic
Portion	Full article
Circulation/distribution	>50,000
Author of this NPG article	yes
Your reference number	
Title of your thesis / dissertation	RATIONALIZING STRUCTURE, STABILITY, AND CHEMICAL BONDING OF PURE AND DOPED CLUSTERS, ISOLATED AND SOLVATED MULTIPLY CHARGED ANIONS, AND SOLID STATE MATERIALS
Expected completion date	Mar 2012
Estimated size (number of pages)	400
Total	Not Available

aggiemail Alina Sergeeva <alina.sergeeva@aggiemail.usu.edu>

RightsLink / Nature Publishing Group Transaction Denied

6 messages

Copyright Clearance Center <rightslink@marketing.copyright.com> **Mon, Jan 9, 2012 at 4:27 AM**
Reply-To: Copyright Clearance Center <reply-fe59107276630d7a7314-14153369_HTML-722925152-114453-171@info.copyright.com>
To: alina.sergeeva@aggiemail.usu.edu

To view this email as a web page, go here.

Do Not Reply Directly to This Email

To ensure that you continue to receive our emails,
please add rightslink@marketing.copyright.com to your address book.

RightsLink | Copyright Clearance Center

Your Order Has Been Denied

Dear Alina Sergeeva,

Your order 500648127 has been denied as a result of the following: As an author of the article you are welcome to use your manuscript and figures as per the license to publish you signed. Please take a look at our author guidelines http://www.nature.com/authors/policies/license.html for further information, or alternatively email me at permisssions@nature.com. Best wishes, Sarah . You will not be charged for this order and a credit will be issued for any monies submitted in this regard to date.

To view the current status of this order, go to https://MyAccount.copyright.com, select View your RightsLink Orders, scroll down to Denied Orders, and click the Order number listed below.

Order Details

User:	Alina P. Sergeeva
Job Ticket Number:	500648127
Type of Use:	A concentric planar doubly π-aromatic B19− cluster
Title:	reuse in a thesis/dissertation
Author:	Wei Huang, Alina P. Sergeeva, Hua-Jin Zhai, Boris B. Averkiev, Lai-Sheng Wang, Alexander I. Boldyrev
Publisher:	Nature Publishing Group
Publication:	Nature Chemistry
Order Date:	Jan 07, 2012
Total::	0.00 USD

G.13:v1.3-rfp

+1-877-622-5543 / Tel: +1-978-646-2777
customercare@copyright.com
http://www.copyright.com

Alina Sergeeva <alina.sergeeva@aggiemail.usu.edu> **Wed, Jan 25, 2012 at 4:38 AM**
To: permisssions@nature.com

Dear Sarah,

My name is Alina P. Sergeeva. I'm a senior graduate student at Utah State University currently finalizing my PhD dissertation. I wanted to use an article of mine (Nature Chem. 2010, 2, 202-206) as a part of my dissertation. I've recently had my order to re-use the article for dissertation (#500648127) denied. See the e-mail below for details.

I read the license to publish as you suggested and I wanted to make sure if I understood it right. Does the license prohibit the use of the article in whole in part at all? Is there anyway I can use the article for my dissertation?

Thank you very much in advance! You help in this matter is greatly appreciated.

Sincerely,

Alina P. Sergeeva

---------- Forwarded message ----------
From: Copyright Clearance Center <rightslink@marketing.copyright.com>
Date: Mon, Jan 9, 2012 at 4:27 AM
Subject: RightsLink / Nature Publishing Group Transaction Denied
To: alina.sergeeva@aggiemail.usu.edu

Your Order Has Been Denied

Dear Alina Sergeeva,

Your order 500648127 has been denied as a result of the following: As an author of the article you are welcome to use your manuscript and figures as per the license to publish you signed. Please take a look at our author guidelines http://www.nature.com/authors/policies/license.html for further information, or alternatively email me at permisssions@nature.com. Best wishes, Sarah . You will not be charged for this order and a credit will be issued for any monies submitted in this regard to date.

To view the current status of this order, go to https://MyAccount.copyright.com, select View your RightsLink Orders, scroll down to Denied Orders, and click the Order number listed below.

Order Details

User:

Alina P. Sergeeva

Job Ticket Number:

500648127

Type of Use:

A concentric planar doubly π-aromatic B19− cluster

Title:

reuse in a thesis/dissertation

Author:

Wei Huang, Alina P. Sergeeva, Hua-Jin Zhai, Boris B. Averkiev, Lai-Sheng Wang, Alexander I. Boldyrev

Publisher:

Nature Publishing Group

Publication:

Nature Chemistry

Order Date:

Jan 07, 2012

Total::

0.00 USD

G.13:v1.3-rfp

+1-877-622-5543 / Tel: +1-978-646-2777
customercare@copyright.com
http://www.copyright.com

[Quoted text hidden]

--

E-mail: alina.sergeeva@aggiemail.usu.edu
Web-site: http://www.chem.usu.edu/~boldyrev/alina/
Department of Chemistry and Biochemistry: http://www.chem.usu.edu/
Utah State University
0300 Old Main Hill

Mail Delivery Subsystem <mailer-daemon@googlemail.com> **Wed, Jan 25, 2012 at 4:38 AM**
To: alina.sergeeva@aggiemail.usu.edu

Delivery to the following recipient failed permanently:

permisssions@nature.com

Technical details of permanent failure:
Google tried to deliver your message, but it was rejected by the recipient domain. We recommend contacting the other email provider for further information about the cause of this error. The error that the other server returned was: 550 550 #5.1.0 Address rejected permisssions@nature.com (state 14).

----- Original message -----

MIME-Version: 1.0
Received: by 10.182.119.73 with SMTP id ks9mr15507219obb.45.1327491523992;
Wed, 25 Jan 2012 03:38:43 -0800 (PST)
Received: by 10.182.51.2 with HTTP; Wed, 25 Jan 2012 03:38:43 -0800 (PST)
In-Reply-To: <3646c4be-e089-46de-b92b-1bb83d0c947b@xtinmta197.xt.local>
References: <3646c4be-e089-46de-b92b-1bb83d0c947b@xtinmta197.xt.local>
Date: Wed, 25 Jan 2012 04:38:43 -0700
Message-ID: <CAMVQ_pJGR0o-4Tst2ZCoRegtexMovh4hPp_ndc4Kc9Kxzi-Nrg@mail.gmail.com>
Subject: Fwd: RightsLink / Nature Publishing Group Transaction Denied
From: Alina Sergeeva <alina.sergeeva@aggiemail.usu.edu>
To: permisssions@nature.com
X-Gm-Message-State: ALoCoQkRDVJrslwsQsNzr9o9QlMN2n
4aTZwNPxeKRwZ3nTJ6jvwWAwaUgWW2BYq4mbxVqM3uDWUU
Content-Type: multipart/alternative; boundary=f46d044480dfbadab104b758b40f

[Quoted text hidden]

Alina Sergeeva <alina.sergeeva@aggiemail.usu.edu> **Wed, Jan 25, 2012 at 4:40 AM**
To: permissions@nature.com

Dear Sarah,

My name is Alina P. Sergeeva. I'm a senior graduate student at Utah State University currently finalizing my PhD dissertation. I wanted to use an article of mine (Nature Chem. 2010, 2, 202-206) as a part of my dissertation. I've recently had my order to re-use the article for dissertation (#500648127) denied. See the e-mail below for details.

I read the license to publish as you suggested and I wanted to make sure if I understood it right. Does the license prohibit the use of the article in whole in part at all? Is there anyway I can use the article for my dissertation?

Thank you very much in advance! You help in this matter is greatly appreciated.

Sincerely,

Alina P. Sergeeva

---------- Forwarded message ----------
From: **Copyright Clearance Center** <rightslink@marketing.copyright.com>
Date: Mon, Jan 9, 2012 at 4:27 AM
Subject: RightsLink / Nature Publishing Group Transaction Denied
To: alina.sergeeva@aggiemail.usu.edu

[Quoted text hidden]

[Quoted text hidden]

Permissions@nature.com <Permissions@nature.com> **Wed, Jan 25, 2012 at 4:44 AM**
To: Alina Sergeeva <alina.sergeeva@aggiemail.usu.edu>

Dear Alina,

You are welcome to use your manuscript and figures as per the license to publish you signed.

Ownership of copyright in the article remains with the Authors, and provided that, when reproducing the Contribution or extracts from it, the Authors acknowledge first and reference publication in the Journal, the Authors retain the following non-exclusive rights:

a) To reproduce the Contribution in whole or in part in any printed volume (book or thesis) of which they are the author(s).

b) They and any academic institution where they work at the time may reproduce the Contribution for the purpose of course teaching.

c) To post a copy of the Contribution as accepted for publication after peer review (in Word or Tex format) on the Authors' own web site or institutional repository, or the Authors' funding body's designated archive, six months after publication of the printed or online edition of the Journal, provided that they also give a hyperlink from the Contribution to the Journals web site.

d) To reuse figures or tables created by them and contained in the Contribution in other works

created by them.

Do let me know if you have any further questions.

Best wishes,
Sarah

Sarah Brooks
.....
Permissions Assistant

nature publishing group
The Macmillan Building
4 Crinan Street
London N1 9XW
e: permissions@nature.com

p: + 44 207 014 4129
f: + 44 207 843 4998

.....
Please consider the environment before printing this e-mail or its attachments

---

From: Alina Sergeeva [mailto:alina.sergeeva@aggiemail.usu.edu]
Sent: Wednesday, January 25, 2012 11:41 AM
To: Permissions@nature.com
Subject: Fwd: RightsLink / Nature Publishing Group Transaction Denied

[Quoted text hidden]

[Quoted text hidden]

Header

left

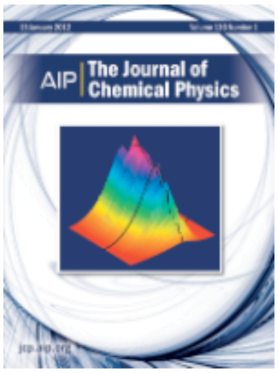

Title: All-boron analogues of aromatic hydrocarbons: B17− and B18−

Author: Alina P. Sergeeva, Boris B. Averkiev, Hua-Jin Zhai, Alexander I. Boldyrev, et al.

Publication: Journal of Chemical Physics

Volume/Issue 134/22

Publisher: American Institute of Physics

Date: Jun 10, 2011

Page Count: 11

Order Completed

Thank you very much for your order.

This is a License Agreement between Alina P. Sergeeva ("You") and American Institute of Physics ("AIP"). The license consists of your order details, the terms and conditions provided by American Institute of Physics, and the payment terms and conditions.

Get the printable license.

License Number	2823740837469
License date	Jan 07, 2012
Licensed content publisher	American Institute of Physics
Licensed content publication	Journal of Chemical Physics
Licensed content title	All-boron analogues of aromatic hydrocarbons: B17− and B18−
Licensed content author	Alina P. Sergeeva, Boris B. Averkiev, Hua-Jin Zhai, Alexander I. Boldyrev, et al.
Licensed content date	Jun 10, 2011
Volume number	134
Issue number	22
Type of Use	Thesis/Dissertation
Requestor type	Author (original article)
Format	Print and electronic
Portion	Excerpt (> 800 words)
Will you be translating?	No
Title of your thesis / dissertation	RATIONALIZING STRUCTURE, STABILITY, AND CHEMICAL BONDING OF PURE AND DOPED CLUSTERS, ISOLATED AND SOLVATED MULTIPLY CHARGED ANIONS, AND SOLID STATE MATERIALS
Expected completion date	Mar 2012
Estimated size (number of pages)	400
Total	0.00 USD

ORDER MORE... CLOSE WINDOW

AMERICAN INSTITUTE OF PHYSICS LICENSE TERMS AND CONDITIONS

Jan 07, 2012

This is a License Agreement between Alina P. Sergeeva ("You") and American Institute of Physics ("AIP") provided by Copyright Clearance Center ("CCC"). The license consists of your order details, the terms and conditions provided by American Institute of Physics , and the payment terms and conditions.

All payments must be made in full to CCC. For payment instructions, please see information listed at the bottom of this form.

License Number	2823740837469
License date	Jan 07, 2012
Licensed content publisher	American Institute of Physics
Licensed content publication	Journal of Chemical Physics
Licensed content title	All-boron analogues of aromatic hydrocarbons: B17− and B18−
Licensed content author	Alina P. Sergeeva, Boris B. Averkiev, Hua-Jin Zhai, Alexander I. Boldyrev, et al.
Licensed content date	Jun 10, 2011
Volume number	134
Issue number	22
Type of Use	Thesis/Dissertation
Requestor type	Author (original article)
Format	Print and electronic
Portion	Excerpt (> 800 words)
Will you be translating?	No
Title of your thesis / dissertation	RATIONALIZING STRUCTURE, STABILITY, AND CHEMICAL BONDING OF PURE AND DOPED CLUSTERS, ISOLATED AND SOLVATED MULTIPLY CHARGED ANIONS, AND SOLID STATE MATERIALS
Expected completion date	Mar 2012
Estimated size (number of pages)	400
Total	0.00 USD
Terms and Conditions	

American Institute of Physics -- Terms and Conditions: Permissions Uses

American Institute of Physics ("AIP") hereby grants to you the non-exclusive right and license to use and/or distribute the Material according to the use specified in your order, on a one-time basis, for the specified term, with a maximum distribution equal to the number that you have ordered. Any links or other content accompanying the Material are not the subject of this license.

1. You agree to include the following copyright and permission notice with the reproduction of the Material: "Reprinted with permission from [FULL CITATION]. Copyright [PUBLICATION YEAR], American Institute of Physics." For an article, the

aggiemail Alina Sergeeva <alina.sergeeva@aggiemail.usu.edu>

request for the permission to use three papers for the thesis/dissertation

2 messages

Alina Sergeeva <alina.sergeeva@aggiemail.usu.edu> **Sat, Jan 7, 2012 at 12:10 PM**
To: contracts-copyright@rsc.org

Dear Madam/Sir,

My name is Alina P. Sergeeva. I'm a senior graduate student at Utah State University currently finalizing my PhD dissertation. I'm hereby asking for the permission to reprint three articles co-authored by me and published in Chem. Commun. and Phys. Chem. Chem. Phys., as a part of the dissertation.

Unfortunately, I encountered a problem with the RightsLink system that you are suggesting to use. The error message I'm getting is:

"This reuse request is not allowed. If you need further assistance, please contact Royal Society of Chemistry at contracts-copyright@rsc.org."

I would very much appreciate if you could send me the permission to use the following three papers by fax or e-mail:

1) Unravelling phenomenon of internal rotation in B_{13}^{+} through chemical bonding analysis. Gerardo Martínez-Guajardo, Alina P. Sergeeva, Alexander I. Boldyrev, Thomas Heine, Jesus M. Ugalde and Gabriel Merino

Chem. Commun. 2011, *47*, 6242-6244 (DOI: 10.1039/C1CC10821B) (communication)

2) Deciphering the mystery of hexagon holes in an all-boron graphene α-sheet.
Timur R. Galeev, Qiang Chen, Jin-Chang Guo, Hui Bai, Chang-Qing Miao, Hai-Gang Lu, Alina P. Sergeeva, Si-Dian Li and Alexander I. Boldyrev
Phys. Chem. Chem. Phys. 2011, *13*, 11575-11578 (DOI: 10.1039/C1CP20439D) (communication)

3) δ-Bonding in the $[Pd_4(\mu_4\text{-}C_9H_9)(\mu_4\text{-}C_8H_8)]^{+}$ sandwich complex.

Alina P. Sergeeva and Alexander I. Boldyrev
Phys. Chem. Chem. Phys. 2010, *12*, 12050-12054 (DOI: 10.1039/C0CP00475H) (communication)

Fax number: +1(435)797-3390

E-mail: alina.sergeeva@aggiemail.usu.edu

I am not a correspondence author.

Thank you very much in advance!

Sincerely,
Alina P. Sergeeva

P.S.

My mailing address:

0300 Old Main Hill

Department of Chemistry and Biochemistry

Utah State University

Logan, UT, 84322-0300

CONTRACTS-COPYRIGHT (shared) <Contracts-Copyright@rsc.org> **Mon, Jan 9, 2012 at 2:08 AM**
To: Alina Sergeeva <alina.sergeeva@aggiemail.usu.edu>

Dear Alina

The Royal Society of Chemistry (RSC) hereby grants permission for the use of your paper(s) specified below in the printed and microfilm version of your thesis. You may also make available the PDF version of your paper(s) that the RSC sent to the corresponding author(s) of your paper(s) upon publication of the paper(s) in the following ways: in your thesis via any website that your university may have for the deposition of theses, via your university's Intranet or via your own personal website. We are however unable to grant you permission to include the PDF version of the paper(s) on its own in your institutional repository. The Royal Society of Chemistry is a signatory to the STM Guidelines on Permissions (available on request).

Please note that if the material specified below or any part of it appears with credit or acknowledgement to a third party then you must also secure permission from that third party before reproducing that material.

For the paper from ChemComm, please ensure that the thesis states the following:

Reproduced by permission of The Royal Society of Chemistry

For the paper from PCCP, please ensure that the thesis states the following:

Reproduced by permission of the PCCP Owner Societies

Please also include a link to the paper on the Royal Society of Chemistry's website.

Please ensure that your co-authors are aware that you are including the paper in your thesis.

Regards

Gill Cockhead

Publishing Contracts & Copyright Executive

Gill Cockhead (Mrs), Publishing Contracts & Copyright Executive

Royal Society of Chemistry, Thomas Graham House

Science Park, Milton Road, Cambridge CB4 0WF, UK

Tel +44 (0) 1223 432134, Fax +44 (0) 1223 423623

http://www.rsc.org

From: Alina Sergeeva [mailto:alina.sergeeva@aggiemail.usu.edu]
Sent: 07 January 2012 19:11
To: CONTRACTS-COPYRIGHT (shared)
Subject: request for the permission to use three papers for the thesis/dissertation
[Quoted text hidden]

Order Completed

Thank you very much for your order.

This is a License Agreement between Alina P. Sergeeva ("You") and Springer ("Springer"). The license consists of your order details, the terms and conditions provided by Springer, and the payment terms and conditions.

Get the printable license.

License Number	2823761271912
License date	Jan 07, 2012
Licensed content publisher	Springer
Licensed content publication	Journal of Cluster Science
Licensed content title	Rational Design of Small 3D Gold Clusters
Licensed content author	Alina P. Sergeeva
Licensed content date	Jan 1, 2011
Volume number	22
Issue number	3
Type of Use	Thesis/Dissertation
Portion	Full text
Number of copies	10
Author of this Springer article	Yes and you are a contributor of the new work
Title of your thesis / dissertation	RATIONALIZING STRUCTURE, STABILITY, AND CHEMICAL BONDING OF PURE AND DOPED CLUSTERS, ISOLATED AND SOLVATED MULTIPLY CHARGED ANIONS, AND SOLID STATE MATERIALS
Expected completion date	Mar 2012
Estimated size(pages)	400
Total	0.00 USD

CLOSE WINDOW

SPRINGER LICENSE
TERMS AND CONDITIONS

Jan 07, 2012

This is a License Agreement between Alina P. Sergeeva ("You") and Springer ("Springer") provided by Copyright Clearance Center ("CCC"). The license consists of your order details, the terms and conditions provided by Springer, and the payment terms and conditions.

All payments must be made in full to CCC. For payment instructions, please see information listed at the bottom of this form.

License Number	2823761271912
License date	Jan 07, 2012
Licensed content publisher	Springer
Licensed content publication	Journal of Cluster Science
Licensed content title	Rational Design of Small 3D Gold Clusters
Licensed content author	Alina P. Sergeeva
Licensed content date	Jan 1, 2011
Volume number	22
Issue number	3
Type of Use	Thesis/Dissertation
Portion	Full text
Number of copies	10
Author of this Springer article	Yes and you are a contributor of the new work
Order reference number	
Title of your thesis / dissertation	RATIONALIZING STRUCTURE, STABILITY, AND CHEMICAL BONDING OF PURE AND DOPED CLUSTERS, ISOLATED AND SOLVATED MULTIPLY CHARGED ANIONS, AND SOLID STATE MATERIALS
Expected completion date	Mar 2012
Estimated size(pages)	400
Total	0.00 USD
Terms and Conditions	

Introduction
The publisher for this copyrighted material is Springer Science + Business Media. By clicking "accept" in connection with completing this licensing transaction, you agree that the following terms and conditions apply to this transaction (along with the Billing and Payment terms and conditions established by Copyright Clearance Center, Inc. ("CCC"), at the time that you opened your Rightslink account and that are available at any time at http://myaccount.copyright.com).

Limited License
With reference to your request to reprint in your thesis material on which Springer Science and

No Amendment Except in Writing
This license may not be amended except in a writing signed by both parties (or, in the case of Springer Science + Business Media, by CCC on Springer Science + Business Media's behalf).

Objection to Contrary Terms
Springer Science + Business Media hereby objects to any terms contained in any purchase order, acknowledgment, check endorsement or other writing prepared by you, which terms are inconsistent with these terms and conditions or CCC's Billing and Payment terms and conditions. These terms and conditions, together with CCC's Billing and Payment terms and conditions (which are incorporated herein), comprise the entire agreement between you and Springer Science + Business Media (and CCC) concerning this licensing transaction. In the event of any conflict between your obligations established by these terms and conditions and those established by CCC's Billing and Payment terms and conditions, these terms and conditions shall control.

Jurisdiction
All disputes that may arise in connection with this present License, or the breach thereof, shall be settled exclusively by the country's law in which the work was originally published.

Other terms and conditions:

v1.2

If you would like to pay for this license now, please remit this license along with your payment made payable to "COPYRIGHT CLEARANCE CENTER" otherwise you will be invoiced within 48 hours of the license date. Payment should be in the form of a check or money order referencing your account number and this invoice number RLNK500694674.
Once you receive your invoice for this order, you may pay your invoice by credit card. Please follow instructions provided at that time.

Make Payment To:
Copyright Clearance Center
Dept 001
P.O. Box 843006
Boston, MA 02284-3006

For suggestions or comments regarding this order, contact RightsLink Customer Support: customercare@copyright.com or +1-877-622-5543 (toll free in the US) or +1-978-646-2777.

Gratis licenses (referencing $0 in the Total field) are free. Please retain this printable license for your reference. No payment is required.

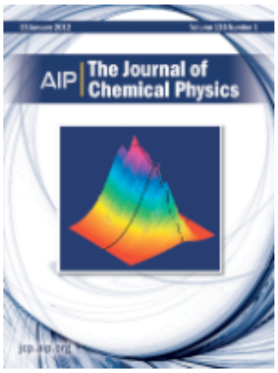

Title: Negative electron binding energies observed in a triply charged anion: Photoelectron spectroscopy of 1-hydroxy-3,6,8-pyrene-trisulfonate

Author: Jie Yang, Xiao-Peng Xing, Xue-Bin Wang, Lai-Sheng Wang, et al.

Publication: Journal of Chemical Physics

Volume/Issue 128/9

Publisher: American Institute of Physics

Date: Mar 4, 2008

Page Count: 4

Quick Price Estimate

I would like to... reuse in a thesis/dissertation

Select your currency USD – $

Requestor Type Author (original article)

Format Print and electronic

Portion Excerpt (> 800 words)

Will you be translating? No

Quick Price Click Quick Price

QUICK PRICE CONTINUE

Content Delivery: Once licensed, you may reuse the content only for the reuse purposes specified. No content delivery is offered through this service.

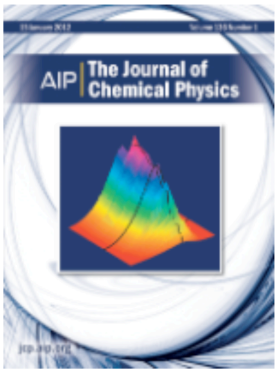

Title: Negative electron binding energies observed in a triply charged anion: Photoelectron spectroscopy of 1-hydroxy-3,6,8-pyrene-trisulfonate

Author: Jie Yang, Xiao-Peng Xing, Xue-Bin Wang, Lai-Sheng Wang, et al.

Publication: Journal of Chemical Physics

Volume/Issue 128/9

Publisher: American Institute of Physics

Date: Mar 4, 2008

Page Count: 4

Order Completed

Thank you very much for your order.

This is a License Agreement between Alina P. Sergeeva ("You") and American Institute of Physics ("AIP"). The license consists of your order details, the terms and conditions provided by American Institute of Physics, and the payment terms and conditions.

Get the printable license.

License Number	2823750502829
License date	Jan 07, 2012
Licensed content publisher	American Institute of Physics
Licensed content publication	Journal of Chemical Physics
Licensed content title	Negative electron binding energies observed in a triply charged anion: Photoelectron spectroscopy of 1-hydroxy-3,6,8-pyrene-trisulfonate
Licensed content author	Jie Yang, Xiao-Peng Xing, Xue-Bin Wang, Lai-Sheng Wang, et al.
Licensed content date	Mar 4, 2008
Volume number	128
Issue number	9
Type of Use	Thesis/Dissertation
Requestor type	Author (original article)
Format	Print and electronic
Portion	Excerpt (> 800 words)
Will you be translating?	No
Title of your thesis / dissertation	RATIONALIZING STRUCTURE, STABILITY, AND CHEMICAL BONDING OF PURE AND DOPED CLUSTERS, ISOLATED AND SOLVATED MULTIPLY CHARGED ANIONS, AND SOLID STATE MATERIALS
Expected completion date	Mar 2012
Estimated size (number of pages)	400
Total	0.00 USD

ORDER MORE... CLOSE WINDOW

AMERICAN INSTITUTE OF PHYSICS LICENSE TERMS AND CONDITIONS

Jan 07, 2012

This is a License Agreement between Alina P. Sergeeva ("You") and American Institute of Physics ("AIP") provided by Copyright Clearance Center ("CCC"). The license consists of your order details, the terms and conditions provided by American Institute of Physics , and the payment terms and conditions.

All payments must be made in full to CCC. For payment instructions, please see information listed at the bottom of this form.

License Number	2823750502829
License date	Jan 07, 2012
Licensed content publisher	American Institute of Physics
Licensed content publication	Journal of Chemical Physics
Licensed content title	Negative electron binding energies observed in a triply charged anion: Photoelectron spectroscopy of 1-hydroxy-3,6,8-pyrene-trisulfonate
Licensed content author	Jie Yang, Xiao-Peng Xing, Xue-Bin Wang, Lai-Sheng Wang, et al.
Licensed content date	Mar 4, 2008
Volume number	128
Issue number	9
Type of Use	Thesis/Dissertation
Requestor type	Author (original article)
Format	Print and electronic
Portion	Excerpt (> 800 words)
Will you be translating?	No
Title of your thesis / dissertation	RATIONALIZING STRUCTURE, STABILITY, AND CHEMICAL BONDING OF PURE AND DOPED CLUSTERS, ISOLATED AND SOLVATED MULTIPLY CHARGED ANIONS, AND SOLID STATE MATERIALS
Expected completion date	Mar 2012
Estimated size (number of pages)	400
Total	0.00 USD
Terms and Conditions	

American Institute of Physics -- Terms and Conditions: Permissions Uses

American Institute of Physics ("AIP") hereby grants to you the non-exclusive right and license to use and/or distribute the Material according to the use specified in your order, on a one-time basis, for the specified term, with a maximum distribution equal to the number that you have ordered. Any links or other content accompanying the Material are not the subject of this license.

1. You agree to include the following copyright and permission notice with the reproduction of the Material: "Reprinted with permission from [FULL CITATION]. Copyright [PUBLICATION YEAR], American Institute of Physics." For an article, the

Title: Photoelectron Spectroscopy of Cold Hydrated Sulfate Clusters, SO42−(H2O)n (n = 4−7): Temperature-Dependent Isomer Populations

Author: Xue-Bin Wang et al.

Publication: The Journal of Physical Chemistry A

Publisher: American Chemical Society

Date: May 1, 2009

Quick Price Estimate

Permission for this particular request is granted for print and electronic formats at no charge. Figures and tables may be modified. Appropriate credit should be given. Please print this page for your records and provide a copy to your publisher. Requests for up to 4 figures require only this record. Five or more figures will generate a printout of additional terms and conditions. Appropriate credit should read: "Reprinted with permission from {COMPLETE REFERENCE CITATION}. Copyright {YEAR} American Chemical Society." Insert appropriate information in place of the capitalized words.

I would like to...	reuse in a Thesis/Dissertation
Requestor Type	Author (original work)
Portion	Full article
Format	Print and Electronic
Will you be translating?	No
Select your currency	USD – $
Quick Price	Click Quick Price

QUICK PRICE CONTINUE

This service provides permission for reuse only. If you do not have a copy of the article you are using, you may copy and paste the content and reuse according to the terms of your agreement. Please be advised that obtaining the content you license is a separate transaction not involving Rightslink.

To request permission for a type of use not listed, please contact the publisher directly.

Title: Flattening a Puckered Pentasilacyclopentadienide Ring by Suppression of the Pseudo Jahn−Teller Effect

Author: Alina P. Sergeeva et al.

Publication: Organometallics

Publisher: American Chemical Society

Date: Sep 1, 2010

Quick Price Estimate

Permission for this particular request is granted for print and electronic formats at no charge. Figures and tables may be modified. Appropriate credit should be given. Please print this page for your records and provide a copy to your publisher. Requests for up to 4 figures require only this record. Five or more figures will generate a printout of additional terms and conditions. Appropriate credit should read: "Reprinted with permission from {COMPLETE REFERENCE CITATION}. Copyright {YEAR} American Chemical Society." Insert appropriate information in place of the capitalized words.

I would like to...	reuse in a Thesis/Dissertation
Requestor Type	Author (original work)
Portion	Full article
Format	Print and Electronic
Will you be translating?	No
Select your currency	USD – $
Quick Price	Click Quick Price

QUICK PRICE CONTINUE

This service provides permission for reuse only. If you do not have a copy of the article you are using, you may copy and paste the content and reuse according to the terms of your agreement. Please be advised that obtaining the content you license is a separate transaction not involving Rightslink.

To request permission for a type of use not listed, please contact the publisher directly.

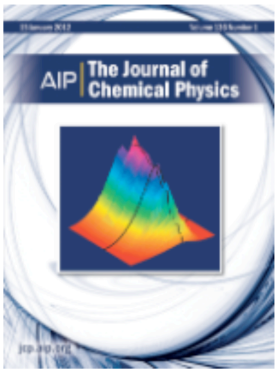

Title: Flattening a puckered cyclohexasilane ring by suppression of the pseudo-Jahn–Teller effect

Author: Konstantin Pokhodnya, Christopher Olson, Xuliang Dai, Douglas L. Schulz, et al.

Publication: Journal of Chemical Physics

Volume/Issue 134/1

Publisher: American Institute of Physics

Date: Jan 7, 2011

Page Count: 5

Quick Price Estimate

I would like to... reuse in a thesis/dissertation

Select your currency USD – $

Requestor Type Author (original article)

Format Print and electronic

Portion Excerpt (> 800 words)

Will you be translating? No

Quick Price Click Quick Price

QUICK PRICE | CONTINUE

Content Delivery: Once licensed, you may reuse the content only for the reuse purposes specified. No content delivery is offered through this service.

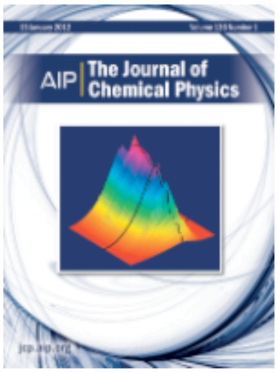

Title: Flattening a puckered cyclohexasilane ring by suppression of the pseudo-Jahn–Teller effect

Author: Konstantin Pokhodnya, Christopher Olson, Xuliang Dai, Douglas L. Schulz, et al.

Publication: Journal of Chemical Physics

Volume/Issue 134/1

Publisher: American Institute of Physics

Date: Jan 7, 2011

Page Count: 5

Order Completed

Thank you very much for your order.

This is a License Agreement between Alina P. Sergeeva ("You") and American Institute of Physics ("AIP"). The license consists of your order details, the terms and conditions provided by American Institute of Physics, and the payment terms and conditions.

Get the printable license.

License Number	2823750713465
License date	Jan 07, 2012
Licensed content publisher	American Institute of Physics
Licensed content publication	Journal of Chemical Physics
Licensed content title	Flattening a puckered cyclohexasilane ring by suppression of the pseudo-Jahn–Teller effect
Licensed content author	Konstantin Pokhodnya, Christopher Olson, Xuliang Dai, Douglas L. Schulz, et al.
Licensed content date	Jan 7, 2011
Volume number	134
Issue number	1
Type of Use	Thesis/Dissertation
Requestor type	Author (original article)
Format	Print and electronic
Portion	Excerpt (> 800 words)
Will you be translating?	No
Title of your thesis / dissertation	RATIONALIZING STRUCTURE, STABILITY, AND CHEMICAL BONDING OF PURE AND DOPED CLUSTERS, ISOLATED AND SOLVATED MULTIPLY CHARGED ANIONS, AND SOLID STATE MATERIALS
Expected completion date	Mar 2012
Estimated size (number of pages)	400
Total	0.00 USD

ORDER MORE... CLOSE WINDOW

AMERICAN INSTITUTE OF PHYSICS LICENSE TERMS AND CONDITIONS

Jan 07, 2012

This is a License Agreement between Alina P. Sergeeva ("You") and American Institute of Physics ("AIP") provided by Copyright Clearance Center ("CCC"). The license consists of your order details, the terms and conditions provided by American Institute of Physics , and the payment terms and conditions.

All payments must be made in full to CCC. For payment instructions, please see information listed at the bottom of this form.

License Number	2823750713465
License date	Jan 07, 2012
Licensed content publisher	American Institute of Physics
Licensed content publication	Journal of Chemical Physics
Licensed content title	Flattening a puckered cyclohexasilane ring by suppression of the pseudo-Jahn–Teller effect
Licensed content author	Konstantin Pokhodnya, Christopher Olson, Xuliang Dai, Douglas L. Schulz, et al.
Licensed content date	Jan 7, 2011
Volume number	134
Issue number	1
Type of Use	Thesis/Dissertation
Requestor type	Author (original article)
Format	Print and electronic
Portion	Excerpt (> 800 words)
Will you be translating?	No
Title of your thesis / dissertation	RATIONALIZING STRUCTURE, STABILITY, AND CHEMICAL BONDING OF PURE AND DOPED CLUSTERS, ISOLATED AND SOLVATED MULTIPLY CHARGED ANIONS, AND SOLID STATE MATERIALS
Expected completion date	Mar 2012
Estimated size (number of pages)	400
Total	0.00 USD
Terms and Conditions	

American Institute of Physics -- Terms and Conditions: Permissions Uses

American Institute of Physics ("AIP") hereby grants to you the non-exclusive right and license to use and/or distribute the Material according to the use specified in your order, on a one-time basis, for the specified term, with a maximum distribution equal to the number that you have ordered. Any links or other content accompanying the Material are not the subject of this license.

1. You agree to include the following copyright and permission notice with the reproduction of the Material: "Reprinted with permission from [FULL CITATION].

Copyright [PUBLICATION YEAR], American Institute of Physics." For an article, the copyright and permission notice must be printed on the first page of the article or book chapter. For photographs, covers, or tables, the copyright and permission notice may appear with the Material, in a footnote, or in the reference list.

2. If you have licensed reuse of a figure, photograph, cover, or table, it is your responsibility to ensure that the material is original to AIP and does not contain the copyright of another entity, and that the copyright notice of the figure, photograph, cover, or table does not indicate that it was reprinted by AIP, with permission, from another source. Under no circumstances does AIP, purport or intend to grant permission to reuse material to which it does not hold copyright.
3. You may not alter or modify the Material in any manner. You may translate the Material into another language only if you have licensed translation rights. You may not use the Material for promotional purposes. AIP reserves all rights not specifically granted herein.
4. The foregoing license shall not take effect unless and until AIP or its agent, Copyright Clearance Center, receives the Payment in accordance with Copyright Clearance Center Billing and Payment Terms and Conditions, which are incorporated herein by reference.
5. AIP or the Copyright Clearance Center may, within two business days of granting this license, revoke the license for any reason whatsoever, with a full refund payable to you. Should you violate the terms of this license at any time, AIP, American Institute of Physics, or Copyright Clearance Center may revoke the license with no refund to you. Notice of such revocation will be made using the contact information provided by you. Failure to receive such notice will not nullify the revocation.
6. AIP makes no representations or warranties with respect to the Material. You agree to indemnify and hold harmless AIP, American Institute of Physics, and their officers, directors, employees or agents from and against any and all claims arising out of your use of the Material other than as specifically authorized herein.
7. The permission granted herein is personal to you and is not transferable or assignable without the prior written permission of AIP. This license may not be amended except in a writing signed by the party to be charged.
8. If purchase orders, acknowledgments or check endorsements are issued on any forms containing terms and conditions which are inconsistent with these provisions, such inconsistent terms and conditions shall be of no force and effect. This document, including the CCC Billing and Payment Terms and Conditions, shall be the entire agreement between the parties relating to the subject matter hereof.

This Agreement shall be governed by and construed in accordance with the laws of the State of New York. Both parties hereby submit to the jurisdiction of the courts of New York County for purposes of resolving any disputes that may arise hereunder.

If you would like to pay for this license now, please remit this license along with your payment made payable to "COPYRIGHT CLEARANCE CENTER" otherwise you will be invoiced within 48 hours of the license date. Payment should be in the form of a check or money order referencing your account number and this invoice number RLNK500694663.
Once you receive your invoice for this order, you may pay your invoice by credit card. Please follow instructions provided at that time.

Make Payment To:
Copyright Clearance Center
Dept 001
P.O. Box 843006
Boston, MA 02284-3006

Copyright Clearance Center

Confirmation Number: 10854333
Order Date: 01/25/2012

Customer Information

Customer: Alina Sergeeva
Account Number: 3000484777
Organization: Alina Sergeeva
Email: alina.sergeeva@aggiemail.usu.edu
Phone: +1 (435)8814408
Payment Method: Invoice

Order Details

Special Orders

Aromaticity and metal clusters

Billing Status: **Not Billed**

Order detail ID:	60748803
ISBN:	978-1-4398-1334-8
Publication year:	2010
Publication Type:	Book
Publisher:	CRC Press
Rightsholder:	TAYLOR & FRANCIS GROUP LLC - BOOKS
Author/Editor:	Alina Sergeeva and Alexander Boldyrev
Your reference:	Alina Sergeeva's thesis, part of chapter 13

Permission Status: **Special Order**
Special Order Update: Forwarded to rightsholder

Permission type:	Republish or display content
Type of use:	Dissertation
Requested use:	Dissertation
Republication title:	RATIONALIZING STRUCTURE, STABILITY, AND CHEMICAL BONDING OF PURE AND DOPED CLUSTERS, ISOLATED AND SOLVATED MULTIPLY CHARGED ANIONS, AND SOLID STATE MATERIALS
Republishing organization:	Utah State University
Organization status:	Non-profit 501(c)(3)
Republication date:	03/31/2012
Circulation/ Distribution:	10
Type of content:	Excerpt
Description of requested content:	three paragraphs of the main text
Page range(s):	1-2
Translating to:	No Translation
Requested content's publication date:	10/15/2010

$TBD

Total order items: 1

Order Total: $TBD
(Excludes $TBD items)

UNIVERSITY OF CALIFORNIA, BERKELEY

BERKELEY • DAVIS • IRVINE • LOS ANGELES • RIVERSIDE • SAN DIEGO • SAN FRANCISCO SANTA BARBARA • SANTA CRUZ

DEPARTMENT OF CHEMISTRY
BERKELEY, CALIFORNIA 94720-1460

Dr. Dmitry Yu. Zubarev

Phone: (510) 642-5911
Fax: (510) 642-1088
E-mail: dmitry.zubarev@berkeley.edu

December 30, 2011

Dear Ms. Alina P. Sergeeva

This letter is to confirm that you have me permission to use our common paper

> "A Photoelectron Spectroscopic and Theoretical Study of B16- and B162-: An All-Boron Naphthalene" Alina P. Sergeeva, Dmitry Yu. Zubarev, Hua-Jin Zhai, Alexander I. Boldyrev, Lai-Sheng Wang, J. Am. Chem. Soc. 2008, 130, 7244-7246 (DOI: 10.1021/ja802494z)

in part or in full for preparation or presentation of your dissertation.

Sincerely,

Dmitry Yu. Zubarev

January 25th, 2012

Hua-Jin Zhai, Ph.D.
Department of Chemistry
Brown University
Providence, RI 02912
Phone: (509) 371-6148
Fax: (509) 371-6139
E-mail: Hua-Jin.Zhai@pnnl.gov

Dear Alina P. Sergeeva,

This letter is to confirm that you have my permission to use our common papers:

- A.P. Sergeeva, D.Yu. Zubarev, H.J. Zhai, A.I. Boldyrev, L.S. Wang, "A Photoelectron Spectroscopic and Theoretical Study of B16- and B162-: An All-Boron Naphthalene", *J. Am. Chem. Soc.* 2008, *130*, 7244-7246 (DOI: 10.1021/ja802494z)
- W. Huang, A.P. Sergeeva, H.J. Zhai, B.B. Averkiev, L.S. Wang, A.I. Boldyrev, "A Concentric Planar Doubly π-Aromatic B19- cluster", *Nature Chemistry* 2010, *2*, 202-206 (DOI: 10.1038/nchem.534)
- A.P. Sergeeva, B.B. Averkiev, H.J. Zhai, A.I. Boldyrev, L.S. Wang, "All-boron analogues of aromatic hydrocarbons: B17- and B18-", *J. Chem. Phys.* 2011, *134*, 224304 (DOI: 10.1063/1.3599452)

in part or in full for preparation or presentation of your dissertation.

Sincerely,

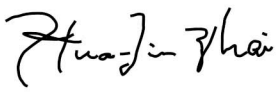

Hua-Jin Zhai

Brown University
Department of Chemistry
324 Brook Street, Box H
Providence, Rhode Island 02912
Tel: (401) 863-3389 Fax: (401) 863-2594
E-mail: Lai-Sheng_Wang@brown.edu
http://www.chem.brown.edu/research/LSWang/

Lai-Sheng Wang
Professor

December 22, 2011

Alina Sergeeva
Department of Chemistry
Utah State University

Dear Alina,

You have my permission to use our following joint papers for your PhD thesis in whatever form suitable.

1) A Photoelectron Spectroscopic and Theoretical Study of B_{16}^- and B_{16}^{2-}: An All-Boron Naphthalene. Alina P. Sergeeva, Dmitry Yu. Zubarev, Hua-Jin Zhai, Alexander I. Boldyrev, Lai-Sheng Wang *J. Am. Chem. Soc.* 2008, *130*, 7244-7246 (DOI: 10.1021/ja802494z) (communication)
2) A Concentric Planar Doubly π-Aromatic B_{19}^- cluster. Wei Huang, Alina P. Sergeeva, Hua-Jin Zhai, Boris B. Averkiev, Lai-Sheng Wang, Alexander I. Boldyrev *Nature Chemistry* 2010, *2*, 202-206 (DOI: 10.1038/nchem.534) (article)
3) All-boron analogues of aromatic hydrocarbons: B_{17}^- and B_{18}^-. Alina P. Sergeeva, Boris B. Averkiev, Hua-Jin Zhai, Alexander I. Boldyrev, and Lai-Sheng Wang *J. Chem. Phys.* 2011, *134*, 224304 (DOI: 10.1063/1.3599452)-- (article)
4) Planarization of B_7^- and B_{12}^- Clusters by Isoelectronic Substitution: AlB_6^- and AlB_{11}^-. Constantin Romanescu, Alina P. Sergeeva, Wei-Li Li, Alexander I. Boldyrev, and Lai-Sheng Wang *J. Am. Chem. Soc.* 2011, *133*, 8646-8653 (DOI: 10.1021/ja2012438) (article)
5) Negative electron binding energies observed in a triply charged anion: Photoelectron spectroscopy of 1-hydroxy-3,6,8-pyrene-trisulfonate. Jie Yang, Xiao-Peng Xing, Xue-Bin Wang, Lai-Sheng Wang, Alina P. Sergeeva, Alexander I. Boldyrev *J. Chem. Phys.* 2008, *128*, 091102-1-4 (DOI: 10.1063/1.2889001) (article)
6) Probing the Electronic Stability of Multiply Charged Anions: The Sulfonated Pyrene Tri- and Tetra-Anions. Xue-Bin Wang, Alina P. Sergeeva, Xiao-Peng Xing, Maria Massaouti, Tatjana Karpuschkin, Oliver Hampe, Alexander I. Boldyrev, Manfred M. Kappes, Lai-Sheng Wang *J. Am. Chem. Soc.* 2009, *131*, 9836-9842 (DOI: 10.1021/ja903615g) (article)
7) Photoelectron Spectroscopy of Cold Hydrated Sulfate Clusters, $SO_4^{2-}(H_2O)_n$ (n = 4-7): Temperature-Dependent Isomer Populations. Xue-Bing Wang, Alina P. Sergeeva, Jie Yang, Xiao-Peng Xing, Alexander I. Boldyrev, Lai-Sheng Wang *J. Phys. Chem. A* 2009, *113*, 5567-5576 (DOI: 10.1021/jp900682g) (article)

Sincerely,

Lai-Sheng Wang

Anhui Institute of Optics and Fine Mechanics

Chinese Academy of Sciences

Hefei 230031, Anhui, P.R. China

Dear Alina P. Sergeeva, December 21, 2011

This letter is to confirm that you have my permission to use our collaborated papers:

A Concentric Planar Doubly π-Aromatic $B19^-$ cluster

Wei Huang, Alina P. Sergeeva, Hua-Jin Zhai, Boris B. Averkiev, Lai-Sheng Wang, Alexander I. Boldyrev

Nature Chemistry 2010, 2, 202-206 (DOI: 10.1038/nchem.534)

in part or in full for preparation or presentation of your dissertation.

Sincerely,

Wei Huang

Jan 09. 2012

Boris Averkiev
Department of Chemistry,
University of Minnesota, 207 Pleasant St. SE,
Minneapolis, MN 55455

December 21, 2011

Dear Alina P. Sergeeva,

This letter is to confirm that you have my permission to use our common papers:

A Concentric Planar Doubly π-Aromatic B_{19}^- cluster.
Wei Huang, Alina P. Sergeeva, Hua-Jin Zhai, Boris B. Averkiev, Lai-Sheng Wang, Alexander I. Boldyrev
Nature Chemistry 2010, *2*, 202-206 (DOI: 10.1038/nchem.534)
(article)

All-boron analogues of aromatic hydrocarbons: B_{17}^- and B_{18}^-.
Alina P. Sergeeva, Boris B. Averkiev, Hua-Jin Zhai, Alexander I. Boldyrev, and Lai-Sheng Wang
J. Chem. Phys. 2011, *134*, 224304 (DOI: 10.1063/1.3599452)
(article)

in part or in full for preparation or presentation of your dissertation.

Sincerely,

Boris Averkiev

Girasoles # 5

Colonia Felipe Ángeles

Zacatecas, Zacatecas

CP 98000

Dear Alina P. Sergeeva,

December 23, 2011

This letter is to confirm that you have my permission to use our common paper:

Unravellingphenomenonofinternalrotation in $B13^{+}$throughchemicalbonding análisis

Gerardo Martínez-Guajardo, Alina P. Sergeeva,Alexander, I. Boldyrev, Thomas Heine, Jesus M. Ugaldedand Gabriel Merino.

Chem. Comm., (2011),**47**, 6242.

In part or in full for preparation or presentation of your dissertation.

Sincerely,

Gerardo Martínez Guajardo.

JACOBS UNIVERSITY

Jacobs University gGmbH, Campus Ring 1, 28759 Bremen

Alina P. Sergeeva
c/o Utah State University
Department of Chemistry and Biochemistry
0300 Old Main Hill
U.S.A.

Prof. Dr. Thomas Heine

School of Engineering & Science
Research III

Phone: +49.421.200-32 23
Fax: +49.421.200-32 29
t.heine@jacobs-university.de

Bremen, January 17, 2012

Dear Alina P. Sergeeva,

This letter is to confirm that you have my permission to use our common papers in part or in full for preparation or presentation of your PhD dissertation.

1. “Unravelling phenomenon of internal rotation in B13+ through chemical bonding analysis”, Gerardo Martínez-Guajardo, Alina P. Sergeeva, Alexander I. Boldyrev, Thomas Heine, Jesus M. Ugalde and Gabriel Merino (*Chem. Commun. 2011, 47, 6242-6244 (DOI: 10.1039/C1CC10821B) (communication*)).

Sincerely,

Prof. Dr. Thomas Heine
School of Engineering and Science, Jacobs University Bremen

eman ta zabal zazu

Dr. Jesus M. Ugalde
Kimika Fakultatea
Euskal Herriko Unibertsitatea
P.K. 1072; 20080 Donostia (Spain)
Voice: +34-943-018190
Fax: +34-943-212236
E-mail: jesus.ugalde@ehu.es
www.ehu.es/chemistry/theory

December 21, 2011

Dear Alina P. Sergeeva,

This letter is to confirm that you have my permission to use our common paper:

- Gerardo Martínez-Guajardo, Alina P. Sergeeva, Alexander I. Boldyrev, Thomas Heine, Jesus M. Ugalde and Gabriel Merino
  Chem. Commun. 2011, **47**, 6242-6244 (DOI: 10.1039/C1CC10821B) (Communication)

in part or in full for preparation or presentation of your dissertation. Sincerely,

Jesus M. Ugalde
Prof. of Chemistry

UNIVERSIDAD DE GUANAJUATO
DEPARTAMENTO DE QUIMICA
DIVISION DE CIENCIAS NATURALES Y EXACTAS
Dr. Gabriel Merino

NORIA ALTA s/n GUANAJUATO, GTO. 36050, MEXICO
TEL (473) 732-0006 ext. 1433
e-mail: gmerino@quijote.ugto.mx

Guanajuato, Gto, México

December 21, 2011

Dear Alina P. Sergeeva,

This letter is to confirm that you have my permission to use our common paper

Martínez-Guajardo, G.; Sergeeva, A. P.; Boldyrev, A. I.; Heine, T.; Ugalde, J. M.; Merino, G. Unravelling phenomenon of almost free internal rotation in planar B_{13}^+ cluster through chemical bonding analysis. Chem. Comm. ***2011***, 47, *6242-6244*.

in part or in full for preparation or presentation of your dissertation.

Sincerely,

Prof. Gabriel Merino
Profesor-Investigador
Profesor Titular

Constantin Romanescu
Brown University
Chemistry Department
324 Brook Street, Providence RI 02912

December 22, 2011

Dear Alina P. Sergeeva,

This letter is to confirm that you have my permission to use our common paper:

Planarization of B_7^- and B_{12}^- Clusters by Isoelectronic Substitution: AlB_6^- and AlB_{11}^-.
Constantin Romanescu, Alina P. Sergeeva, Wei-Li Li, Alexander I. Boldyrev, and Lai-Sheng Wang, *J. Am. Chem. Soc.* 2011, *133*, 8646-8653 (DOI: 10.1021/ja2012438)

in part or in full for preparation or presentation of your dissertation.

Sincerely,

Constantin Romanescu

Chemistry Department

Brown University

324 Brook St, Providence, RI, 02912

December 22, 2011

Dear Alina P. Sergeeva,

This letter is to confirm that you have my permission to use our common papers:

Planarization of B_7^- and B_{12}^- Clusters by Isoelectronic Substitution: AlB_6^- and AlB_{11}^-.

Constantin Romanescu, Alina P. Sergeeva, Wei-Li Li, Alexander I. Boldyrev, and Lai-Sheng Wang *J. Am. Chem. Soc.* 2011, *133*, 8646-8653 (DOI: 10.1021/ja2012438)

in part or in full for preparation or presentation of your dissertation.

Sincerely,

Wei-Li Li

Department of Chemistry and Biochemistry
Utah State University
0300 Old Main Hill
Logan, UT 84322-0300
USA

Dear Alina P. Sergeeva,

January 5, 2012

This letter is to confirm that you have my permission to use our common paper:

1) Deciphering the mystery of hexagon holes in an all-boron graphene α-sheet. Timur R. Galeev, Qiang Chen, Jin-Chang Guo, Hui Bai, Chang-Qing Miao, Hai-Gang Lu, Alina P. Sergeeva, Si-Dian Li, and Alexander I. Boldyrev, Phys. Chem. Chem. Phys., **2011**, *13*, 11575-11578.

in part or in full for preparation or presentation of your dissertation.

Sincerely,

Timur R. Galeev

山西大學
SHANXI UNIVERSITY

Qiang Chen
Institute of Molecular Sciences
Shanxi University
Taiyuan 030006
Shanxi, China
Dec.23, 2011

Dear Alina P. Sergeeva:

I am very glad to know that you will graduate next Spring. I permit you to use the following paper as part of your dissertation to which you made the major contribution:

"Deciphering the mystery of hexagon holes in an all-boron graphene α-sheet." Timur R. Galeev, Qiang Chen, Jin-Chang Guo, Hui Bai, Chang-Qing Miao, Hai-Gang Lu, Alina P. Sergeeva, Si-Dian Li and Alexander I. Boldyrev, *Phys. Chem. Chem. Phys.* 2011, *13*, 11575-11578 (DOI:10.1039/C1CP20439D)

With best regards

Yours Sincerely

Qiang Chen

地　　址：山西省太原市坞城路 92 号
邮　　编：030006
电　　话：0086-351-7010255
传　　真：0086-351-7011981
网　　址：Http://www.sxu.edu.cn
电子信箱：Xiaoban@sxu.edu.cn

山西大學
SHANXI UNIVERSITY

Jin-Chang Guo
Institute of Molecular Sciences
Shanxi University
Taiyuan 030006
Shanxi, China
Dec.23, 2011

Dear Alina P. Sergeeva:

I am very glad to know that you will graduate next Spring. I permit you to use the following paper as part of your dissertation to which you made the major contribution:

"Deciphering the mystery of hexagon holes in an all-boron graphene α-sheet." Timur R. Galeev, Qiang Chen, Jin-Chang Guo, Hui Bai, Chang-Qing Miao, Hai-Gang Lu, Alina P. Sergeeva, Si-Dian Li and Alexander I. Boldyrev, *Phys. Chem. Chem. Phys.* 2011, *13*, 11575-11578 (DOI:10.1039/C1CP20439D)

With best regards

Yours Sincerely

郭谨昌

Jin-Chang Guo

地　址：山西省太原市坞城路 92 号
邮　编：030006
电　话：0086-351-7010255
传　真：0086-351-7011981
网　址：Http://www.sxu.edu.cn
电子信箱：Xiaoban@sxu.edu.cn

山西大學
SHANXI UNIVERSITY

Hui Bai
Institute of Molecular Sciences
Shanxi University
Taiyuan 030006
Shanxi, China
Dec.23, 2011

Dear Alina P. Sergeeva:

I am very glad to know that you will graduate next Spring. I permit you to use the following paper as part of your dissertation to which you made the major contribution:

"Deciphering the mystery of hexagon holes in an all-boron graphene α-sheet." Timur R. Galeev, Qiang Chen, Jin-Chang Guo, Hui Bai, Chang-Qing Miao, Hai-Gang Lu, Alina P. Sergeeva, Si-Dian Li and Alexander I. Boldyrev, *Phys. Chem. Chem. Phys.* 2011, *13*, 11575-11578 (DOI:10.1039/C1CP20439D)

With best regards

Yours Sincerely

白慧

Hui Bai

地　　址：山西省太原市坞城路 92 号
邮　　编：030006
电　　话：0086-351-7010255
传　　真：0086-351-7011981
网　　址：Http://www.sxu.edu.cn
电子信箱：Xiaoban@sxu.edu.cn

山西大學
SHANXI UNIVERSITY

Chang-Qing Miao
Institute of Molecular Sciences
Shanxi University
Taiyuan 030006
Shanxi, China
Dec.23, 2011

Dear Alina P. Sergeeva:

I am very glad to know that you will graduate next Spring. I permit you to use the following paper as part of your dissertation to which you made the major contribution:

"Deciphering the mystery of hexagon holes in an all-boron graphene α-sheet." Timur R. Galeev, Qiang Chen, Jin-Chang Guo, Hui Bai, Chang-Qing Miao, Hai-Gang Lu, Alina P. Sergeeva, Si-Dian Li and Alexander I. Boldyrev, *Phys. Chem. Chem. Phys.* 2011, *13*, 11575-11578 (DOI:10.1039/C1CP20439D)

With best regards

Yours Sincerely

Chang-Qing Miao 苗常青

地　址：山西省太原市坞城路 92 号
邮　编：030006
电　话：0086-351-7010255
传　真：0086-351-7011981
网　址：Http://www.sxu.edu.cn
电子信箱：Xiaoban@sxu.edu.cn

山西大學
SHANXI UNIVERSITY

Hai-Gang Lu
Institute of Molecular Sciences
Shanxi University
Taiyuan 030006
Shanxi, China
Dec.23, 2011

Dear Alina P. Sergeeva:

I am very glad to know that you will graduate next Spring. I permit you to use the following paper as part of your dissertation to which you made the major contribution:

"Deciphering the mystery of hexagon holes in an all-boron graphene α-sheet." Timur R. Galeev, Qiang Chen, Jin-Chang Guo, Hui Bai, Chang-Qing Miao, Hai-Gang Lu, Alina P. Sergeeva, Si-Dian Li and Alexander I. Boldyrev, *Phys. Chem. Chem. Phys.* 2011, *13*, 11575-11578 (DOI:10.1039/C1CP20439D)

With best regards

Yours Sincerely

Hai-Gang Lu 吕海港

地　　址：山西省太原市坞城路 92 号
邮　　编：030006
电　　话：0086-351-7010255
传　　真：0086-351-7011981
网　　址：Http://www.sxu.edu.cn
电子信箱：Xiaoban@sxu.edu.cn

山西大學
SHANXI UNIVERSITY

Prof. Dr. Si-Dian Li
Institute of Molecular Sciences
Shanxi University
Taiyuan 030006
Shanxi, China
Dec.23, 2011

Dear Alina P. Sergeeva:

I am very glad to know that you will graduate next Spring. I and my colleagues of course permit you to use the following paper as part of your dissertation to which you made the major contribution:

"Deciphering the mystery of hexagon holes in an all-boron graphene α-sheet." Timur R. Galeev, Qiang Chen, Jin-Chang Guo, Hui Bai, Chang-Qing Miao, Hai-Gang Lu, Alina P. Sergeeva, Si-Dian Li and Alexander I. Boldyrev, *Phys. Chem. Chem. Phys.* 2011, *13*, 11575-11578 (DOI: 10.1039/C1CP20439D)

With best regards

Yours Sincerely

Si-Dian Li

地　　址：山西省太原市坞城路 92 号
邮　　编：030006
电　　话：0086-351-7010255
传　　真：0086-351-7011981
网　　址：Http://www.sxu.edu.cn
电子信箱：Xiaoban@sxu.edu.cn

Institute of Modern Physics

Chinese Academy of Sciences

509 Nanchang Rd.

Lanzhou 730000 China P.R.

Dear Alina P. Sergeeva, December 21, 2011

This letter is to confirm that you have my permission to use our common papers:

1) Negative electron binding energies observed in a triply charged anion: Photoelectron spectroscopy of 1-hydroxy-3,6,8-pyrene-trisulfonate.
Jie Yang, Xiao-Peng Xing, Xue-Bin Wang, Lai-Sheng Wang, Alina P. Sergeeva, Alexander I. Boldyrev
J. Chem. Phys. 2008, *128*, 091102-1-4 (DOI: 10.1063/1.2889001)
(article)

2) Probing the Electronic Stability of Multiply Charged Anions: The Sulfonated Pyrene Tri- and Tetra-Anions.
Xue-Bin Wang, Alina P. Sergeeva, Xiao-Peng Xing, Maria Massaouti, Tatjana Karpuschkin, Oliver Hampe, Alexander I. Boldyrev, Manfred M. Kappes, Lai-Sheng Wang
J. Am. Chem. Soc. 2009, *131*, 9836-9842 (DOI: 10.1021/ja903615g)
(article)

3) Photoelectron Spectroscopy of Cold Hydrated Sulfate Clusters, $SO_4^{2-}(H_2O)_n$ (n = 4-7): Temperature-Dependent Isomer Populations.
Xue-Bing Wang, Alina P. Sergeeva, Jie Yang, Xiao-Peng Xing, Alexander I. Boldyrev, Lai-Sheng Wang
J. Phys. Chem. A 2009, *113*, 5567-5576 (DOI: 10.1021/jp900682g)
(article)

in part or in full for preparation or presentation of your dissertation.

Sincerely,

Jie Yang

College of Materials Sciences and Optelectronics Technology,
Graduate University of Chinese Academy of Sciences,
19A Yuquan Road, Shijingshan District, Beijing

Dear Alina P. Sergeeva, December 24, 2011

This letter is to confirm that you have my permission to use our common papers:

1. Negative electron binding energies observed in a triply charged anion: Photoelectron spectroscopy of 1-hydroxy-3,6,8-pyrene-trisulfonate. Jie Yang, Xiao-Peng Xing, Xue-Bin Wang, Lai-Sheng Wang, Alina P. Sergeeva, Alexander I. Boldyrev J. Chem. Phys. 2008, 128, 091102-1-4 (DOI: 10.1063/1.2889001) (article)

2. Probing the Electronic Stability of Multiply Charged Anions: The Sulfonated Pyrene Tri- and Tetra-Anions. Xue-Bin Wang, Alina P. Sergeeva, Xiao-Peng Xing, Maria Massaouti, Tatjana Karpuschkin, Oliver Hampe, Alexander I. Boldyrev, Manfred M. Kappes, Lai-Sheng WangJ. Am. Chem. Soc. 2009, 131, 9836-9842 (DOI: 10.1021/ja903615g)(article)

3. Photoelectron Spectroscopy of Cold Hydrated Sulfate Clusters, SO42-(H2O)n (n = 4-7): Temperature-Dependent Isomer Populations.Xue-Bing Wang, Alina P. Sergeeva, Jie Yang, Xiao-Peng Xing, Alexander I. Boldyrev, Lai-Sheng WangJ. Phys. Chem. A 2009, 113, 5567-5576 (DOI: 10.1021/jp900682g)(article)

in part or in full for preparation or presentation of your dissertation.

Sincerely,

Xiaopeng Xing

Pacific Northwest National Laboratory

Chemical & Materials Sciences Division
P.O. Box 999, MS K8-88
Richland, WA 99352

Xue-Bin Wang

Scientist

Tel: 509-371-6132
Fax: 509-371-6139
E-mail: xuebin.wang@pnnl.gov

Dear Alina P. Sergeeva, Dec.22, 2011

This letter is to confirm that you have my permission to use our common papers:

(1) Negative electron binding energies observed in a triply charged anion: Photoelectron spectroscopy of 1-hydroxy-3,6,8-pyrene-trisulfonate.
Jie Yang, Xiao-Peng Xing, Xue-Bin Wang, Lai-Sheng Wang, Alina P. Sergeeva, Alexander I. Boldyrev. *J. Chem. Phys.* 2008, *128*, 091102-1-4 (DOI: 10.1063/1.2889001) (article)
(2) Probing the Electronic Stability of Multiply Charged Anions: The Sulfonated Pyrene Tri- and Tetra-Anions.
Xue-Bin Wang, Alina P. Sergeeva, Xiao-Peng Xing, Maria Massaouti, Tatjana Karpuschkin, Oliver Hampe, Alexander I. Boldyrev, Manfred M. Kappes, Lai-Sheng Wang. *J. Am. Chem. Soc.* 2009, *131*, 9836-9842 (DOI: 10.1021/ja903615g) (article)
(3) Photoelectron Spectroscopy of Cold Hydrated Sulfate Clusters, $SO_4^{2-}(H_2O)_n$ (n = 4-7): Temperature-Dependent Isomer Populations.
Xue-Bing Wang, Alina P. Sergeeva, Jie Yang, Xiao-Peng Xing, Alexander I. Boldyrev, Lai-Sheng Wang. *J. Phys. Chem. A* 2009, *113*, 5567-5576 (DOI: 10.1021/jp900682g) (article)

in part or in full for preparation or presentation of your dissertation.

Sincerely,

Xue-Bin Wang

Maria Massaouti has not responded to my request for the permission letter

Dipl. Chem. Tatjana Karpuschkin
Karlsruhe Institute of Technology (KIT)
Institute of Nanotechnology
Hermann-von-Helmholtz-Platz 1
76344 Eggenstein-Leopoldshafen, Germany

January 24, 2011

Dear Alina P. Sergeeva,

This letter is to confirm that you have my permission to use our common papers:

Probing the Electronic Stability of Multiply Charged Anions:The Sulfonated Pyrene Tri- and Tetra-Anions.
Xue-Bin Wang, Alina P. Sergeeva, Xiao-Peng Xing, Maria Massaouti, Tatjana Karpuschkin, Oliver Hampe, Alexander I. Boldyrev, Manfred M. Kappes, Lai-Sheng Wang
*J. Am. Chem. Soc.*2009,*131*, 9836-9842(DOI: 10.1021/ja903615g)

in part or in full for preparation or presentation of your dissertation.

Sincerely,

Tatjana Karpuschkin

Karlsruhe Institute of Technology

KIT-Campus North | INT | P.O.Box 3640 | 76021 Karlsruhe, Germany

Institut für Nanotechnologie

Directors: Prof. Dr.-Ing. Horst Hahn
Prof. Dr. Manfred Kappes
Prof. Dr. Jean-Marie Lehn

Hermann-von-Helmholtz-Platz 1
76344 Eggenstein-Leopoldshafen, Germany

PD Dr. Oliver Hampe

Phone: +49 721 608-2-6416
Fax: +49 721 608-2-6368
Email: Oliver.Hampe@kit.edu

Date: 2011-12-22

Mrs.
Alina P. Sergeeva

Department of Chemistry and Biochemistry:
Utah State University
0300 Old Main Hill
USA

Dear Alina P. Sergeeva,

This letter is to confirm that you have my permission to use our common paper

"Probing the Electronic Stability of Multiply Charged Anions: The Sulfonated Pyrene Tri- and Tetra-Anions"
Xue-Bin Wang, Alina P. Sergeeva, Xiao-Peng Xing, Maria Massaouti, Tatjana Karpuschkin, Oliver Hampe, Alexander I. Boldyrev, Manfred M. Kappes, Lai-Sheng Wang
J. Am. Chem. Soc. 2009, 131, 9836-9842 (DOI: 10.1021/ja903615g)

in part or in full for preparation or presentation of your dissertation.

Sincerely,

Karlsruher Institut für Technologie

Karlsruhe Institut für Technologie (KIT),
Institut für Physikalische Chemie, Fritz Haber Weg 2, 76131 Karlsruhe

Institut für Physikalische Chemie
Abteilung Physikalische Chemie mikroskopischer Systeme
Prof. Dr. Manfred Kappes

Fritz-Haber-Weg 2, Geb. 30:44, Zi. 504
76131 Karlsruhe

Telefon: 0721 608-42094
Fax: 0721 608-47232
E-Mail: manfred.kappes@kit.edu
Web: www.kit.edu

Bearbeiter/in:
Unser Zeichen:
Datum: 22.12.2011

Alina P. Sergeeva,
Department of Chemistry and Biochemistry
Utah State University
0300 Old Main Hill

USA

Dear Alina P. Sergeeva,

This letter is to confirm that you have my permission to use our common paper

Probing the Electronic Stability of Multiply Charged Anions: The Sulfonated Pyrene Tri- and Tetra-Anions,
Xue-Bin Wang, **Alina P. Sergeeva**, Xiao-Peng Xing, Maria Massaouti, Tatjana Karpuschkin, Oliver Hampe, Alexander I. Boldyrev, **Manfred M. Kappes**, Lai-Sheng Wang , ***J. Am. Chem. Soc***. 2009, *131*, 9836-9842 (DOI: 10.1021/ja903615g)

in part or in full for preparation or presentation of your dissertation.

Sincerely,

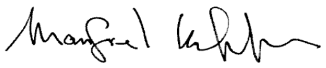

Manfred M. Kappes

Center for Nanoscale Science and Engineering
NORTH DAKOTA STATE UNIVERSITY
Research 2, R102U
1805 NDSU Research Park Dr.
Fargo, ND 58102

Dear Alina P. Sergeeva, January 8, 2012

This letter is to confirm that you have my permission to use our common papers:

"Flattening a puckered cyclohexasilane ring by suppression of the pseudo-Jahn-Teller effect."
Konstantin Pokhodnya, Christopher Olson, Xuliang Dai, Douglas L. Schulz, Philip Boudjouk, Alina P. Sergeeva, and Alexander I. Boldyrev
J. Chem. Phys. 2011, *134*, 014105 (DOI: 10.1063/1.3516179)

in part or in full for preparation or presentation of your dissertation.

Sincerely,

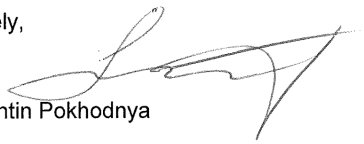

Konstantin Pokhodnya

Christopher Olson has not responded to my request for the permission letter.

Xuliang Dai replied back in an e-mail saying that I have his permission, though he has not provided me with the signed permission letter.

January 11, 2012

Dear Alina P. Sergeeva,

This letter is to confirm that you have my permission to use our common papers: "Flattening a puckered cyclohexasilane ring by suppression of the pseudo-Jahn-Teller effect." Konstantin Pokhodnya, Christopher Olson, Xuliang Dai, Douglas L. Schulz, Philip Boudjouk, Alina P. Sergeeva, and Alexander I. Boldyrev. *J. Chem. Phys.* 2011, *134*, 014105 (DOI: 10.1063/1.3516179) in part or in full for preparation or presentation of your dissertation.

Sincerely,

Douglas L. Schulz, Ph.D.
Senior Research Scientist,
Center for Nanoscale Science & Engineering
NORTH DAKOTA STATE UNIVERSITY
Research 2
1805 NDSU Research Park Dr.
Fargo, ND 58102

NDSU NORTH DAKOTA STATE UNIVERSITY

Office of the Vice President for Research, Creative Activities and Technology Transfer

NDSU Dept. 4000
1735 NDSU Research Park Drive
R1, P.O. Box 6050
Fargo, ND 58108-6050

701.231.6542
Fax 701.231.6736
www.ndsu.edu/ndsu/vprcatt/

January 9, 2012

Ms. Alina Sergeeva
Department of Chemistry and Biochemistry
Utah State University

Dear Ms. Sergeeva:

This letter is to confirm that you have my permission to use our common papers, "Flattening a puckered cyclohexasilane ring by suppression of the pseudo-Jahn-Teller effect" by Konstantin Pokhodnya, Christopher Olson, Xuliang Dai, Douglas L. Schulz, Philip Boudjouk, Alina P. Sergeeva, and Alexander I. Boldyrev. *J. Chem. Phys.* 2011, *134*, 014105 (DOI: 10.1063/1.3516179), in part or in full for preparation or presentation of your dissertation.

Sincerely,

Philip Boudjouk, Ph.D.
Vice President
Office of the Vice President for Research, Creative Activities and Technology Transfer

CURRICULUM VITAE

Alina P. Sergeeva

Department of Chemistry and Biochemistry

Utah State University

0300 Old Main Hill, Logan, UT 84322-0300

E-mail: alina.sergeeva@aggiemail.usu.edu

Website: http://www.chem.usu.edu/~boldyrev/alina

EDUCATION

2007-2012 Ph. D. in Chemistry with an emphasis in physical and theoretical chemistry, Department of Chemistry and Biochemistry, Utah State University, Logan, UT, GPA=4.0

2002-2007 B.Sc. in Chemistry, Department of Science, Peoples' Friendship University of Russia, Moscow, GPA=4.0

RESEARCH EXPERIENCE

2007-present Research Assistant, Alexander I. Boldyrev's Research Group, Department of Chemistry and Biochemistry, Utah State University, Logan, UT, USA.

Development of chemical bonding theory in pure and doped clusters composed of boron, gold, aluminum, transition metals,† etc. via introducing multiple aromaticity/antiaromaticity/conflicting aromaticity concepts and performing the newly developed Adaptive Natural Density Partitioning method. Extending the gained experience in chemical bonding from cluster species to solids.

Interpretation of photoelectron spectra of novel clusters that have the potential to be building blocks of future nanomaterials and nanocatalysts.*#

Investigating peculiarities of multiply charged anions: stability, reactivity, phenomenon of negative electron binding energy, mechanisms of solvation, etc.*§

Rationalizing non-stability of high-symmetry structures via Jahn-Teller Effects (Pseudo Jahn-Teller Effect, Renner-Teller Effect).◊

Investigating the nature of molecular motors.††

In collaboration with:

* Professor Lai-Sheng Wang, Brown University

Professor Kit H. Bowen, Johns Hopkins University

§ Prof. Manfred M. Kappes and Prof. Oliver Hampe, The Institute of Nanotechnology, Karlsruhe, Germany

◊ Dr. Konstantin Pokhodnya, Center of Nanoscale Science and Engineering, North Dakota State University

† Prof. Philippe F. Weck, University of Nevada Las Vegas

†† Prof. Gabriel Merino, Universidad de Guanajuato, Mexico

†† Prof. Thomas Heine, Jacobs University, Germany

†† Prof. Jesus Ugalde, Donostia International Physics Center, Spain

TEACHING EXPERIENCE

2011 Teaching Assistantship, General Chemistry 1210 Recitations

2010 Teaching Assistantship, General Chemistry 1210 Recitations

2010 Process Oriented Guided Inquiry Learning (POGIL) Workshop, at the three day POGIL Regional Meeting, Westminster College, Salt Lake City, UT, 7/13/2010-7/15/2010

2007 Utah State University Teaching Assistant Workshop

2006 One semester course in pedagogy, PFUR, Moscow

MENTORING

Graduate Students:

2011 - present Aleksandr S. Ivanov, under collaboration of USU&PFUR.

2009 – present Timur R. Galeev, under collaboration of USU&PFUR.

2009 – present Ivan Popov, under collaboration of USU&PFUR.

2009 Caleb Allpress, at USU during his rotation in Alex Boldyrev's Group.

2008 Andrey Vorobiev, under collaboration of USU&PFUR.

Undergraduate Students:

2009 – 2010 Aleksandr S. Ivanov, under collaboration of USU&PFUR, whose B. Sc. thesis done under my mentorship was considered to be the best as of 2010 at the Department of Physical-Mathematical and Natural Sciences, PFUR, Moscow.

2008 – 2009 Ivan Popov, under collaboration of USU&PFUR, whose B. Sc. thesis done under my mentorship was considered to be the best as of 2009 at the Department of Physical-Mathematical and Natural Sciences, PFUR, Moscow.

Highschool Students:

2011 Philip Cutler, from Logan High School during his Summer Internship Program organized at USU.

2010 Dustin Hicken, from Logan High School during his Summer Internship Program organized at USU.

2009 Rebekah Jung, from Intech Collegiate High School during her Summer Internship Program organized at USU.

2008 Ellie Edwards, from Intech Collegiate High School during her Summer Internship Program organized at USU.

PROFESSIONAL AFFILIATIONS AND STUDENT ORGANIZATIONS

2009 – 2011 Departmental Representative of Graduate Student Senate at USU

2008 – present Member of American Chemical Society

AWARDS AND HONORS

2012 The Marjorie H. Gardner Teaching Award, USU.

2012 The 2011-2012 College of Science Ph. D. Graduate Researcher of the Year, USU.

2011 American Chemical Society Physical Chemistry Division Outstanding Student Poster Award at the 242nd ACS National Meeting, Denver, CO.

2011 The School of Graduate Studies Dissertation Fellowship, Utah State University.

2011 The Outstanding Graduate Student in Chemistry Award, Utah State University.

2010 American Chemical Society Physical Chemistry Division Outstanding Student Poster Award at the 239th ACS National Meeting, San Francisco, CA.

2010 IBM-Zerner Award for Graduate Students at the 50th Sanibel Symposium, Quantum Theory Project, St. Simons Island, GA.

2008 Award for Early Research Progress in Chemistry, Utah State University.

2007 B.Sc. Honor Diploma, Peoples' Friendship University of Russia.

LIST OF PUBLICATIONS (as of April 15, 2012)

2012

20. A photoelectron spectroscopy and ab initio study of B_{21}^-: Negatively charged boron clusters continue to be planar at 21. Zachary A. Piazza, Wei-Li Li, Constantin Romanescu, Alina P. Sergeeva, Lai-Sheng Wang, and Alexander I. Boldyrev J. Chem. Phys. 2012, 136, 104310 (DOI: 10.1063/1.3692967) (article)

2011

19. All-boron analogues of aromatic hydrocarbons: B_{17}^- and B_{18}^-. Alina P. Sergeeva, Boris B. Averkiev, Hua-Jin Zhai, Alexander I. Boldyrev, and Lai-Sheng Wang. J. Chem. Phys. 2011, 134, 224304 (DOI: 10.1063/1.3599452) (article)

This article was selected for the JCP Editors' Choice for 2011

18. Rational Design of Small 3D Gold Clusters. Alina P. Sergeeva and Alexander I. Boldyrev. J. Clust. Sci. 2011, 22, 321-329 (DOI: 10.1007/s10876-011-0386-2) (article)

17. Deciphering the mystery of hexagon holes in an all-boron graphene α-sheet. Timur R. Galeev, Qiang Chen, Jin-Chang Guo, Hui Bai, Chang-Qing Miao, Hai-Gang Lu, Alina P. Sergeeva, Si-Dian Li, and Alexander I. Boldyrev. Phys. Chem. Chem. Phys. 2011, 13, 11575-11578 (DOI: 10.1039/C1CP20439D) (communication)

16. Planarization of B_7^- and B_{12}^- Clusters by Isoelectronic Substitution: AlB_6^- and AlB_{11}^-. Constantin Romanescu, Alina P. Sergeeva, Wei-Li Li, Alexander I. Boldyrev, and Lai-Sheng Wang. J. Am. Chem. Soc. 2011, 133, 8646-8653 (DOI: 10.1021/ja2012438) (article)

15. Unravelling phenomenon of internal rotation in B_{13}^+ through chemical bonding analysis. Gerardo Martínez-Guajardo, Alina P. Sergeeva, Alexander I. Boldyrev, Thomas

Heine, Jesus M. Ugalde, and Gabriel Merino. Chem. Comm., 2011, 47, 6242-6244 (DOI: 10.1039/c1cc10821b) (communication)

This communication was featured on the cover of Issue 22 of Chemical Communications.

14. Flattening a puckered cyclohexasilane ring by suppression of the pseudo-Jahn-Teller effect. Konstantin Pokhodnya, Christopher Olson, Xuliang Dai, Douglas L. Schilz, Philip Boudjouk, Alina P. Sergeeva, and Alexander I. Boldyrev. J. Chem. Phys., 2011, 134, 014105 (DOI: 10.1063/1.3516179) (article)

13. Chemical Bonding and Aromaticity in Trinuclear Transition-Metal Halide Clusters. Philippe F. Weck, Alina P. Sergeeva, Eunja Kim, Alexander I. Boldyrev, and Kenneth R. Czerwinski. Inorg. Chem., 2011, 50, 1039-1046 (DOI: 10.1021/ic101779w) (article)

2010

12. Aromaticity in Metals: From Clusters to Solids. Alina P. Sergeeva and Alexander I. Boldyrev. In Aromaticity and Metal clusters. Atoms, Molecules, and Clusters. Structure, Reactivity, and Dynamics book series. P. K. Chattaraj, Ed.; CRC Press, Taylor & Francis Group, Boca Raton, 2010, pp. 55-68. (ISBN: 9781439813348) (invited chapter)

11. δ-Bonding in the $[Pd_4(\mu_4\text{-}C_9H_9)(\mu_4\text{-}C_8H_8)]^+$ sandwich complex. Alina P. Sergeeva and Alexander I. Boldyrev. Phys. Chem. Chem. Phys., 2010, 12, 12050-12054 (DOI: 10.1039/C0CP00475H) (communication)

10. Flattening a Puckered Pentasilacyclopentadienide Ring by Suppression of the Pseudo Jahn-Teller Effect. Alina P. Sergeeva and Alexander I. Boldyrev. Organometallics, 2010, 29, 3951-3954 (DOI: 10.1021/om1006038) (article)

9. Combined Experimental and Theoretical Investigation of Three-Dimensional, Nitrogen-Doped, Gallium Cluster Anions. Haopeng Wang, Yeon Jae Ko, Kit H. Bowen,

Alina P. Sergeeva, Boris B. Averkiev and Alexander I. Boldyrev. J. Phys. Chem. A, 2010, 114, 11070-11077 (DOI: 10.1021/jp101419b) (article)

8. Recent Advances in All-Transition Metal Aromaticity and Antiaromaticity. Alina P. Sergeeva, Boris B. Averkiev, and Alexander I. Boldyrev. In Metal-Metal Bonding. Structure and Bonding book series. G.Parkin, Ed.; Volume 136, Springer, Berlin/Heidelberg, 2010, pp. 275-306. (ISBN: 978-3-642-05242-2; DOI: 10.1007/978-3-642-05243-9_8) (invited chapter)

7. The Chemical bonding of Re_3Cl_9 and $Re_3Cl_9^{2-}$ revealed by the Adaptive Natural Density Partitioning analyses. Alina P. Sergeeva and Alexander I. Boldyrev. Comments Inorg. Chem., 2010, 31, 2-12 (DOI: 10.1080/02603590903498639) (article)

6. B_{19}^-: A Concentric Planar Doubly π-Aromatic Cluster. Wei Huang, Alina P. Sergeeva, Hua-Jin Zhai, Boris B. Averkiev, Lai-Sheng Wang, and Alexander I. Boldyrev. Nature Chem., 2010, 2, 202-206 (DOI: 10.1038/nchem.534) (article)

This article was highlighted in News of the Week section of C&EN, Vol. 88, Issue 28, p. 9. 2009, as well as **in Chemistry World, Vol.7, No.3, 2010.**

5. Probing the Electronic Stability of Multiply Charged Anions: The Sulfonated Pyrene Tri- and Tetra-Anions. Xue-Bin Wang, Alina P. Sergeeva, Xiao-Peng Xing, Maria Massaouti, Tatjana Karpuschkin, Oliver Hampe, Alexander I. Boldyrev, Manfred Kappes, and Lai-Sheng Wang. J. Am. Chem. Soc., 2009, 131, 9836-9842 (DOI: 10.1021/ja903615g) (article)

4. Photoelectron Spectroscopy of Cold Hydrated Sulfate Clusters, $SO_4^{2-}(H_2O)_n$ (n = 4–7): Temperature-Dependent Isomer Populations. Xue-Bin Wang, Alina P. Sergeeva, Jie

Yang, Xiao-Peng Xing, Alexander I. Boldyrev, and Lai-Sheng Wang. J. Phys .Chem. A, 2009, 113, 5567-5576 (DOI: 10.1021/jp900682g) (article)

3. Multifold Aromaticity, Multifold Antiaromaticity, and Conflicting Aromaticity: Implications of Stability and Reactivity of Clusters. Dmitry Y. Zubarev, Alina P. Sergeeva, and Alexander I. Boldyrev. In Chemical Reactivity Theory. A Density Functional View. Chattaraj, P. K., Ed.; CRC Press. Taylor & Francis Group: New York, 2009, pp. 439-452. (ISBN: 978-1-4200-6543-5) (invited chapter)

2008

2. A Photoelectron Spectroscopic and Theoretical Study of B_{16}^- and B_{16}^{2-}: An All-Boron Naphthalene. Alina P. Sergeeva, Dmitry Y. Zubarev, Hua-Jin Zhai, Lai-Sheng Wang, and Alexander I. Boldyrev. J. Am. Chem. Soc., 2008, 130, 7244-7246 (DOI: 10.1021/ja802494z) (communication)

1. Negative Electron Binding Energies Observed in a Triply Charged Anion: Photoelectron Spectroscopy of 1-Hydroxy-3,6,8-Pyrene-Trisulfonate ($HPTS^{3-}$). Jie Yang, Xiao-Peng Xing, Xue-Bin Wang, Lai-Sheng Wang, Alina P. Sergeeva, and Alexander I. Boldyrev. J. Chem. Phys., 2008, 128, 091102-1-4(DOI: 10.1063/1.2889001) (article)

PRESENTATIONS AT PROFESSIONAL MEETINGS

August 28 – September 1, 2011 (Poster presentation) "Rationalizing chemical bonding in molecular Wankel motors" Division of Physical Chemistry, at the 242nd National ACS Meeting & Exposition, Denver, CO.

March 21-25, 2010 (Poster presentation) "Structure, stability and unique chemical bonding of pure boron clusters: All-boron hydrocarbon analogs" Division of Physical Chemistry, at the 239th National ACS Meeting & Exposition, San Francisco, CA.

March 21-25, 2010 (Poster presentation) "Deciphering chemical bonding: From clusters to solids" Division of Inorganic Chemistry, at the 239th National ACS Meeting & Exposition, San Francisco, CA.

February 24 - March 2, 2010 (Poster presentation) "Towards unified chemical bonding theory" at the 50th Sanibel Symposium, Quantum Theory Project, St. Simons Island, GA.

June 13, 2009 (Poster presentation) "Ab Initio, Photoelectron Spectroscopy, and Mass-Spectroscopic probing of negative electron binding energy, electronic structure and stability of isolated and solvated multiply-charged anions" at the celebration of 40 Years of Ion chemistry, Carl Lineberger and His Co-Conspirators, Boulder, CO.

August 17-21, 2008 (Poster presentation) "Peculiarities of 1-hydroxy-3,6,8-pyrene-trisulfonate triply charged anion" at the 236th National ACS Meeting, Philadelphia, PA.